

Archive ouverte UNIGE

https://archive-ouverte.unige.ch

Thèse 2023

Open Access

This version of the publication is provided by the author(s) and made available in accordance with the copyright holder(s).

Targeting the Glucocorticoid Pathway Improves the Outcome of Immunotherapy in a Renal Cancer Model

Poinot, Hélène

How to cite

POINOT, Hélène. Targeting the Glucocorticoid Pathway Improves the Outcome of Immunotherapy in a Renal Cancer Model. Doctoral Thesis, 2023. doi: 10.13097/archive-ouverte/unige:172584

This publication URL: https://archive-ouverte.unige.ch/unige:172584

Publication DOI: 10.13097/archive-ouverte/unige:172584

© This document is protected by copyright. Please refer to copyright holder(s) for terms of use.

UNIVERSITÉ DE GENÈVE

FACULTÉ DES SCIENCES

Section de Sciences Pharmaceutiques

Département d'Immunopharmacologie du cancer

Professeur C. Bourquin

Docteur A. Pommier

Targeting the Glucocorticoid Pathway Improves the Outcome of Immunotherapy in a Renal Cancer Model

THÈSE

présentée aux Facultés de médecine et des sciences de l'Université de Genève pour obtenir le grade de Docteur ès sciences en sciences de la vie, mention Sciences Pharmaceutiques

par

Hélène POINOT

de

Gif-sur-Yvette, France

Thèse N°238

GENÈVE

Centre d'impression Uni Mail

2023



DOCTORAT ÈS SCIENCES EN SCIENCES DE LA VIE DES FACULTÉS DE MÉDECINE ET DES SCIENCES MENTION SCIENCES PHARMACEUTIQUES

Thèse de Mme Hélène POINOT

intitulée :

« Targeting the Glucocorticoid Pathway Improves the Outcome of Immunotherapy in a Renal Cancer Model »

Les Facultés de médecine et des sciences, sur le préavis de Madame Carole BOURQUIN, Professeure ordinaire et directrice de thèse (Section des sciences pharmaceutiques), Monsieur Aurélien POMMIER, Maître assistant et co-directeur de thèse (Section des sciences pharmaceutiques), Monsieur Yogeshvar KALIA, Professeur ordinaire (Section des sciences pharmaceutiques), Monsieur Eric FERAILLE, Professeur associé (Département de physiologie cellulaire et métabolisme), Madame Camilla JANDUS, Professeure assistante (Département de pathologie et immunologie) et Monsieur Nicola VANNINI, Docteur (Department of oncology, University of Lausanne, UNIL, CHUV, Ludwig Institute for Cancer Research Lausanne) autorisent l'impression de la présente thèse, sans exprimer d'opinion sur les propositions qui y sont énoncées.

Genève, le 12 septembre 2023

Thèse - 238 -

Le Doyen Faculté de médecine

A.C. cicl

La Doyenne Faculté des sciences

N.B. - La thèse doit porter la déclaration précédente et remplir les conditions énumérées dans les "Informations relatives aux thèses de doctorat à l'Université de Genève".



Table of Contents

Acknowledgments	V
Résumé en français	VIII
Abstract	X
1) Introduction	1
I. The immune system and cancer	1
I.A. Immune cells	2
I.A.1. Myeloid cells	2
I.A.2. Lymphoid cells	3
I.B. Immune checkpoints	4
I.B.1. Expression and function	4
I.B.2. Treatment in cancer	4
I.C. Resistance to immunotherapy	6
II. Renal cancer	7
II.A. The kidneys	7
II.A.1. Anatomy and histology of the kidneys	7
II.A.2. Function of the kidney	8
II.A.2.a. Detoxification	8
II.A.2.b. Hormones secreted by the kidney	9
II.A.2.c. Blood pressure regulation	10
II.B. Renal cell carcinoma	11
II.B.1. Classification and physiopathology	11
II.B.2. Molecular mechanisms	12
II.B.2.a. Von Hippel-Lindau pathway	12
II.B.2.a.i. The hypoxia pathway	12
II.B.2.a.ii. Vascular endothelial growth factor	13
II.B.2.a.iii. Mammalian target of rapamycin pathway	13

II.B.2.b. Von Hippel-Lindau gene mutation	13
II.B.3. Immune infiltration	14
II.B.4. Epidemiology	14
II.B.4.a. Sex-biased effect in clear cell renal cell carcinoma	14
II.B.4.b. Risk factors in clear cell renal cell carcinoma	15
II.B.5. Treatment of clear cell renal cell carcinoma	16
II.B.5.a. Targeted therapies	16
II.B.5.b. Immunotherapies	17
II.B.5.c. Resistance	19
II.B.5.d. Biomarkers	20
II.C. Clear cell renal cell carcinoma models	20
II.C.1. Cellular model used in research	20
II.C.2. In vivo models used in research	21
III. Glucocorticoids: Origin and biological activity	22
III.A. Steroidogenesis	22
III.B. Hypothalamic-pituitary-adrenal axis	23
III.B.1. Anatomy	23
III.B.2. Hormone secretion and circadian cycle	24
III.A. Glucocorticoid signaling	24
III.A.1. Glucocorticoid receptor	24
III.A.1.a. Expression	24
III.A.1.b. Activity, target genes, and effects of the glucocorticoid receptor	25
III.A.2. Mineralocorticoid receptor	26
III.A.3. Interrelation between glucocorticoids and sex steroid pathways	27
III.B. Production of glucocorticoids in peripheral organs	28
III.B.1. 11β-hydroxysteroid dehydrogenases type 1	28
III.B.2. 11β-hydroxysteroid dehydrogenases type 2	30
III.C. Glucocorticoid pathways and the immune system	32

III.C.1. Effects of glucocorticoids on immune differentiation	32
III.C.2. Effects of glucocorticoids on immune activation	33
III.C.3. Effects of the circadian cycle on immune cells	33
III.D. Glucocorticoids in cancer	34
III.D.1. Link between cancer and glucocorticoids	34
III.D.1.a. Therapeutic glucocorticoid use with immunotherapy	34
III.D.1.b. Endogenous glucocorticoids	34
III.D.2. Inhibition of the glucocorticoid pathway in patients	35
III.D.2.a. Glucocorticoid receptor inhibitors	35
III.D.2.b. 11β-hydroxysteroid dehydrogenases type 1 inhibitors	36
III.D.2.b.i. Use in clinic	36
III.D.2.b.ii. ABT-384	37
2) Aim of the Thesis	
3) Results	39
I. Activation of endogenous glucocorticoids by HSD11B1 inhibits the antitumor immune	response in
renal cancer	39
I.A. Introduction	39
I.B. Manuscript submitted	40
II. HSD11B1 inhibitors for use in immunotherapy and the uses thereof	81
II.A. Introduction and contributions	81
II.B. Patent WO2021180643	82
II.C. Supplementary results	116
II.C.1. Materials and methods	116
II.C.2. Results	117
III. Effect of <i>Hsd11b1</i> genetic modulation on the antitumor immune response in a renal ca	ancer model
	119
III.A. Material and methods	120
III.B. Effect of intratumoral HSD11B1 over-expression on the antitumor immune re	sponse in a
subcutaneous tumor model	122

III.C. Impact of <i>Hsd11b1</i> kr	ockout in mice on the antitumor immune response in a subcutaneous
tumor model	
III.D. Discussion	
IV. Effect of glucocorticoid re	ceptor antagonism on tumor growth and antitumor immune response
IV.A. Material and method	s 129
IV.B. Results	
IV.C. Discussion	
4) General Discussion	
I. Impact of stress-induced gl	ucocorticoids on the anti-PD-1 response in cancer140
II. Role of HSD11B1 and the o	lual effect of its inhibitor ABT-384 on the antitumor immune response
in a renal cancer model	
III. Glucocorticoid receptor a	s a new target for improving immune checkpoint blockade response
IV. Repurposing drugs in cand	er treatment to improve patients' quality of life144
V. Beyond glucocorticoids: Th	ne steroid pathway and its impact on renal cancer development 145
5) Conclusion and Perspectives.	
6) Bibliography	
7) Appendices	
I. Supplementary data	
II. Abbreviations	
III. List of Figures and Tables	
IV. Curriculum vitae	186

Acknowledgments

First, I would like to thank Pr Carole Bourquin for giving me the opportunity to do my PhD thesis in her lab.

A special thanks to Dr Aurélien Pommier, my supervisor and mentor, for his advices and support to accompany my development in research all along my PhD.

I also wish to thank Pr Yogeshvar Kalia, Pr Eric Feraille, Pr Camilla Jandus and Dr Nicola Vannini for accepting to examine my thesis. I would especially like to thank Pr Kalia who supported me during the last weeks of my PhD.

During my thesis I met wonderful colleagues who helped me a lot and with whom I had really nice time. Some of them became friends, but all counted for me.

Thanks to Betül Taskoparan for being the first teacher in my daily lab life issue. I miss our time thinking and troubleshooting about experiments and particularly in molecular biology.

To Bart Boersma, I wish to thank you a lot for your help and for the great collaboration we have working together. I really enjoy all our brain storming on DB's project and all these times I was observing your new technics or helping you in the lab to change my mind during the writing of my thesis.

To Montserrat Alvarez, I would like to give my most sincere thanks for your daily support in the lab. None of us would be able to work in so nice conditions without all the work you are doing with all the orders, stock, lab management and help during experiments.

To Barbara Pinheiro and Isis Senoner, I wish to thank you both for the kind help you gave me, especially with the genotyping.

I would like to thank Viola, Sandra, Julia and Betül for sharing their experience and for their help during the beginning of my PhD. Thanks also for the "out of the lab" time, for the pizza evenings in the lab, for the Ciné transat, and for the great time in Sardinia and Turkey!

Thanks to Betül, Eloïse, Isis, Montsé, Aurélien, Bart, Guillaume, and Jérémie for their help during my numerous end-of-experiment days. I could not do it without your help.

A special thanks to Guillaume Disner for being my first master student. I learned a lot with you on my side, and you will stay forever my best-first student.

Laure et Anthony, merci pour votre aide en attente 7. Pour les questions via Pyrat ou emails quand mes requêtes semblaient bizarres. Pour avoir répondu à tous mes « c'est normal ça ? » et « comment tu fais ça ? ». Et pour votre bonne humeur à chaque fois que j'arrivais en bas !

Finally, this journey would not have been possible without all the little attentions that many have given me all along.

À Patricia Delcros, merci mille fois de m'avoir aidée lors de la recherche de mon stage de fin d'étude, de m'avoir fait confiance et ouvert ton réseau. Merci aussi à Frederic Duchenes pour la confiance que vous m'avez accordée sans laquelle je n'aurais pas eu l'occasion de faire mon stage chez Pierre Fabre. Sans votre confiance à tous deux, cette aventure des 5 dernières années n'aurait pas été possible.

Montsé, merci d'avoir toujours fait attention à comment j'allais. Merci pour tous tes petits messages et tous tes « ça va ? » qui étaient toujours véridiques et pas juste des questions rhétoriques. Merci pour tous tes conseils (et pas seulement au sujet des expériences de labo). Merci aussi pour tous les moments « out-of-lab » que tu as si souvent organisés. Et pour finir, merci de partager mon amour inconditionnel des paillettes et du bricolage!

Sofia, I appreciated so much your support during the last months of this journey, our laughs in the office, our discussion about "life", our mutual love for coffee. I wish that you keep having so much enthusiasm in your future researcher life.

To the Turkish crew, Betül, Melis, Burak, Giray and Dogukan, I had such great time with you in Switzerland, France or Turkey. Teşhekular!

Bart you made my life in the lab so beautiful! You made me laugh so many times (even though there were also quite some moments when you laugh about me especially about my beautiful accent). I could not survive this last few years without you. I am looking forward to meet you in other labs or out of the CMU (specially to crush you at Mario Kart).

Joé et Margherita, vous êtes arrivées assez tard dans cette aventure qu'a été ma thèse. Mais les super moments que l'on a passés au théâtre ou pendant MT180, m'ont soutenue et portée pendant la dernière ligne droite. Merci pour tous ces moments et j'ai hâte pour tous les suivants !

Aux cousins Poillibert, je vous ai peu vu ces dernières années, mais chaque rencontre reste gravée en moi. Merci pour ces bons moments de relâche, et pour votre soutien lors de MT180 (je suis sûre que les votes se sont envolés grâce à vous !).

À Camille et Florence, un immense merci pour votre soutien indéfectible, pour votre présence à tout moment, pour vos « interventions urgentes » et votre disponibilité pour venir me changer les idées. Les mots me manquent pour exprimer à quel point vous m'avez soutenu dans les moments difficiles, à quel point vous avez été un pilier pour moi. Et à quel point je chéris les moments de rire et joie que l'on a partagés et qui j'en suis sûre s'enrichiront de plein d'autres dans les années à venir.

Aurélien, je n'aurais jamais assez de temps pour exprimer la reconnaissance que j'éprouve. Ta confiance en mes capacités me dépasse. Merci. Merci pour le début chez Pierre Fabre. Merci de m'avoir fait confiance pour cette thèse. Merci de m'avoir poussée parfois, retenue d'autre fois, soutenue toujours. C'est difficile de mettre un mot sur ce que tu représentes, mais je pense que le plus approprié serait « mentor » même s'il sonne un peu comme « vieux sage » (et bien sûr je ne me permettrais pas ce qualificatif d'âge). Tu es un excellent enseignant et un très bon manager. Et même si ne plus travailler avec toi me fait peur, je sais que tu m'as donné les armes pour la suite de ma carrière.

Maman, Papa, merci d'avoir été présents pendant ces années difficiles. D'avoir pris des vacances dans le coin pour que je puisse venir. De m'avoir conseillé sur comment allier vie pro et vie perso. D'avoir mis le holà quand c'était trop. A Jean-Baptiste, Claire et Margot, merci pour votre soutien indéfectible et votre adaptabilité à mon emploi du temps. Merci pour tous les fous rire que l'on partage à chaque fois que l'on se voit. Mon cœur se serre quand je pense à tous les 5 et je ne sais pas comment vous dire ce que je ressens. Mais vous savez.

Résumé en français

Le cancer est la seconde cause de décès dans le monde et le cancer rénal en est le dixième le plus courant dans les pays développés. Ceux ayant un cancer rénal répondent habituellement aux inhibiteurs de checkpoint immunitaires (ICI) qui ont pour but de restaurer une réponse immunitaire antitumorale chez les patients. Cependant des mécanismes de résistance existent et, aux Etats-Unis, le taux de survie à 5 ans est de seulement 12 % pour les patients atteints d'un cancer rénal métastatique. C'est pourquoi, de nouveaux traitements sont nécessaires afin de surmonter les mécanismes de résistance aux actuelles immunothérapies. L'un des potentiel mécanisme de résistance est l'altération du métabolisme des cellules tumorales et des cellules immunitaires, résultant en une diminution de l'immunité antitumorale. Parmi les changements métaboliques observés au niveau tumoral, la voie de la stéroïdogenèse pourrait jouer une importante fonction de modulation de la réponse immune. Cependant le rôle des stéroïdes endogènes dans la résistance aux immunothérapies contre le cancer est aujourd'hui peu compris. Dans cette thèse, nous avons étudié le potentiel thérapeutique d'une inhibition de la voie des glucocorticoïdes endogènes afin d'améliorer la réponse immune antitumorale et l'efficacité des ICI dans le cancer rénal.

En utilisant des outils bio-informatiques, l'analyse de données du TCGA nous a permis de mettre en évidence que la voie des glucocorticoïdes était fortement associée avec le pronostic clinique des patients souffrant d'un cancer du rein. La 11-béta-hydroxystéroïde déshydrogénase de type 1 (HSD11B1) régénère les glucocorticoïdes inactifs en glucocorticoïdes actifs. Il s'agit du principal producteur de glucocorticoïdes dans les tissus périphériques non surrénaliens. De façon intéressante, l'expression d'HSD11B1 est associée avec un mauvais pronostic clinique et corrèle avec l'expression de gènes immunosuppresseurs chez les patients atteints d'un cancer du rein. Nous avons aussi découvert qu'HSD11B1 était principalement exprimé dans les cellules immunes infiltrant la tumeur rénale.

Suite à l'observation de l'expression d'HSD11B1 associée à un aspect immun, nous avons étudié l'impact de l'activité d'HSD11B1 dans les cellules immunes. Grâce à des tests *in vitro* murins et humains, nous avons démontré que l'inhibition d'HSD11B1 augmentait l'élimination des cellules tumorales par les lymphocytes T, et cela en stimulant leur activation médiée par un antigène. Nous avons également établi que le traitement avec un inhibiteur d'HSD11B1 synergisait avec un anti-PD-1 pour améliorer l'efficacité de l'ICI. Par conséquent, dans le but déclaré de réutiliser les inhibiteurs d'HSD11B1 dans le traitement contre le cancer, plusieurs inhibiteurs ont été testés, et un brevet a été déposé pour protéger leurs utilisations en association avec un ICI.

Puisque l'activation immunitaire était améliorée par l'inhibition d'HSD11B1 in vitro, nous avons étudié l'effet d'une inhibition de la voie des glucocorticoïdes sur la réponse immune antitumorale in vivo. La

combinaison d'un inhibiteur d'HSD11B1 et d'un ICI ou de resiquimod a démontré une amélioration de l'efficacité des immunothérapies dans des modèles murins de cancer du rein sous-cutané et intra-rénal. La voie des glucocorticoïdes a aussi été ciblée via l'inhibition du récepteur aux glucocorticoïdes par la mifepristone. L'association de mifepristone et d'anti-PD-1 a montré un meilleur résultat que la monothérapie dans un modèle murin de cancer du rein sous-cutané. Cette association a révélé une augmentation dans la tumeur de voies de signalisation liées à la réponse immune, et impliquées dans le métabolisme du collagène. Cependant des investigations plus poussées doivent être effectuées afin de comprendre les mécanismes sous-jacents impliquées dans cette réponse immunitaire antitumorale, plus particulièrement au sujet du rôle du métabolisme du collagène et son impact sur l'activité des cellules immunes.

En conclusion, cette thèse soutient l'hypothèse que l'utilisation d'un inhibiteur pharmacologique d'HSD11B1, et plus généralement, l'inhibition de la voie des glucocorticoïdes, en association avec une immunothérapie, pourrait être bénéfique chez certains patients atteints d'un cancer du rein. Ces découvertes mettent en évidence le rôle des glucocorticoïdes endogènes dans la réponse immunitaire antitumorale, et ouvrent la voie à de nouvelles combinaisons thérapeutiques pour traiter le cancer du rein, plus particulièrement pour les patients présentant des résistances aux ICI.

Abstract

Cancer is the second cause of death worldwide and renal cancer is the tenth most common cancer in developed countries. Even though patients with renal cancer usually respond to immune checkpoint inhibitors (ICI) which aim to restore the antitumor immune response in patients, resistance mechanisms occur and the 5-year survival rate in USA is only 12 % of patients with metastatic disease. Therefore, novel treatments are required to overcome resistance mechanisms to current immunotherapies in renal cancer. One of the potential resistance mechanisms is the alteration of tumor and immune cell metabolism, which results in a reduction of antitumor immunity. Neosteroidogenesis occurs in tumor and endogenous steroids have strong immunomodulatory functions, but their role in resistance to immunotherapy in cancer is poorly understood. In this thesis, we explored the potential of inhibiting the endogenous glucocorticoid pathway to improve the antitumor immune response and the efficacy of ICI in renal cancer.

Using bioinformatic analysis of TCGA data, we found that the glucocorticoid pathway was strongly associated with clinical outcome of renal cancer patients. The 11 beta-hydroxysteroid dehydrogenase type 1 (HSD11B1) regenerates inactive glucocorticoids into active glucocorticoids and is the main peripheral glucocorticoid producer. Interestingly, *HSD11B1* expression was associated with a poor clinical outcome and correlated with immunosuppressive gene expression in renal cancer patients. We also found that HSD11B1 was mainly expressed in immune infiltrated cells in human renal cancer samples.

Having observed that HSD11B1 expression was associated with immune components, we investigated the impact of HSD11B1 activity in immune cells. In murine and human *in vitro* assays, we demonstrated that HSD11B1 inhibition increases the T cell dependent killing of tumor cells by stimulating the antigenmediated T cell activation, and treatment with an HSD11B1 inhibitor synergized with anti-PD-1 to improve the efficacy of ICI. Therefore, with the stated goal of repurposing HSD11B1 inhibitor in cancer treatment, several HSD11B1 inhibitors were tested and a patent was filed to protect the use of HSD11B1 inhibitor in combination with ICI.

As immune activation was improved by HSD11B1 inhibition *in vitro*, we investigated the effect of the glucocorticoid pathway inhibition on the antitumor immune response *in vivo*. HSD11B1 inhibition in combination with ICI or resiquimod demonstrated an improvement of the efficacy of immunotherapy in subcutaneous and intra-renal mouse cancer models. Targeting the glucocorticoid pathway was also achieved through inhibition of the glucocorticoid receptor with mifepristone. Combination with mifepristone and anti-PD-1 showed a better outcome in subcutaneous renal mouse cancer than monotherapy, with an enhancement of immune related pathways and collagen metabolism in the

tumor. However, further studies need to be carried out to understand the underlying mechanisms involved in this antitumor immune response, especially the role of the collagen metabolism and its impact on immune cell activity.

To conclude, this thesis supports the hypothesis that the use of HSD11B1 pharmacological inhibitor and more generally, inhibition of the glucocorticoid pathway, in combination with immunotherapy could be beneficial in some renal cancer patients. These findings highlight the role of endogenous glucocorticoids on the antitumor immune response and pave the way for new treatment combinations in renal cancer, especially for patients exhibiting resistance to ICI.

I. The immune system and cancer

Cancer, the second most common cause of death in Europe and the USA in 2020,^{1,2} results from an abnormally excessive proliferation of cells. Cancer is characterized by ten hallmarks described by Hanahan and Weinberg, which recapitulate the tumor cell capabilities such as the resistance to cell death, the induction of angiogenesis, and the replicative immortality.³ The immune system plays a crucial role in cancer development and avoiding immune destruction is one of the ten hallmarks. Some of immune system functions and interactions with tumors are described in the cancer-immunity cycle in Figure 1.⁴ Through tumor development, tumor cell death occurs, which causes tumor antigens to be released. Antigen-presenting cells (APCs) in the tumor microenvironment, such as dendritic cells (DCs), take up, process, and present antigens to T cells in the lymph nodes. Once activated by DCs, T cells are capable of trafficking through the circulation to the tumor, specifically recognizing tumor cells, and then killing them.

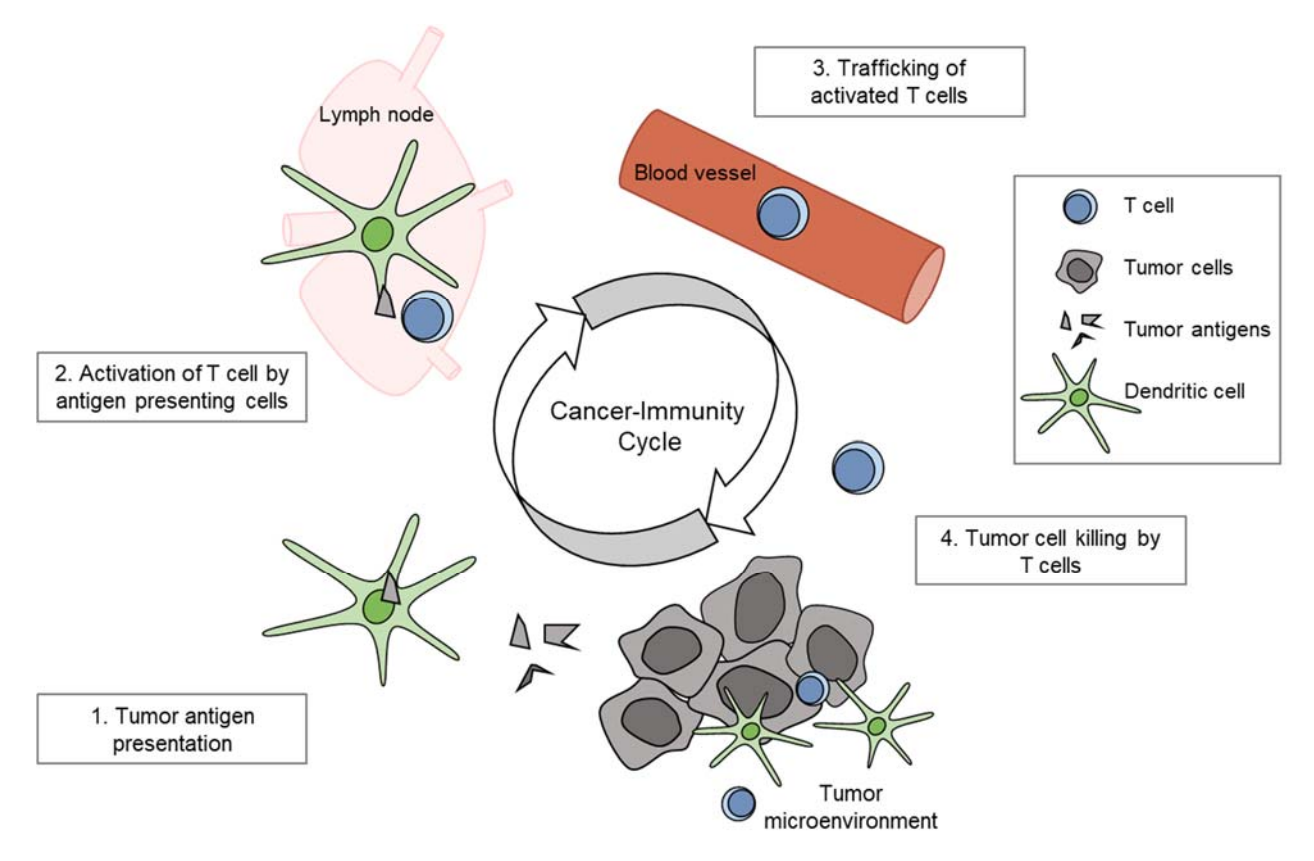


Figure 1: The cancer-immunity cycle: A schematic representation of immune activity during cancer development. Adapted from Chen and Mellman, Immunity, 2013.

However, immune system activity can also favor tumor progression, such as through the selection of immune-resistant tumor cells. Indeed, adaptation mechanisms have developed in tumor cells, such as

the loss of tumor-antigen expression or the secretion of immunosuppressive molecules. This dual role of the immune system – simultaneously anti- and pro-tumoral – is known as cancer immunoediting. ^{5–7} It is divided into the following three main phases, which do not all always occur: tumor cell elimination, equilibrium, and tumor cell escape. First, in the elimination or immunosurveillance phase, immune system activity leads to the killing of tumor cells, as described in Figure 1. Then, the antitumor immune response is initiated through the activation of innate immune cells by danger signals produced by tumor cells, such as type I interferon or HMGB1, ⁸ and through the activation of the adaptive immune system starting with APCs. ⁹ However, some tumor cells are able to adapt and avoid immunosurveillance, which is where cancer enters a phase of equilibrium; here, the adaptive immune system maintains tumor cells in a dormant state. Over time, the selection of more aggressive tumor cell variants occurs, increasing the presence of tumor cells that are able to escape from immune cells surveillance, such as through the loss of antigen expression. The proliferation of these immune-resistant cells leads to tumor progression and the last phase of cancer immunoediting, namely tumor cell escape.

The immune system consists of several subpopulations, which have antitumoral or pro-tumoral effects. Cytotoxic T cells and DCs are potent antitumor immune cells, and myeloid-derived suppressor cells, M2-macrophages, or regulatory T cells belong to immunosuppressive populations and favor tumor development. To understand their role in a tumoral context and how treatment could potentiate their antitumor effects, and reverse their pro-tumoral effects, a brief overview of the immune system is provided in the following subsections.

I.A. Immune cells

I.A.1. Myeloid cells

DCs are the first actor in the adaptative immune response due to their ability to process and present extracellular antigens to lymphocytes, thus activating them in an antigen-specific manner. This antigen-presentation process is called cross-presentation, and it is particularly critical in a tumor context. ^{10,11} This is because it allows the presentation of antigens from tumor cells to CD8⁺ T cells, which are then able to recognize and eliminate them. After the phagocytosis of tumor cell fragments, antigens are transferred into the cytosol of DCs, where they are processed and presented on the MHC class I protein. DCs are essential for inducing a potent antitumor immune response through the activation of CD8⁺ T cells. ¹² To allow the proper activation of T cells, DCs express co-stimulator proteins, such as CD40, CD80, and CD86, which interact with molecules on T cells, such as CD40L or CD28, and secrete immunostimulatory cytokines, such as IL-12, IL-6, or TNF-α. However, DCs can also acquire a

regulatory profile that expresses inhibitory molecules, such as PD-L1, PD-L2, or OX40L, or secreting cytokines such as TGF- β , leading to a tolerant microenvironment that promotes tumor growth. ¹³

Macrophages are innate immune cells that can be divided into subpopulations such as M1-like macrophages, which are also called classically activated macrophages, and M2-like macrophages. M1-like macrophages have a pro-inflammatory phenotype and promote an antitumor response, while M2-polarized macrophages are anti-inflammatory and lead to a tolerant response to tumors. $^{14-16}$ Furthermore, M1-like macrophages have a high antigen presentation capacity and produce inflammatory cytokines, whereas M2-like macrophages poorly present antigens and secrete anti-inflammatory cytokines, such as IL-10 and TGF-β.

In the myeloid lineage, neutrophils and myeloid-derived suppressor cells (MDSCs) are two subpopulations that are particularly involved in the immunosuppression of the tumor microenvironment. Neutrophils are able to have antitumor activity, through reactive oxygen species production or the activation of innate and adaptive immune cells, but they also display pro-tumor functions with the secretion of pro-angiogenic factors and their ability to remodel the extra-cellular matrix.¹⁷ The MDSC population is composed of several immature cells, which exhibit an immunosuppressive function. As they originate from several myeloid populations, their difference is based on their functions and not on their surface markers, which do not allow them to be differentiated from neutrophils or monocytes in mice contrary to human. MDSCs can produce TGF- β and VEGF; consume arginine and tryptophan, which are amino acids required for T cell activity; and express co-inhibitory receptors such as PD-L1.

I.A.2. <u>Lymphoid cells</u>

Lymphocytes are also divided into two populations, namely antibody producer B cells and T cells, which recognize specific antigens after activation through T cell receptors interacting with antigens bound to the MHC protein on APCs. T cells are further classified into two subpopulations with distinct functions, depending on their expression of transmembrane proteins, the first of which is CD4⁺ T cells. These act as helpers of the immune response during the activation of CD8⁺ T cells, which are cytotoxic cells that kill pathogens or abnormal cells, such as tumor cells.

The second subpopulation is CD8⁺ T cells, which play a crucial role in the antitumor immune response because they are cytotoxic tumor-infiltrating lymphocytes (TILs). TILs are involved in the killing of tumoral cells.²¹ Therefore, high CD8⁺ T cell infiltration in a tumor is correlated with a good prognosis in patients with most solid cancer types.^{22–25}

Furthermore, CD4⁺ T cells can differentiate into several subpopulations with more tolerant (e.g., T_H2 phenotype) or pro-inflammatory (e.g., T_H1 or T_H17) phenotypes.^{26,27} One of the tolerant CD4⁺ T cell subpopulations is the T regulatory population (T_{reg}), which is highly involved in cancer.²⁸ Indeed, T_{reg} promotes a pro-tumorigenic context in the tumor microenvironment by secreting immunosuppressive cytokines, such as IL-10 and TGF- β , and expressing co-inhibitory receptors, such as CTLA-4 and PD-1.

T cells are affected by tumor cells through the expression of co-inhibitory receptors or the secretion of anti-inflammatory cytokines, which leads to a tolerant phenotype in infiltrated T cells. TILs either become anergic, which is a deficient activation state due to a lack of IL-2 production or co-stimulatory molecules, or exhausted, which refers to a state of decreased efficacy after chronic T cell activation.²⁹

I.B. Immune checkpoints

I.B.1. Expression and function

Immune checkpoints are co-inhibitory receptors expressed during the activation of immune cells. They provoke the inhibition of the immune system, which is analogous to a negative feedback on the immune response. This physiological mechanism is crucial for the homeostasis of the immune system, especially to prevent auto-immune reactions.

PD-1, also known as CD274, is a protein encoded by the *PDCD1* gene and expressed at the surface of T cells during activation, and binding to its ligands PD-L1 or PD-L2 leads to the exhaustion of T cells.²⁹ The PD-1 pathway contributes to the homeostasis of the immune system under normal conditions, preventing T cell overstimulation leading to auto-immune disease. PD-L1 and PD-L2 are expressed by APCs and cancer cells.

CTLA-4 is another transmembrane protein expressed on the surface of T cells. It is also expressed upon activation and competes for the B7 receptor on APCs. Thus, the T cell coreceptor CD28 is no longer able to interact with B7 and T cells become exhausted.³⁰

Due to their immunosuppressive effect, immune checkpoints are targeted in cancer treatment, especially PD-1 and CTLA-4 on T cells.³¹ New anti-cancer treatments targeting immune checkpoints have been developed over the last 30 years.^{12,32,33} These immunotherapeutic treatments are aimed at increasing the detection and killing of tumor cells by the immune system through enhancing immune activation and tumor immune infiltration.

I.B.2. Treatment in cancer

New immunotherapies called immune checkpoint inhibitors (ICIs) have been developed during the last decade, which reverse the inhibition in immune cells and restore the antitumor immune response. The

ICIs currently used in clinics are listed in Table 1. They target T lymphocyte populations, and although PD-L1 is expressed on APC or tumor cells, the aim is to block its interaction with T cells. Other ICIs are under development, especially those that target macrophages as they have a phagocytic activity and antigen presentation capacity, which is beneficial for the antitumor immune response.³⁴

Targeted receptor	Molecule	Approved indications
		Advanced melanoma
CTLA-4	Ipilimumab	Advanced renal cell carcinoma
		Advanced colorectal cancer
		Melanoma
		Lung cancer
		Hodgkin lymphoma
		Renal cell carcinoma
	Nivolumab	Urothelial cancers
PD-1	Pembrolizumab Cemiplimab	Advanced colorectal cancer
PD-1		Hepatocellular carcinoma
		Head and neck squamous cell carcinoma
		B cell lymphoma
		Merkel cell carcinoma
		Esophageal and gastric adenocarcinoma
		Cutaneous squamous cell carcinoma
		Lung cancer
	Atezolizumab	Breast cancer
PD-L1	Avelumab	Renal cell carcinoma
	Durvalumab	Urothelial cancers
		Merkel cell carcinoma

Table 1: Immune checkpoint inhibitors and their current indications.³⁵

Furthermore, while ICIs have demonstrated remarkable efficacy compared with other therapies in multiple types of cancer, $^{36-41}$ a major disadvantage is their side effects in patients. Because ICIs target immune cells, they trigger immune-related adverse events (irAEs). Despite a similar to lower number of fatal irAEs compared with other anti-cancer treatments (0.3 to 1.3 % for ICIs, 0.9 % for platinum-based chemotherapy, and 4 % for VEGF-targeted therapy), ICIs induce a high number of grade \geq 3 irAEs (6 % of anti-PD-1-treated patients, 24 % of anti-CTLA-4-treated patients, and 55 % of patients with a combination of both). However, the occurrence of irAEs can also be correlated with the establishment of a proper immune response as well as serve as a biomarker of the antitumor immune response. 43,44

I.C. Resistance to immunotherapy

The discovery of ICIs was a breakthrough in cancer treatment. Yet, many patients do not respond to these immunotherapies due to *de novo* or acquired resistance mechanisms. Indeed, only 19–45 % of patients with melanoma and non-small-cell lung cancer respond to anti-PD-1 monotherapy, and 30 % of patients with melanoma who respond relapse over time.⁴⁵ Moreover, some types of cancers have a high rate of non-responder patients, such as metastatic castration-resistant prostate cancer and pancreatic ductal adenocarcinoma.⁴⁶

Resistance to ICIs can result from tumor-cell intrinsic factors, such as mutations during the cancer immunoediting phase (e.g., the loss of MHC-I molecules or absence of neo-antigens), 47,48 or from tumor-cell extrinsic factors, such as immune cells infiltrating the tumor micro-environment, such as T_{reg} , M2-macrophages, or MDSCs. Several tumor-cell extrinsic factors are described in the following paragraphs.

In most cancers, patients with a high tumor mutational burden exhibit high tumor T cell infiltration as well as an enhanced response to immune checkpoint blockade.^{49–51} Indeed, to obtain a good antitumor immune response, functional and activated immune cells are required in the tumor, such as effector CD8⁺ T cells. To achieve such tumor infiltration, CD8⁺ T cells require potent activation by DCs and an environment in which they do not become exhausted.¹² Therefore, tumors with a low mutational burden are often less infiltrated by immune cells and are called "cold tumor". The absence of immune infiltrate is a cause of resistance to ICI.⁵²

Angiogenesis is involved in resistance to ICIs as vessels are involved in immune cell trafficking. Indeed, the increase of pro-angiogenic factor VEGF signaling decreases CD8 $^{+}$ T effector cells and increases T_{reg} infiltration in tumors. The normalization of tumor vessels is associated with the resolution of immunotherapy resistance.

Furthermore, composition in the tumor microenvironment is a cause of ICI resistance. The secretion of molecules such as VEGF, TGF- β , and adenosine results in impaired T cell functions and immunosuppression. Moreover, the deprivation of some amino acids, such as tryptophan, or a lack of glucose lead to changes in the immunometabolism and the loss of T cell killing ability. 46

In addition, the gut microbiota also impacts the response to ICIs and therefore the appearance of resistance. Antibiotic usage prior to immunotherapy was found to modify the gut microbiota and induce resistance in patients with metastatic renal cell carcinoma who responded less to anti-PD-1 treatment.⁴⁶ This resistance can be abolished and the ICI response restored with fecal microbiota transplantation from immunotherapy responders.¹²

Although chemotherapy, radiotherapy, and surgery do not target the patient's immune cells, these treatments have an effect on the immune compartment.^{54–56} For instance, chemotherapy damages the peripheral immune system, which may be deleterious to anti-PD-1 therapy, but also increases the tumor infiltration of DCs, which is beneficial for immune checkpoint blockade.^{57,58} Therefore, their impact on the immune system must be considered – especially to overcome resistance – when they are used in combination with immunotherapies, such as ICIs, especially regarding the timing of treatment (i.e., neoadjuvant or concomitant treatments).

This list of causes of ICI resistance is not exhaustive,^{59–61} and new treatment combinations must be identified to restore the efficacy of ICIs in patients.

II. Renal cancer

II.A. The kidneys

II.A.1. Anatomy and histology of the kidneys

Each kidney is protected by the renal capsule, a fibrous connective tissue. The functional unit of the kidney is the nephron, which is a network of two separate fluid circulations integrated together, constituted of blood vessels around tubes that collect urine. Nephrons are located in the outer region of the kidney, which is called the cortex; however, some of them extend deep into the inner part, which is called the medulla. A nephron is composed of the corpuscle and collecting tubules, which start from the corpuscle by the proximal tubule, and continue with the loop of Henle, distal tubule, and connecting tubule before the collecting duct, which collects urine before the ureter. The anatomy of the nephron is detailed in the schema in Figure 2.

The corpuscle consists of the glomerulus and its capsule and contains a large network of capillaries. These blood vessels are formed of specialized fenestrated glomerular endothelial cells and perivascular epithelial cells, which are called podocytes. Podocytes wrap the capillaries and form a barrier with vessel endothelial cells as illustrated in Figure 2. This barrier is permeable to water and small molecules, both electrolytes and nonelectrolytes, crossing from the blood to the capsule due to blood hydrostatic pressure produced by heart beats.

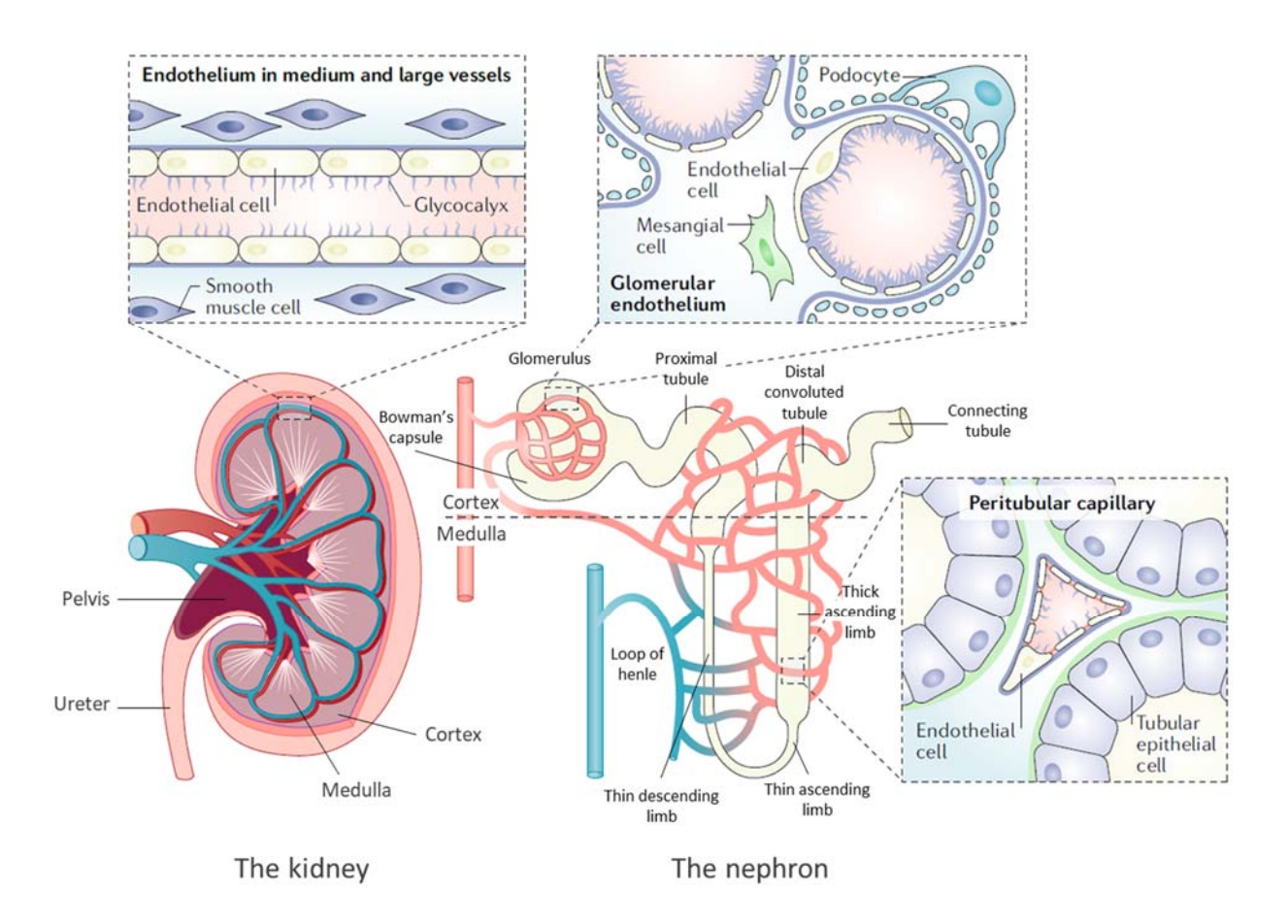


Figure 2: Anatomy of the kidney and the associated histology. Adapted from Jourde-Chiche et al, Nat. Rev., 2019.

II.A.2. Function of the kidney

The kidney is a well-irrigated organ as it receives 20–25 % of cardiac output, which represents 1 L/min of blood.^{66,67} The blood comes from the aorta and is filtered in the nephron. It coordinates several functions in the body, such as the detoxification of metabolic blood waste, in addition to secreting hormones involved in blood pressure, bone homeostasis, and erythropoiesis.^{65,68}

II.A.2.a. <u>Detoxification</u>

The nephron is composed of the corpuscle, where water and molecules are filtered out of the blood, and collecting tubules in which water and some salts are reabsorbed into the blood.

The filtration of blood in the glomerulus produces a fluid that contains water and electrolytic molecules, such as sodium, calcium, potassium, magnesium, phosphate, and bicarbonate, and also nonelectrolytic molecules, such as glucose, amino acids, urea, uric acid, and creatinine. In the subsequent tubules of the nephron, endothelial cells passively or actively reabsorb molecules and

water,⁶⁹ leading to the reabsorption of 99 % of the initially filtered fluid.⁷⁰ The molecules that are actively reabsorbed are sodium, potassium, calcium, phosphate, and uric acid, as the electrochemical gradient is the opposite of their transport.⁷¹ Urea, water, chloride, and some bicarbonate and phosphate are passively reabsorbed in the same direction as the electrochemical gradient.⁷⁰ The maintenance of the homeostasis of calcium, phosphate, and magnesium by the kidney is crucial as these molecules are second messengers for numerous signaling pathways and physiological events, such as bone formation.⁷¹ Proximal and distal tubule cells also secrete molecules of high molecular weight that are not filtered through glomerulus fenestrated vessels, or molecules in excess in the blood,⁶⁹ such as hydrogen, ammonia, or drug and chemical exogenous molecules. The excretion of hydrogen and the reabsorption of buffers from the urine allow a normal pH level to be maintained in the blood. The filtration function is quantified by the glomerular filtration rate, which is measured by the administration of a compound filtered by the glomerulus.^{72,73}

Kidney metabolism follows oscillations with lower activity during the rest phase of the day, which is aligned with the circadian rhythm explained in 1)III.B.2. Furthermore, 13 % of renal transcripts are rhythmically expressed during the circadian cycle, and some of them encode transport proteins such as water channel aquaporins. This explains why the excretion of water and molecules is decreased during inactive phases.⁷⁴

II.A.2.b. <u>Hormones secreted by the kidney</u>

The kidney regulates blood pressure and red blood cell production by secreting hormones and plays a role in the production of vitamin D.

Blood pressure is partly regulated by the kidney through the production of renin, which is a component of the renin-angiotensin-aldosterone system. Terminally, renin production leads to aldosterone release and an increase in blood pressure, which is explained in detail in the next section.⁷⁵

In the renal cortex, pericytes, which are components of blood vessels, produce erythropoietin. Erythropoietin is a cytokine that allows the differentiation and production of erythrocytes in the bone marrow. ⁷⁶ Hypoxia increases its secretion by renal pericytes, favoring red blood cell production by the bone marrow, leading to an increase of oxygen transport in the blood and thus the resolution of hypoxia. ⁷⁷ With their role in erythropoietin secretion and plasma volume regulation, kidneys are crucial for maintaining the hematocrit within a normal range.

In addition, the kidney is also involved in the production of vitamin D. Indeed, even though 25-hydroxyvitamin D is produced initially by the liver, the most active form (1,25(OH)₂D) is obtained after

hydroxylation by renal enzymes in tubules. The active form of vitamin D is crucial for calcium absorption and the effective homeostasis of osteoclasts in bones.⁷¹

II.A.2.c. Blood pressure regulation

Blood pressure is regulated by several hormones, one of which is produced in the kidney. In the distal convoluted tubule, the macula densa consists of 10–20 specialized epithelial cells in contact with cells from the blood vessels of the glomerulus, which are called juxtaglomerular cells. Both are components of the juxtaglomerular apparatus. Depending on the salt concentration in the urine, macula densa cells produce and send paracrine signals to the juxtaglomerular cells, which release renin. Renin is the first hormone of the renin-angiotensin-aldosterone system, which controls blood pressure. ^{62,78} It is an enzyme secreted in the blood that cleaves the hormone angiotensinogen, which is produced by the liver. As illustrated in Figure 3, cleaved angiotensinogen forms angiotensin I, which is converted into angiotensin II in the lung. ⁷⁹ Angiotensin II stimulates vasoconstriction and the production of aldosterone by the adrenal gland. Aldosterone is a mineralocorticoid that promotes the reabsorption of Na⁺ in the ascending limb of the loop of Henle, distal convoluted tubule, and collecting duct. ⁷⁰ The reabsorbed sodium generates an osmotic effect that causes the retention of water in the blood, which increases blood pressure. ⁸⁰ Therefore, renin secretion terminally produces increased blood pressure.

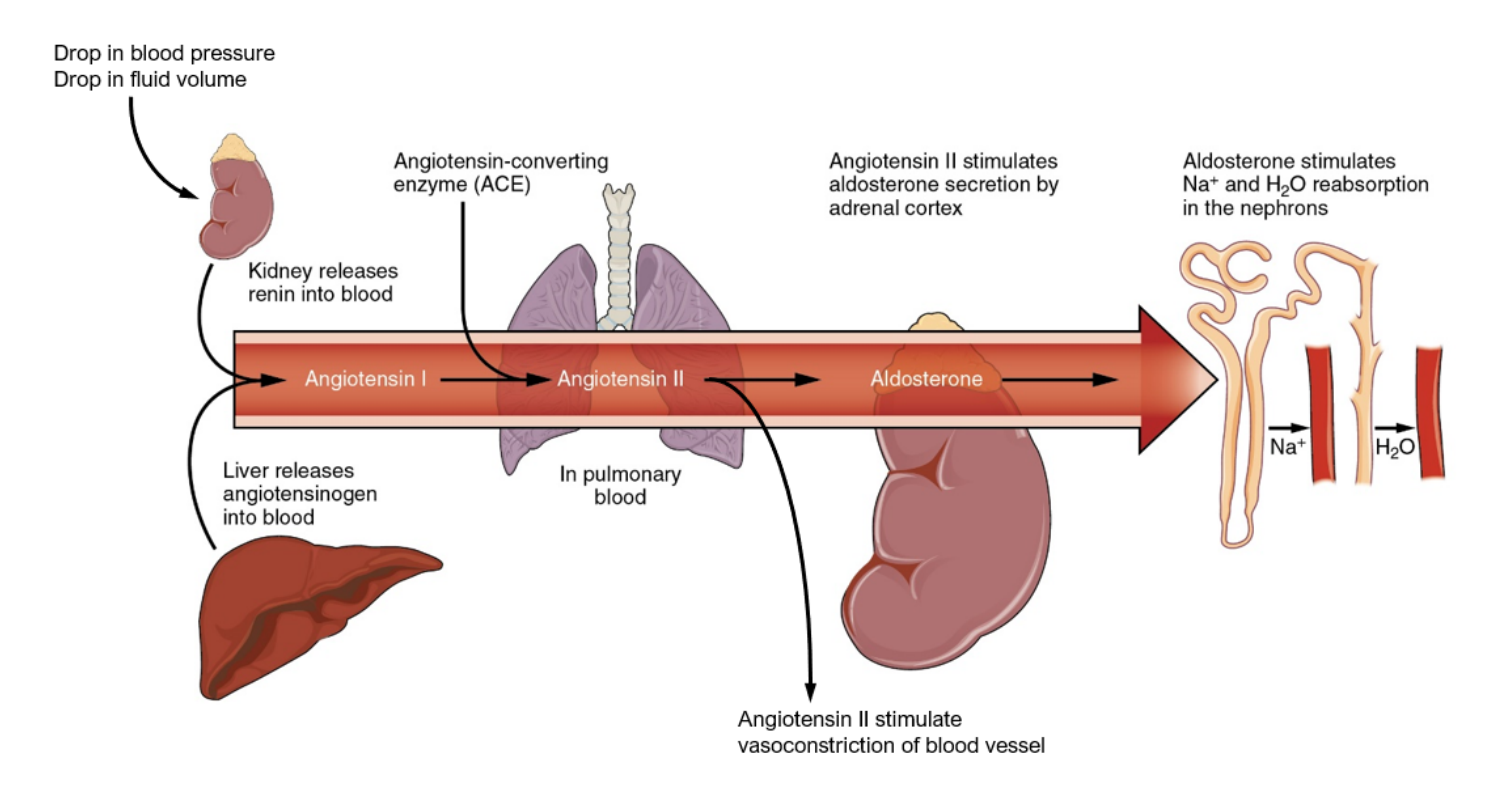


Figure 3: Renin-angiotensin system for the regulation of blood pressure. Adapted from Gordon Betts et al., Anatomy and Physiology, 2013.

II.B. Renal cell carcinoma

II.B.1. Classification and physiopathology

Renal cell carcinoma (RCC) is classified into the following three main types based on their histology:^{81,82} clear cell RCC (ccRCC), papillary RCC (pRCC), and chromophobe RCC (chRCC). ccRCC represents 75 % of RCC,⁸³ whereas pRCC and chRCC represent 15 % and 5 % of RCC, respectively.⁸⁴

Papillary RCC is further divided into two types. The less aggressive type 1 is characterized by an increase in signaling of the MET receptor tyrosine kinase, while the NRF2-antioxidant response element pathway is increased in type 2.85 Chromophobe RCC is the least aggressive form of RCC. Common mutations of the TP53 and mTOR pathway genes are found in 50 % of tumors, while the modification of the telomerase gene is found in 10 %.81 ccRCC is mainly characterized by the deletion or loss of function of the VHL tumor-suppressor gene.81 However, the mutation of this gene is not sufficient for triggering ccRCC formation. Papillary and chromophobe RCC have better prognoses than ccRCC, with only 7 % of chRCC patients developing metastasis disease83 compared with 30 % of ccRCC patients.86

The stages of renal cancer are classified through the tumor-node-metastasis (TNM) system for solid tumors. 82 This system considers the size of the primary tumor; the invasion in adjacent lymph nodes, renal vein, or adrenal gland; and presence of metastasis in other organs. Patients with RCC can be distributed into four stages with the TNM classification as described in Table 2. The Fuhrman grading system is also used to evaluate tumors in patients with RCC. It is based on the histology of the tumor and the presence of nucleoli in cell nuclei or multilobed nuclei. Although historically divided into four groups, studies have demonstrated that division into only two or three groups has as much statistical power in terms of patient survival prediction. 87

	T1: primary tumor confined to kidney < 7 cm
Stage I	NO: no metastasis in regional lymph nodes
	M0: no distant metastasis
	T2: primary tumor confined to kidney > 7 cm
Stage II	NO: no metastasis in regional lymph nodes
	M0: no distant metastasis
	T3: invasion of the primary tumor in peripheral tissues and veins without affecting the
Stage III	adrenal gland or renal fascia
	or N1: presence of metastasis in regional lymph nodes
	with M0: no distant metastasis

Stage IV	T4: invasion of the primary tumor in the adrenal gland or beyond the renal fascia
Stage IV	or M1: presence of distant metastasis

Table 2: ccRCC stages from the tumor-node-metastasis (TNM) classification

ccRCC and pRCC arise from epithelial cells of the proximal tubule of the nephron, while chRCC develops from intercalated cells of the distal tubule.⁸¹ However, this origin is not certain for ccRCC, as some expression markers could be explained by an origin from epithelial cells of the distal tubule,⁸⁴ even though they could be gained during the dedifferentiation of cells that occurs during tumorigenesis. ccRCC is a highly vascularized tumor and the preferential metastatic sites are the lung, liver, and bones. Histologically, it is defined by clear cytoplasmic cells due to a high accumulation of lipids and glycogen as illustrated in Figure 4.⁸⁸ However, ccRCC – and especially the metastatic stage of the disease – can present different histological features, such as eosinophilic cytoplasm.⁸⁹

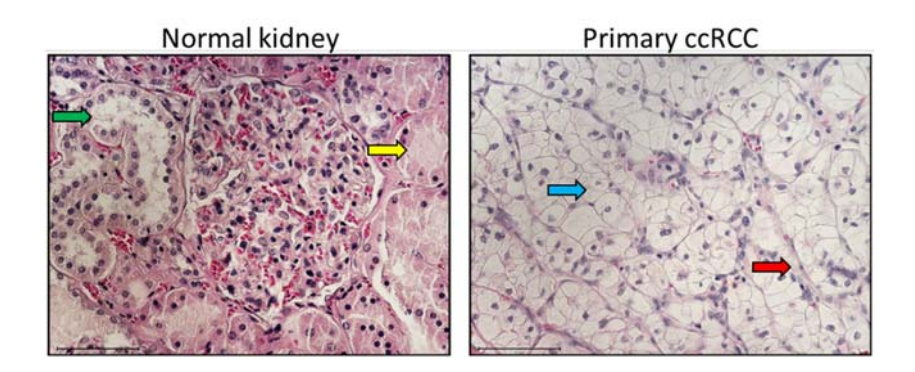


Figure 4: Section of normal kidney and primary ccRCC stained with hematoxylin and eosin. Normal structures of the glomerulus (yellow arrow) and tubule (green arrow) can be seen in the normal kidney and not in the ccRCC. Cells with large and clear cytoplasm are typical of ccRCC, with a distinct cell membrane (blue arrow) and infiltrated blood vessel (red arrow). Magnification: 40 X, scale bar: 75 µm. Sharma et al, J. Exp. Clin. Cancer Res., 2021

II.B.2. Molecular mechanisms

II.B.2.a. Von Hippel-Lindau pathway

In humans, the *von Hippel-Lindau* (*VHL*) tumor suppressor gene is located on the chromosome arm 3p. VHL is a cellular protein that is involved in the management of hypoxia and is a component of the ubiquitination complex involved in proteasome degradation.

II.B.2.a.i. The hypoxia pathway

The main actor of the hypoxia signaling pathway is hypoxia-inducible factor 1 (HIF-1), 90 which is a transcription factor constituted by two dimers, namely HIF-1 α and HIF-1 β . HIF-1 β is constitutively expressed and located in cell nuclei, while HIF-1 α is modulated by the oxygen level, located in the cytoplasm, and able to translocate into the nucleus. Under normoxic conditions, the presence of oxygen allows the hydroxylation of HIF-1 α , which is then sensitive to proteasome degradation. Under normal conditions, VHL protein binds to HIF-1 α to ubiquitinate it and send it for proteasome degradation. As HIF-1 α cannot translocate to the nucleus, heterodimers cannot interact together to act as a transcription factor. Under hypoxic conditions, VHL protein is not functional, and HIF-1 α is not hydroxylated nor ubiquitinated and can translocate into the nucleus to form a heterodimer with HIF-1 β , which acts as a transcription factor and regulates target genes.

II.B.2.a.ii. Vascular endothelial growth factor

One of the target genes of the HIF-1 pathway is the *vascular endothelial growth factor* (*VEGF*) gene. The VEGF family includes five proteins in mammals, which bind to three transmembrane tyrosine kinase receptors. VEGF-A is the main pro-angiogenic cytokine in adults and can be produced by fibroblasts and immune cells, but also some tumor cells. VEGF-A binds to its receptors – VEGFR-1 or VEGFR-2 – and triggers signaling pathways that lead to angiogenesis, cell migration, and vascular permeability.

II.B.2.a.iii. Mammalian target of rapamycin pathway

The PI3K/Akt/mTOR pathway (phosphoinositide 3-kinase, serine/threonine kinase Akt, mammalian target of rapamycin) can be activated through several signals, including metabolic inducers such as glucose or amino acids, but also through growth factors and their tyrosine kinase receptor. Activation of the mTOR pathway leads to the inhibition of apoptosis, promotion of cell proliferation, and angiogenesis through increases in the HIF-1 α level and VEGF-A production. The VHL pathway is connected to the mTOR pathway through the interaction of VHL with the mTORC1 subunit RAPTOR. This interaction inhibits the pathway as RAPTOR cannot form mTORC1 complex.

II.B.2.b. Von Hippel-Lindau gene mutation

While ccRCC has a low tumor mutation burden, some specific mutations are observed in tumors. The most common mutation is the functional biallelic inactivation of the *VHL* gene, which occurs in more than 90 % of ccRCC cases, most commonly through the loss of the 3p chromosomic region.^{81,84} Additionally, the 3p chromosomic region includes three other genes that are commonly mutated in ccRCC, namely polybromo 1 (*PBRM1*), SET domain-containing 2 (*SETD2*), and BRCA1-associated protein 1 (*BAP1*),⁸¹ which are three proteins involved in chromatin remodeling. *VHL* inactive mutation or

deletion leads to the activation of HIF- 1α and the mTOR pathway. As previously explained, the activation of HIF- 1α and the mTOR pathway directly or indirectly leads to a high production of VEGF and enhances angiogenesis and cell proliferation. This explains the high vascularization of ccRCC tumors.

II.B.3. Immune infiltration

ccRCC tumors are highly immune infiltrated, with an average of 30 % of cells in the tumor being immune cells. ^{96,97} The tumor microenvironment in ccRCC is more immune infiltrated than in a normal kidney, ⁹⁸ with mainly T lymphocytes, even though the mutational burden is low and there is a heterogeneous macrophage population. ^{96,99,100} It is also the cancer type that is the most infiltrated in T cells in TCGA cohorts. ⁹⁷ However, unlike most solid tumors, tumor immune infiltration in ccRCC is not correlated with a good prognosis in patients. Moreover, a high number of CD8⁺ T cells – which are normally tumor cell-killing T cells but can become exhausted – correlates with late-stage and poor overall survival, especially in male ccRCC patients. ⁹⁹ It seems that high T_H17, M1 macrophages, and DC infiltration are correlated with a good prognosis in patients, who benefited from immune checkpoint blockade, ¹⁰¹ whereas T_H2, T_{reg} or M2, or naïve macrophage infiltration is associated with a poor prognosis. ⁹⁷

Moreover, VEGF pathway activation, which is a key in ccRCC tumor progression, also plays a role in immune compartment development such as DC or T cells.¹⁰² VEGF-A inhibits NF-κB through VEGFR-1 in DCs and prevents their maturation. Moreover, in the presence of IL-4 and IL-10, VEGF-A promotes the M2 polarization of macrophages.¹⁰³ It enhances the expression of immune checkpoints in CD8⁺ T cells, such as CTLA-4 or PD-1, through VEGFR-2 signaling.¹⁰⁴ VEGF interferes with the homing and circulation of immune cells through the downregulation of CXCL10 and 11 (chemokines necessary for T cell recruitment) and the chemoattraction of myeloid cells, such as M2-macrophages, MDSCs, and monocytes.^{105,106}

II.B.4. Epidemiology

In 2020, RCC accounted for 2.2 % of all cancers worldwide.¹⁰⁷ Patients are often diagnosed unexpectedly during unrelated imaging scans because the disease stays asymptomatic; therefore, one-third of patients are diagnosed at metastatic stages. Moreover, the survival prognosis is highly dependent on the stage: Patients in stage I, in which the tumor is localized, have a 5-year survival rate of 93 %, whereas patients with a metastatic disease in stage IV only have a 5-year survival rate of 12 %.⁸³

II.B.4.a. Sex-biased effect in clear cell renal cell carcinoma

A sexual dimorphism exists in cancer development and treatment response. In renal cancer, the age-standardized rate was twice as high in men than in women in 2020 for incidence and mortality. ¹⁰⁷ However, several analyses of gender-related differences in the efficacy of immune checkpoint blockade in metastatic ccRCC patients have produced controversial data. Some analyses have demonstrated that men have a significantly reduced risk of death compared with women with immune checkpoint blockade treatment, while others have not demonstrated any significant differences between men and women. ^{108–111} In melanoma and non-small-cell lung cancer, women seem to have a better overall survival rate than men; however, they benefit less from immunotherapy than men. ¹¹²

RCC has higher incidence and mortality rates in men than in women, 113 which could be explained by a protective role of female hormones in RCC growth and survival. Indeed, several studies have indicated an impact of the age of the first menarche, first delivery, use of contraceptive therapies, or hysterectomy on the risk of RCC. 108,113 However, despite a potential protective role of female hormones, the obtained results have not all been statistically significant and consistent. 114 Nevertheless, RCC cells express more estrogen receptor β than breast cancer cells and its activation inhibits RCC cell proliferation and increases apoptosis. 115 Moreover, more than 50 % of tumors express the androgen receptor, and no difference in expression exists between women and men. This expression is associated with worse prognosis and more aggressive features. 116

In addition, the interrelation of steroid pathways also leads to sex differences in ccRCC development. ccRCC tumors express, from the highest to the lowest level, mineralocorticoid, glucocorticoid, androgen, estrogen, and progesterone receptor. The most potent androgen, dihydrotestosterone, can bind to the glucocorticoid receptor, which can regulate androgen receptor target genes and promote RCC cancer cell growth. This is a potential mechanism for explaining the higher risk of ccRCC in men. Moreover, the expression of the isoform estrogen-receptor- β leads to an antitumor effect, which could also partially explain the difference of incidence rates in ccRCC in favor of women.

II.B.4.b. Risk factors in clear cell renal cell carcinoma

In addition to the sexual dimorphism, several factors increase the risk of ccRCC development. Age is a critical risk factor as the risk of mutation increases with time. As in several other types of cancer, smoking and a high body mass index increase the risk of RCC (relative risk [RR] for ccRCC = 1.5 for current smokers and 1.8 for obese people). Moreover, diet, drug use, and exposure to chemicals increase the risk of ccRCC development, which is because the kidney is involved in the detoxification of all hazardous exogenous molecules from the body. The kidney is a highly vascularized organ, and an increase in blood pressure can damage the glomerulus and the capsule in the nephron; therefore, hypertension increases the risk of RCC (RR = 2.3-2.4 in Europeans). Metabolic syndrome, especially

due to insulin resistance caused by type 2 diabetes, is also an independent risk factor, with the stage of ccRCC (odds ratio = 4.028),¹¹⁸ mortality, and incidence of ccRCC being higher in patients with metabolic syndrome than those of other patients. In patients with RCC, obesity has a detrimental effect on the anti-PD-1 treatment response, which is in opposition to the obesity paradox that occurs in some cancer types, such as melanoma; that is, while obesity increases the risk of cancer development, obese patients respond better to immune checkpoint blockade than non-obese patients.¹¹⁹ However, obesity seems to be beneficial to RCC patients during targeted therapies, such as VEGF inhibitors. These studies must be confirmed in RCC to obtain a clear consensus regarding obesity's effect on therapeutic responses.¹¹⁹

Prognostic factors can be determined for metastatic RCC patients using the International Metastatic RCC Database Consortium risk calculator. This tool stratifies patients into good and bad prognosis groups depending on their daily life abilities, time from diagnosis to treatment, line of treatment currently used, hemoglobin, neutrophils, platelets, and calcium levels.

II.B.5. <u>Treatment of clear cell renal cell carcinoma</u>

In this section, ccRCC treatments are described; however, treatment plans follow the same approach in pRCC and chRCC. Depending on the stage of the disease, patients will receive more or less aggressive treatments, but treatment plans usually start with surgery followed by tyrosine-kinase inhibitor alone or in combination if metastasis is present. Surgical resection of the kidney is the main first-line treatment in ccRCC. Nephrectomy can be partial in some patients, but most of the time surgeons perform simple or radical nephrectomy, which consists of removing the kidney, adrenal gland, surrounding fat, and adjacent lymph node. However, 30 % of patients with a localized tumor who received a nephrectomy eventually relapse and develop metastasis. 124

II.B.5.a. Targeted therapies

Before 2000, due to ccRCC chemotherapy and radiotherapy resistance, the recommended treatment was cytokines, such as IL-2 and interferon, which had efficacy in almost 10 % of patients but severe side effects, such as cardiac and respiratory toxicity. From the 2000s onwards, new treatments called targeted therapies started to be used as the standard of care in ccRCC: tyrosine kinase inhibitors (TKIs) have been developed, targeting angiogenesis through VEGFR inhibition, as well as inhibitors of the mTOR pathway, and used in the treatment of metastatic disease.

As VEGF promotes angiogenesis in tumors, ccRCC is a highly vascularized tumor and can be sensitive to therapies that inhibit pro-angiogenesis factors or receptors. Mechanism of action of these therapies is described in Figure 5. The treatments used in clinics target the VEGF receptor through the inhibition

of the tyrosine kinase subunit of the receptor, such as sunitinib or axitinib, but also through the direct inhibition of VEGF-A, such as bevacizumab, which is a neutralizing antibody of VEGF. Other growth factor receptors with tyrosine kinase activity can be targeted, such as AXL, c-MET, PDGF-R, or FGF-R, due to their upregulation under VEGF signaling and/or their positive effect on tumor invasion, proliferation, and survival. Moreover, resistance to VEGFR inhibition can be overcome by targeting several receptors, such as the mechanism of action of cabozantinib, which is an inhibitor of several tyrosine kinase receptors, such as VEGFR, AXL, and c-MET. VEGF pathway inhibition leads to the normalization of tumor vascularization, a rise in tumor hypoxia, and an increase in the number of tumor-infiltrating immune cells. Moreover, as the inactivation of VHL increases the mTOR pathway and favors tumor proliferation, mTOR inhibitors are used in ccRCC treatment management. These molecules are from the same family as rapamycin, such as the everolimus.

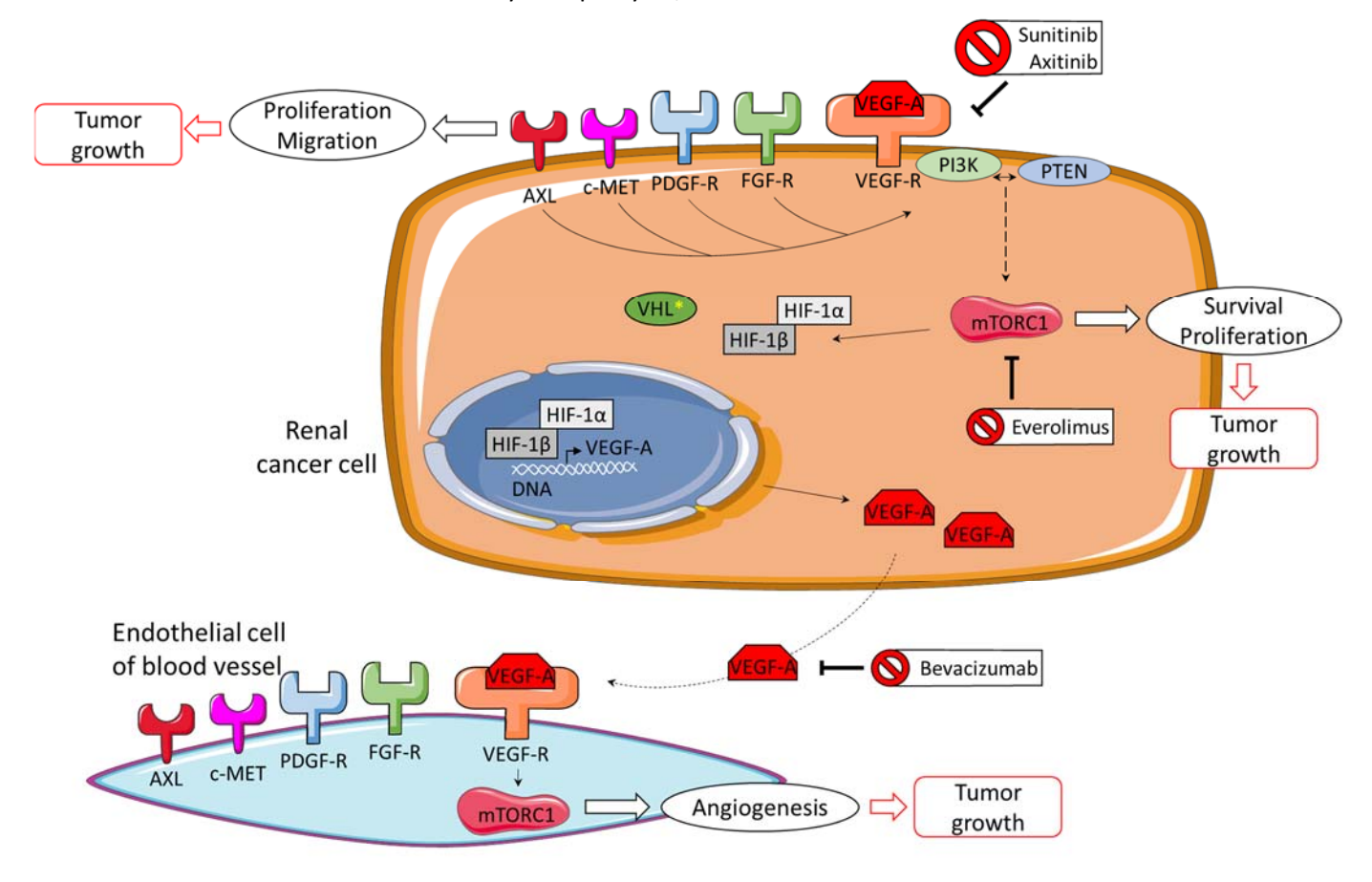


Figure 5: Pathways and current drugs in metastatic renal-cell carcinoma. Adapted from Choueiri and Motzer, N. Engl. J. Med., 2017.

II.B.5.b. Immunotherapies

When ICIs was approved in the clinic for several solid tumors, the standard of care for ccRCC changed drastically. It is a cancer known to be sensitive to ICIs, and these molecules, such as anti-PD-1 or anti-CTLA-4, can be used alone or in combination with other therapies. Anti-CTLA-4 is indicated in ccRCC,

but the most commonly used immunotherapies target PD-1 and PD-L1. 99 Since 2018, some combinations of ICIs and TKI have been used as the first-line treatment for metastatic ccRCC, such as anti-PD-1 pembrolizumab with TKI against VEGFR axitinib. $^{102,125-127}$ Moreover, the inhibition of the VEGF pathway increases T cells' infiltration into the tumor and decreases the immunosuppressive microenvironment with the inhibition of T_{reg} and MDSC, 126 which could improve the efficacy of immune checkpoint blockade. To select the proper treatment, physicians consider the risk of the patient, which they assess using the stage, size, grade, and necrosis (SSIGN) score using the TNM classification and histology of the tumor. The guidelines recommended by the ESMO committee are presented in Figure 6 for first-, second-, and third-line treatments. 128

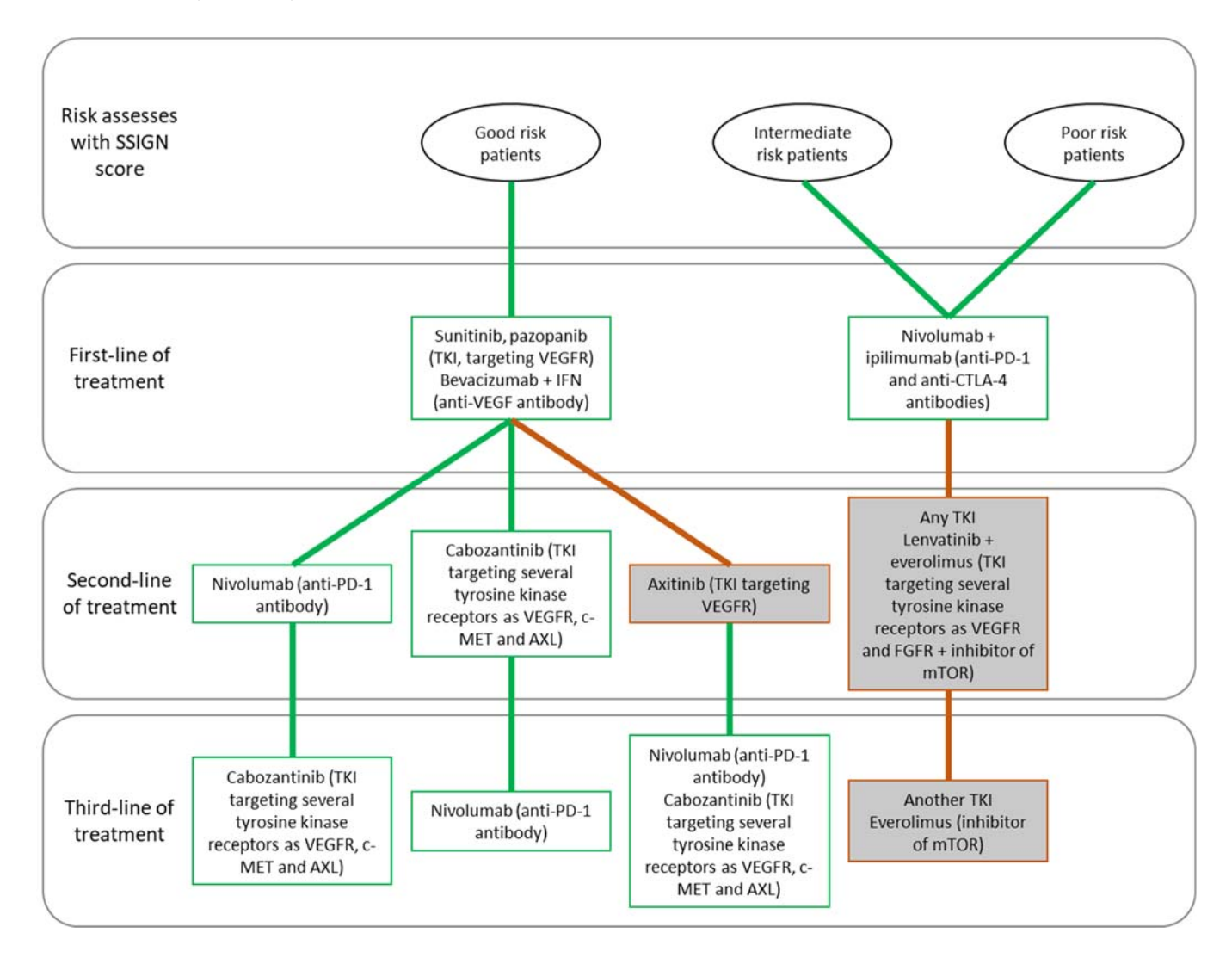


Figure 6: Algorithm for treatment choice in ccRCC. The treatment is chosen depending on the line of treatment, risk of the patients, and availability of treatment. Box outlined in green: standard of care; box outlined in orange: options if standard of care is not available. SSIGN score: stage, size, grade, and necrosis score. Adapted from Escudier et al, Ann. Oncol., 2019.

II.B.5.c. Resistance

Inhibiting the HIF pathway with VEGF inhibitors or the mTOR pathway can lead to the inhibition of ccRCC progression during the first months of treatment. However, patients who respond first can develop adaptive resistance to these targeted therapies. While the arrival of ICIs has drastically increased the efficacy of ccRCC treatment in recent years, some patients exhibit primary resistance and acquired resistance. Indeed, the combination of anti-PD-1 and TKI (pembrolizumab + axitinib) had an overall response of 55 % in untreated metastatic ccRCC, and anti-PDL-1 (nivolumab) in second-line treatment had a 25 % overall response. Thus, a need exists for new treatments to overcome these resistances, especially adjuvant treatments. To find new treatment strategies, we must first understand the origins of these resistances. Some of them are detailed in the following paragraphs.

Immune cells that infiltrate ccRCC are mainly immune suppressive cells, such as myeloid-derived suppressor cells or exhausted T cells expressing PD-1, which inhibit the antitumor response. 125 Moreover, the epithelial-mesenchymal transition is a crucial factor in the development of metastasis, and it is increased through HIFa pathway activation, which favors the loss of epithelial cell adhesion molecules and increases tumor cell dissemination. ¹²⁴ The endothelial compartment also plays a critical role in treatment resistance; indeed, tumor endothelial cells can be modified by reactive oxygen species and VEGF expressed in the tumor microenvironment. This leads to its role of immune regulator with increased infiltration of immune suppressive cells rather than effector cells. 124 This could explain why patients who do not respond to nivolumab treatment have a higher endothelial compartment in the tumor microenvironment than those who respond to immune checkpoint blockade. 96 Hypoxia can induce resistance due to the production of an acidic environment - which favors the immune suppressive phenotype of immune cells – as well as its effect on the expression of immune checkpoints. Indeed, hypoxia, mainly through HIFa, increases the expression of PD-L1 and VISTA, another immune checkpoint, on myeloid cells (MDSCs, DCs, and macrophages), leading to the inhibition and exhaustion of T effector cells. The acidic environment also directly inhibits T cell proliferation and activation as well as promotes tumor-associated macrophages, Treg, and hypoxic MDSCs, which are more immunosuppressive. 124

The anti-angiogenic treatments used to reduce the blood supply to tumors can also lead to secondary hypoxia. Hypoxia increases the expression of the P-glycoprotein membrane exporter, which is a protein implicated in the drug efflux that decreases the level of TKI inhibitors inside the cells.¹²⁴

Therefore, one of the trails followed to overcome RCC resistance is to combine immune checkpoint blockade together, with or without TKI, despite the high toxicity observed.

II.B.5.d. Biomarkers

To ensure accuracy in the prognosis and treatment choice for patients, research is being conducted on new biomarkers in ccRCC, since none are currently validated and used in clinical settings. Despite PD-L1 expression in 25 % of ccRCC tumors, it has no predictive role in patient outcomes. Several proteins are under investigation, such as the ubiquitin conjugating enzyme E2 C, for which a high expression promotes the proliferation and migration of cancer cells in ccRCC, thus predicting poor prognosis in patients. Opa interacting protein 5 expression correlates with immune infiltration in ccRCC and is a negative prognostic marker; thus, its oncogenic role needs to be examined precisely. Insulin growth factor-like receptor 1 is expressed in T cells and has a high expression associated with high myeloid-derived suppressor cell infiltration in ccRCC, which is an indicator of poor prognosis in patients.

Immune infiltration is also a biomarker of good or bad prognosis in ccRCC as well as a marker for predicting anti-PD-1 immunotherapy response. However, as explained in 1)II.B.3, strong immune infiltration is not correlated with a good prognosis in patients with ccRCC. The presence of different immune cells in the tumor can interfere in the treatment response as well as tumor growth. Gene signatures are under investigation for predicting prognosis and immunotherapy response, such as the immune-related prognostic differential gene signature, ¹⁰¹ which considers the expression of immune genes, such as WNT5A, IL4R, and genes expressed by cancer cells or stromal cells.

II.C. Clear cell renal cell carcinoma models

II.C.1. Cellular model used in research

Several cell lines have been derived and designed to study RCC *in vitro*, especially resistances to treatment. Different human cell lines are used in research to study ccRCC.¹³² The ones most commonly used are listed as follows:

- A-498 is a *VHL*-mutated cell line used to study ccRCC; however, some studies have discussed its ccRCC origin and demonstrated a more papillary origin.
- 786-O also does not express functional VHL, enhancing the HIF and VEGF pathways, leading to a ccRCC model.
- Caki-1 cells do not express a wild-type VHL protein but produce a high amount of VEGF and form tumors with a clear cell histology in mice. They are used as a metastatic ccRCC model.
- Caki-2 cells express wild-type VHL protein. It is a tumor cell line originally from a primary kidney tumor usually used as a ccRCC model, although it exhibits more characteristics of pRCC.

In a mouse model, the cell line most extensively used as a syngeneic model for mimicking ccRCC is the Renca cell line, which comes from a spontaneous renal adenocarcinoma of Balb/c mouse. Despite a

VhI deletion, Renca cells do not recapitulate all of the common ccRCC mutations observed in humans. Indeed, unlike in humans, *VhI*, *Pbrm1*, *Setd2*, and *Bap1* are not localized on the same chromosome in mice; therefore, *VhI* deletion does not lead to mutations in the other genes. However, *VhI* deletion does lead to increases in HIF-1 α and VEGF in the same way as in human ccRCC.¹³³

II.C.2. *In vivo* models used in research

To study the tumor microenvironment's components, several in vivo tumor models have been developed through implanting tumor cells in naïve mice or spontaneously forming tumors in genetically engineered animals. The easiest model to implement is the ectopic injection of Renca cells subcutaneously into the flank of mice, which generates a localized solid tumor. This is an extensively used model due to convenience during injection and tumor measurement. However, this simple model does not recapitulate the main characteristics of human ccRCC, such as the vascularization and tumor microenvironment found in the kidney as well as metastases development. ¹³⁴ Orthotopic models are also used to study ccRCC. Renca cells are then injected under the kidney capsule or directly into the kidney, allowing the development of a primary renal tumor and metastases in the lung, lymph nodes, liver, and peritoneum. Both of these orthotopic models demonstrate a progressive tumor growth in the kidney and spontaneous metastasis formation. The contralateral kidney does not develop metastases, preventing death due to renal failure. The subcapsular injection allows a slow growth with the detection of a tumor after 7-10 days, whereas direct injection into the kidney is more rapid in tumor progression but less invasive during injection as it does not require suturing. These orthotopic models allow the primary localized tumor as well as early- and late-stage metastases to be studied with nephrectomy, mimicking the human disease history. 134 Renca cells can also be injected intraperitoneally or intravenously to generate metastatic models in the peritoneum or lung. However, these models do not recapitulate the human RCC as there is no kidney tumor, even though they are used to study treatment against metastases in RCC.¹³⁴

To generate a model as similar as possible to the human disease, several genetically engineered animals have been produced. However, none of them recapitulate all of the characteristics of human RCC, despite a clear gene mutation origin in human patients. Considering that the mutation of the *VHL* gene is one of the main drivers of ccRCC in humans, complete *vhl* knockout (KO) has been performed in zebrafish. This deletion generates abnormalities in the proximal tubules of the kidney, leading to ccRCC but also an early death for an unknown reason. Because of this premature death, this model can only be used for early-stage ccRCC. Moreover, the total inactivation of *Vhl* in mice is lethal during development. Therefore, several models have been generated with the conditional deletion of *Vhl*, whether in proximal or distal tubular epithelial cells or collecting duct cells. Nevertheless, none of these

mouse models have exhibited ccRCC formation despite the presence of several anomalies, especially clear cells and cysts. 129 These results indicate that vhl mutation is lethal or insufficient for generating ccRCC in zebrafish or mouse models, and contributions from other oncogenes or tumor suppressor genes might be necessary for kidney tumorigenesis. As two of the most well-known tumor suppressor genes, PTEN and TP53, are often mutated in cancers, the mutation of Pten and VhI or Tp53 and VhI, have been trialed but they do not mimic patients. Indeed, the first combination does not lead to ccRCC formation, while the second is not similar to the molecular features found in patients, even though it leads to tumorigenesis in the kidney. As already mentioned, in human ccRCC, VhI deletion can lead to Pbrm1, Setd2, or Bap1 mutation due to their close location on the chromosome 3, but not in mice as they are not on the same chromosome. Therefore, genetically engineered mice with mutations of these genes and Vhl could be a relevant model for ccRCC. The simultaneous deletion of Vhl and Pbrm1 as well as the deletion of Vhl and only one allele of Bap1 (Bap1 deficiency is lethal in mice) have been performed.¹³⁶ These mice developed cysts and tumors in their kidneys, mimicking the main features of human ccRCC at the cellular and molecular levels as they presented an increase in HIF target gene expression and mTOR signaling as in human patients. 129

III. Glucocorticoids: Origin and biological activity

III.A. Steroidogenesis

Steroids hormones are composed of three main families, namely mineralocorticoids, glucocorticoids, and sex hormones, ¹³⁷ all of which are produced from cholesterol. As Figure 7 indicates, steroidogenesis starts with the steroidogenic acute regulatory protein (StAR), which transports cholesterol from the outer to the inner mitochondrial membrane. In the inner mitochondrial membrane, cholesterol is converted into pregnenolone, the precursor of all steroids. 138 CYP11A1 converts cholesterol into pregnenolone in a reaction that is limiting for the rest of the steroidogenesis (Figure 7). 139 Several subsequent enzymatic reactions by cytochromes P (CYP) and hydroxysteroid dehydrogenases (HSD) produce mineralocorticoids, glucocorticoids, and sex hormones. Aldosterone is the main mineralocorticoid that plays a role in the renin-angiotensin-aldosterone system, which was previously explained in 1)II.A.2.c. Glucocorticoids are composed of cortisol and corticosterone as the active compounds and cortisone and 11-dehydrocorticosterone (11-DHC) as their inactive forms. They can be inactivated or reactivated through enzymatic reaction by HSD11B1/2. In humans, the predominant compounds are cortisol and cortisone, whereas they are corticosterone and 11-DHC in rodents. The sex hormones are estrogens in females, such as estrone and estradiol, and androgens in males, such as dehydroepiandrosterone and testosterone.

Steroidogenesis occurs in the adrenal gland, but also in peripheral organs for terminal enzymatic reactions, such as the kidney for glucocorticoids, testicles for androgens, and ovaries for estrogens. These hormones circulate freely or are bound to proteins such as glucocorticoids, which are 90 % bound to corticosteroid-binding globulin or albumin. Only 5–10 % of free plasmatic glucocorticoids are bioavailable for the targeted tissues and cells.

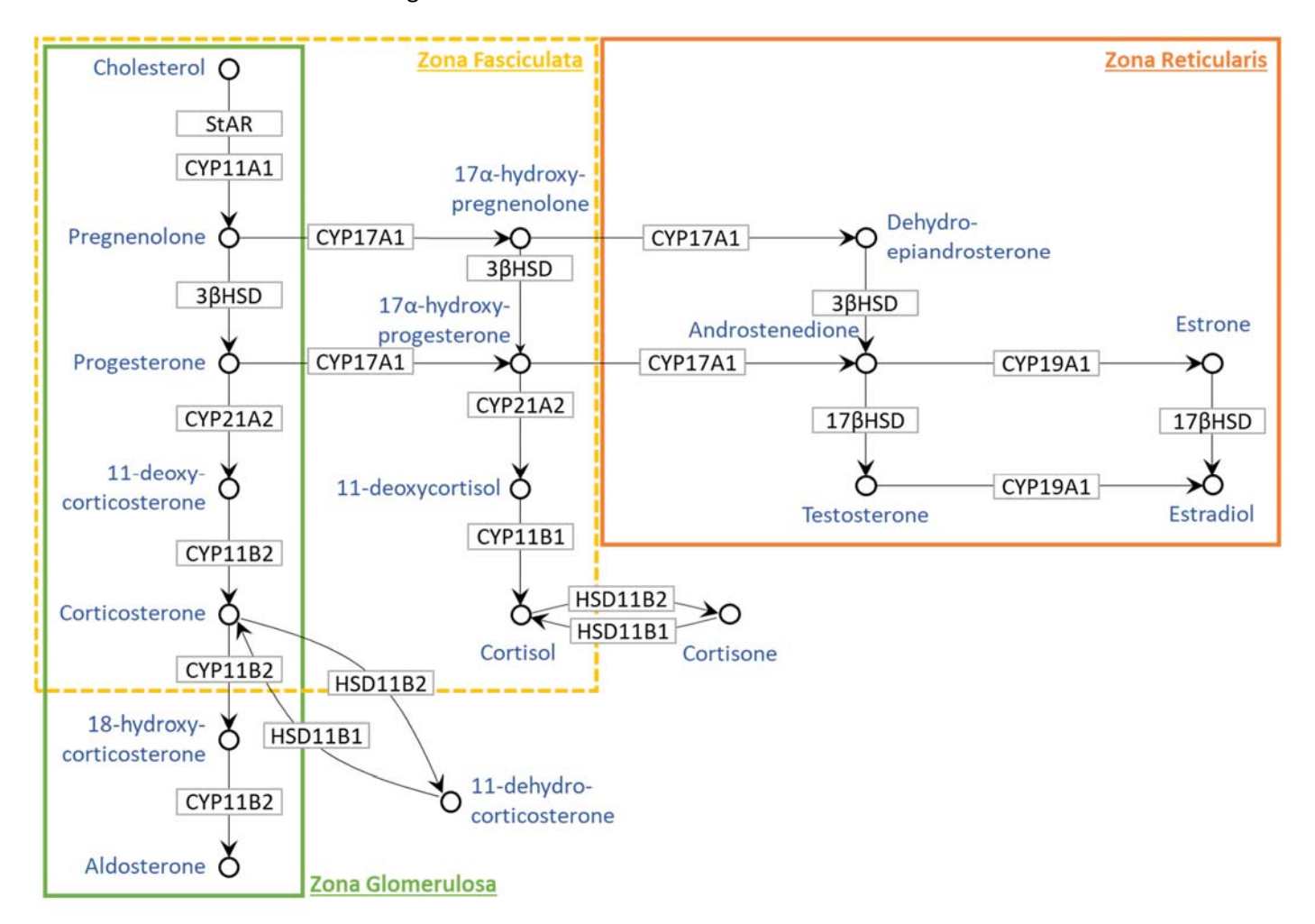


Figure 7: Steroidogenesis pathway that occurs in the adrenal gland and its spatial localization.

III.B. Hypothalamic-pituitary-adrenal axis

Glucocorticoid secretion follows a cycle throughout the day called the circadian cycle. The hypothalamic-pituitary-adrenal (HPA) axis controls the release of cortisol by the adrenal gland.

III.B.1. Anatomy

The HPA pathway involves several hormones that are produced in different organs: the hypothalamic paraventricular nuclei, the anterior pituitary, and the adrenal gland. The hypothalamic paraventricular nuclei are part of the hypothalamus and are connected to the anterior pituitary at the base of the brain. Adrenal glands are located above the kidneys and consist of three layers that produce

steroids.¹⁴¹ As schematized in Figure 7, the external zona glomerulosa synthetizes mineralocorticoids; the zona fasciculata, in the middle, produces glucocorticoids; and the internal layer, called the zona reticularis, produces sex hormones.

III.B.2. Hormone secretion and circadian cycle

In physiological conditions, stress stimuli such as hypoglycemia, or activity signals provoked by the release of vasopressin hormone, lead to the activation of the HPA axis, which regulates glucocorticoid secretion.¹⁴² The HPA axis is also stimulated by external stress stimuli, such as infections, which increase pro-inflammatory cytokines secreted by immune cells.¹⁴³

First, the hypothalamic paraventricular nuclei produce corticotropin-releasing hormone (CRH), which then activates the release of adrenocorticotropic hormone (ACTH) from the anterior pituitary. Finally, ACTH promotes glucocorticoid secretion from the adrenal gland into the blood circulation. In Glucocorticoids have a negative feedback effect on the HPA axis. Moreover, a high concentration of glucocorticoids inhibits CRH secretion by the hypothalamic paraventricular nuclei, decreasing the stimulation on the adrenal gland and thus glucocorticoid production. This negative feedback of glucocorticoids on the HPA axis is not through a direct effect of the glucocorticoid receptor on CRH transcription, but rather because of modulations of several signaling pathways in CRH-producer neurons, which are not yet completely understood. In Indiana I

Humans are diurnal, meaning that their activity period is during the day. Thus, their plasmatic glucocorticoids increase in the morning to reach a peak, and then decrease in the afternoon to reach a nadir at night. Add Rodents have an opposite circadian cycle as they are nocturnal animals.

Aldosterone synthesis is also increased upon ACTH stimulation in the adrenal gland; thus, its concentration increases under stress conditions. Physiologically, its production is increased by angiotensin II signaling and mainly regulated at the level of CYP11B2, the last enzyme of its metabolism as illustrated in Figure 7.

III.A. Glucocorticoid signaling

III.A.1. Glucocorticoid receptor

III.A.1.a. Expression

The *NR3C1* gene encodes the glucocorticoid receptor (GR), which belongs to the same nuclear family receptor as the other steroid receptors. It is constituted of a DNA binding region, a ligand binding domain, and dimerization contact regions in between two transactivation domains.¹⁴⁷ The GR ligand-binding domain, which forms an internal pocket, accepts endogenous glucocorticoids such as cortisol

or corticosterone or exogenous glucocorticoids such as dexamethasone. The classical GR α isoform, which is ubiquitously expressed, binds glucocorticoids and mediates most of their effects. The GR β isoform acts as a dominant negative and does not bind ligands but rather inhibits GR α 's effects on reducing the glucocorticoid effect, especially in immune cells.¹⁴⁸ In the kidney, GR is particularly expressed in the proximal tubules and the glomeruli, while in ccRCC tumors, a high expression correlates with a less aggressive cancer.¹¹⁴

III.A.1.b. Activity, target genes, and effects of the glucocorticoid receptor

The GR is located in the cell cytoplasm, where it is bound to heat shock proteins, restraining the receptor into the cytoplasm in the absence of glucocorticoids. The binding of the ligand into the ligand-binding-domain pocket induces a change in conformation of the GR as well as the dissociation of heat shock proteins. GR can dimerize and translocate from the cytosol to the nucleus. ¹⁴⁹

The activation of GR triggers two separate pathways – namely the non-classical pathway, which involves the activation of kinases, and the classical signaling pathway, which leads to the modification of the transcription. The non-classical signaling pathway of the GR involves non-genomic activity, such as activation in the cytosol of the kinase signaling pathway, ¹⁴⁰ and leads to fast signaling. ¹³⁷ In the classical signaling pathway, the GR can bind specific DNA sequences in the promoter regions of its target genes. These DNA regions are called glucocorticoid response elements and are DNA consensus sequences. DNA tethering of the GR induces a modification of conformation, dependent of the DNA consensus sequence, allowing the recruitment of other transcription factors and activator or repressor proteins. ¹⁴⁰ In addition to DNA binding, GR activity involves protein-protein interactions between the nuclear receptor and other transcription factors, impacting the transcription of genes that do not contain GRE. ¹⁴⁸ The regulation of steroid receptor activation is mainly caused by pre-receptor regulation with the modulation of ligand availability. ¹⁵⁰ Acquired resistance to glucocorticoids appears because of the downregulation of GR expression, but also because of the abrogation of GR dimerization without an impact on the expression level. ¹⁵¹

GR signaling plays a role in several physiological functions that are important during the entire life course. For instance, during fetal development, glucocorticoids are particularly critical for the maturation of organs, especially in the lungs for the establishment of proper respiration. Indeed, GR signaling leads to the maturation of specialized lung cells producing surfactant. Moreover, glucocorticoids are known to inhibit the immune response and have an anti-inflammatory effect, and they are used therapeutically for this purpose.

The regulation of the immune response through GR signaling involves interactions with AP-1 and NFk-B, two transcription factors involved in immune cytokine expression, and inhibits their effects. ¹⁵² The

GR can also bind to glucocorticoid response elements in the DNA promoter region of pro-inflammatory immune genes and decrease their transcription by preventing the fixation of NF κ -B. Overall, GR signaling decreases pro-inflammatory immune gene transcription, such as IL-2, IL-1, TNF- α , and MHC type I and promotes the transcription of immune checkpoints, such as PD-L1, ^{152,153} and anti-inflammatory genes, such as IL-10 and TSC22D3 (GILZ). ¹³⁷

III.A.2. Mineralocorticoid receptor

The mineralocorticoid receptor is another steroid receptor to which aldosterone can bind. Similar to the GR, the mineralocorticoid receptor is a nuclear receptor located in the cytosol, and it translocates in the nucleus to act as a transcription factor upon ligand binding and dimerization. An inactive mineralocorticoid receptor is bound to cytosolic chaperon proteins, which are consequently dissociated from the conformational change that occurs during ligand binding. Moreover, the mineralocorticoid receptor can heterodimerize with the GR, which is broadly expressed in the kidney. The mineralocorticoid receptor is expressed in aldosterone-target cells, such as in the distal part of the nephron, the loop of Henle, distal tubules, and collecting ducts of the nephron, the loop of Henle aldosterone pathway.

The mineralocorticoid receptor has structural similarities with the GR, leading to an equivalent affinity of glucocorticoids and aldosterone for the mineralocorticoid receptor. Thus, the mineralocorticoid receptor can be activated by glucocorticoids in most cells as its concentration is higher than aldosterone. The signaling through aldosterone binding occurs in cells that express HSD11B2, which can inactivate glucocorticoids, as explained in Figure 8.

In aldosterone-sensitive cells, mineralocorticoid receptor activation produces non-genomic as well as genomic effects. Non-genomic effects are fast and include calcium transfer and the generation of reactive oxygen species through NADPH oxidase, which are necessary for vasoconstriction and ion homeostasis in the kidney. Genomic effects lead to the modulation of target-gene transcription, such as the ionic membrane transporter. ¹⁵⁶

The mineralocorticoid receptor is also involved in non-aldosterone-sensitive cells. For instance, it can regulate inflammation through its expression in macrophages, as demonstrated in cardiac fibrosis. ¹⁵⁷ Moreover, mineralocorticoid signaling has been detected in neurons of the hypothalamic paraventricular nuclei and the hippocampus. ^{150,155} This expression in these cells is involved in the control of the HPA axis, and the possibility of heterodimerization with the GR could play a role in the regulation of the circadian rhythm; however, the mechanism is yet to be completely elucidated. ^{155,158,159}

III.A.3. Interrelation between glucocorticoids and sex steroid pathways

Crucial differences are observed between men and women in their response to glucocorticoids. Men have a higher basal glucocorticoid level and exhibit a stronger increase in glucocorticoid levels in response to psychological stress than premenopausal women. Moreover, exogenous glucocorticoid treatment leads to a shorter decrease in pro-inflammatory cytokines in women than in men. Indeed, women are known to have a more reactive immune system than men, which correlates with a higher prevalence of auto-immune diseases in women and a higher susceptibility to infections for men. Indeed,

Several mechanisms can explain the sex differences in glucocorticoid response, such as the sex dimorphism of enzymes producing glucocorticoids or the cross-talk between sex hormones and glucocorticoid receptor (GR) signaling.

The enzymes involved in glucocorticoid synthesis are sexually dimorphic. HSD11B1 and HSD11B2, which are direct producers of glucocorticoids (Figure 7), are less expressed in females than males.

Indeed, estrogen downregulates HSD11B1 expression, leading to a lower glucocorticoid production in females than in males in cells involved in estrogen and glucocorticoid production, such as adipocytes.

Moreover, the expression of CYP11A1 and CYP17A1, which are involved at the beginning of glucocorticoid synthesis (Figure 7), decreases with estrogen exposition. These decreases lead to a reduction of cortisol production, as one study demonstrated in a zebrafish model.

166

In addition to sex differences in the expression of glucocorticoid producer enzymes, the glucocorticoid signaling pathway is connected to sex hormones. First, glucocorticoids regulate other steroids, such as estrogen production, by enhancing the activity of aromatase P450, which produces estrogen from androgens in adipose tissue. ¹⁶⁷ However, while they increase estrogen production, glucocorticoids also inhibit estrogen receptor signaling by antagonizing the receptor or binding target gene promoters. ^{168,169} This antagonism leads to a displacement of estrogen receptors away from their response element on DNA. Conversely, estrogen receptors inhibit the GR's function through the post-translational modification of the receptor. ¹⁷⁰ Moreover, heterodimerization of the GR leads to the regulation of different target genes than monomer or homodimers, and a ligand-bound GR can be dimerized with other steroid receptors, such as mineralocorticoid receptors ¹⁵⁰ or androgen receptors. ¹⁷¹ Finally, receptors for glucocorticoids, mineralocorticoids, and sex hormones have similarities in the tertiary structures of their ligand-binding domain, ¹⁴⁷ allowing conformationally similar ligands to bind with different affinities, as presented in Table 3. This table presents the ranking of steroid affinities for the different steroid receptors. As the values of each affinity vary between sources, only an overall ranking is described without dissociation-constant values.

Receptor	Affinity
GR	Dexamethasone > Cortisol/corticosterone > Aldosterone > Estradiol ≈ Progesterone ≈
	Testosterone
MR	Aldosterone ≈ Cortisol/corticosterone ≈ Progesterone > Dexamethasone > Estradiol ≈
	Testosterone
AR	Testosterone >> Estradiol ≈ Progesterone > Dexamethasone ≈ Cortisol/corticosterone >
	Aldosterone
ER	Estradiol >>> Aldosterone ≈ Dexamethasone ≈ Cortisol/corticosterone ≈ Progesterone ≈
	Testosterone
PR	Progesterone >> Estradiol > Testosterone ≈ Aldosterone > Dexamethasone ≈
	Cortisol/corticosterone

Table 3: Ranking of steroid affinity for steroid receptors. AR: androgen receptor, ER: estrogen receptor, GR: glucocorticoid receptor, MR: mineralocorticoid receptor, PR: progesterone receptor.

Interrelations in these steroid pathways lead to several effects on physiological functions, such as the immune response. Signaling through glucocorticoid, progesterone, and androgen receptors mainly results in anti-inflammatory effects, whereas signaling through estrogen receptors leads to pro- or anti-inflammatory effects, depending on the receptor isoforms and estrogen doses. Glucocorticoid receptors can bind progesterone, leading to a repression of cyclooxygenase 2 and an inhibition of the NFĸ-B pathway.¹⁷⁸ Cyclooxygenase 2 is an enzyme that produces prostaglandins and is known to increase inflammation, which induces a decrease in pro-inflammatory cytokines.^{164,179} Despite mutual inhibition between the GR and the estrogen receptor, some evidence exists of co-operation between these two nuclear receptors for the inhibition of pro-inflammatory proteins, such as CD69 or IL-6, for enhancing an anti-inflammatory context.¹⁶⁹

III.B. Production of glucocorticoids in peripheral organs

The 11β -hydroxysteroid dehydrogenases type 1 and 2 (HSD11B1 and HSD11B2) are isozymes involved in the activation and inactivation of intracellular glucocorticoids in peripheral, non-adrenal organs. ¹⁸⁰

III.B.1. <u>11β-hydroxysteroid dehydrogenases type 1</u>

HSD11B1 is a 34 kDa protein located in the membrane of the endoplasmic reticulum, with its active enzymatic site in the lumen of the organelle as illustrated in Figure 8. It is encoded by the *HSD11B1* gene on chromosome 1 in humans and mice. 180

HSD11B1 acts mainly as a reductase to produce active glucocorticoids (cortisol and corticosterone) from inactive glucocorticoids (cortisone and 11-DHC) using NADP(H) as a co-factor. HSD11B1 closely

interacts with hexose-6-phosphate dehydrogenase (H6PDH), another transmembrane protein of the endoplasmic reticulum that produces the NADP(H) required for its reductase activity. In the absence of NADP(H), HSD11B1 can also act as a dehydrogenase and produce ketone. The substrates of HSD11B1 dehydrogenase are cortisol, corticosterone, and some synthetic glucocorticoids such as prednisolone. The dehydrogenase activity has been described in enzymatic assays lacking NADP(H) as a co-factor; however, *in vivo*, HSD11B1 mainly exerts a reductase function.

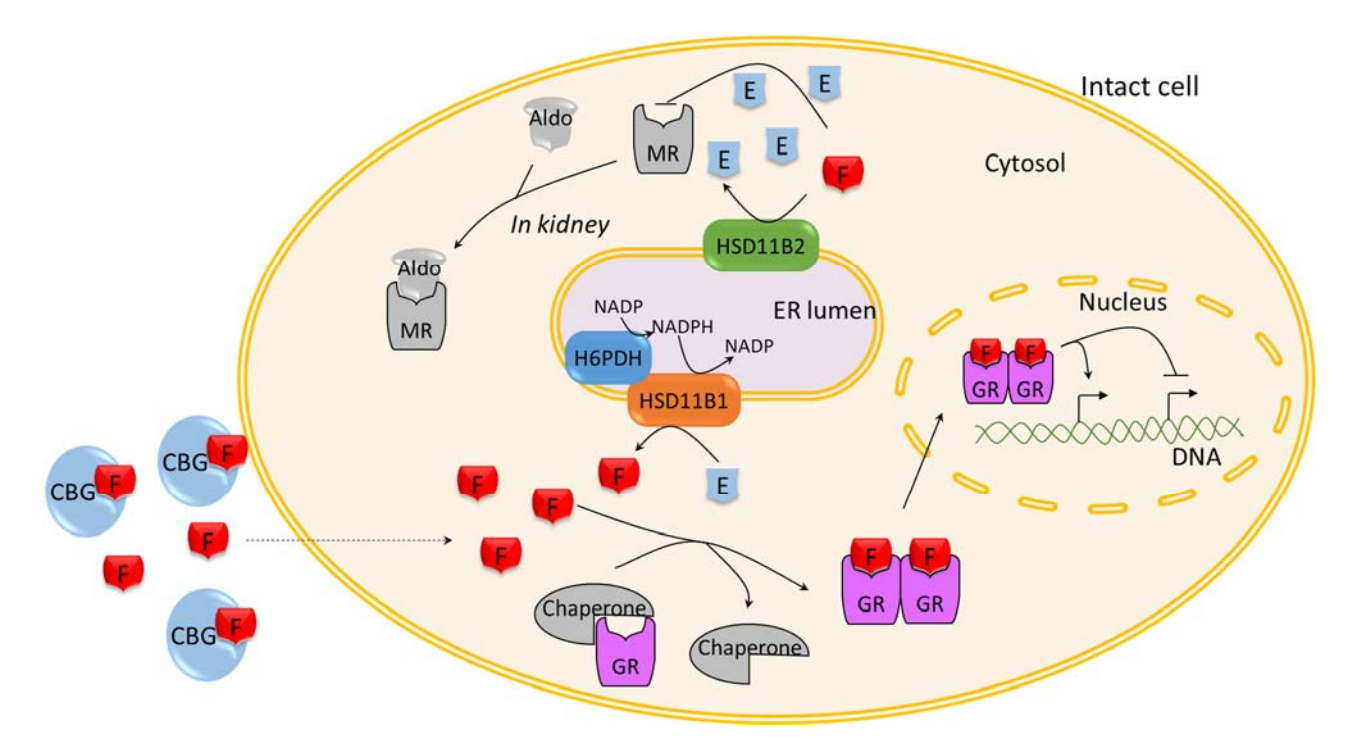


Figure 8: Glucocorticoid pathway in peripheral organ cells. Aldo: aldosterone, DNA: deoxyribonucleic acid, E: cortisone or 11-DHC, ER: endoplasmic reticulum, F: cortisol or corticosterone, GR: glucocorticoid receptor, HSD11B1/2: 118-hydroxysteroid dehydrogenases 1/2, H6PDH: hexose-6-phosphate dehydrogenase, MR: mineralocorticoid receptor, NADP/H: nicotinamide adenine dinucleotide phosphate. Adapted from Chapman, Holmes and Seckl, Physiol. Rev., 2013.

HSD11B1 is ubiquitously expressed and its activity regulates many physiological functions, such as systemic glucocorticoid levels, angiogenesis, the HPA axis, adipogenesis, and the immune response.

The liver is the organ that expresses the highest level of HSD11B1 and generates 20-40 % of the total daily glucocorticoid production, ¹⁸⁰ independently of the HPA axis. Thus, the systemic amount of endogenous glucocorticoids depends on not only adrenal production but also the peripheral activity of HSD11B1.

Furthermore, HSD11B1 can inhibit angiogenesis *via* its activity in endothelial cells and macrophages. ¹⁸¹ Enhancing HSD11B1 expression in vascular endothelial cells decreases angiogenesis. ¹⁸² Macrophages

are also particularly crucial for the formation of new vessels,¹⁸³ and the KO of *HSD11B1* in this cell type enhances angiogenesis.¹⁸³ The anti-angiogenic effect of HSD11B1 is also due to its inhibitory role in pro-angiogenic factors. For instance, IL-1, a major pro-angiogenic cytokine, is downregulated by HSD11B1-produced glucocorticoids. However, HSD11B1 does not have any effect on VEGF-A, the main pro-angiogenic growth factor, as its expression was not modified in *Hsd11b1*-/- mice, although an increase in angiogenesis was observed in them.¹⁸⁴

Moreover, the expression of *HSD11B1* in the central nervous system¹⁴⁴ participates in the regulation of systemic glucocorticoid amounts by the HPA axis. An increase in glucocorticoid levels enhances the transcription of the *HSD11B1* gene, which is regulated by the GR, resulting in a higher intracellular concentration of glucocorticoids. The increase of glucocorticoid production by HSD11B1 in neurons is crucial for the negative feedback loop of glucocorticoid signalization. Indeed, it increases the glucocorticoid amounts directly in the neurons, which induces CRH downregulation and ultimately inhibits glucocorticoid adrenal production.¹⁸⁵

In addition, HSD11B1 is involved in the regulation of metabolic homeostasis. It regulates adipogenesis, as was demonstrated in *HSD11B1* KO mice that were resistant to diet-induced obesity. The expression of HSD11B1 in adipocytes increases their differentiation and adipogenesis as well as the formation of white adipose tissue. In addition, HSD11B1 expression in adipocytes is enhanced by insulin, which is often over-secreted in metabolic syndrome, maintaining adipogenesis dysregulation. HSD11B1 inhibition reduces risk factors in metabolic syndrome, such as the cardiovascular risk of obese patients. Drugs targeting HSD11B1 in this indication have been developed to reduce metabolic disorders in patients (as detailed in 1)III.D.2.b.i).

Lastly, the immune response can be modulated by HSD11B1 activity through its expression in immune cells. HSD11B1's effects on immune cells during the immune response are explained in the next section (1)III.C).

III.B.2. 11β-hydroxysteroid dehydrogenases type 2

HSD11B2 is a 42–44 kDa cytosolic protein anchored in the endoplasmic reticulum membrane and encoded by the *Hsd11b2* gene in chromosome 16 in humans and chromosome 8 in mice. ^{180,189} Its expression is more restricted than that of its isozyme HSD11B1, as it is only expressed in the kidney, colon, some parts of the brain, and placenta, but not in immune cells. HSD11B2 acts as a dehydrogenase in the same proportion as its isozyme HSD11B1. As Figure 8 indicates, HSD11B2 inactivates cortisol and corticosterone into cortisone and 11-DHC with the cofactor NAD⁺. ¹⁸⁰

Furthermore, HSD11B2 activity is important for several physiological functions in adults as well as during development. A critical function is the regulation of aldosterone signaling. The mineralocorticoid receptor has a similar affinity for active glucocorticoids (cortisol or corticosterone) as it does for aldosterone, 150 but its affinity for inactive glucocorticoids (cortisone or 11-DHC) is low. As HSD11B2 transforms active into inactive glucocorticoids, the intracellular level of the active form decreases and the mineralocorticoid receptor is less bound by glucocorticoids. Therefore, the mineralocorticoid receptor is free to bind aldosterone. Despite a higher concentration of glucocorticoids than aldosterone in the blood, it is the intracellular steroid concentration that is decisive in determining which steroid will bind the mineralocorticoid receptor. In this context, the presence of HSD11B2 allows the mineralocorticoid receptor to be protected from glucocorticoids and the possibility of aldosterone binding. 150 Thus, the co-expression of HSD11B1/2 enzymes, which regulate the amounts of intracellular glucocorticoids, with the mineralocorticoid receptor, affects its specific activity.¹⁵⁴ For instance, in the distal nephron, where aldosterone regulates salt-water homeostasis, HSD11B2 and the mineralocorticoid receptor are co-expressed, allowing a binding of aldosterone to its receptor.¹⁵⁴ Moreover, in some parts of the brain, such as the paraventricular nucleus cells, HSD11B2 is expressed at a low level. 190,191 In these cells, mineralocorticoid receptor signaling leads to increased activity of the sympathetic system, such as cardiac activity. HSD11B2 allows this signaling to be regulated through aldosterone binding and not glucocorticoids. ¹⁹⁰ In some patients, the mutation of HSD11B2 leads to severe hypertension due to glucocorticoid-induced activation of the mineralocorticoid receptor. 192

Moreover, HSD11B2 is particularly important during fetal development,¹⁹³ especially in the placenta and the brain of the fetus. Early exposure to glucocorticoids could affect the maturation of organs of the embryo and decrease the birth weight of the baby.¹⁸⁰ However, they are necessary for the late maturation of organs, such as the liver and lungs. Indeed, at the end of pregnancy, glucocorticoid exposure allows the maturation of specialized lung cells, which produce surfactant.¹⁹⁴ Thus, HSD11B2 is particularly expressed in the placenta to inactivate active glucocorticoids coming from the mother before the embryo.¹⁹⁵ At the end of pregnancy, HSD11B2 expression decreases and HSD11B1 expression begins, allowing maturation through the glucocorticoid exposure of organs, such as the lungs. HSD11B2 is also particularly expressed in the brain of the fetus.¹⁹¹ Brain cells in development are sensitive to glucocorticoids, which lead to the defective differentiation of neurons. Indeed, repeated therapeutic administration of glucocorticoids during pregnancy prevents the maturation of astrocytes and cell junctions in the brain of the fetus.¹⁹⁶ Moreover, during pregnancy, the consumption of glycyrrhetinic acid, an HSD11B2 inhibitor present in licorice, leads to cognitive disorders and

hyperactivity of the HPA axis in children. ¹⁸⁰ Therefore, *HSD11B2* expression and its timing are particularly crucial during fetal development.

III.C. Glucocorticoid pathways and the immune system

As described in 1)III.A.1.b, glucocorticoids have an effect on immune genes through binding to the GR, inhibiting inflammation, and decreasing the activation of immune cells. Glucocorticoids also modulate the differentiation and polarization of immune cells.

III.C.1. Effects of glucocorticoids on immune differentiation

Glucocorticoid signaling is involved in the activation of myeloid cells, such as neutrophil activation, ¹⁹⁷ macrophage polarization, or DC maturation. 198 HSD11B1 is dynamically expressed during the polarization of naïve macrophages into M1 macrophages. 143 Then, glucocorticoids can be reactivated by HSD11B1, leading to an anti-inflammatory phenotype that drives a fast resolution of inflammation. 143 Macrophages from mice that lack Hsd11b1 in myeloid phagocytes exhibit a faster polarization into M2 macrophages than macrophages from WT mice. 183 These changes in macrophages are caused by the change in the intracellular level of glucocorticoids and not the modification of the plasma level. 183 Knowing that M2 macrophages are known to be involved in angiogenesis and HSD11B1 promotes an M1 phenotype in macrophages, 199 HSD11B1-produced glucocorticoids impair the homeostasis of angiogenesis through their effects in macrophages. This has also been demonstrated in Hsd11b1 KO mice that display a pro-angiogenic context. 181,183,184 Through the inhibition of macrophage maturation, glucocorticoids induce decreases in IFN-y and IL-12 secretion, which are cytokines produced by M1 macrophages and DCs. Glucocorticoids are also involved in the maturation of DCs, which leads to the downregulation of IFN-y and IL-12 secretion in particular. Moreover, HSD11B1 increases during the maturation of DCs, and its activity is especially increased following an innate immune signal but not after adaptative immune activation. ¹⁹⁸ Thus, an innate immune response leads to an increase of HSD11B1-produced glucocorticoids and decreases of IFN-y and IL-12 secretion by DCs, preventing T_H1 polarization and inducing a tolerogenic phenotype in T cells.

Glucocorticoids are also critical during thymic T cell development and T cell polarization. The GR is expressed in all T cells and glucocorticoids are produced de novo in the thymus by the thymic epithelial cells and T cells, which express HSD11B1 and CYP11A1. 137,139,140 GR activation induces the apoptosis of T cells in both negative and positive selections in the thymus. 169 Moreover, the glucocorticoid pathway is involved in the polarization of T cells, 140,180 and T cell subpopulations have different sensitivities to glucocorticoids. Glucocorticoid signaling leads to the strong inhibition of $T_{H}1$ and moderate inhibition of $T_{H}2$ but permits the development of $T_{H}17$. Furthermore, it induces a loss of the anti-apoptotic

protein BCL-2 in T_H1 cells, thereby promoting their apoptosis, whereas BCL-2 is increased in T_H17 by IL-17 signaling, which is enhanced by glucocorticoids. In secondary lymphoid organs, GR activation in T cells promotes T_{reg} differentiation with the activation of the transcription factor TSC22D3 (GILZ), which induces $TGF-\theta$ receptor and FOXP3 expression, a receptor and a transcription factor that promote T_{reg} differentiation. In the secondary lymphoid organs, GR activation in T cells promotes T_{reg} differentiation.

III.C.2. Effects of glucocorticoids on immune activation

Immune activation is a dynamic process that induces an increase of HSD11B1-produced active glucocorticoids, especially in immune cells. It is inhibited by GR signaling, leading to the resolution of the immune response. The modulation of the immune response through glucocorticoids occurs in both lymphoid and myeloid cells.

In lymphoid cells, *HSD11B1* expression is increased by pro-inflammatory cytokine signals and during TCR activation in T cells. ¹⁸⁰ GR activation leads to an inhibition of co-stimulatory receptor expression, such as *CD28* and pro-inflammatory cytokines, and induces the expression of immune checkpoints, such as *PDCD1* (PD-1), *CTLA*-4, and *TIM3*. ¹⁴⁰

In myeloid cells, HSD11B1 is expressed during inflammation in neutrophils and DCs, leading to the production of active glucocorticoids. However, *HSD11B1* is also a target gene of glucocorticoids, which increase its expression, amplifying the effects of active glucocorticoids and inhibiting inflammation.¹⁹⁷ This dynamic increase of intracellular glucocorticoid amounts due to HSD11B1 in myeloid cells leads to a modulation of the immune response.¹⁹⁷ Glucocorticoid signaling inhibits DC activation with the downregulation of MHC type II, co-stimulatory proteins, and cytokines. Moreover, the expression of *TSC22D3* (GILZ) is induced by glucocorticoids in DCs and represses the transcription of immune genes, leading to a tolerant phenotype that impairs the inhibition of tumor growth.²⁰⁰ GR activation also decreases the *CD11B* expression of neutrophils, which is an important integrin involved in migration into inflamed tissues.¹⁹⁷

Overall, glucocorticoid signaling, especially via intracellular HSD11B1-produced glucocorticoids, induces an autocrine feedback in immune cells, acting as an immune checkpoint and allowing inflammation to be controlled. 180,197

III.C.3. Effects of the circadian cycle on immune cells

Through the circadian cycle, the plasmatic glucocorticoid level is modulated, which particularly affects T cell trafficking. Lymphocytes migrate from the blood to lymphoid tissues where they can be activated by APCs. This T cell trafficking fluctuates over 24 h, with the lymphocytes being located more in the lymphoid tissues during the active period and more in the blood during the low-glucocorticoid

period.¹⁴⁰ In T cells, glucocorticoids enhance IL-7R transcription, leading to an IL-7 driven CXCR4 expression, which is a surface chemokine receptor leading to migration into lymphoid tissues. Therefore, glucocorticoid circadian fluctuation leads to the rhythmic expression of CXCR4 on the T cell surface.^{201,202} This effect of the circadian cycle impacts the resolution of inflammation depending on the timing of the immune challenge. Indeed, during the active period, T cells are located in the lymphoid tissues ready to be activated; therefore, an infection that occurs during this period will be resolved faster than that in periods in which T cells are in the blood.^{201,202}

III.D. Glucocorticoids in cancer

III.D.1. Link between cancer and glucocorticoids

III.D.1.a. Therapeutic glucocorticoid use with immunotherapy

In the clinic, synthetic glucocorticoids are used as anti-inflammatory treatment for their immune inhibitory effects through steroid receptors. In cancer treatment, glucocorticoids are especially administered to manage side effects during immunotherapy. This usage raises the problem of damping the immunotherapy response due to systemic immunosuppression provoked by glucocorticoids. Several studies have demonstrated that glucocorticoids have a negative effect on patients' survival if the treatment is administered before the immune checkpoint blockade. However, the use of glucocorticoids to manage side effects due to immune checkpoint blockade does not impair the clinical benefit of immunotherapy. In some cases, patients need to receive glucocorticoids before immunotherapy, such as in the case of intracranial metastasis for reducing brain edema. Then, anti-CTLA-4 can be used as an ICI to reduce glucocorticoids' negative effect on the immune system. Indeed, dexamethasone, a synthetic glucocorticoid, increases the expression of CTLA-4 in T cells, which can be reversed with CTLA-4 blockade, unlike PD-1 blockade.

Overall, the timing of glucocorticoid treatment is crucial for avoiding the detrimental effects of their immunosuppression on the immune checkpoint blockade response.²⁰⁷ Indeed, the antitumor immune response seems to follow glucocorticoid administration if it was initiated before glucocorticoid treatment.²⁰⁷

III.D.1.b. Endogenous glucocorticoids

Much evidence exists to support the involvement of GR activation and endogenous glucocorticoid production in tumor and metastasis development.²⁰⁸

The expression of GR in tumors was associated with poor prognosis in patients, late stages of cancer, and a higher risk of relapse compared with patients with low GR tumor expression in epithelial ovarian

cancer and ER⁻ breast cancer.^{209,210} Furthermore, GR inhibitor treatment in a pancreatic cancer model promoted tumor immune infiltration and increased the immune checkpoint blockade response.¹⁵³ Moreover, the expression of the GR in some cancer cells (pancreatic, prostate, or breast) increased the level of transcription factors involved in the epithelial-mesenchymal transition, leading to the intravasation of cancer cells and metastasis formation.¹⁵³

In addition, the increase of circulating endogenous glucocorticoids caused by psychological stress suppressed the immunogenic effect of chemotherapies, which was restored with the use of a GR antagonist. On Moreover, psychological stress increases TSC22D3 expression in mouse DCs. TSC22D3 (GILZ) is a glucocorticoid-induced protein that interacts especially with NFK-B, which drives the tolerogenic phenotype in DCs and the induction of T_{reg} through FOXP3 expression, thereby decreasing the antitumor immune response. This was confirmed by the KO of TSC22D3 in DCs or the inhibition of the GR, which increased the immunogenicity in the tumor.

Furthermore, glucocorticoid variations caused by the circadian rhythm affect metastasis formation in breast cancer. ²¹¹ During low glucocorticoid periods (e.g., sleep), circulating tumor cells express more mitotic genes and perform more intravasation into the blood or lymphatic vessels than during the active phase of the day, leading to the generation of metastases. ²¹¹ Moreover, chronic disruptions to the circadian cycle, such as working night shifts, enhance the ability of breast cancer cells to form metastases. ²¹² This abnormal glucocorticoid variation promotes the epithelial-mesenchymal transition of cancer cells and decreases the efficacy of the antitumor immune response. ²¹²

Finally, intra-tumoral glucocorticoid synthesis promotes tumor progression. *HSD11B1* is expressed in breast cancer cells, and its inhibition represses metastasis propagation.²¹³ Immune cells that infiltrate the tumor also produce steroids, which promote an immunosuppressive tumor microenvironment. Deleting *CYP11A1* from T cells increases the number of pro-inflammatory cells infiltrating the tumor, such as M1 macrophages or non-exhausted T cells,¹³⁹ thereby increasing the antitumor immune response.

Thus, the production of glucocorticoids (adrenal and intra-tumor steroid biosynthesis) and GR activation are detrimental to a proper antitumor immune response. Inhibition of the pathway could reverse this immunosuppression, leading to an enhanced antitumor immune response.

III.D.2. <u>Inhibition of the glucocorticoid pathway in patients</u>

III.D.2.a. Glucocorticoid receptor inhibitors

Since glucocorticoid signaling is involved in cancer progression, GR inhibitors could reduce tumor growth. Several GR inhibitors, whether specific or not to the receptor, are being studied as cancer treatments in clinical trials.

RU486 (mifepristone), used as an abortive drug for its progesterone receptor antagonism, inhibits the GR. RU486 has effects on the HPA axis, which depends on the treatment dose, administration route, and frequency. It can produce an abolition of the HPA axis with low ACTH and glucocorticoid secretion or a disinhibition of the axis with higher corticosterone in the plasma. Overall, the trend indicates an abolition of the HPA axis during continuous or daily repeated *per os* administration of RU486. RU486 also inhibits steroidogenesis enzymes, such as 21-hydroxylase, 11-hydroxylase, and 3-hydroxysteroid dehydrogenase, which can modify the synthesis of many other steroids, such as aldosterone or androstenedione. In rodents, the clearance of RU486 is fast because the drug is not bound to the plasma α 1-glycoprotein, unlike in humans where the half-life is longer. RU486 has been studied in several clinical trials to improve the survival of cancer patients, such as in prostate cancer, in which RU486 has a low effect, probably because the treatment increases androgens in favor of cancer progression. This increase in sex hormones could be counteracted with a combination of androgen receptor inhibitor and RU486.

There are also specific GR inhibitors that do not target steroid receptors other than the GR, such as CORT125281 (exacorilant)²¹⁵ or CORT125134 (relacorilant) from Corcept Therapeutics. Their effects are being studied in several clinical trials to improve patients' life with cancer, but also in metabolic disorder, Cushing's syndrome, and Alzheimer's disease.

III.D.2.b. <u>11β-hydroxysteroid dehydrogenases type 1 inhibitors</u>

Compared with GR inhibition, the main advantage of HSD11B1 inhibition is that the receptor would still be functional and potentially activated by synthetic glucocorticoids if any strong side effect was to occur.

III.D.2.b.i. Use in clinic

Several clinical trials are ongoing in phase 1 or 2 for testing HSD11B1 inhibitors in different diseases, such as Alzheimer's disease, Cushing's syndrome, type 2 diabetes, obesity, and metabolic syndrome. These inhibitors are well tolerated by patients. ¹⁹⁷ In preclinical studies and in clinical trials on patients with type 2 diabetes, selective HSD11B1 inhibitor treatment demonstrated improvements in glycemic control, insulin sensitivity, and lipid metabolism disorder. ¹⁹⁷ The inhibition of HSD11B1 in patients is not reflected in the plasma cortisol level, which means that there is no compensation of the adrenal pathway through an increase in ACTH. ¹⁸⁰ HSD11B1 inhibition has an effect on immune cells, with a

reduction of pro-inflammatory cells infiltrating adipose tissue in obesity and decreases of macrophages and T cells in an atherosclerosis model. 197

One of the tested HSD11B1 inhibitors is AZD4017. It leads to an increase in the observed muscle mass, which can be related to the expression of HSD11B1 and the GR in skeletal muscle cells and the intracellular level of glucocorticoid in these cells. Moreover, androgen levels have been found to be increased in these patients, which can also affect muscle tissue. The lipid profile is also modified with AZD4017 treatment, with the total cholesterol and LDL cholesterol being reduced.

III.D.2.b.ii. ABT-384

ABT-384 is an inhibitor of HSD11B1 that has already been tested in humans in a phase 2 clinical trial for Alzheimer's disease. However, this clinical trial was prematurely ended due to a lack of efficacy of the drug compared with the current treatment for Alzheimer's. This pharmacological inhibitor was demonstrated to be safe for a daily dose, which fully inhibits HSD11B1. 224

It is metabolized through CYP3A, and two metabolites of ABT-384 have a potent HSD11B1 inhibition activity. Therefore, the use of CYP3A inhibitors, such as some antibiotics (e.g., clarithromycin), can affect the clearance of ABT-384. However, as the therapeutic index is high, there is a low risk of side effects during such co-medication.²²⁴ In the case of co-administration with CYP3A inducers, such as rifampicin, the dose of ABT-384 might need to be increased to reach the same efficacy.

2) Aim of the Thesis

The development of immune checkpoint blockade has been found to improve the overall survival of cancer patients who failed to respond to previous treatments, such as chemotherapy or radiotherapy.^{36,38} Even though immune checkpoint blockades have demonstrated high efficacy in the treatment of many solid tumors, only 25 % of patients with ccRCC have an objective response after 2 years, which highlights the presence of resistance mechanisms to ICIs in RCC.^{125,225–228}

As already described in 1)II.B.3, ccRCC is a tumor that is highly immune infiltrated, which correlates with a poor prognosis for patients.^{99,229} As strong immune infiltration in solid tumors is associated with an increased chance of immunotherapy response in most cancers,²³⁰ this correlation is a paradox that suggests the interesting role of the immune system in RCC.

Moreover, glucocorticoids are known to possess anti-inflammatory and immunosuppressive activity, as explained in 1)III.C. Moreover, in patients with cancer, stress that leads to a high level of glucocorticoids decreases their overall survival.^{200,231,232} The kidneys are highly involved in the production and elimination of glucocorticoids. They express HSD11B2, which produces a substrate for active glucocorticoid synthesis.

The aim of this project was to investigate the role of HSD11B1 and endogenous glucocorticoids in the antitumor immune function in renal cancer. Accordingly, the project's objectives were as follows:

- To investigate the therapeutic potential of HSD11B1 inhibition in renal cancer models;
- To protect the use of HSD11B1 inhibitors for their use in combination with immunotherapy in cancer treatment;
- To test the impact of *Hsd11b1* genetic modulation in a renal cancer model with overexpression in tumor cells and KO in the host mouse;
- To study the effect of glucocorticoid receptor antagonism in combination with immune checkpoint blockade on the antitumor immune response in a renal cancer model.

3) Results

I. Activation of endogenous glucocorticoids by HSD11B1 inhibits the antitumor immune response in renal cancer

I.A. Introduction

Endogenous steroids and particularly glucocorticoids modulate immune cell differentiation and activity. To understand the role of endogenous glucocorticoids in the resistance to immune checkpoint blockade, we investigated the role of the glucocorticoid producer HSD11B1 in renal cancer.

Specifically, we studied a human database of gene expression in tumors and found that *HSD11B1* expression is associated with a poor prognosis in renal cancer. In human and murine immune cell assays, we demonstrated an inhibitory activity of HSD11B1 on the immune response. Moreover, in renal cancer models, we demonstrated that HSD11B1 inhibition improves immunotherapy response.

I.B. Manuscript submitted

Authors

Hélène Poinot^{1,2}, Eloïse Dupuychaffray^{1,2}, Grégoire Arnoux³, Montserrat Alvarez^{1,2}, Jérémie Tachet^{1,2}, Ounss Ezzar^{1,2}, Jonathan Moore⁴, Olivia Bejuy⁵, Eulalia Olesti^{1,2}, Gioele Visconti^{1,2}, Víctor González-Ruiz^{1,2}, Serge Rudaz^{1,2}, Jean-Christophe Tille⁶, Clarissa Daniela Voegel⁷, Patrycja Nowak-Sliwinska^{1,2,4}, Carole Bourquin*^{1,2,8} and Aurélien Pommier*^{1,2}

¹School of Pharmaceutical Sciences, University of Geneva, Geneva, Switzerland

²Institute of Pharmaceutical Sciences of Western Switzerland, University of Geneva, Geneva, Switzerland

³Department of Cell Physiology and Metabolism, Faculty of Medicine, University of Geneva, Geneva, Switzerland

⁴Translational Research Centre in Oncohaematology, Faculty of Medicine, University of Geneva, Geneva, Switzerland

⁵CIBM Center for Biomedical Imaging, Faculty of Medicine, University of Geneva, Geneva, Switzerland

⁶Division of Clinical Pathology, Geneva University Hospitals, Geneva, Switzerland

⁷Department of Nephrology and Hypertension, Inselspital, Bern University Hospital, University of Bern, Bern, Switzerland

⁸Department of Anesthetics, Pharmacology, Intensive Care and Emergencies, Faculty of Medicine, University of Geneva, Geneva, Switzerland

* Corresponding authors

Title

Activation of endogenous glucocorticoids by HSD11B1 inhibits the antitumor immune response in renal cancer

Abstract

Although immune-based therapies have revolutionized the management of cancer, novel approaches are urgently needed to improve their outcome. We investigated the role of endogenous steroids in the resistance to cancer immunotherapy, as these have strong immunomodulatory functions. Using a publicly available database, we found that the intratumoral expression of 11 beta-hydroxysteroid dehydrogenase type 1 (HSD11B1), which regenerates inactive glucocorticoids into active glucocorticoids, was associated with poor clinical outcome and correlated with immunosuppressive gene signatures in patients with renal cell carcinoma (RCC). HSD11B1 was mainly expressed in tumorinfiltrating immune myeloid cells as seen by immunohistochemistry in RCC patient samples. Using peripheral blood mononuclear cells from healthy donors or immune cells isolated from the tumor of RCC patients, we showed that the pharmacological inhibition of HSD11B1 improved the response to the immune checkpoint inhibitor anti-PD-1. In a subcutaneous mouse model of renal cancer, the combination of an HSD11B1 inhibitor with anti-PD-1 treatment increased the proportion of tumorinfiltrating dendritic cells. In an intrarenal mouse tumor model, HSD11B1 inhibition increased the survival of mice treated with anti-PD-1. In addition, inhibition of HSD11B1 sensitized renal tumors in mice to immunotherapy with resiguimod, a Toll-like receptor 7 agonist. Mechanistically, we demonstrated that HSD11B1 inhibition combined with resiquimod increased T cell-mediated cytotoxicity to tumor cells by stimulating the antigen-presenting capacity of dendritic cells. In conclusion, these results support the use of HSD11B1 inhibitors to improve the outcome of immunotherapy in renal cancer and highlight the role of the endogenous glucocorticoid metabolism in the efficacy of immunotherapy.

Keywords

Immunotherapy, Renal cancer, HSD11B1, Glucocorticoids, Steroidogenesis

Cancer immunotherapy has revolutionized the field of oncology by prolonging patient survival. In clear cell renal cell carcinoma (ccRCC), immune checkpoint inhibitors are approved for first-line treatment of metastatic disease and have improved overall survival across multiple clinical trials. However, only 10% of patients with advanced ccRCC achieve complete response to checkpoint inhibitors. Since expression of PD-L1 does not predict response to treatment in renal cancer, it is urgent to identify the factors of resistance to checkpoint inhibition and to develop novel combination therapies to improve the outcome of immunotherapy.

Steroid hormones such as glucocorticoids play a role in regulating various physiological functions, including the immune response.⁴ Following treatment with immune checkpoint inhibitors, exogenous glucocorticoids are prescribed to control immune-related adverse events, but whether endogenous steroid hormones influence the response to immunotherapy in ccRCC is unknown.⁵

Although systemic levels of steroids are mostly governed by their production in the gonads and the adrenal gland, their biological activity is highly regulated in peripheral tissues in which the final steps of steroidogenesis can occur. This regulation has been demonstrated in several tissues and cell types, including immune cells.⁶ In particular, glucocorticoids in peripheral tissues are activated by 11 beta-hydroxysteroid dehydrogenase type 1 (HSD11B1) and inactivated by 11 beta-hydroxysteroid dehydrogenase type 2 (HSD11B2), a mechanism which contributes to the local regulation of the stimulation of the glucocorticoid receptor.⁷ In cancer, evidence of intratumoral steroidogenesis was first shown in hormone-sensitive cancers such as breast and prostate tumors.^{8,9} More recently, the expression of genes involved in steroidogenesis was characterized as a signature for survival of patients with hormone-independent cancers such as gastric cancer and gastrointestinal stromal tumors.^{10,11}

Since steroids are important modulators of the immune response, we investigated whether the enzymes involved in steroid metabolism were associated with clinical outcome and antitumor immune responses in ccRCC. Our results shed light on the inhibitory function of glucocorticoid regeneration through HSD11B1 in the immune response against renal cancer.

Materials and Methods

See Supplemental Information

Results

HSD11B1 expression in tumors correlates with poor clinical outcome in patients with renal cancer.

In order to identify clinically impactful genes that influence the antitumor immune response, we correlated the intratumoral expression of genes involved in steroidogenesis with the outcome of ccRCC patients and looked for an association with immunosuppressive markers using the TCGA repository. We found that high expression of HSD11B1, HSD17B1, CYP21A2 and STAR was associated with poor overall survival while on the contrary, high expression of AKR1C2, HSD17B2, AKR1C4, AKR1C1, HSD11B2, HSD17B8 was associated with a longer overall survival (OS) in patients (Fig 1 A). This analysis drew our attention to the glucocorticoid pathway, as four genes were related to cortisol metabolism (Fig 1 B, Fig S1 A). The CYP21A2 and HSD11B1 enzymes support the production of cortisol, while HSD11B2 and AKR1C4 are involved in cortisol inactivation and degradation. This finding indicated that patients with high expression of cortisol-producing enzymes or a low expression of cortisol-inactivating enzymes had reduced OS. Hierarchical clustering analysis revealed five main patient populations with one cluster of patients expressing low levels of these enzymes and four clusters mainly defined by the strong expression of each individual gene, demonstrating that HSD11B1, CYP21A2, AKR1C4 and HSD11B2 were mutually exclusively expressed in ccRCC patients (Fig 1 C). Survival analyses of the patient populations defined by the hierarchical clustering clearly showed that patients defined by high expression of HSD11B1 or CYP21A2 had a negative outcome compared to the patients defined by high expression of AKR1C4 or HSD11B2 (Fig 1 D). Since CYP21A2 is not only involved in the cortisol synthesis pathway but also regulates the mineralocorticoid synthesis pathway, we then focused our analysis on HSD11B1, which is directly and specifically involved in cortisol regeneration. The log-rank test showed a greater impact of HSD11B1 on survival when the patient population was defined by the clustering analyses (HR=2.187, 95%CI: 1.511-3.166) (Fig S1 B) compared to the median-based method (HR= 1.3, 95%CI:1.17-1.45) (Fig 1 A). Among the 39 cancer subtypes tested in TCGA, the expression of HSD11B1 was found to correlate with a poor prognosis only in stomach adenocarcinoma and renal cancer. Renal cancer was the cancer type most significantly associated with shorter OS (Fig S2).

Since HSD11B1 is involved in cortisol regeneration, which may lead to local immunosuppression, ¹² we hypothesized that ccRCC patients defined by a high *HSD11B1* could be associated with an immunosuppressive gene expression pattern. Interestingly, patients with high expression of *HSD11B1* had a higher expression of *PDCD-1* (coding for PD-1), *LAG-3*, *CTLA-4* and genes involved in a Th2 immune response (Fig 1 E).

In order to confirm the expression of HSD11B1 at the protein level in renal tumors and to identify the positive cells, we stained twenty tumors from ccRCC patients by immuno-histochemistry. As shown in Fig 2 A, a positive staining of HSD11B1 was mainly detected in infiltrating cells with 11/20 patients

showing more than 1% of HSD11B1-positive cells (Fig 2 B). Morphological analysis of the staining by a pathologist suggested that HSD11B1-positive cells were immune cells of the myeloid lineage, especially macrophages and neutrophils (Fig S3). Co-staining of HSD11B1 with CD68⁺ cells confirmed that HSD11B1 was expressed in tumor-infiltrating macrophages (Fig 2 C).

HSD11B1 activity inhibits antigen-mediated T cell activation and limits the response to anti-PD-1 treatment in human PBMC and tumor-infiltrating immune cells.

A key function of myeloid cells is to stimulate the adaptive T cell response against cancer. ¹³ We tested the functional impact of HSD11B1 activity in peripheral blood mononuclear cells (PBMCs) healthy human donors and human immune cells isolated from RCC tumors. An antigen recall assay was performed to test whether HSD11B1 could impact antigen-dependent T cell activation and the response to anti-PD-1 treatment in these cells. T cell activation, measured by IFN-γ secretion, was detected only in the presence of antigen stimulation and was increased by anti-PD-1 treatment. Treatment with cortisone, an inactive HSD11B1 substrate, reduced T cell activation both in isotype and anti-PD-1 treated conditions, suggesting that immune cells were able to metabolize cortisone into the active hormone cortisol through HSD11B1. The inhibitory effect of cortisone on T cell activation was reversed using ABT-384, an HSD11B1 inhibitor, demonstrating that the cortisone-mediated inhibition of the immune response was driven by HSD11B1 (Fig 3 A). Interestingly, while treatment with cortisone blocked the efficacy of anti-PD-1 treatment in this assay, the addition of ABT-384 restored T cell activation toward a level comparable with the non-cortisone-treated condition.

The effect of HSD11B1 activity was then tested on immune cell subsets isolated from RCC tumors. Although only one out of four patients tested showed a response to antigen recall, we observed a reduction of the T cell response in cortisone-treated samples in both isotype and anti-PD-1 conditions, which was reversed by ABT-384 (Fig 3 B). These results demonstrated that HSD11B1 can inhibit the antigen-specific response in tumor-infiltrating immune cells.

HSD11B1 inhibition impacts the immune phenotype in anti-PD-1-treated subcutaneous renal tumors in mice.

Since HSD11B1 inhibition improved the T cell response to an immune checkpoint inhibitor *in vitro*, we tested the therapeutic potential of combining an HSD11B1 inhibitor with anti-PD-1 in mice. First, cortisold4 was administered to non-tumor-bearing mice treated with ABT-384 and HSD11B1 activity was quantified. We observed a complete inhibition of HSD11B1 activity as demonstrated by the low level of cortisol-d3 measured in the plasma of inhibitor-treated mice (Fig 4 A). In mice bearing subcutaneous murine renal cancer (Renca) tumors, anti-PD-1 treatment partially inhibited tumor growth. No efficacy of monotherapy with the HSD11B1 inhibitor was observed when compared to the vehicle-treated control group (Fig 4 B). Furthermore, there was no effect of the combination treatment with the HSD11B1 inhibitor and anti-PD-1 on tumor growth compared to the anti-PD-1 treated group. Regarding the tumor immune phenotype, intratumoral CD4+ effector cells were increased in the combination group compared to the anti-PD-1 monotherapy group (Fig 4 C). In addition, a decrease of the myeloid-derived suppressor cell to dendritic cell ratio (MDSC/DC) in the combination group compared to anti-PD-1 monotherapy-

treated group was observed (Fig 4 D and Fig S4). Thus, although HSD11B1 inhibition did not confer higher antitumoral efficacy to anti-PD-1 treatment, the combination impacted the tumor immune phenotype.

Combination of an HSD11B1 inhibitor with anti-PD-1 therapy increases the survival of mice bearing orthotopic renal tumors.

As HSD11B2 provides the substrates for HSD11B1 and higher levels of HSD11B2 activity have been described in the kidney compared to other tissues, 14 we hypothesized that the inhibition of HSD11B1 could be more impactful in an orthotopic model of renal cancer. We observed a lower ratio of the murine active hormone corticosterone to the inactive murine precursor 11-dehydrocorticosterone (11-DHC) in the kidney than in the plasma of naive mice, confirming a predominant activity of HSD11B2 in kidneys (Fig 5 A). We then confirmed that administration of ABT-384 inhibited HSD11B1 activity in the kidney of naive mice (Fig 5 B). The combination of the HSD11B1 inhibitor with anti-PD-1 was then tested in mice bearing orthotopic Renca tumors and tumor growth was assessed by MRI and PET scans (Fig 5 C). Treatment with ABT-384 decreased the corticosterone-to-11-DHC ratio in the plasma of tumor-bearing mice (Fig 5 D). The survival of the mice treated with anti-PD-1 was not different from the isotype control group, indicating that anti-PD-1 was not effective in this model (Fig 5 E, Fig S5 A). The probability of survival at day 32 was 100% for mice treated with the combination treatment, 70% for the control group or the mice treated with anti-PD-1 monotherapy and 40% in mice having received the HSD11B1 inhibitor monotherapy. Thus, a decrease of corticosterone levels through HSD11B1 inhibition may improve the efficacy to anti-PD-1 treatment in this model, although the difference was not significant. Interestingly, a higher corticosterone-to-11-DHC ratio was associated with an increased tumor size in the combination group only, suggesting that low levels of corticosterone correlated with an improved response to anti-PD-1 treatment (Fig S5 B to E). These results indicated that a decrease of corticosterone levels through HSD11B1 inhibition may improve the efficacy of anti-PD-1 treatment in mice bearing intrarenal tumors.

HSD11B1 inhibition confers sensitivity to the innate immune stimulating agent resiquimod in mice bearing subcutaneous Renca tumors.

As HSD11B1 was mainly expressed in myeloid cells of RCC patients, and since we observed an increase of the MDSC/DC ratio in response to HSD11B1 inhibition in anti-PD-1-treated tumors, we tested whether HSD11B1 activity modulated the anti-tumor response to resiquimod (R848), which is a TLR7/8 agonist. We have previously shown that R848 enhances antitumor CD8+ responses and decreases intratumoral myeloid-derived suppressor cells. 15,16 Quantification of the corticosterone-to-11-DHC ratio showed no effect of R848 treatment on the plasma concentration of these steroids (data not shown). In tumor-bearing mice, although no reduction of tumor growth was observed either with R848 or with ABT-384 as monotherapies, the combination of both led to a decrease in tumor size at 14 days post-engraftment (Fig 6 A). Interestingly, a reduction in tumor-infiltrating CD4+ T cells and an increase in tumor-infiltrating CD8+ T cells were observed in the combination group, as seen by the significant decrease of the CD4+/CD8+ ratio (Fig 6 B, Fig S6 B and C). In addition, the combination treatment induced a decrease of the mannose receptor (CD206) protein expression in tumor-infiltrating macrophages, suggesting a switch toward a proinflammatory phenotype (Fig 6 C). Although not

significant, the combination therapy was also associated with a slight reduction in the MDSC/DC ratio (Fig 6 D). These results suggested that stimulation of the myeloid compartment by a TLR7/8 agonist in combination with HSD11B1 inhibition improves the antitumor immune response.

HSD11B1 inhibits T cell-mediated tumor cytotoxicity by down-regulating the activation of myeloid cells.

In order to better characterize the effect of HSD11B1 inhibition on the antitumor immune response in the context of TLR7 stimulation, we tested the impact of HSD11B1 activity on the capacity of mouse dendritic cells to initiate an antitumor immune response against renal cancer cells. HSD11B1 expression was confirmed in mouse bone marrow-derived dendritic cells (BMDC) (Fig 7 A). Dendritic cells were activated by R848 to prime cytotoxic T cells (Fig. 7 B). Treatment with 11-DHC led to downregulation of surface CD86 and MHCII indicating decreased BMDC activation, which was reversed by HSD11B1 inhibition (Fig 7 C and D). CD8+ T cells and Renca H2-kb GFP cells were then cocultured with the dendritic cells (Fig 7 B). Exposure to 11-DHC enhanced tumor cell growth, suggesting that myeloid cells primed T-cell-mediated cytotoxicity against tumor cells less efficiently (Fig 7 E). HSD11B1 inhibition restored the antitumor immune response in the presence of 11-DHC to the levels seen with the vehicle-treated control (Fig 7 E). In the absence of immune cells, the growth of Renca H2-kb GFP cells did not change in response to 11-DHC or HSD11B1 inhibition (data not shown). These results demonstrated that BMDC are sensitive to 11-DHC and that HSD11B1 inhibits the anti-cancer immune response through a downregulation of the antigen presentation capacity of the dendritic cells.

Discussion

Unprecedented advances have been made in the treatment of renal cancer through the use of immune checkpoint blockade, but some drivers of resistance are still unknown. In RCC a high CD8⁺ T cell infiltration is associated with a lower probability of response to anti-PD-1 therapy and with a worse prognosis, in contrast to what is seen in many other types of cancer.^{18,19} To the best of our knowledge, it is not fully understood why inflamed renal tumors do not respond well to immune checkpoint inhibitors, although a low tumor mutational burden and specific somatic mutations may play a role.^{19,20} Here we propose HSD11B1 as a novel factor contributing to resistance to immunotherapy in renal cancer.

Among all the cancer types available in the TCGA database, the poor prognostic value of intratumoral *HSD11B1* expression was seen mainly in patients with renal cancer. One explanation may be the high level of activity in the kidney of its isoenzyme HSD11B2, which inactivates cortisol or corticosterone into cortisone or 11-DHC and thus produces the substrate for HSD11B1.^{14,21} Accordingly, we observed a lower corticosterone/11-DHC ratio in the kidney than in the plasma of mice. The therapeutic efficacy of HSD11B1 inhibition in combination with immunotherapy was higher for orthotopic Renca tumors than for subcutaneous tumors, supporting the hypothesis that HSD11B1 activity may have more impact in the kidney, where higher levels of its substrates are present than in other organs. Consistently with this concept, we found that *HSD11B1* expression was also associated with poor prognosis in stomach adenocarcinoma, and it has been shown that *HSD11B2* is also expressed in the gastrointestinal tract.²² In addition, *HSD11B1* overexpression or gain mutations were associated with poor clinical outcome in patients with gastrointestinal stromal tumors.¹¹

The inhibition of HSD11B1 may have a different impact according to the type of immunotherapy, as we observed a greater benefit of HSD11B1 inhibition for combination treatment with R848 than with anti-PD-1 immunotherapy in subcutaneous models. This may be due to the mode of action of R848 which activates myeloid cells through TLR7, in contrast to anti-PD1 treatment which acts directly on T cell function. We propose that HSD11B1 contributes to cancer-associated immunosuppression by regulating the activation of myeloid cells and their capacity to induce an effective T cell response. This is supported by the expression pattern of HSD11B1, which we found mainly in tumor-infiltrating macrophages in human RCC samples, in agreement with previous observations in RCC and in melanoma.^{23,24} Consistently with our results, a recent study reported a higher infiltration of macrophages in RCC samples expressing a higher level of HSD11B1, supporting the link between HSD11B1 expression and myeloid cell in the tumor microenvironment.²³ In mice, we observed a decrease in expression of the antiinflammatory marker CD206 on tumor-infiltrating macrophages in response to HSD11B1 inhibition, suggesting a shift towards a more inflammatory phenotype. Indeed, we showed that HSD11B1 inhibition improved the ability of both human and mouse myeloid cells to prime T cells. In the context of vaccination, inhibition of HSD11B1 was shown to synergize with CpG, a TLR9 agonist, to enhance T cell responses, suggesting that the amplification of endogenous glucocorticoids by HSD11B1 is an important mechanism for the regulation of the activity of antigen-presenting cells.²⁵

3) Results

In tumors, activation of the glucocorticoid receptor by its ligand leads to a decrease in the expression of co-stimulatory molecules such as *CD28* and of pro-inflammatory cytokines, and to an increased expression of immune checkpoints such as *PDCD1* (PD-1), *CTLA-4*, and *TIM3.*²⁶ This is consistent with our observation that immune checkpoints are more highly expressed in RCC tumors with elevated *HSD11B1* expression. Within tumor-infiltrating CD8⁺ T cells, the glucocorticoid receptor was shown to be highly expressed in exhausted CD8⁺ T cells and to promote the upregulation of genes associated with T cell dysfunction.²⁷ Thus, glucocorticoid receptor activity is associated with the suppression of CD8⁺ T cell responses.

The functional relevance of the immunosuppression induced by endogenous glucocorticoids is supported by the emerging link between psychological stress and the outcome of cancer immunotherapy. Production of systemic glucocorticoids limits antitumor immune responses by abrogating type I interferon responses in dendritic cells.²⁸ This mechanism is in line with our results showing that suppression of glucocorticoid production in dendritic cells through HSD11B1 inhibition supports their ability to prime a cytotoxic T cell response. In addition, our findings are consistent with a recent study demonstrating that HSD11B1 limits the response to PD-1 blockade in melanoma.²⁴

In conclusion, this work supports the hypothesis that the combination of an HSD11B1 inhibitor with immune checkpoint blockade may be beneficial in renal cancer patients, highlighting the role of endogenous glucocorticoid metabolism in the efficacy of immunotherapy. Although not used in the clinic to date, HSD11B1 inhibitors have been widely developed in the framework of metabolic diseases.²⁹ Our study provides a rationale to further investigate whether these inhibitors could be repurposed for the treatment of cancer by boosting antitumor immunity.

Acknowledgments

This work was supported by Horizon 2020 UE No 641549 (SEFRI 15.0243), the Swiss National Science Foundation 310030_182317 and IZSTZ0_198887, the Swiss Cancer Research Foundation KFS 4535-08-2018-R, Innosuisse 44124.1 IP-LS, the Boninchi Foundation and the Schmidheiny Foundation. The authors thank Magdalena Rausch for support during the isolation of immune cells from RCC patients, Stéphane Germain for his help in the setting up of the orthotopic tumor model and Didier J. Colin who is the responsible of the small animal preclinical imaging platform of Geneva.

Author contribution

AP, CB and HP designed and planned the study. HP, ED, GA, MA, JT, OE, JM, OB, EO, GV, CDV and AP performed the experiments and collected and analyzed the data. VGR, SR, JCT, and PNS contributed essential expertise and tools. AP, CB and HP wrote the paper. The paper was reviewed and approved by all authors.

Declaration of interest statement

No potential conflict of interest was reported by the authors.

Data availability statement

The data that support the findings of this study are available from the corresponding authors, [CB, AP], upon reasonable request.

Reference list

References are included in the Bibliography of the Thesis.

Appendices

Supplemental Figures and Methods following the figures captions.

Figures

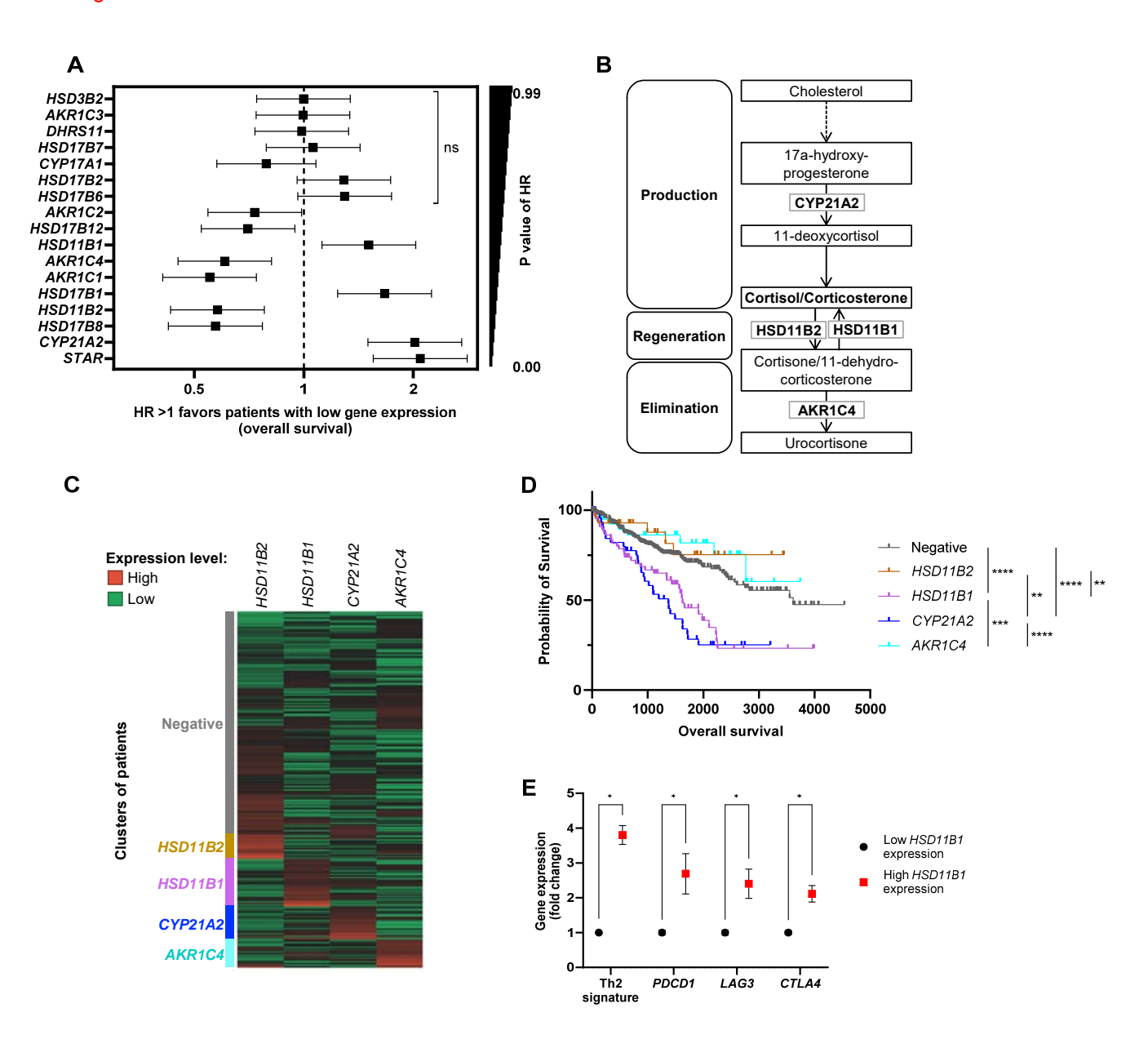


Figure 1: The intratumoral expression of genes involved in glucocorticoid metabolism correlates with clinical outcomes in patients with ccRCC.

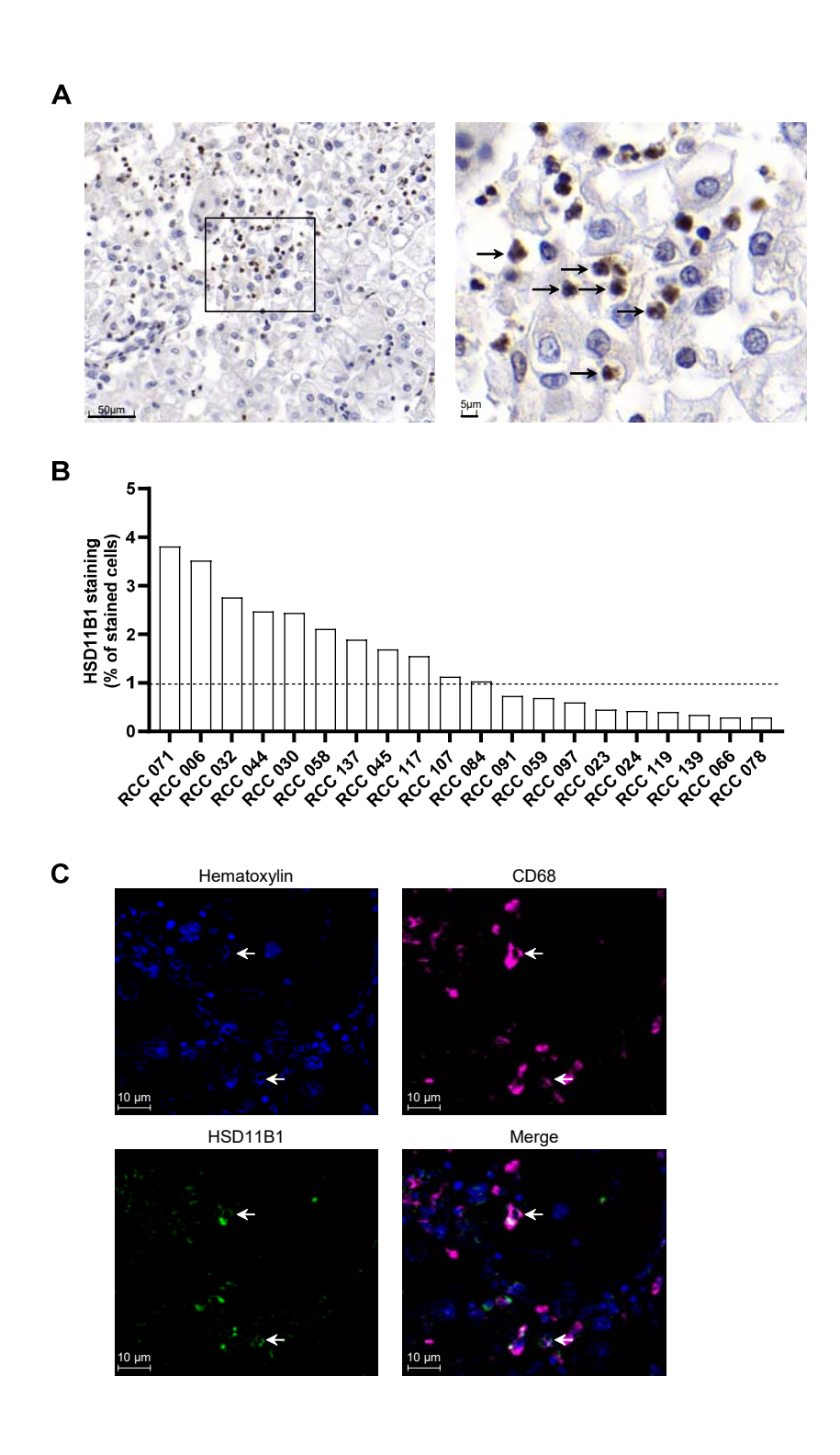


Figure 2: HSD11B1 is expressed in tumor-infiltrating macrophages.

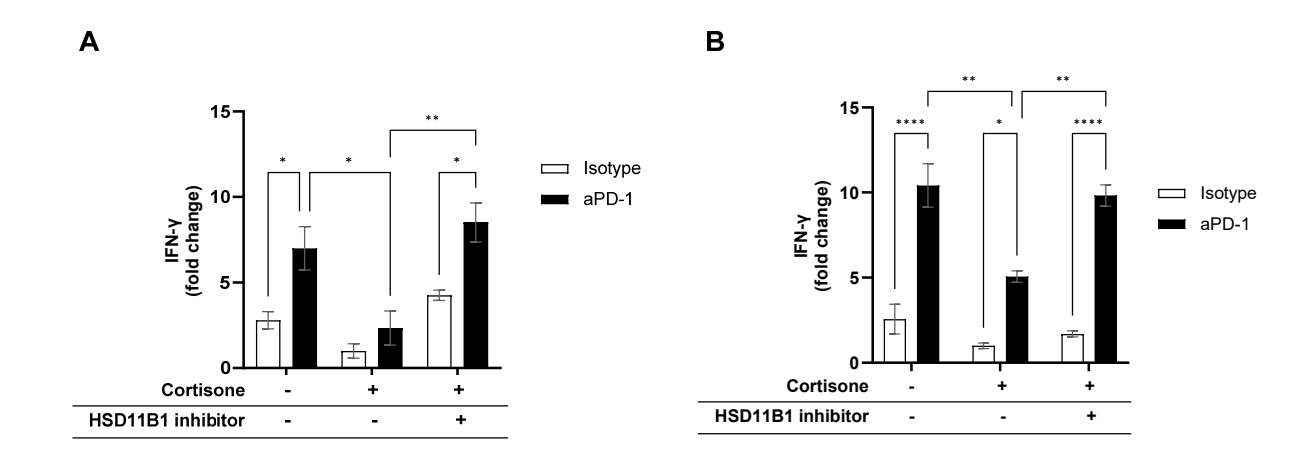


Figure 3: HSD11B1 activity inhibits the antigen-mediated T cell activation and the response to anti-PD-1 treatment in human immune cells.

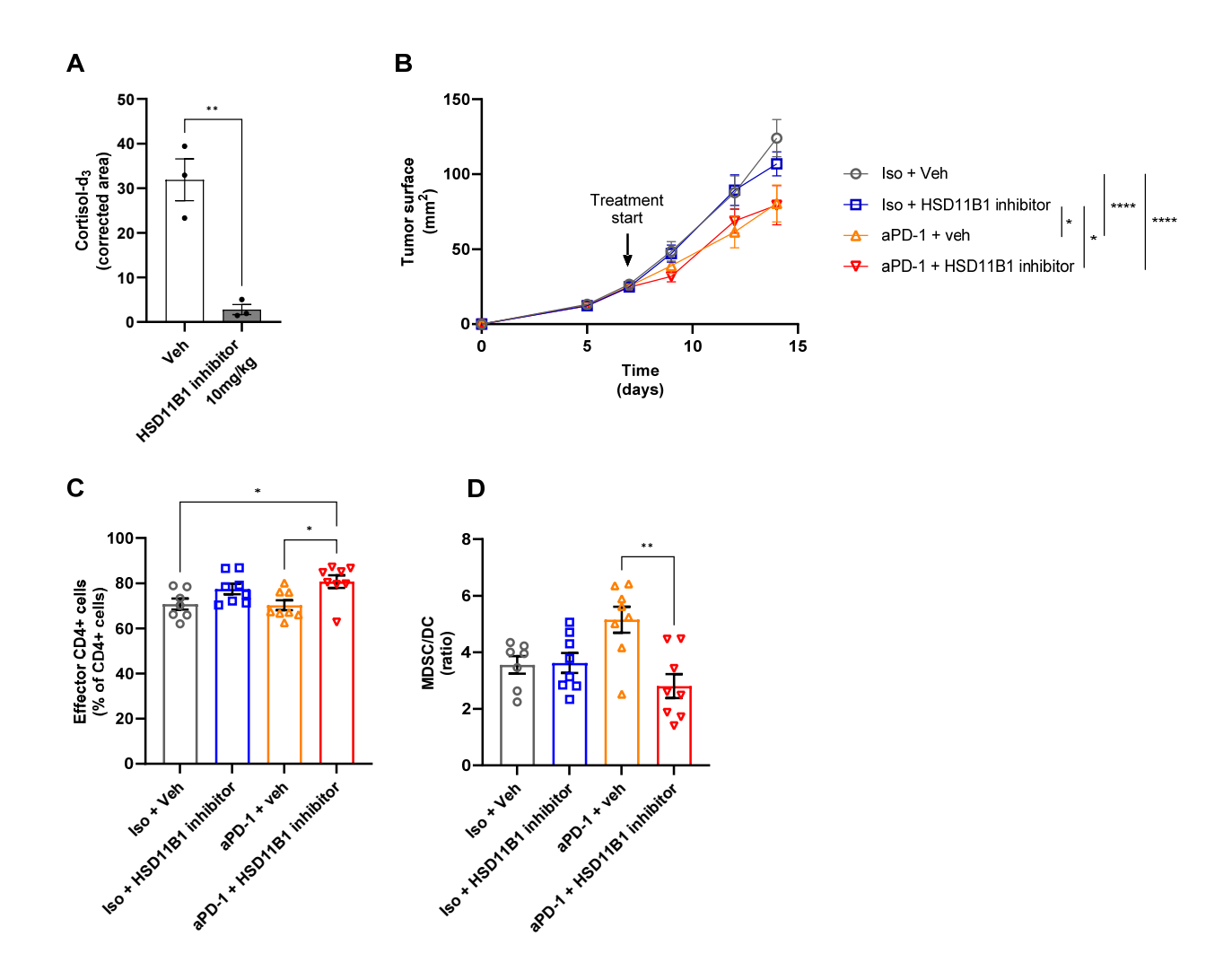


Figure 4: HSD11B1 inhibition impacts the tumor immune phenotype in anti-PD-1-treated subcutaneous Renca tumors.

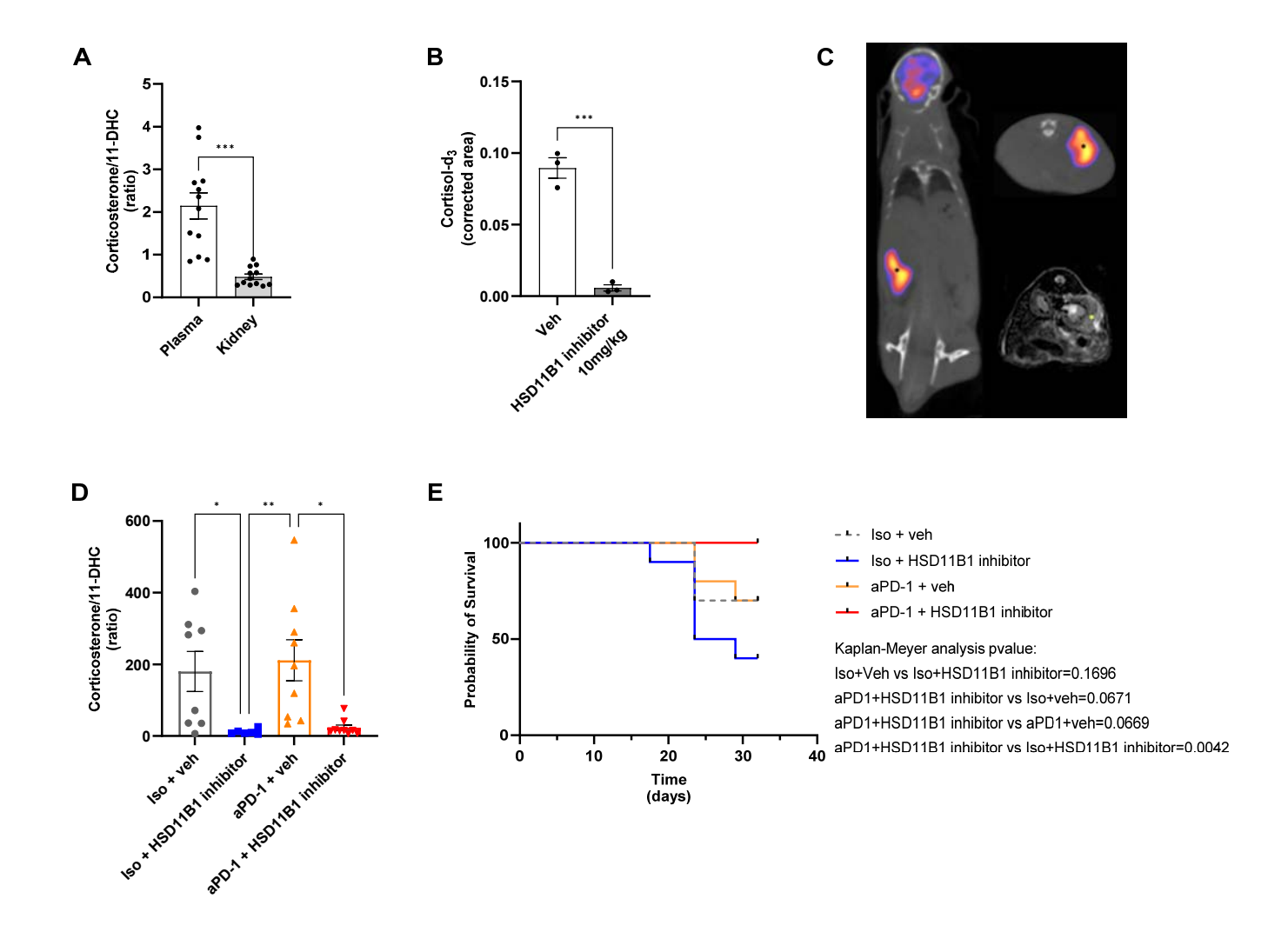


Figure 5: Combination of an HSD11B1 inhibitor with anti-PD-1 increases the survival of mice bearing intrarenal tumors.

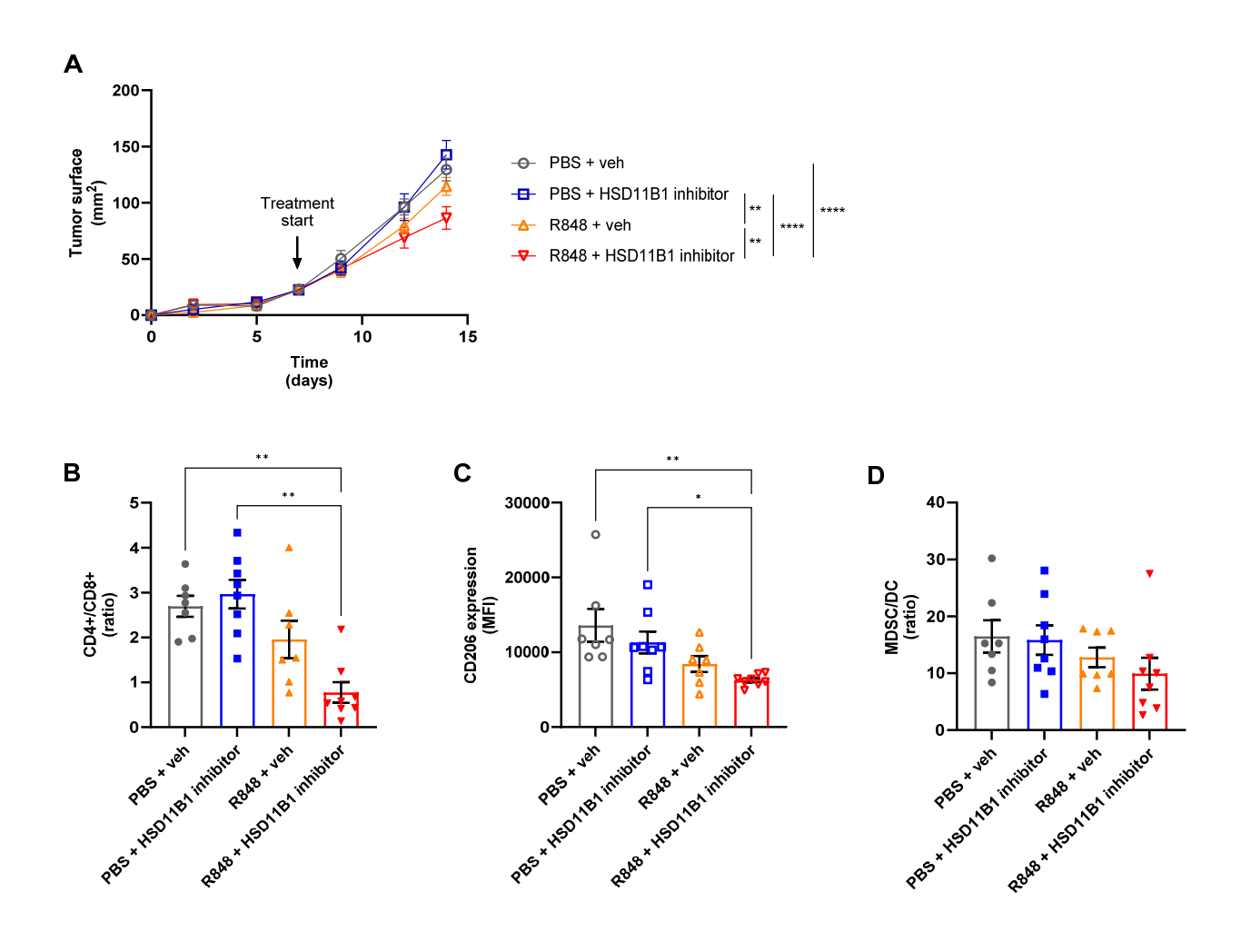


Figure 6: Combination of HSD11B1 inhibition with the innate immunostimulant R848 confers better antitumor sensitivity than monotherapy.

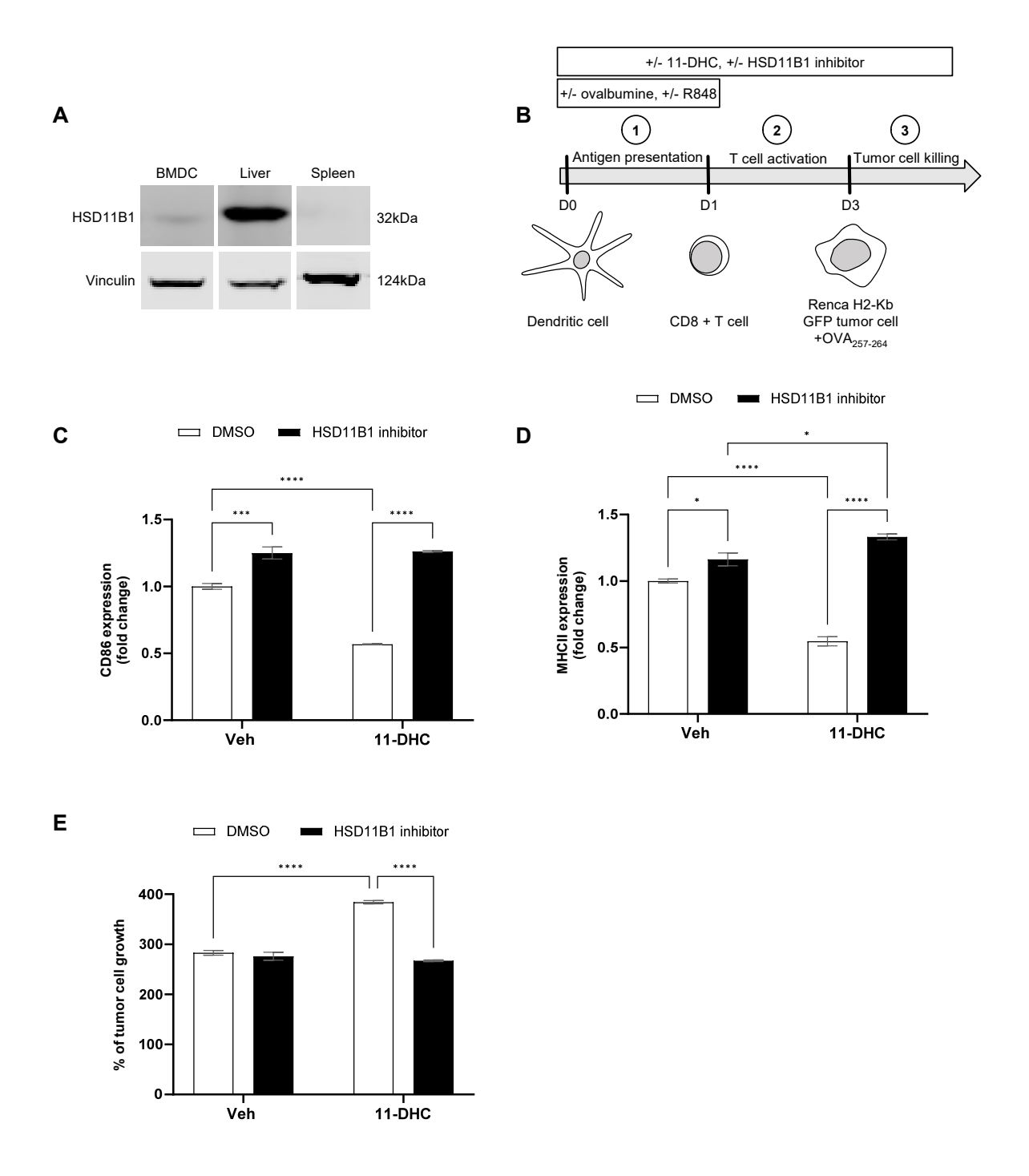


Figure 7: HSD11B1 inhibits dendritic cell activation and T cell-mediated tumor cytotoxicity in a cellular assay.

Figure captions

Figure 1:

A. Forest plot showing the hazard ratio (HR) for overall survival (OS) in ccRCC patients with high versus low expression of genes involved in steroidogenesis. Patients were dichotomized into high vs. low gene expression groups based on the median expression values as threshold. HR is represented on a logarithmic scale, HR>1 indicates that high expression of the gene correlates with a shorter OS. **B.** Simplified diagram of the glucocorticoid pathway. **C.** Heat map representing hierarchical clustering analysis of genes involved in glucocorticoid metabolism. **D.** Probability of survival for patients segregated based on the hierarchical clustering. ** p-value<10⁻², *** p-value<10⁻³, **** p-value<10⁻⁴. **E.** Expression levels for immune checkpoints and Th2 gene signature in patients with high vs. low HSD11B1 expression. Data are shown as mean +/- SEM of 445 (low *hsd11b1* expression) and 57 patients (high *hsd11b1* expression), **** p-value<10⁻⁶.

Figure 2:

A. Human RCC tumor sample stained for HSD11B1 (brown) by immunohistochemistry. The right picture is a zoom in section. The arrows indicate infiltrating cells positive for HSD11B1 with a macrophage morphology. **B.** Percentage of cells positive for HSD11B1 in tumors from 20 patients with RCC. **C.** Representative immunohistochemistry staining for CD68, HSD11B1 and hematoxylin in four RCC tumor specimens from patients. Arrows show colocalization of HSD11B1 and CD68.

Figure 3:

Relative IFN-γ levels secreted by PBMC from a healthy donor (**A**) and immune cells enriched from a human RCC tumor (**B**), following antigen recall stimulation. There was no effect of ABT-384 on the level of IFN-γ in absence of cortisone. Fold change compared to the condition with cortisone, isotype and without HSD11B1 inhibitor is represented as mean +/- SEM of 3 technical replicates in one experiment. * p-value<0.05, ** p-value<10⁻², *** p-value<10⁻³, **** p-value<10⁻⁴. **A**. Data are representative of 3 independent experiments on the same donor. Similar results were obtained with 2 other donors tested in one experiment. **B**. Out of 4 patients tested, only the patient shown had a response to antigen recall.

Figure 4:

A. Determination of HSD11B1 activity by the measurement of plasma cortisol-d₃ levels in naive mouse after administration of cortisol-d4 +/- the HSD11B1 inhibitor ABT-384. Data are shown as mean +/- SEM of 3 mice per group. ** p-value<10⁻². **B.** Growth kinetics of subcutaneous Renca tumors. Data are shown

as mean of tumor area +/- SEM of 8 mice per group. Statistical analysis at day 14, * p-value<0.05, **** p-value<10⁻⁴. **C-D.** Immunophenotyping results of the tumor by FACS. CD44⁻CD62L⁻ CD4⁺ were defined as effector CD4⁺ cells and are represented as % of total CD4⁺ cells (**C**). MDSC/DC ratio calculated based on the % of MDSC/CD45⁺ cells and % of DC/CD45⁺ cells (Fig S4). (**D**). Data are shown as mean +/- SEM of 8 mice per group. * p-value<0.05, ** p-value<10⁻².

Figure 5:

A. Comparison of corticosterone/11-DHC ratio in plasma and kidney of naive mice. Data are shown as mean +/- SEM of 12 mice per group. *** p-value=5x10⁻⁴. **B.** Determination of HSD11B1 activity by the measurement of cortisol-d₃ levels in kidneys of naive mice after administration of cortisol-d₄ +/- the HSD11B1 inhibitor ABT-384. Data are shown as mean +/- SEM of 3 mice per group. *** p-value<10⁻³. **C.** Representative images of a mouse with an intrarenal Renca tumor. Coronal (left) and axial views (upper right) of the [¹⁸F]FDG PET/CT scan (back of the mouse on the top). The lower right image corresponds to the axial view of the MRI scan. Tumor is pointed by the asterisks. **D.** Corticosterone/11-DHC ratio in plasma of renal tumor-bearing mice. Data are shown as mean +/- SEM of 6 to 9 mice per group. * p-value<0.05, ** p-value<10⁻². **E.** Probability of survival over time in mice bearing intrarenal Renca tumors based on the tumor volume. Tumor volume >200 mm³ considered as event of death. 10 mice per group. Statistical analysis: log-rank (Mantel-Cox) test.

Figure 6:

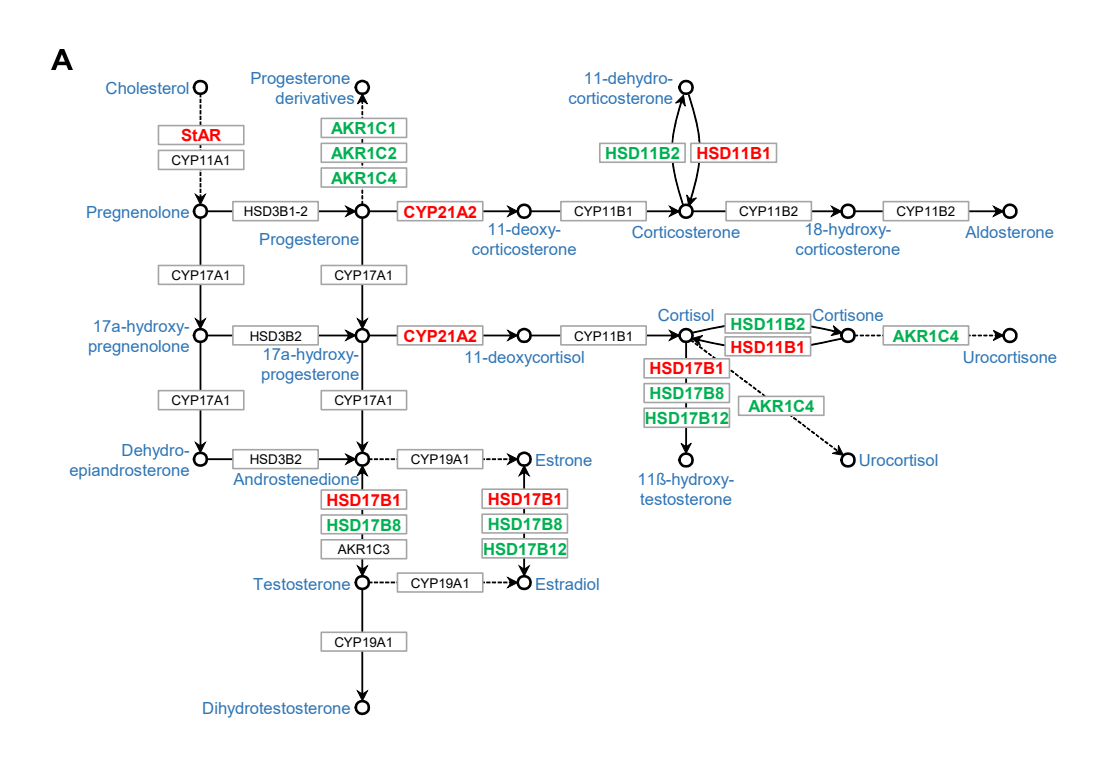
A. Growth kinetics of subcutaneously implanted Renca tumors. Treatments were initiated at day 7. Data are shown as mean of tumor area +/- SEM of 7 to 8 mice per group. Statistical analysis at day 14, ** p-value<10⁻², **** p-value<10⁻⁴. **B-D.** Immunophenotyping results of the tumors by flow cytometry. Percentage of CD4⁺, CD8⁺ (**B**), MDSC, and DC (**D**) represented as ratio of cell populations. CD206 expression (**C**) represented as mean fluorescence intensity (MFI) of CD206 on macrophages in the tumor. Data are shown as mean +/- SEM of 7 to 8 mice per group. * p-value<0.05, ** p-value<10⁻².

Figure 7:

A. HSD11B1 expression by Western blot in mouse bone marrow-derived dendritic cells, liver and spleen. **B.** Experimental design of T cell-mediated tumor cytotoxicity assay. **C, D.** Surface CD86 (**C**) and MHCII (**D**) molecules on bone marrow-derived dendritic cells measured by flow cytometry at D1. Results are expressed as fold change of the MFI, relative to the control condition. Data are shown as mean +/- SEM of 3 technical replicates of one experiment. **E.** Measurement of Renca H2-Kb GFP tumor cell growth exposed to antigen stimulated CD8+T cells. Results are expressed as % of tumor cell growth normalized to the seeding density. Data are shown as mean +/- SEM of 3 replicates and representative of 3 independent experiments. * p-value<0.05, *** p-value<10-3, **** p-value<10-4.

Supplementary information to Poinot et al.

Supplementary figures



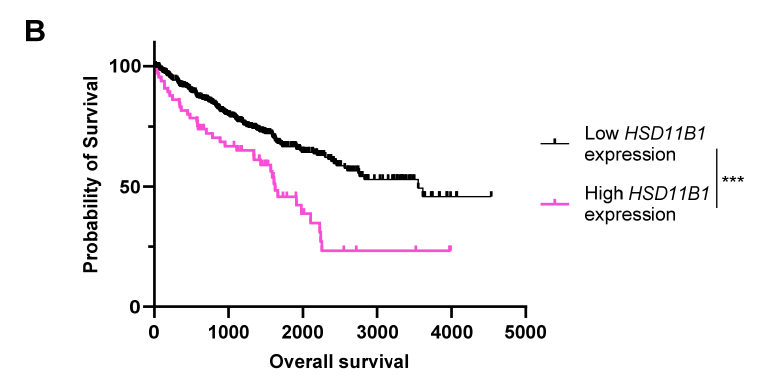


Figure S1: The expression of HSD11B1 correlates with clinical outcome in patients with renal cancer.

A. Steroidogenesis pathway. Steroids are represented as circle with their name in blue. Enzymes are represented in rectangles, in green for a correlation with good prognosis in RCC patients, in red for a correlation with poor prognosis in RCC patients. **B.** Kaplan-Meyer curves showing the probability of survival over time for ccRCC patients segregated based on the hierarchical clustering. The low *HSD11B1* expression group includes patients of Negative, *HSD11B2*, *CYP21A2* and *AKR1C4* clusters (Fig 1C). Statistical analysis: Log-rank (Mantel-Cox) test, *** p-value<10-3.

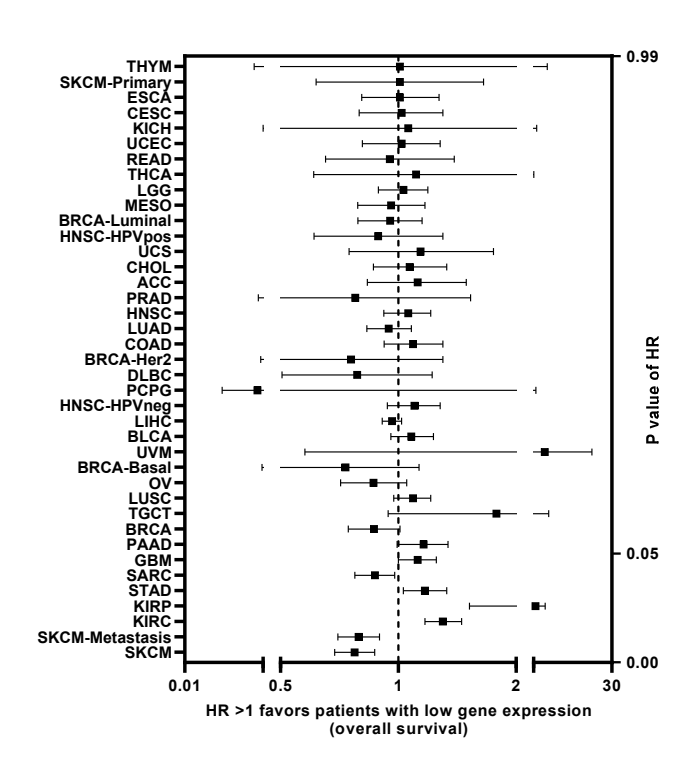


Figure S2: Correlation between HSD11B1 expression and survival in multiple cancer types.

Forest plot showing the hazard ratio (HR) for overall survival (OS) in cancer patients with high versus low expression of HSD11B1. Patients were segregated into high versus low HSD11B1 expression groups based on the median expression values as threshold by TIMER (Tumor IMmune Estimation Resource). The impact of the HSD11B1 expression level on OS was determined with Cox Proportional-Hazards model and the HR are represented with 95% confidence interval. HR is represented on a logarithmic scale, HR>1 indicates that high expression of HSD11B1 correlates with a shorter OS. Tested cancers were ranked by their p-value.

ACC: adrenocortical carcinoma, BLCA: bladder urothelial carcinoma, BRCA: breast invasive carcinoma, CESC: cervical and endocervical cancer, CHOL: cholangiocarcinoma, COAD: colon adenocarcinoma, DLBC: diffuse large B-cell lymphoma, ESCA: esophageal carcinoma, GBM: glioblastoma multiforme, HNSC: head and neck cancer, KICH: kidney chromophobe, KIRC: kidney renal clear cell carcinoma, KIRP: kidney renal papillary cell carcinoma, LGG: lower grade glioma, LIHC: liver hepatocellular carcinoma, LUAD: lung adenocarcinoma, LUSC: lung squamous cell carcinoma, MESO: mesothelioma, cystadenocarcinoma, PAAD: OV: ovarian serous pancreatic adenocarcinoma, PCPG: pheochromocytoma and paraganglioma, PRAD: prostate adenocarcinoma, READ: rectum adenocarcinoma, SARC: sarcoma, SKCM: skin cutaneous melanoma, STAD: adenocarcinoma, TGCT: testicular germ cell tumors, THCA: thyroid carcinoma, THYM: thymoma, UCEC: uterine corpus endometrial carcinoma, UCS: uterine carcinosarcoma, UVM: uveal melanoma.

HSD11B1 staining

ID	Macrophages			1 staining ation	Follow-up	Grade
patients			Core	Margin	period (days)	
RCC 6	+	n.a.	+	-	7019	1
RCC 23	-	-	n.d.	n.d.	7215	1
RCC 24	-	-	n.d.	n.d.	6511	1
RCC 30	+	-	+	-	8865	1
RCC 32	+	+	+	-	730	3
RCC 44	-	-	+	-	5615	1
RCC 45	+	+	+	-	921	3
RCC 58	+	+	+	-	372	4
RCC 59	+	+	n.d.	n.d.	50	3
RCC 66	-	-	n.d.	n.d.	5175	1
RCC 71	-	-	+	-	5396	1
RCC 78	-	-	n.d.	n.d.	192	3
RCC 84	-	-	n.d.	n.d.	493	3
RCC 91	-	-	n.d.	n.d.	4962	1
RCC 97	-	-	n.d.	n.d.	5828	1
RCC 107	-	-	n.d.	n.d.	162	3
RCC 117	-	-	+	n.a.	656	3
RCC 119	-	-	n.d.	n.d.	2567	3
RCC 137	+	+	+	+	5302	1
RCC 139	-	-	n.d.	n.d.	3814	3

Figure S3: Expression of HSD11B1 in tumor infiltrating cells.

Immunohistochemistry slides of RCC patient tumor samples were analyzed for HSD11B1 expression by a pathologist. An HSD11B1 positive staining is represented by +, and negative staining by -. Macrophages and neutrophils were identified by their morphological characteristics as described in the supplementary material and methods. Follow-up period and grade of the disease are indicated for each patient. n.d.: not defined. n.a.: not applicable.

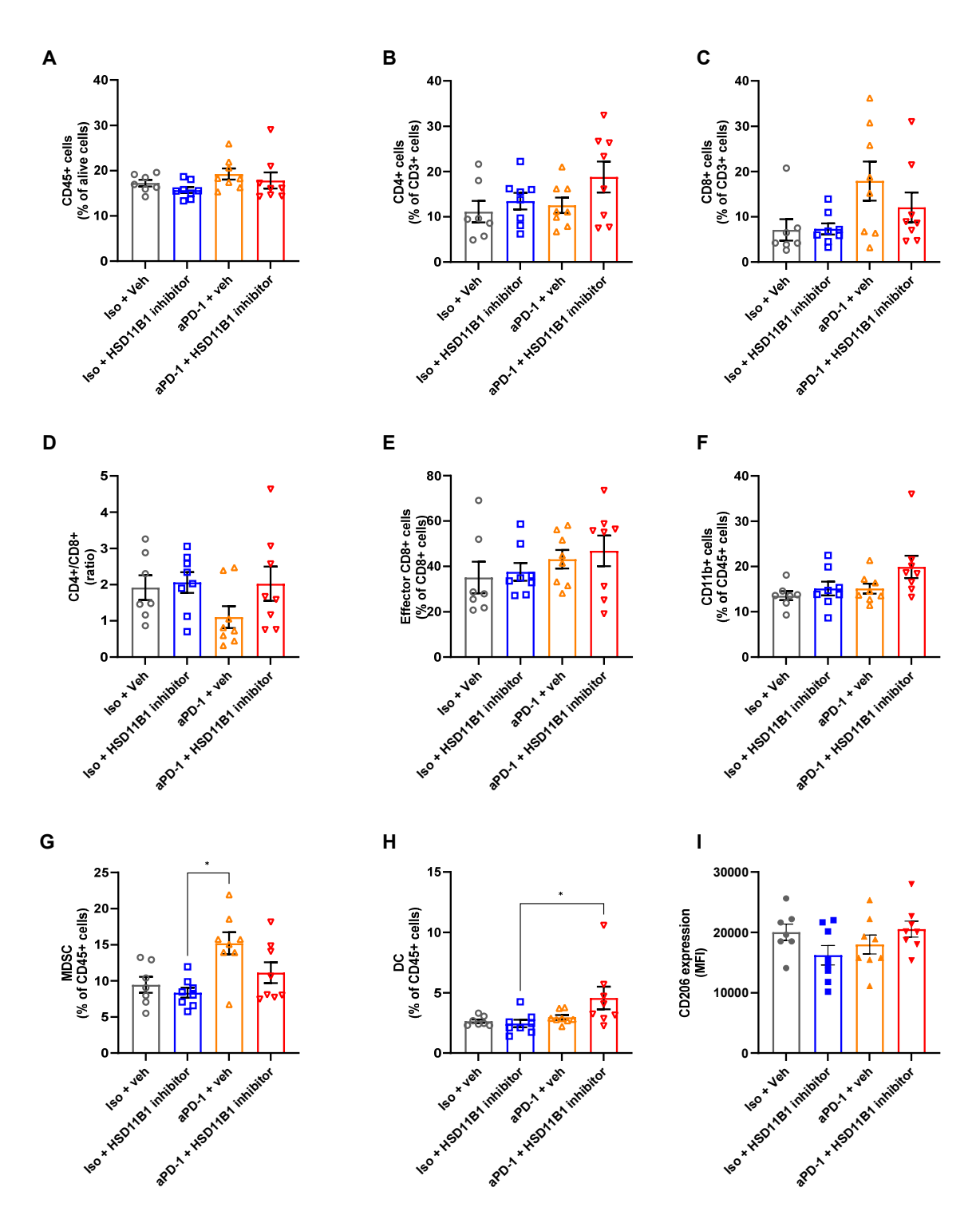


Figure S4: Effect of HSD11B1 inhibition on the tumor immune phenotype in anti-PD-1-treated subcutaneous Renca tumors.

Immunophenotyping of the tumor by flow cytometry. Percentage of each subpopulation represented as % of live cells (**A**) or as % of CD45⁺ cells (**F-H**). Percentage of CD4⁺ and CD8⁺ represented as % of CD3⁺ cells (**B-C**) and as ratio of cell populations (**D**). CD44⁻CD62L⁻ CD8⁺ were defined as effector CD8⁺ cells and represented as % of CD8⁺ cells (**E**). CD206 expression (**I**) represented as mean fluorescence intensity (MFI) of CD206 on macrophages in the tumor. Data are shown as mean +/- SEM of 8 mice per group. * p-value≤0.05.

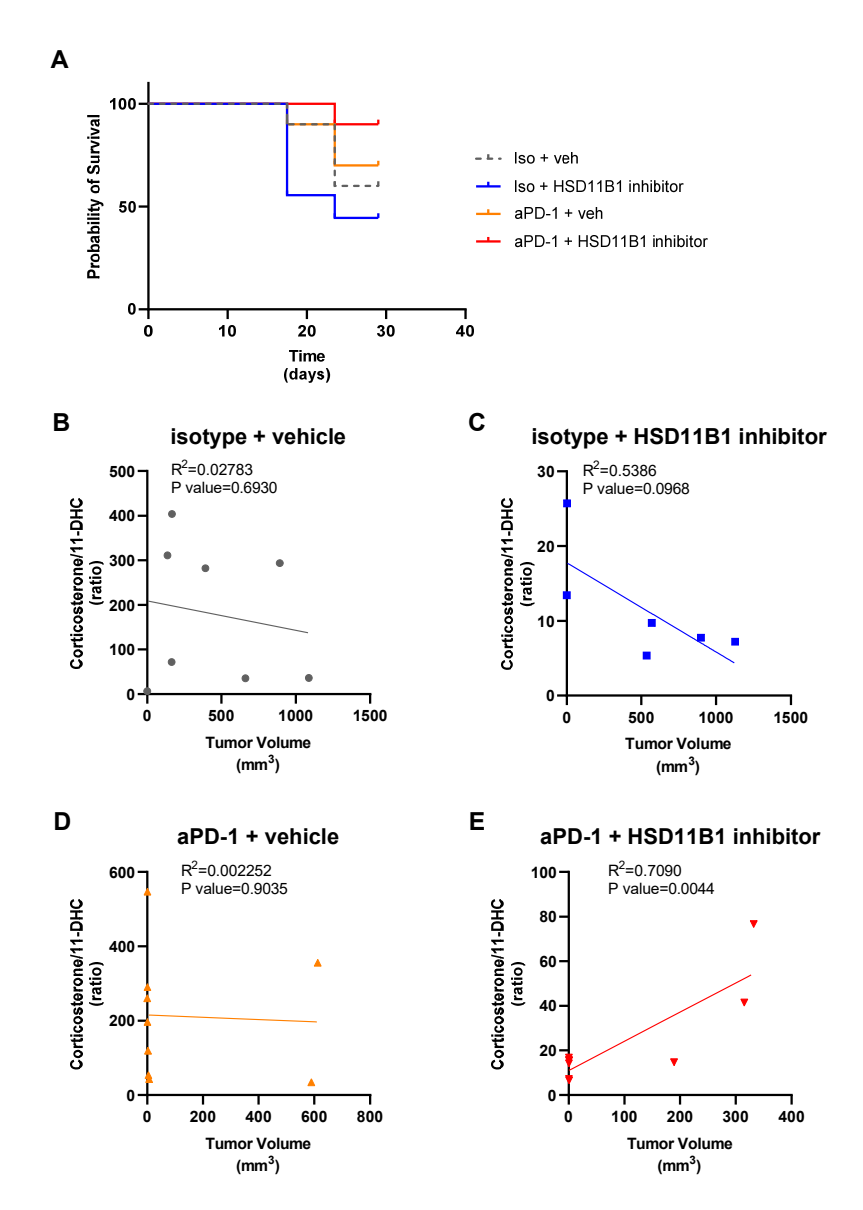


Figure S5: HSD11B1 may improve the efficacy of anti PD-1 treatment in intrakidney tumorbearing mice

A. Growth of intra-renal Renca tumors of the experiment represented in figure 5 C-E. Treatment was initiated at day 7. Kaplan-Meyer curve showing the probability of survival over time. Survival was defined by the tumor metabolic activity measured by PET, with a PET signal over 2 considered as event of death. 10 mice per group. **B-E.** Relationship between corticosterone to 11-DHC ratio in the plasma and last tumor volume before death. 6 to 9 mice per group. Statistical analysis: Simple linear regression.

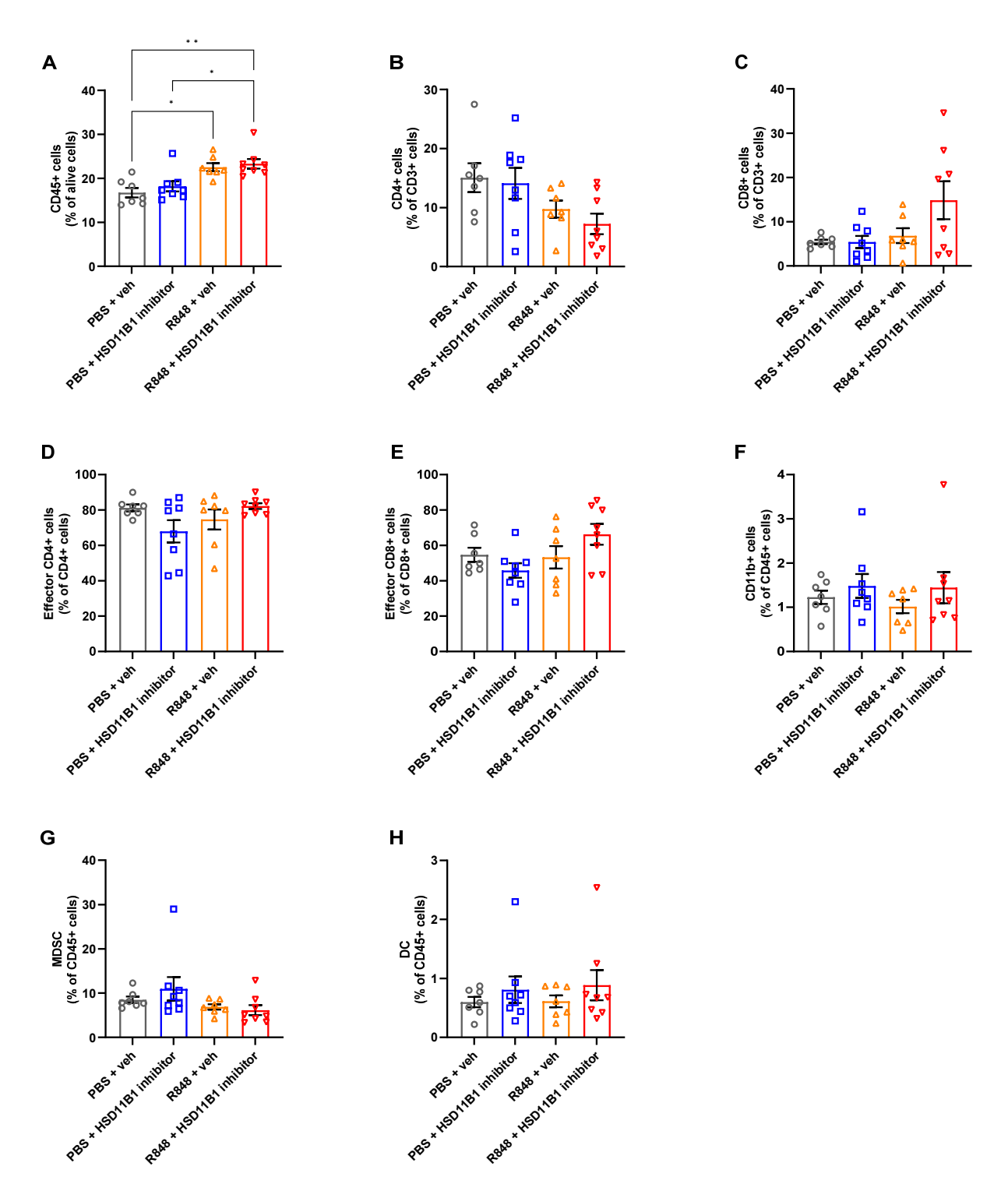
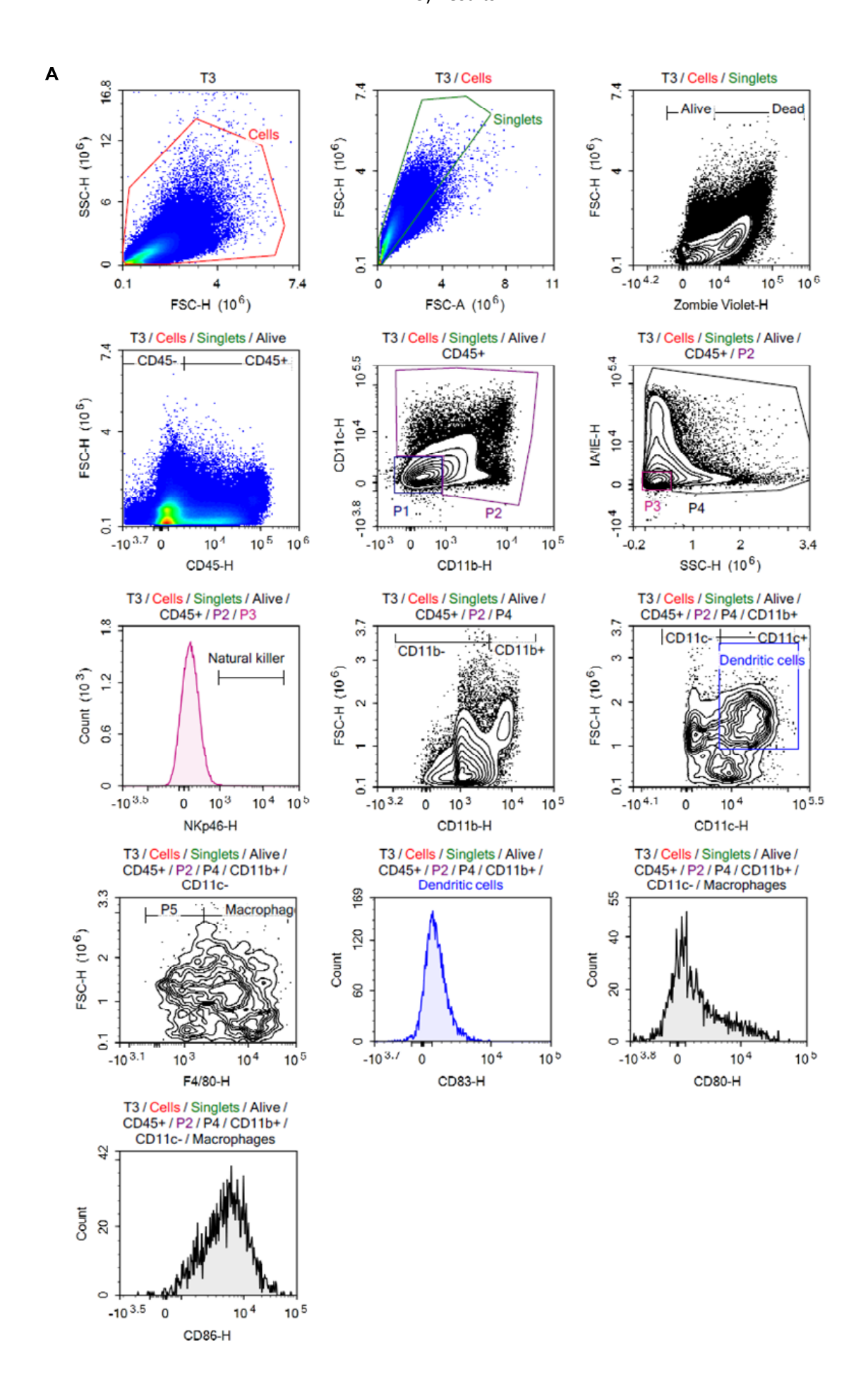
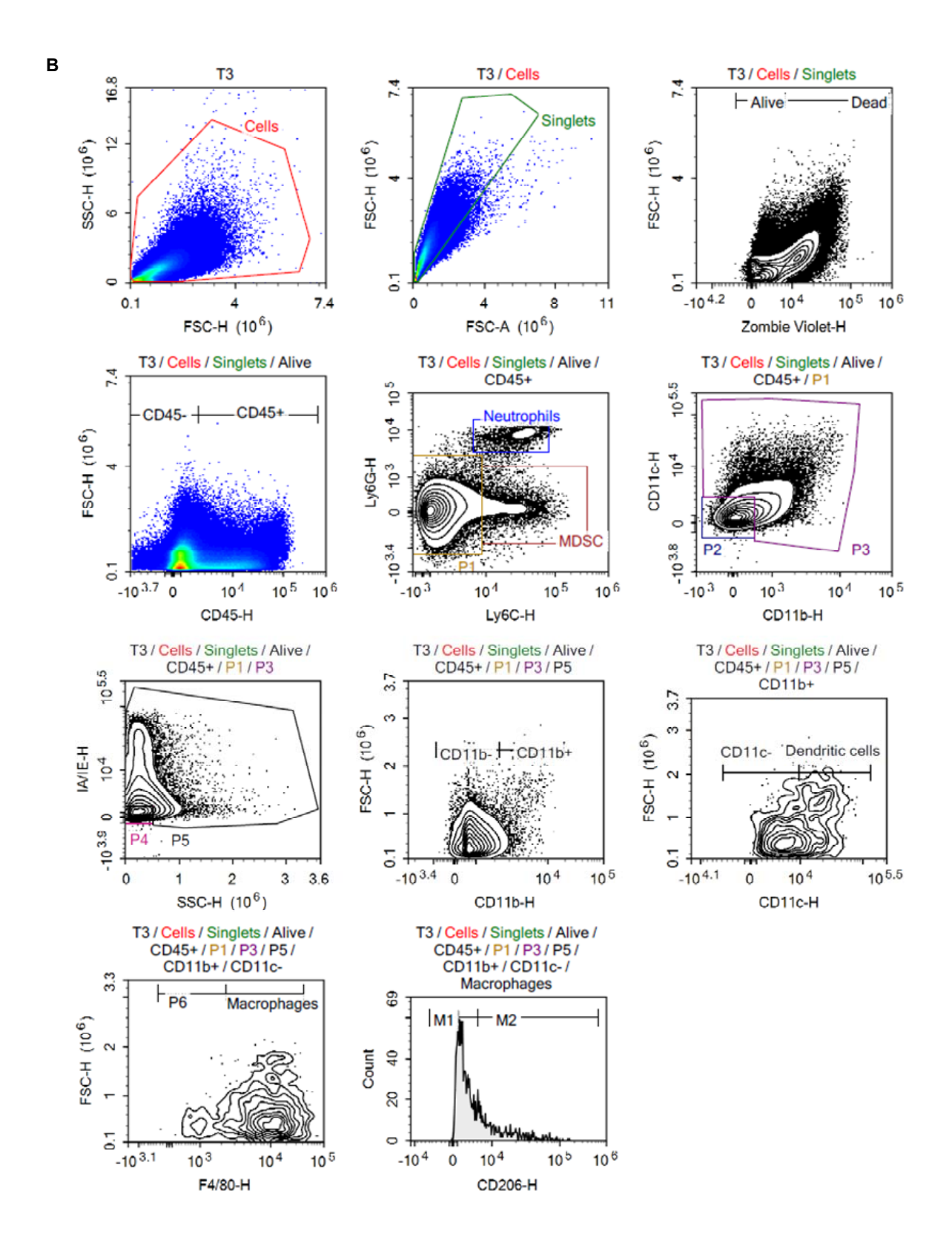


Figure S6: Immunophenotyping of subcutaneous Renca tumors in mice treated with an HSD11B1 inhibitor and the innate immune-activating agent R848.

Immunophenotyping results of the tumor by flow cytometry. Percentage of subpopulations represented as % of live cells (**A**), CD45⁺ cells (**F-H**), CD3⁺ cells (**B**, **C**), CD4⁺ cells (**D**) or CD8⁺ cells (**E**). Data are shown as mean +/- SEM of 7 to 8 mice per group. * p-value≤0.05, ** p-value<10⁻².





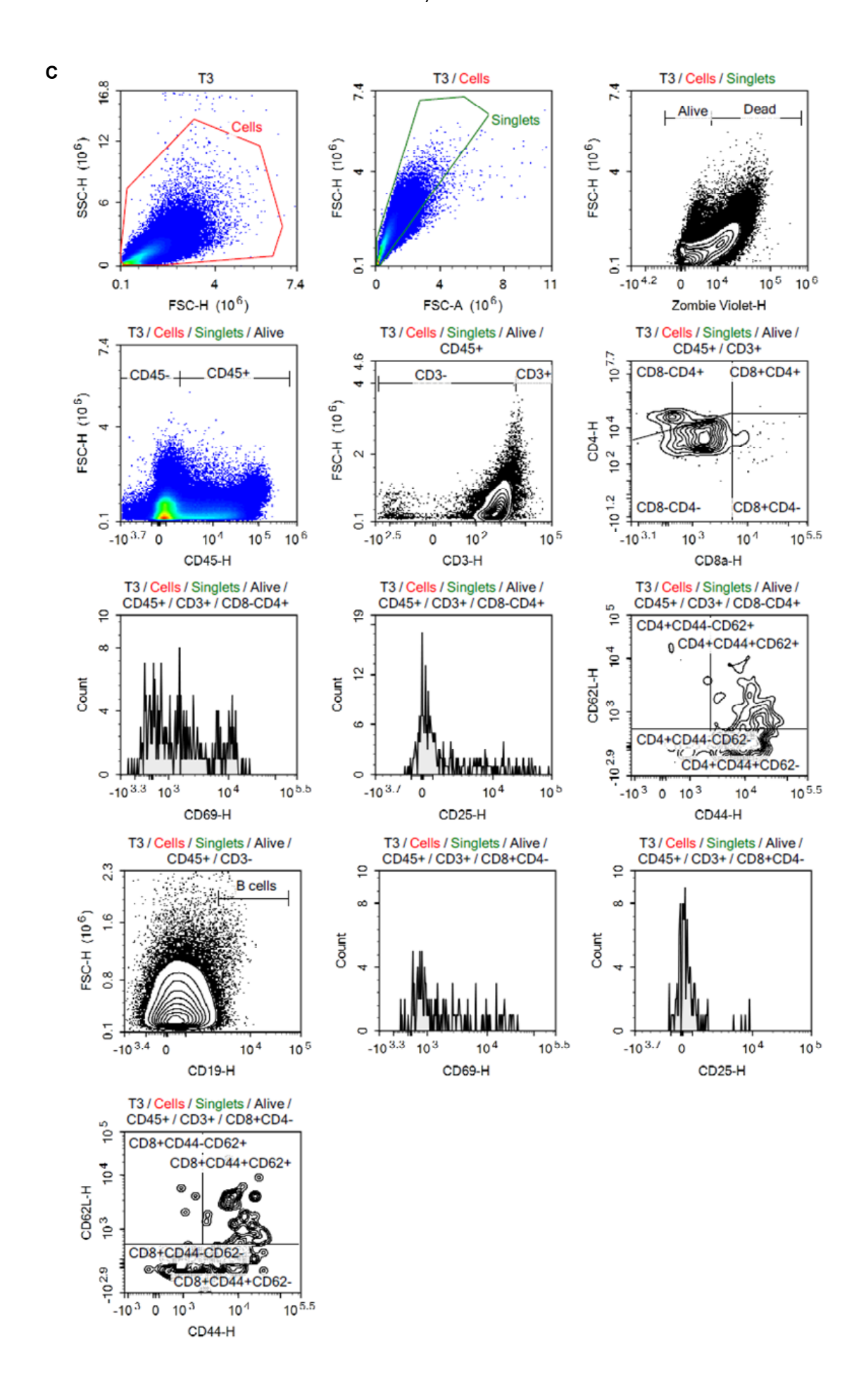


Figure S7: Gating strategies used for immunophenotyping of subcutaneous Renca tumors.

Immunophenotyping results by flow cytometry of the tumor number 3 of the experiment presented in Figure 6. **A.** Gating strategy of the "myeloid activation markers" panel of antibodies. NK cells were identified in this gating strategy by NKp46 positive staining. Activation level of macrophages and DC were defined with CD80, CD86 and CD83 staining. **B.** Gating strategy of the "myeloid population markers" panel of antibodies. Population of MDSC, DC, and macrophages were identified in this gating strategy as explained in the "Flow cytometry" paragraph of material and methods. **C.** Gating strategy of the "lymphoid population markers" panel of antibodies. Population of B cells, CD4+ and CD8+ T cells as well as subpopulations of T cells and their level of activation were defined in this gating strategy.

Supplementary materials and methods

Patient material

The prognostic value of genes involved in steroidogenesis was tested in 533 clear cell renal cancer patients using RNA sequencing and clinical data from the TCGA. Genes involved in steroidogenesis were defined from the steroid hormone biosynthesis pathway from the KEGG pathway database. HSD11B1 staining was performed by immunohistochemistry on FFPE samples from the primary tumors of ccRCC patients from the Geneva University Hospital biobank. 10 patients with poor prognosis and 10 patients with good prognosis were chosen to avoid a selection bias linked to disease stage. For the activation assay of immune cells isolated from RCC patients, RCC tumors were collected by the surgeons at the Geneva University Hospital. The study methodology was reviewed by the Swiss Ethics Committees on Research Involving Humans and approved by the Commission Cantonale d'éthique de la recherche de Genève (2017-00364, to PNS).

Immunohistochemistry

Antigen retrieval was processed for 64 min with EDTA buffer (pH 8) and incubated for 32 min at 1:50 with HSD11B1 polyclonal rabbit antibodies. Primary antibodies were detected with anti-rabbit HRP complex and revealed by diaminobenzidine using automated routine procedures. Brown coloration corresponds to a positive staining.

Counterstained mounted slides were scanned, and HSD11B1 staining was quantitated with DEFINIENS software. Tumoral stained areas were considered as regions of interest (ROI) and were digitally marked. Then the algorithm counted the number of positively stained cells and the total number of cells in each selected ROI. The percentage of positive stained cells was calculated as follows: number of positive cells/total number of cells X 100.

For morphological analysis, macrophages were characterized as large round cells with a non-segmented nucleus shifted to the periphery and an apparent cytoplasm. Neutrophils were characterized as small cells with scant cytoplasm and a tri-lobulated nucleus.

Multiplex immunohistochemistry

FFPE tissue sections were cut at 4 µm and floated onto a 45 C water bath to be mounted on positively charged glass slides. After overnight drying, tissue sections were dewaxed by immersion in xylene, and rehydrated in ethanol of decreasing concentrations. After heat-mediated antigen retrieval of the slides in pH 6 citrate buffer (10 min), endogenous peroxidases, non-specific proteins, endogenous biotins, and avidins were blocked with corresponding blocking solutions from Dako™. Primary antibody was incubated on tissue sections, followed by a biotinylated secondary antibody and a streptavidin-HRP complex revealed by AEC chromogen. Slides were coated with a glass coverslip with an aqueous mounting solution and scanned into MRXS images. Glass coverslips were removed by immersion in hot water, and AEC staining washed in ethanol of increasing concentrations. Antibodies were stripped by boiling tissue sections in pH 6 citrate buffer for 10 to 20 min, and putative residual antibodies were blocked by Fab fragments directed against host of the previous primary antibody used. Then,

multispectral immunohistochemistry was performed which consists of sequential cycles of staining with primary antibodies revealed by AEC chromogen, tissue section scanning, removal of AEC chromogen with ethanol, antibody stripping, and blocking with Fab fragments.

For the image processing, whole slide multiplexed images coming from the same tissue section were processed with an in-house code developed in Matlab R2022b (The MathWorks). Briefly, individual scans were aligned at a cellular level, according to the same reference image by using manual control points. Afterwards, hematoxylin and AEC immunohistochemical chromogenic staining of each image were unmixed and a single multiplexed image was exported.

Human antigen recall assay

PBMC were isolated from buffy coats of healthy donors (Centre de Transfusion Sanguine, Geneva, agreement n°758). Briefly, buffy coats were diluted by a factor 2 in PBS and centrifugated on a density gradient medium (Lymphoprep) at 1200 g for 30 min at room temperature using SepMate tubes. PBMC were collected above the density gradient and washed 3 times in PBS (400 g, 10 min, room temperature). After counting, PBMC were frozen at 1.5x10⁷ cells/mL for subsequent use (working on ice, freezing in Corning CoolCell Freezing container at -80 °C 24 h before storing in liquid N2) or tested for antigen response. Culture medium was filtered through 4 μm filters. The antigens were used at a final concentration of 1 or 0.1 μg/mL for CMV and 0.5 μg/mL for tetanus toxoid. Anti-PD-1 antibody and its isotype control were used at 1 or 0.1 μg/mL. Cortisone was used at a final concentration of 50 ng/mL. For the antigen recall assay, PBMC were thawed, carefully washed in culture medium (or used directly after isolation), counted, added at 2x10⁵ cells/well to a 96-well plate previously prepared with 2 X compounds, and incubated 6 days at 37 °C, 5 % CO₂. Response to antigen was monitored via IFN-γ production measured by ELISA. ABT-384 alone do not activate immune cells with or without Antigen stimulation (data not shown).

Activation assay of immune cells isolated from RCC patients.

Tumors from RCC patients were collected from the surgeon, mechanically and enzymatically (collagenase I and IV) dissociated and immune cells were enriched with a density gradient centrifugation on Lymphoprep medium as for PBMC. After enrichment and washing, cells were seeded in a 96-well plate at 1.92x10⁵ cell/well in wells previously prepared with 2 X compounds. Culture medium was identical to the one used for PBMC, activation was done with a mix of antigens (0.1 μg/mL of CMV, 0.5 μg/mL of tetanus toxoid from Astarte, 0.5 μg/mL of tetanus toxoid from Calbiochem, 300 nM of MPLA), during 6 days of incubation at 37 °C 5 % CO₂. Response to antigen was monitored via IFN-γ production measured by ELISA. One out of the four patients tested showed a response to antigen recall. The absence of T cell activation observed in the three other donors was attributed either to a low level of tumor immune cell infiltration or to the absence of reactivity against cytomegalovirus and tetanus toxoid antigens.

Genetic modification of MHC H2-Kb Renca cell line

The Renca cell line was genetically modified to express MHC H2-Kb Class I instead of MHC H2-Kd Class I normally express in BALB/c background. CRISPR/Cas9 was used to remove the H2-Kd gene and replace by the H2-Kb gene which was brought through a minicircle template as previously described. Modified Renca cells were termed Renca H2-Kb for further usage. Overexpression of *gfp* was performed on the Renca H2-Kb cells using lipofectamine transfection (manufacturer protocol) with plasmid containing *gfp* (plasmid #52961 from Addgene modified to replace *cas9* by *gfp*) and the cells renamed Renca H2-Kb GFP.

Differentiation and activation of bone marrow-derived dendritic cells

Bone marrow from 6 to 15-week-old C57BL/6 mice was flushed out of tibia and femur postmortem. After a 40 μ m filtration, a red-blood-cell lysis was performed on the bone marrow cells. After washing and counting, the cells were incubated at 2.5x10⁶ cells/mL in 6-well plates with 20 ng/mL GM-CSF at 37 C 5 % CO₂ for 2 days (BMDC medium in cell media table at the end of the materials and methods section). At day 2, half of the medium from each well was removed, centrifuged, and the cells resuspended in the same volume of fresh medium with 40 ng/mL GM-CSF and added back to their wells. At the end of day 3, the cells were collected with all the medium, centrifuged and resuspended in the double amount of fresh medium with 20 ng/mL GM-CSF and incubated for 3 additional days at 37 °C. At day 6 of the differentiation process, bone marrow-derived dendritic cells (BMDC) were collected, pooled, washed and distributed in 96-well plates at 1.5x10⁵ cells/well in presence of the following compounds for 24 or 48 h. R848 was used at a final concentration of 100 nM, the HSD11B1 inhibitor (BMS-823778 or ABT-384) at 1 μ M, and 11-dehydrocorticosterone at 20 ng/mL. Cell surface proteins on BMDC were measured by flow cytometry with an antibody panel composed of antibodies against myeloid activation markers. IL-6 concentration in supernatant was measured by ELISA after 24 or 48 h of activation.

Antigen-specific T cell-mediated cytotoxicity of tumor cells

At day 6 of the BMDC differentiation, $2x10^4$ BMDC were seeded in 96-well plates in presence of the BMDC stimulation mix composed of R848 (100 nM) and ovalbumine (25 µg/mL) and treated with 11-DHC or vehicle and HSD11B1 inhibitor or vehicle. At day 7 of the BMDC differentiation, a spleen was collected from a 6 to 15-week-old TCR transgenic OT-I mouse (C57BL/6 background, Charles River), passed through a 40 µm cell strainer, and red blood cell lysis was performed. After washing and counting, CD8+ T cells were isolated through negative selection with a magnetic bead-based isolation kit following the manufacturer's protocol and the purity was checked by flow cytometry. Isolated CD8+ T cells were added to the BMDC at $1x10^5$ cells/well in T cell medium after removing 50 % of the media. At day 9, H2-Kb-recombined Renca GFP+ cells were pulsed with 2 µg/mL of the ovalbumin antigenic peptide SIINFEKL (OVA₂₅₇₋₂₆₄) for 1 h at 37 °C. 2.5x10³ cells were added to the co-culture wells. 3 hours after seeding, the confluency of Renca H2-Kb GFP was measured and used as baseline for further comparison. Renca H2-Kb GFP growth was then followed during 5 days with the Incucyte live-cell analysis system.

Mice

All animal experiments were authorized by Geneva cantonal authorities (Service de la consommation et des affaires vétérinaires) and followed the 3Rs principles to reduce, refine and replace animal experimentation. For subcutaneous tumor experiments, 6-week-old BALB/c mice were injected with 1x10⁶ Renca cells in 100 µL of PBS into the flank. After 5 to 7 days, tumors were palpable and measured with a caliper. Mice were assigned to treatment groups in order to obtain groups of comparable tumor area average, but were not moved from their initial cages to avoid stress and conflict. Area was measured 3 times per week.

For the orthotopic tumor experiment, $100 \, \mu L$ of $0.1 \, mg/kg$ buprenorphine was administered subcutaneously to 6-week-old BALB/c at least 20 min before the intervention. Mice were exposed to 2 % isoflurane for the induction of the anesthesia and 0.5 % to 1 % for the maintenance (in an individual mask on a heating pad). An incision of 0.5 to 0.7 cm was made in the skin of the mouse's flank without opening the peritoneum. The experimenter localized the kidney, pulled and maintained it close to the skin incision, and slowly injected the cells. 10^5 Renca cells in $10 \, \mu L$ were slowly injected into the kidney with a Hamilton syringe (needle of 30 G, 20 mm of length, bevel of $12 \, ^\circ$) with the needle inserted at $30 \, ^\circ$ at a depth of 4 mm (speed of injection around 1 $\mu L/s$, followed by a pause of 5 s before removing the needle). The incision was closed with surgical glue and mice checked twice a day for 3 days. $15 \, days$ after injection, tumor volumes of orthotopic renal cancer model were assessed with magnetic resonance imaging (MRI) and tumor activity was followed by [18 F]FDG-PET/CT imaging once a week. To represent survival, tumor volume >200 mm 3 was considered as event of death in figure 5A and PET signal >2 in figure S5A.

For both subcutaneous and intra-kidney tumor experiments, mice were treated as follow. Treatment of mice was initiated at day 7 after tumor cell injection. The HSD11B1 inhibitor ABT-384 or vehicle (0.5 % methylcellulose, 0.2 % Tween-80) were administered orally once a day in the morning at 10 mg/kg in 200 μ L (with a PTFE feeding needle, 20 G, diameter 1.5 in., length 1.9 mm). Resiquimod (R848) or vehicle (PBS) were injected subcutaneously on two consecutive days repeated every 4 days, at 10 μ g/mouse in 100 μ L. Anti-PD-1 antibodies or isotype were injected intraperitoneally three times a week at 200 μ g/mouse in 200 μ L.

For MRI acquisitions, mice were exposed to 4 % isoflurane for the induction of the anesthesia and 0.5 to 2 % for the maintenance during the scan. 3T MRI acquisitions were performed with a mouse whole body transmit-receiver coil. T2-weighted fast spin echo FatSat images were acquired in the axial plane with acquisition parameters as follows: repetition time 7275 ms, echo time 104 ms, 10 excitations, field of view 40 × 40 mm², acquisition matrix 128 × 128, spatial resolution 0.31 × 0.31 mm², slice thickness 0.5 mm, no interslice gap, bandwidth 25,000 Hz, automatic fat saturation, scan durations 19 min 58 s.

For PET/CT acquisitions, mice were anesthetized with 4 % isoflurane and injected in the retro-orbital venous sinus with 4 to 5 megabecquerel (MBq) of [18F]FDG. Mice were then left awake for an uptake period of 60 min. Mice were anesthetized again with 4 % isoflurane and maintained with 2 % during the scans. Imaging chambers were heated to maintain a body temperature of 37 °C. PET and CT images were acquired on a preclinical PET/SPECT/CT scanner. CT images were obtained at 75 peak

kilovoltage (kVp), 150 mA, and 1'024 projections were acquired during the 360 ° rotation with a field of view of 84.6 mm (1.4 magnification). PET scans were acquired for a total duration of 10 min. CT scans were reconstructed with the built-in Triumph XO software using a filtered back-projection algorithm with a matrix of 512 and a voxel size of 165 μm. PET scans were reconstructed with the built-in LabPET software using an OSEM3D (20 iterations) algorithm, and images were calibrated in Bq/mL by scanning a phantom cylinder. The Imalytics software version 3.0 (Gremse-IT GmbH, Aachen, Germany) was used to quantitatively analyze PET and MRI datasets. CT and PET scans were co-registered and PET series were converted to display standardized uptake values (SUVs) adjusted to the body weight of the animals. Maximum SUVs (maxSUVs) were quantified in the regions of interest corresponding to renal tumors and used in subsequent analyses. MRI images were used to quantify tumor volumes by tracing renal tumors.

Steroid hormone determination in plasma

To measure steroid hormone concentrations in the plasma, blood was terminally collected from mice through cardiac puncture immediately after CO₂ euthanasia. Blood was collected in a heparin tube and kept on ice until centrifugation (2000 g, 10 min, 4 °C). The plasma corresponding to the upper phase was collected into clean tubes and snap frozen for mass spectrometric analysis of steroids²⁵⁵. Plasma samples were purified using solid phase extraction on an OasisPrime HLB 96-Well Plate. A Vanquish UHPLC (equipped with an ACQUITY UPLC HSS T3 Column, 100 Å, 1.8 μm, 1 mm x 100 mm column) was coupled to a Q Exactive Plus Orbitrap. Separation was achieved using gradient elution over 12 min using water and methanol both supplemented with 0.1 % formic acid (all Sigma-Aldrich, Buchs, Switzerland) as mobile phases. Data analysis was performed using TraceFinder 4.1 (Thermo Fisher Scientific, Reinach, Switzerland). Steroid hormone concentrations were calculated in nmol/L.

Tumor collection

Tumors were collected post mortem, weighed and divided for subsequent RNA analysis (snap freezing on dry ice) or flow cytometry analysis. To obtain cell suspensions for flow cytometry, tumors were digested in 1 mL of tumor dissociation enzyme mix in Gentle MACS C tubes with the program 37C_m_TDK_2 of the Gentle MACS Dissociator. After digestion, enzymes were inactivated with 10 mL of medium containing FBS, and the tumor suspension was filtered through a 40 µm cell strainer before washing in PBS and aliquoting in 96-well plates for subsequent staining. Each tumor suspension was separately stained with 3 different antibody panels: myeloid population markers, myeloid activation markers, or lymphoid population markers.

Pharmacodynamics of ABT-384

During 5 days, naive 6-week-old BALB/c males were treated with ABT-384 (synthetized by Spirochem) or vehicle (0.5 % methylcellulose, 0.2 % Tween-80) orally once daily in the morning at 10 mg/kg in 200 μ L (with a PTFE feeding needle, 20 G, diameter 1.5 in., length 1.9 mm). The last day, mice were subcutaneously injected with 360 μ g of cortisol-d4 (hydrocortisone-9,11,12,12-d4) in 200 μ L (15 mg/kg, dilution at 1.8 mg/mL in PBS+DMSO (6.8 %)) 6 hours after ABT-384 treatment. Cortisol-d4 is converted into cortisone-d3 *in vivo* by HSD11B2 which is the substrate of HSD11B1. Cortisone-d3 is then

converted into cortisol-d3 by HSD11B1. Conversion into cortisol-d3 was measured to assess HSD11B1 activity. Mice were euthanized 2.5 to 3.5 hours after cortisol-d4 injection and blood was collected post-mortem.

Steroid hormone determination in kidney and plasma after cortisol-d₄ injection

Mouse kidneys were collected post mortem and frozen on dry ice. For liquid chromatography-mass spectrometry (LC-MS), 400 μ L of aqueous 0.1 % formic acid were added to 150 mg of frozen tissue and homogenized with a tissue homogenizer (30 Hz, 2 min, 4 C). Then, 800 μ L of cold acetonitrile were added to precipitate proteins. After vortexing (10 s) and centrifugation (10 min, 13000 rpm, 4 °C), 250 μ L of supernatant were collected. 10 μ L of internal standard solution (aldosterone-d7 at 1 μ g/mL) were added and liquid-liquid extraction (LLE) was conducted by adding 0.5 mL of sodium phosphate buffer (1 M, pH 7), 2 mL of saturated NaCl, and 250 μ L of K₂CO₃ (25 % w/v). After vortexing for 5 s, 6 mL of ethyl acetate were added and the tubes placed into a rotary mixer for (30 min, 35 rpm) for LLE extraction. After centrifugation (10 min, 3500 rpm, and 4 °C), the organic phase was transferred into fresh tubes and evaporated until dryness at reduced pressure. Samples were reconstituted with 100 μ L of water:acetonitrile (50:50 v/v), centrifuged again (10 min, 13000 rpm, 4 °C) and supernatants were transferred to liquid chromatography (LC) vials for injection.

Plasma was collected as described above. Then, 10 μ L of internal standard (aldosterone-d7 at 1 μ g/mL) were added to 100 μ L of plasma, and the samples were processed for LLE as for the kidney samples.

LC-MS measurements were performed on an Agilent Infinity 1290 UHPLC system consisting of a binary solvent delivery pump, a flexible cube module, a flow-through-needle autosampler, and a column oven. The LC was coupled to an Agilent G6490A triple quadrupole mass spectrometer through an Agilent Jet Stream ESI source. Data was acquired in dynamic multiple reaction monitoring (dMRM).

All separations were conducted on a Phenomenex core-shell column (Kinetex C18 100 Å, 2.1 x 150 mm, 1.7 μ m, Phenomenex, Torrance, USA) equipped with the corresponding pre-column, and using water (A) and acetonitrile (B) as mobile phases, both containing 0.1 % formic acid and applying a gradient from 2 % to 100 % B in 14 min. The column temperature and flow rate were set at 30 °C and 300 μ L·min⁻¹, respectively.

Source conditions were: gas temperature 250 °C, gas flow 14 L·min⁻¹, nebulizer pressure 20 psi, sheath gas heater 400 °C, sheath gas flow rate 11 L·min⁻¹ and capillary voltage 3000 V.

Mass spectrometric conditions (MS/MS transitions, cone voltage, collision energy) were optimized using the Optimizer version B.08.00 software (Agilent Technologies, Santa Clara, US) by flow injection analysis of individual steroid standard (1 μ g·mL⁻¹) using a mixture of water:acetonitrile (50:50 v/v) containing 0.1 % formic acid at a flow rate of 100 μ L·min⁻¹. The obtained precursor and product ions, the collision energies (CE) and retention times monitored for each compound are reported in the table below. For all transitions, precursor and product ion selection was performed with a resolution of 0.7 Da. Two transitions (quantifier and qualifier) of the main isotopic form for analytes and internal standard

were selected for quantification and confirmation. Data acquisition and instrument control were performed using MassHunter version B.08.00 (Agilent Technologies, Santa Clara, US).

The y-axis of Figure 4A and 5B represents the intensity of the mass spectrometry signal of cortisol-d3 corrected by the one from the internal standard (aldosterone-d7). Raw values for steroid quantification were normalized by the weight of each kidney tissue sample.

Retention	Name	Prec Ion	Prod Ion	CE (\(\)	Polarity
time (min)	Name	(<i>m/z</i>)	(<i>m/z</i>)	CE (V)	lolanty
6.21	Aldosterone-d ₇ (internal	366.2	338.2	12	NEG
0.21	standard)	368.2	350.4	16	POS
6.60	Cortisol-d ₃	366.2	121.1	24	POS
0.00	Ooi tisoi-uş	366.2	97.1	44	POS
6.61	Cortisol-d ₄	367.2	121.1	24	POS
0.01	O0111301-04	367.2	97.1	44	POS
6.65	Cortisol	363.2	121.0	36	POS
0.00	Oortisor	363.2	109.1	36	POS
6.65	Cortisol- ¹³ C ₃	366.2	312.0	12	POS
0.00	O0111301- 03	366.2	124.1	24	POS
6.72	Cortisone-d ₃	364.2	121.0	32	POS
0.72	Oortioone d ₅	364.2	97.0	40	POS
6.75	Cortisone	361.2	163.0	20	POS
0.70	Oortioone	361.2	121.0	28	POS
6.75	Cortisone- ¹³ C ₃	364.2	166.0	24	POS
0.75	Oortisone- Os	364.2	124.2	32	POS
7.58	Corticosterone	347.0	239.0	12	POS
7.50	001110001010110	347.0	112.0	36	POS
7.35	11-Dehydrocorticosterone	345.0	121.1	28	POS
7.00	11 Delly droot droot crone	345.0	107.0	48	POS

Flow cytometry

Cells were stained with a Zombie viability marker in PBS during 20 min at 4 °C in the dark. After PBS wash (400 g, 5 min, 4 °C), the cells were resuspended in the antibody panels and incubated 15 min at 4 °C. Samples were read with a Novocyte3000 (violet, blue and red lasers, 13 colors) and analysis done with NovoExpress Software.

Gating strategies for the 3 antibody panels are shown in Figure S7. MDSCs were defined as CD45+ Ly6C+ and removed from the following analysis as presented in the gating strategy of the "myeloid population markers" panel (Figure S7B). Macrophages were defined as CD45+ CD11b+ CD11c- F4/80+ as presented in the gating strategy of the "myeloid population markers" panel (Figure S7B). DC were

defined as CD45+ CD11b+ CD11c+ as presented in the gating strategy of the "myeloid population markers" panel (Figure S7B).

Statistical analyses

All statistical analyses were performed using GraphPad Prism software except the hierarchical clusters and heat maps which were generated by using TIBCO Spotfire.

For the TCGA data analyses, patients were dichotomized into two groups based on the high versus low expression of each individual genes (median as threshold). The impact of the expression level on overall survival (OS) was assessed using the Cox proportional-hazards model in GraphPad Prism. All the analyzed genes were ranked according to their p-value and plotted with their hazard ratio (HR) generated by the Cox regression model. HR were used to estimate the probability of an event (death of the patient) occurring in the high and low group of patients. HR are represented with 95 % confidence interval. A HR > 1 favors patients with low gene expression. In hierarchical clustering analysis, patients were ranked according to the level of expression of genes involved in glucocorticoid metabolism (AKR1C4, CYP21A2, HSD11B1, HSD11B2). The Ward's clustering method was used, with half-square Euclidean for the distance measure, mean value for the ordering of gene expression, and Z score calculation for the normalization and correlation of OS was shown using Kaplan-Meyer plot based on the identified clusters. A Gehan-Breslow-Wilcoxon test was used to assess the difference of survival between the groups. Immune infiltrate analysis was performed on the five clusters of patients already identified by hierarchical clustering analysis. For this, the mRNA expression of immune checkpoints (PDCD-1, LAG-3, and CTLA-4) was evaluated in each patient as well as a Th2 gene signature. 256 The expression levels for immune checkpoints and the Th2 gene signature in patients with high vs low HSD11B1 expression were compared with a multiple unpaired t test, two-stage step-up, desired FDR = 1 %.

For all the comparisons of quantitative variables in conditions involving more than one categorical variable, data were analyzed with ordinary two-way ANOVA, alpha 0.05, Tukey's multiple comparison tests (IFN-γ concentrations in Fig 3 A and B, tumor surfaces in Fig 4 B and Fig 6 A, expression of CD86 and MHCII and percentage of growth in Fig 7 C, D and E).

For parameters not following normal distribution, a Wilcoxon test with two-tailed p-value was performed (corticosterone/11-DHC ratio in plasma and kidney in Fig 5 A). When multiple comparisons were needed, a Kruskal-Wallis test were performed with Dunn's multiple comparison tests (immunophenotyping results of the tumor in Fig 4 C and D, and in Fig 6 B-D, corticosterone/11-DHC ratio in plasma in Fig 5 D).

For parameters following normal distribution, an unpaired t test with two-tailed p-value was performed (cortisol-d₃ levels in plasma (Fig4 A) and in kidneys (Fig 5 B)).

Cell media

Medium	Product	Provider	Ref. number
	RPMI	Gibco	21875034
	10 % FBS		
PBMC culture	1 % MEM Non-Essential Amino Acids	Gibco	11140035
medium	10 mM Hepes	Gibco	15630056
	100 U/mL penicillin/streptomycin	Gibco	15140122
	2 mM L-glutamine	Gibco	25030024
PBMC freezing	PBMC culture medium		
medium	40 % FBS		
medidiii	10 % DMSO		
	PBS		
FACS buffer	0.5 % BSA		
	2 mM EDTA		
	RPMI	Gibco	21875034
	10 % FBS		
BMDC	100 U/mL penicillin/streptomycin	Gibco	15140122
medium	2 mM L-glutamine	Gibco	25030024
	0.5 mM sodium pyruvate	Gibco	11360039
	50 μM 2-mercaptoethanol	Gibco	31350010
	RPMI-Very low endotoxin	Bioswisstec AG	M3440
	10 % FBS		
	100 U/mL penicillin/streptomycin	Gibco	15140122
	2 mM L-glutamine	Gibco	25030024
T cell medium	1 mM sodium pyruvate	Gibco	11360039
	1 % MEM Non-Essential Amino Acids	Gibco	11140035
	50 μM 2-mercaptoethanol	Gibco	31350010
	0.5 % BSA		
	2 mM EDTA		

FACS panels

Panel	Antibody	Dilution in FACS buffer	Provider	Ref. number
	anti-mouse CD16/32	1/100	Biolegend	101319
mouse BMDC	anti-CD11c	1/200	Biolegend	117331
activation	anti-CD80	1/200	Biolegend	104729
	anti-PD-L1	1/200	Biolegend	124331

	anti-MHC II	1/200	Miltenyi	130-102-168
	anti-CD40	1/200	eBioscience	12-0401-82
	anti-CD11b	1/200	BD Bioscience	550993
	anti-MHC I	1/200	eBioscience	17-5958-80
	anti-CD86	1/200	Biolegend	105030
	anti-mouse CD16/32	1/100	Biolegend	101319
	anti-CD3	1/200	Biolegend	100203
mouse T cell purity	anti-CD8a	1/200	Biolegend	100708
	anti-CD4	1/200	Biolegend	100559
	anti-CD19	1/200	Biolegend	115512
	anti-mouse CD16/32	1/100	Biolegend	101319
	anti-CD45	1/200	Biolegend	103154
4	anti-Ly6C	1/200	Biolegend	128033
mouse tumor	anti-CD11b	1/200	Biolegend	101233
immunophenotyping:	anti-IA/IE	1/200	Biolegend	107641
myeloid population markers	anti-CD206	1/200	Biolegend	141710
markers	anti-F4/80	1/200	Biolegend	123146
	anti-Ly6G	1/200	Biolegend	127616
	anti-CD11c	1/200	Biolegend	117318
	anti-mouse CD16/32	1/100	Biolegend	101319
	anti-CD45	1/200	Biolegend	103154
	anti-CD11b	1/200	Biolegend	101233
mouse tumor	anti-CD80	1/200	Biolegend	104729
immunophenotyping:	anti-IA/IE	1/200	Biolegend	107641
myeloid activation	anti-CD86	1/200	Biolegend	105043
markers	anti-NKp46	1/200	Biolegend	137604
	anti-F4/80	1/200	Biolegend	123146
	anti-CD11c	1/200	Biolegend	117318
	anti-CD83	1/200	Biolegend	121510
	anti-mouse CD16/32	1/100	Biolegend	101319
	anti-CD45	1/200	Biolegend	103154
	anti-CD69	1/200	Biolegend	104532
mouse tumor	anti-CD44	1/200	Biolegend	103049
immunophenotyping:	anti-CD19	1/200	Biolegend	115543
lymphoid population	anti-CD3	1/200	Biolegend	100203
markers	anti-CD62L	1/200	Biolegend	104408
	anti-CD8a	1/200	Biolegend	100762
	anti-CD4	1/200	Biolegend	100422
	anti-CD25	1/200	Biolegend	102012

Reagents

Experiment	Product	Provider	Ref. number	
Immunohistochemistry	Polyclonal rabbit antibodies of HSD11B1	Sigma	HPA 042186	
Multiplex	Thermoscientific Superfrost™ Gold Plus	Thermofischer,		
immunohistochemistry glass slides		Massachusetts, USA		
	SepMate tubes	StemCell	85450	
	CMV	Astarte	1004	
	Tetanus toxoid	Astarte	1002	
Human antigen recall	Tetanus toxoid	Calbiochem	582231-25UG	
assay	Anti-PD-1, Humanized Antibody	BioVision	A1306	
assay	Human IgG4, κ Isotype Control Antibody	BioVision	A1101	
	Cortisone	Sigma	C2755	
	ELISA MAX™ Standard Set Human IFN- γ	Biolegend	430101	
Tumor-derived immune	MPLA	Avanti	699800P-1MG	
cell activation	MPLA	Avanti	099800F-1101G	
Genetic modification of Renca cells	Lipofectamine™ 2000	Invitrogen	11668019	
Differentiation and activation of BMDC	ELISA MAX™ Standard Set Mouse IL-6	Biolegend	431301	
Antigen-specific T cell-	ovalbumine	Invivogen	Vac-pova-100	
mediated tumor	CD8a+ T Cell Isolation Kit, mouse	Miltenyi	130-104-075	
cytotoxicity assay	SIINFEKL	Invivogen	vac-sin	
<i>In vivo</i> tumor model	R848	Invivogen	tlrl-r848-5	
III vivo tumoi modei	Surgical glue, VetBond		1469SB	
Storoid magaziroment in	heparin tube	BD	365966	
Steroid measurement in	OasisPrime HLB 96-Well Plate	Waters, UK		
plasma	ACQUITY UPLC HSS T3 Column	Waters, Switzerland		
Tumor processing for	Tumor Dissociation Kit, mouse	Miltenyi	130-096-730	
immunophenotyping	Gentle MACS C tube	Miltenyi	130-096-334	
FACS staining	Zombie Violet™ Fixable Viability Kit	Biolegend	423113	

Instruments

Experiment	Machine	Provider
Immunohistochemistry	Ventana System on Automates Benchmark Ultra	Roche
Multiplex immunohistochemistry	Pannoramic 250 Flash III scanner	3D Histech, Budapest, Hungary

Mouse MRI	nanoScan	Mediso, Medical Imaging Systems, Budapest, Hungary
Mouse PET	Triumph	Trifoil Imaging, Chatsworth, USA
Steroid measurement in	Vanquish UHPLC	Thermo Fisher Scientific, Reinach, Switzerland
plasma	Q Exactive Plus Orbitrap	Thermo Fisher Scientific, Reinach, Switzerland
Steroid measurement in kidney and plasma after cortisol-d ₄ injection	Agilent Infinity 1290 UHPLC system	Agilent Technologies, Santa Clara, US

References:

References are included in the Bibliography of the Thesis.

II. HSD11B1 inhibitors for use in immunotherapy and the uses thereof

II.A. Introduction and contributions

Numerous HSD11B1 inhibitors have already been developed in the clinic, especially within the scope of metabolic diseases, as explained in 1)III.D.2.b. However, none of these pharmacological inhibitors have been pursued in the clinic. To improve anti-PD-1 response, we hypothesized that HSD11B1 could be a pharmacological target for removing immune suppression by decreasing glucocorticoid levels. Thus, the repurposing of selective HSD11B1 inhibitors in cancer treatment was considered based on our findings. Therefore, to protect the use of HSD11B1 inhibitors in combination with immune checkpoint blockade, a patent has been filed,²⁵⁷ which is presented below, followed by some supplementary data.

The authors' contributions to this work are detailed as follows:

Aurélien Pommier, Carole Bourquin, and Hélène Poinot designed and planned the study. Aurélien Pommier and Carole Bourquin are the inventors of the patent. Hélène Poinot performed and analyzed the experiment's proof of concept with PBMCs (Figure 1 and supplementary results). Aurélien Pommier performed and analyzed the experiment with tumor cell killing with the help of Montserrat Alvarez (Figure 2). Aurélien Pommier supervised the study. Aurélien Pommier wrote the application with the help of attorneys (Reuteler & cie) and Hélène Poinot.

II.B. Patent WO2021180643

Field of the invention

The present invention relates to the agents useful in combination with immunotherapy, in particular for increasing responsiveness to immunotherapy treatments. The invention further relates to methods and compositions useful in the treatment of cancers, in particular solid tumor cancers.

Background

Immunotherapy of cancer aiming to stimulate the immune system against tumor cells has seen unprecedented success in recent years. The term immunotherapy regroups several therapeutic approaches including the use of immune checkpoint inhibitors, cell transfer therapies, monoclonal antibodies, treatment vaccines, immune system modulators and immunoconjugates. Although the use of immunotherapy is increasing, an objective clinical response is still observed only in a minority of patients. The determinant factors driving resistance to immunotherapy are not fully understood and the identification of immunosuppressive molecular pathways able to reduce the efficacy of immunotherapy is of high interest to improve clinical outcome of patients with cancer. Biological processes critical to antitumour immunity, such as interferon signalling, antigen presentation (Kalbasi et al., 2020, Nat Rev Immunol, 20(1), 25-39), loss of MHCI or mutation in beta-2 microglobulin and PD-L1 (Programmed death-ligand 1) expression in tumors (Syn, et al., 2017, Lancet Oncol, 18(12), e731e741) have been described as important factors involved in sensitivity to immunotherapy. Other efforts have shed light on the immunological implications of canonical cancer signalling pathways, such as WNT-β- catenin signalling, cell cycle regulatory signalling, mitogen- activated protein kinase signalling and pathways activated by loss of the tumour suppressor phosphoinositide phosphatase PTEN (Phosphatase and tensin homologue on chromosome 10) in the context of immune checkpoint inhibitors treatment (Kalbasi et al., 2020, supra). In the field of adoptive cell therapies, growing experience with these agents has revealed that limitations to durable remissions after chimeric antigen receptor (CAR) T cell therapy includes poor CAR T cell persistence in leukemia (Shah et al., 2019, Nat Rev Clin Oncol, 16(6), 372-385). CAR T cell persistence is also considered as an important obstacle to overcome in order to reach efficacy of adoptive T cell therapies in solid tumors (Shah et al., 2019, supra).

Acquired resistance to checkpoint inhibition such as anti-PD-1 therapy is also a problem, with approximately one quarter of responders who later present a disease progression (*Ribas et al., 2016, JAMA, 315:1600–9*).

Therefore, it is critical to identify and target novel biological mechanisms involved in resistance to immunotherapy.

Endogenous glucocorticoids are steroid hormones derived from cholesterol, which have diverse physiological effects. In humans, cortisol is the main active glucocorticoid which controls several biological mechanisms in cells by binding to the glucocorticoid receptor. The activated glucocorticoid receptor-cortisol complex up-regulates the expression of target genes in the nucleus (a process known as transactivation) and represses the expression of genes involved in inflammation and immune response by preventing the translocation of other transcription factors such as NF-kB and AP1 (transrepression). Glucocorticoid receptor is expressed in key immune cells involved in antitumor immunity such as T cells (*Purton et al., 2004, J. Immunol, 173(6), 3816-24*), dendritic cells and macrophages (*Heasman et al., 2003, J. Endocrinol, 178(1), 29-36*).

The activation of glucocorticoid receptor depends on the regulation of cortisol bioavailability. At systemic level, glucocorticoids are first secreted by the adrenal gland in response to hypothalamic pituitary stimulation. Second, the human liver/splanchnic bed contributes between 20 and 40% of daily cortisol production (*Andrew et al., 2002, J. Clin. Endocrinol. Metab., 87(1), 277-85; Basu et al., 2004, Diabetes, 53(8), 2051-9*) thus making a major impact on the half-life of cortisol. In tissues, the level of active cortisol can be controlled by 11-beta-hydroxysteroid dehydrogenase Type 1 (HSD11B1) and Type 2 (HSD11B2) enzymes. HSD11B1 is a low affinity enzyme with Km for cortisone in the micromolar range that prefers NADPH/NADP- (nicotinamide adenine dinucleotide phosphate) as cofactors. HSD11B1 is widely expressed with a distribution similar reported in rodents, non-human primates and humans (*Agarwal et al., 1989, J. Biol. Chem, 264(32),18939-43; Moisan et al., 1990, J. Neuroendocrinol, 2(6), 853-8; Tannin et al., 1991, J. Biol. Chem, 266(25), 16653-8*).

HSD11B1 expression is found in liver (*Tannin et al., 1991, supra; Moisan et al., 1990, Endocrinology, 127(3), 1450-5*), brain (*Moisan et al., 1990, supra; Lakshmi, et al., 1991, Endocrinology, 128(4), 1741-8*), uterus (*Burton et al., 1998, Endocrinology, 139(1), 376-82*), placenta (*Waddell et al., 1998, Endocrinology, 139(4), 517-23*), adipose tissues (*Bujalska et al., 1997, Lancet, 349(9060): p. 1210-3*), skeletal muscle (*Whorwood et al., 2002, Diabetes, 51(4), 1066-75*), heart (*Walker et al., 1991, Endocrinology, 129(6), 3305-12*) and immune and inflammatory cells (*Gilmour et al., 2006, J. Immunol., 176(12), 7605-11*). Most studies have shown that HSD11B1 functions primarily as a reductase in intact cells converting inactive 11-ketoglucocorticoids (i.e., cortisone or dehydrocorticosterone) to active 11-hydroxycorticoids (i.e., cortisone or corticosterone), and thereby amplifies glucocorticoid action in a tissue-specific manner.

Importantly, glucocorticoids have both anti-inflammatory and immunosuppressive activity. The intensity of their immunomodulatory effect depends not only on circulating levels but also on the tight regulation at the pre-glucocorticoid receptor level where HSD11B1 and HSD11B2 have a critical impact.

In recent years, glucocorticoids have gained interest in the field of cancer research. Studies in breast, prostate and ovarian cancer have shown a correlation between high levels and activity of GR in tumors and poor outcome (*Arora et al., 2013, Cell, 155(6),1309-22; Pan et al., 2011, Cancer Res, 71(20), 6360-70; Veneris et al., 2017, 146(1), 153-160*).

HSD11B2 catalyses the conversion of cortisol to the inactive metabolite cortisone modulating thereby the intracellular glucocorticoid levels. HSD11B2 is mainly expressed and active in the kidney and its primary function is to protect the nonselective mineralocorticoid receptor from occupation by glucocorticoids. *Cirillo et al., 2017, British Journal of Cancer, 117, 984-993* raised the possibility that different tumor cell types can produce cortisol and that it was possible to modulate the bioavailability of cortisol by manipulation of HSD11B2.

Zhang et al., 2005, J. Immunol, 174(2), 879-89 demonstrate that inhibition of HSD11B1 in T cell increases their activation levels, while Rocamora-Reverte et al. 2017, Cell Death Dis, 8(7), e2948 showed that activation of glucocorticoids by HSD11B1 in T cells participates to autonomous cell death.

Inhibition of 11-beta-hydroxysteroid dehydrogenase enzymes in a living system has been described for the treatment of various conditions by the administration of an inhibitor of conversion of cortisol-to-cortisone or of an inhibitor of conversion of cortisone-to-cortisol (WO 2004/027047). WO 2006/097337 described the generation of specific inhibitors against HSD11B1 and/or HSD11B2 to either selectively or combined inhibition of the enzymes and to allow fine tuning of local cortisol levels to compensate for cortisol excess or deficiencies. It indicated that the use of inhibitors against HSD11B2 would be preferred for the treatment of cancer and/or cell proliferation.

The preferred inhibition of HSD11B2 claimed in WO 2006/097337 was based on the direct antiproliferative effect of cortisol on tumor cells. Indeed, since HSD11B2 could provide an enzymatic shield that may protect the tumor cells from the antiproliferative effects of the glucocorticoids, the specific inhibition of HSD11B2 over HSD11B1 was preferred. However, based on the low number of patients currently responding to immunotherapy (only about 20-40% of patients respond to immunotherapy as reported by *Sharma et al., 2017, Cell 168(4), 707–723)*, there is still a critical need to discover novel therapeutic methods to improve the efficacy of immunotherapy that would overcome these shortcomings.

Summary of the Invention

The invention is based on the unexpected finding that resistance to immunotherapy can derive from a reduced efficacy of the antitumor immune response which is induced by the enzymatic conversion of inactive 11-ketoglucocorticoids (i.e., cortisone or dehydrocorticosterone) to active 11-hydroxycorticoids (i.e., cortisone or corticosterone). The invention further relates to the finding that the use of selective inhibitors of HSD11B1 in combination with immunotherapy induces an increased response to immunotherapy, which would be beneficial for the treatment of cancer.

Therefore, the invention further relates to a newly developed combination, which has a surprisingly effective anticancer activity, and would be useful in preventing intrinsic or acquired resistance to immunotherapy in particular in malignant and resistant cancers such as melanoma, lung carcinoma, glioblastoma, renal carcinoma, gastrointestinal stromal tumor and leukemia.

According to one aspect of the invention, is provided a selective HSD11B1 inhibitor for use in the treatment of a cancer, wherein said HSD11B1 inhibitor is to be administered in combination with immunotherapy.

According to another aspect of the invention, is provided a combination of at least one selective HSD11B1 inhibitor and at least one agent useful in immunotherapy for use in the treatment of a cancer.

According to another aspect of the invention, is provided a use of a combination of the invention for the preparation of a pharmaceutical composition for the treatment of cancer.

According to another aspect of the invention, is provided a pharmaceutical composition comprising at least one selective HSD11B1 inhibitor, at least one agent useful in immunotherapy and at least one pharmaceutically acceptable carrier and its use as a medication.

According to another aspect of the invention, is provided a method for treating a subject who is suffering from a cancer, said method comprising administering a therapeutically effective amount of an agent inducing selective HSD11B1 inhibition or any suitable pharmaceutically acceptable formulation thereof, in a subject in need thereof in combination with immunotherapy.

In another embodiment, the invention provides a method of identifying agents useful in the potentiation of immunotherapy, said method comprising identifying agents that are able to inhibit selectively HSD11B1, in particular as described herein.

Description of the figures

Figure 1 represents the immune activation induced by a combination according to the invention based on **A:** the levels of IFNγ measured in PBMC supernatant after the combined use of various HSD11B1 inhibitors (BMS-823778 (1), PF-915275 (2), 10J (3) and carbenoxolone (4)) with anti-PD-1

immunotherapy (G4K) in human immune cells compared to vehicle and isotype control; **B**: the fold changes in IFNy levels measured in PBMC supernatant after the combined use of various HSD11B1 inhibitors ((1), (2), (3) and (4), AZD4017 (5), BI-135585 (6), AZD8329 (7), ABT-384 (8) and MK-0736 (9)) or DMSO control (10)with anti-PD-1 immunotherapy (G4K) in human immune cells compared to isotype control in the absence of cortisone as described in Example 1.

Figure 2 represents A: growth of tumor cells cultured with immune cells and the combination of: a: vehicle control and isotype; b: HSD11B1 inhibitor (1) and isotype; c: vehicle control and anti-PD-1 immunotherapy (G4K) or d: HSD11B1 inhibitor (1) and anti-PD-1 immunotherapy (G4K) B: growth of tumor cells with immune cells treated with HSD11B1 inhibitors (1), (4), (8), (9) or vehicle control, as described in Example 2.

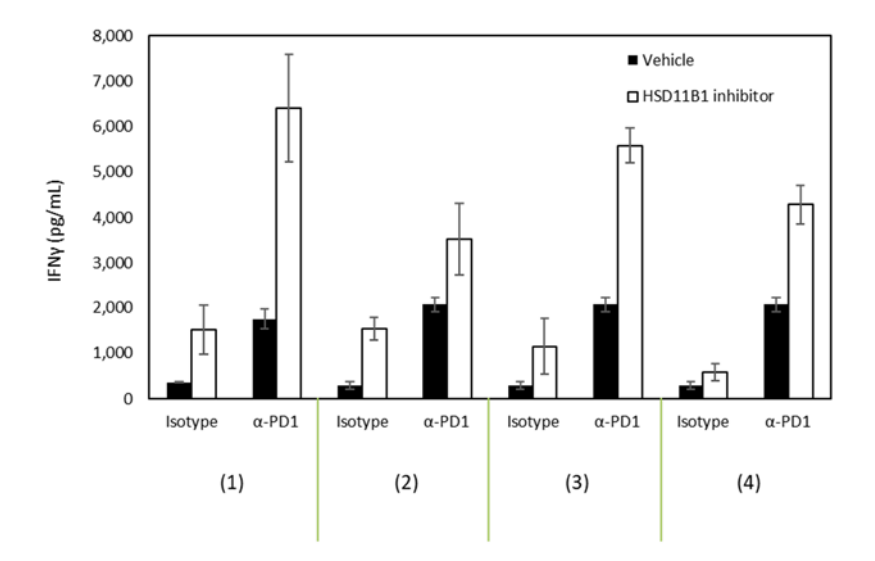


Figure 1A

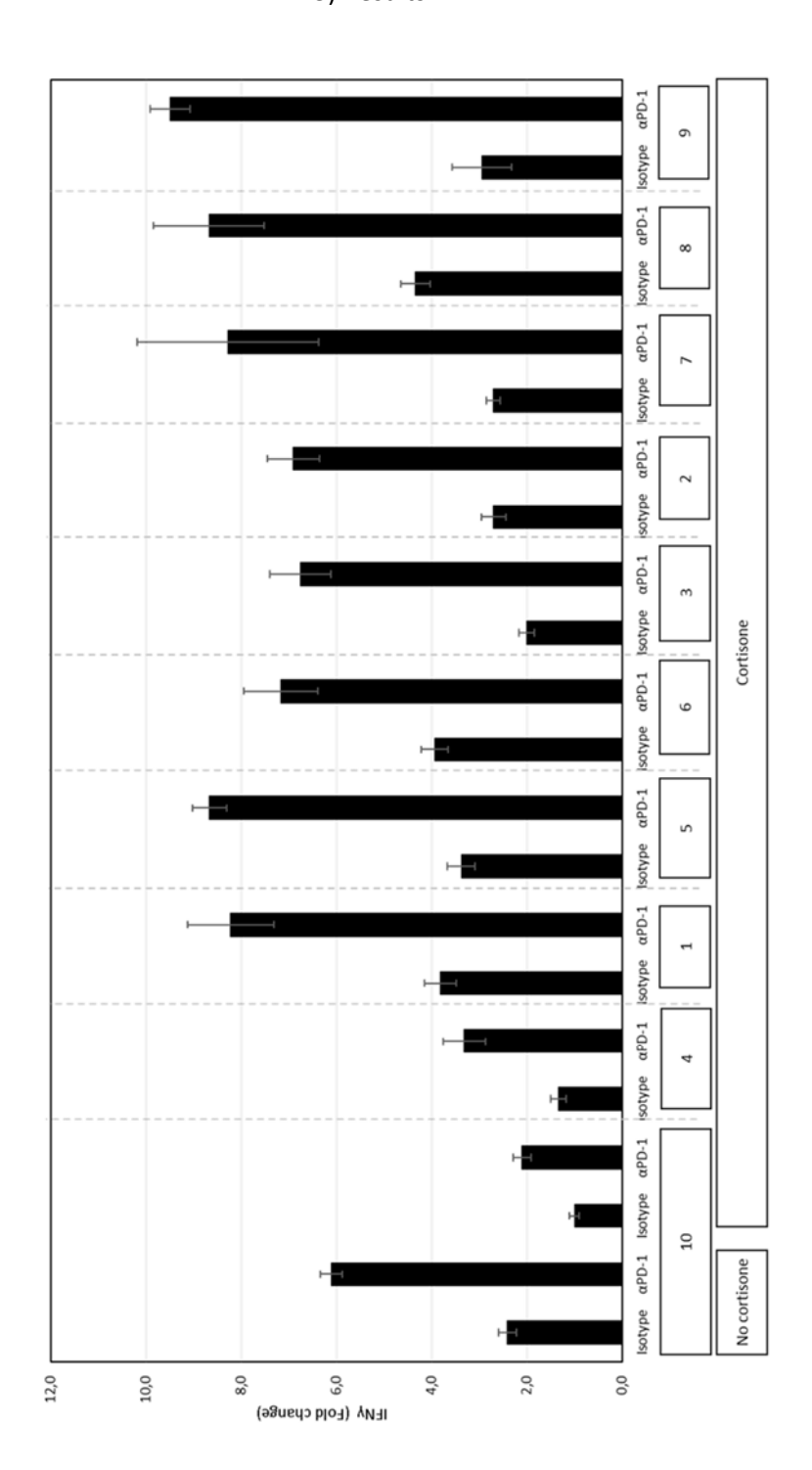
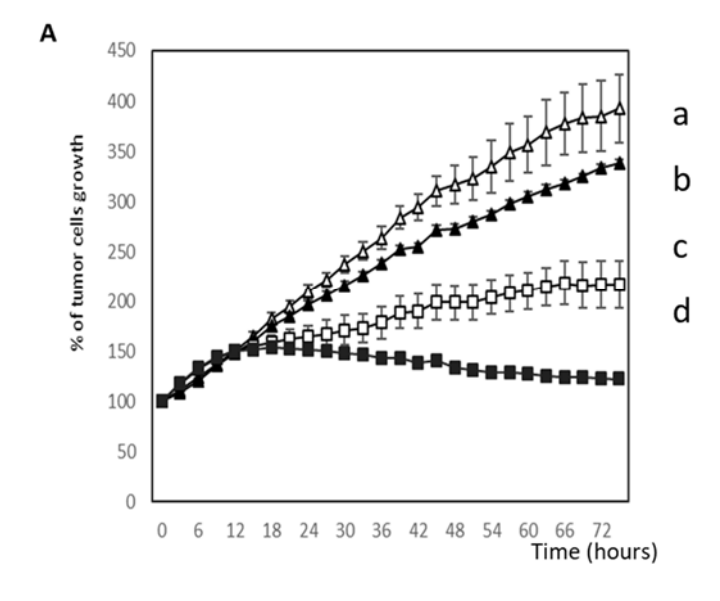


Figure 1B



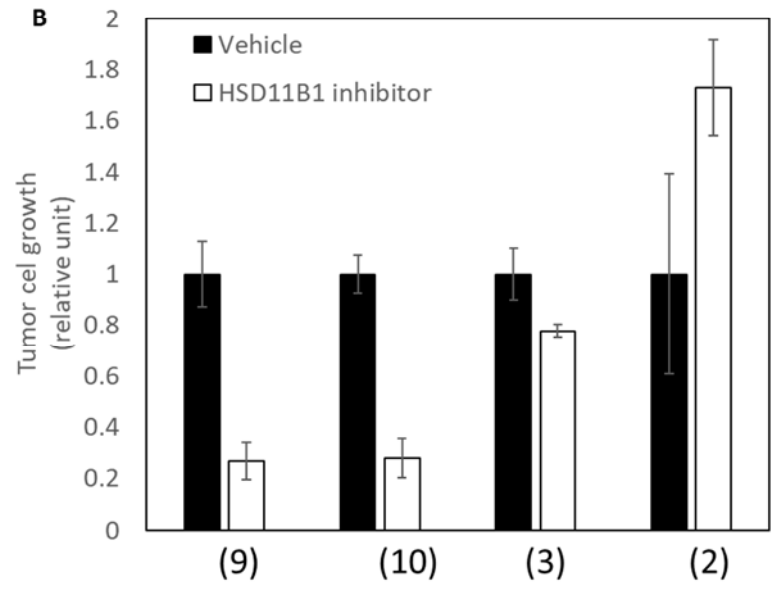


Figure 2

Detailed description

The expression "pharmaceutically acceptable salts" refers to salts of the below-specified compounds. Examples of such salts include, but are not restricted, to base addition salts formed by reaction of those compounds with organic or inorganic bases or inorganic acids (e.g. hydrochloric acid and the like).

As used herein, "treatment" and "treating" and the like generally mean obtaining a desired pharmacological and physiological effect. The effect may be prophylactic in terms of preventing or partially preventing a disease, symptom or condition thereof and/or may be therapeutic in terms of a partial or complete cure of a disease, condition, symptom or adverse effect attributed to the disease.

The term "treatment" as used herein covers any treatment of a melanoma in a mammal, particularly a human, and includes inhibiting the disease, i.e., arresting its development; or relieving the disease, i.e., causing regression of the disease and/or its symptoms or conditions such as improvement or remediation of damage.

The term "efficacy" of a treatment or method according to the invention can be measured based on changes in the course of disease or condition in response to a use or a method according to the invention. According to a particular embodiment, the efficacy of a combined use according to the invention can be measured through the assessment of efficacy of a compound combination of the invention, in particular long-term efficacy regarding repression of tumor growth, progression and dissemination, decrease of the number of cancer cells or their proliferation rate in combination with immunotherapy as compared to the efficacy of each compound of the combination, taken alone. According to another embodiment, the efficacy of a combined use according to the invention can be assessed by the monitoring of immune activation (eg. IFNy expression in peripheral blood) the observation of progression free survival (defined by the RECIST criteria) and overall survival in human patients.

According to another aspect, the efficacy of a combined use according to the invention can be assessed for example through the observation of IFNy secretion level for example by ELISA in an antigen recall assay using peripheral blood mononuclear cells (PBMC) isolated from healthy donors or by assessing the immune cell killing potential of T cells against cancer cells in mouse as described herein.

The term "subject" as used herein refers to mammals. For examples, mammals contemplated by the present invention include humans, primates, domesticated animals such as cattle, sheep, pigs, horses, laboratory rodents, other pets and the like.

The term "selective HSD11B1 inhibitors" refers to agents inhibiting HSD11B1 with a selectivity over HSD11B2 >100. The selectivity of HSD11B1 inhibition over HSD11B2 inhibition can be determined by scintillation proximity assay (Mundt et al., 2005, ASSAY and Drug Development Technologies 3(4), DOI: 10.1089/adt.2005.3.367). Examples of selective HSD11B1inhibitors are provided herein.

The expression "11-beta-hydroxysteroid dehydrogenase Type 1 (HSD11B1) inhibitor" refers to agents able to inhibit HSD11B1. Inhibition of HSD11B1 can be assessed for example by measuring the enzymatic transformation of HSD11B1 substrates (11-DHC or cortisone) into products (corticosterone or cortisol) by ELISA or mass spectrometry or in yeast cell based assays described *Vanella et al., 2016, Microb Cell Fact., 15:* 52, or cell-based assays on human 11 β -HSD1 transfected HEK-293 cell line with an Scintillation Proximity Assay (WO 2006/100502) or by molecular modelling of the crystal structure of one subunit of human 11 β -HSD1 such as described by *Quian et al., Molecules, (9). pii: E1222*.

Inhibition of HSD11B1 can be also assessed at the functional level for example by testing the inhibitory effect of immune suppression of HSD11B1 products on immune cells as described in this invention. HSD11B1 inhibitors can be small molecules inhibitors, peptides, mAbs, chimeric proteins or fusion proteins, aptamers (including peptide aptamers, DNA and RNA aptamers), soluble receptors and such agents may be acting by silencing, or down-regulating HSD11B1 at the genetic level by nucleic acid interaction, nucleic acid mutations or deletion aiming to abrogate the enzymatic activity of HSD11B1 using CRISPR-Cas9 technologies or by systemic administration of RNA interference delivered by liposomes or nanoparticles in humans.

HSD11B1 inhibitors can be administered in humans or on isolated immune cells in case of adoptive transfer therapy (e.g. CAR T cells).

Among those agents, some HSD11B1 inhibitors were actively developed for the treatment of different diseases including diabetes, metabolic diseases, obesity, Alzheimer, intraocular hypertension, arteriosclerosis or NAFLD (Non-Alcoholic Fatty Liver Disease) by several companies. All of these compounds failed in clinical trials so far. Some of them are still on clinical trial (AZD4017, from AstraZeneca in Phase II for intra ocular pressure intracranial hypertension). None of them has been tested in oncology. For example, HSD11B1 inhibitors according to the invention have been described in Table 1 below.

Table 1

Chemotypes	Common names of examples	Description of the chemotypes
	of specific compounds	
3,4,5-trisubstituted-4-	MK-0736 (9)	Compounds described in PCT/WO2010/68580, in
1,2,4-triazole		particular compounds of the following structure as
		described in PCT/US2004/133011 and
		PCT/US2009/066939, in particular, compounds of the
		following structures
		$\mathbf{R^4} - \mathbf{X} - \mathbf{N} $

Chemotypes	Common names of examples	Description of the chemotypes
	of specific compounds	
	BMS 823778 (1)	Compounds of the following structure as described in
		PCT/US/2011/288051
		$Q = \begin{pmatrix} N & N & N \\ N & N & N \\ R_{3b} & R_{3b} \end{pmatrix}$
		and in particular compounds of the following structure
		R N-N
		as described in <i>Li et al., 2018, ACS Med Chem Lett.,</i>
		9(12):1170-1174
	MK0916	Compounds of the following structures as described in
		PCT/US/2004/004891, PCT/US/2004/0106664
		PCT/US/2005/001928
		$(R^1)_3 \xrightarrow{N-N} R^3$
N-(thiazol-2-yl)	BVT2733	Compounds described in PCT/SE2001/01155 PCT/WO
benzenesulfonamide		2001/090090 and in particular compounds of the following
in particular		structure
arylsulfonamides		T- R N X R ²
thiazoles		S S S
		as described in PCT/US/2010/0113435

Chemotypes	Common names of examples	Description of the chemotypes
	of specific compounds	
	BVT-3498	Compounds described in PCT/SE/2001/01155, and
		PCT/US/2010/011343 and in particular compounds of the
		following structure
		$ \begin{array}{cccccccccccccccccccccccccccccccccccc$
		as described in PCT/US/2004/0224996
S-(1-H-pyrazol-4-	UE2343	Compounds of the following structure as described in
yl)thiophene-3-		Webster, 2017, british journal of pharmacology,
carboxamide		174(5):396-408.
		N N N R
Spirocyclic ureas	10J (3)	Compounds of the following structure as described in
		PCT/US2007/018789
		$(\mathbb{R}^{2})_{p2} \underbrace{\downarrow}_{M} \underbrace{\downarrow}_{M} \underbrace{\downarrow}_{N} \downarrow$
		In particular of the following structure
		R 3 4 5 5 X
		as described in <i>Tice et al., 2010, Bioorg. Med. Chem. Lett.,</i>
		20(3):881-6

Chemotypes	Common names of examples	Description of the chemotypes
	of specific compounds	
Adamantanes	ABT-384 (8)	Compounds of the following structures as described in
		PCT/US2005/245534, PCT/US/2005/277647
		PCT/WO/2009/026422, PCT/US/2010/222316 and <i>Rhode</i>
		et al., 2006, Bioorganic & Medicinal Chemistry Letters,
		16(23):5958-5962
		H R ³ R ⁴ R ⁵ R ⁵ R ¹ R ⁵ R ¹ R ⁵ R ⁶ R ⁶
Carbamoyl	AZD8329 (7)	Compounds described in PCT/US/2009/0221660
		PCT/US/2011/002853 or PCT/US/2011/0028529,
		PCT/US/2011/022427, in particular compounds of the
		following structure as PCTUS/2008/0269288,
		PCT/US/2009/312372, PCT/US/2009/030607
		HO X
		or of the following structures as described in
		PCT/US/20110224273 or <i>Scott et al., 2012,</i> J. Med. Chem.,
		55, 22, 10136-10147
		HO X A Y R A S R A

Chemotypes	Common names of examples	Description of the chemotypes	
	of specific compounds		
Thiazolones	AMG-221	Compounds as described in PCT/WO/2009/002445,	
		PCT/WO/2010/008729, PCT/WO/2010/014586,	
		PCT/WO/2012/051139, in particular, compounds of the	
		following structures	
		as described in PCT/US/2008/045503, in particular	
		compounds of the following structures	
		R^{6} R^{7} R^{5} R^{2} R_{1} R^{6} R^{7}	
		as described in <i>Véniant et al., 2010,</i> J. Med. Chem. <i>2010,</i>	
		53, 11, 4481-4487	
Arylsulfonamide	PF-915275	Compounds of the following structure	
		as described in PCT/US/2007/0072914 or in <i>Siu et al.</i> ,	
		2009, Bioorg Med Chem Lett., 19(13):3493-7	

Chemotypes	Common names of examples	Description of the chemotypes
	of specific compounds	
Cyclohexylcarbamoyl	AZD4017	Compounds of the following structures as described in
		PCT/US/2008/0269288, PCT/US/2009/312372 and
		PCT/US/2009/030607
		$\begin{array}{cccccccccccccccccccccccccccccccccccc$
		or in Scott, et al., 2012, Journal of medicinal chemistry or
		having the following structures
		F S F S C S S S S S S S S S S S S S S S
Sulfonamides	HSD-016	Compounds of the following structure as described in
		PCT/US/2010/029648, PCT/US/2007/0219198
		$R^1 - X - Y$ W^2 $V - R^2$
	BI 135585 (6)	Compounds of the following structures as described in
		PCT/US2011/040443, PCT/US/2013/0244993
		$\begin{array}{c ccccccccccccccccccccccccccccccccccc$
		or in Zuang, bioorganic and medicinal chemistry, 2017,
		25(14) :3649-3657
		N R

Chemotypes	Common names of examples	Description of the chemotypes
	of specific compounds	
Pyrazoles		Compounds of the following structure as described in PCT/EP/2007/052269 R ₅ NR ₁ R ₂ R ₄
Alkyl-pyridazine		Compounds of the following structures as described in PCT/EP/2007/056347
Glycyrrhetinic acid derivatives (comparative compounds- non-selective HSD11B1 inhibitors)		Compounds of the following structure CH3 CH3 CH3 CH3 CH3 CH3 CH3 CH

According to a particular embodiment, a HSD11B1 inhibitor according to the invention is selected from an adamantane, in particular an adamantyltriazole, an arylsulfonamide, in particular an arylsulfonamidothiazole, an anilinothiazolone, a spirocyclic urea and a 3,4,5-trisubstituted-4-1,2,4-triazole as described in *Anagnostis et al.*, 2013, 62(1):21-33; Webster et al., 2017, supra.

According to another particular embodiment, a HSD11B1 inhibitor according to the invention is selected from adamantyltriazoles, arylsulfonamidothiazoles, anilinothiazolones, spirocyclic ureas as described in *Anagnostis et al.*, 2013, supra; Webster et al., 2017, supra.

According to another particular embodiment, a HSD11B1 inhibitor according to the invention is selected from 3,4,5-trisubstituted-4-1,2,4-triazole, N-(thiazol-2-yl) benzenesulfonamide, S-(1-H-pyrazol-4-yl)thiophene-3-carboxamide, cyclohexylcarbamoyl spirocyclic ureas, arylsulfonamides, adamantanes, sulphonamides, carbamoyl, and thiazolones as described above.

According to another particular embodiment, a HSD11B1 inhibitor according to the invention is an arylsulfonamide, for example an arylsulfonamidothiazole.

According to another particular embodiment, a HSD11B1 inhibitor according to the invention is BVT2733, PF-915275 or analogues thereof as described therein.

According to another particular embodiment, a HSD11B1 inhibitor according to the invention is an anilinothiazolone.

According to another further particular embodiment, a HSD11B1 inhibitor according to the invention is AMG-221 or analogues thereof as described therein.

According to another particular embodiment, a HSD11B1 inhibitor according to the invention is a spirocyclic urea.

According to another further particular embodiment, a HSD11B1 inhibitor according to the invention is 10J or analogues thereof as described therein.

According to another particular embodiment, a HSD11B1 inhibitor according to the invention is a 3,4,5-trisubstituted-4-1,2,4-triazole.

According to another further particular embodiment, a HSD11B1 inhibitor according to the invention is BMS-823778 or analogues thereof as described therein.

According to another particular embodiment, a HSD11B1 inhibitor according to the invention is an adamantane.

According to another further particular embodiment, a HSD11B1 inhibitor according to the invention is ABT-384 or analogues thereof as described therein.

According to a particular embodiment, a selective HSD11B1 inhibitor according the invention is a selective over HSD11B2 with a factor of 100 or more.

For example, according to a further particular embodiment, HSD11B1 inhibitors are selected from compounds and pharmaceutically acceptable salts thereof reported in Table 2 below:

Table 2

Common name	Structure	IUPAC name
10J	CO₂H	(+/-)-2-(7-bromo-1'-((2-adamantyl)
(CAS number: 1009373-58-3)	NH NH	carbamoyl)-2,3-dihydrospiro [indene-1,4'-
(3)	Br	piperidine]-3-yl) acetic acid
spirourea		

Common name	Structure	IUPAC name
PF-915275	O H N NH2	N-(6-aminopyridin-2-yl)-4-(4-
(CAS number: 857290-04-1)	Solution	cyanophenyl) benzenesulfonamide
(2)		
arylsulfonamide	N	
BVT2733	CI CH ₃	3-chloro-2-methyl-N-[4-[2-(4-
(CAS number: 376640-41-4)	S.H. N.	methylpiperazin-1-yl)-2-oxoethyl]-1,3-
Arylsulfonamide	ÖÖ Ś N−CH₃	thiazol-2-yl]benzenesulfonamide
BMS-823778		2-[3-[1-(4-chlorophenyl)cyclopropyl]-
(CAS number: 1140898-87-8)	H₃C H₃C → OH	[1,2,4] triazolo[4,3-a]pyridin-8-yl]propan-
(1)	N,	2-ol
3,4,5-trisubstituted-4-1,2,4-	N N	
triazole	₹ C} cı	
MK-0736	F F	3-{4-[3-
(CAS number 719272-79-4)	N-N	(ethanesulfonyl)propyl]bicyclo[2.2.2]octa
(9)		n-1-yl}-4-methyl-5-[2-
	=20	(trifluoromethyl)phenyl]-4H-1,2,4-triazole
AMG-221- BVT-83370	,° \	(5S)-2-[[(1S,2S,4R)-2-
(CAS number 1095565-81-3)		bicyclo[2.2.1]heptanyl] imino]-5-methyl-
anilinothiazolone	N S	5-propan-2-yl-1,3-thiazolidin-4-one
AZD8329	HO	4-[4-(2-adamantylcarbamoyl)-5- <i>tert</i> -butyl
(CAS number 1048668-70-7)		pyrazol-1-yl]benzoic acid
(7)	7 8	
ABT-384	o NN NN	4-[[2-methyl-2-[4-[5-
(CAS number 868623-40-9)	H,N O N,	(trifluoromethyl)pyridin-2-yl]piperazin-1-
(8)	N N	yl]propanoyl]amino]adamantane-1-
adamantane	F	carboxamide
BVT-3498	<u></u>	3-chloro-2-methyl-N-[4-[2-(3-
(CAS number 376641-49-5)		oxomorpholin-4-yl) ethyl]-1,3-thiazol-2-
	H N	yl]benzenesulfonamide
MK0916	CI	3-[1-(4-chlorophenyl)-3-fluorocyclobutyl]-
(CAS number 633317-53-0)	FIN. N	4,5-dicyclopropyl-1,2,4-triazole

Common name	Structure	IUPAC name
AZD4017	0	2-[(3 <i>S</i>)-1-[5-(cyclohexylcarbamoyl)-6-
(CAS number	N OH	propyl sulfanylpyridin-2-yl]piperidin-3-
1024033-43-9)	S N N	yl]acetic acid
(5)		
HSD-016	Q FF	(2R)-1,1,1-trifluoro-2-[3-[(2R)-4-[4-fluoro-
(CAS number 946396-92-5)	N S OH	2-(trifluoromethyl)phenyl]-2-
	F F F	methylpiperazin-1-
	Ė '	yl]sulfonylphenyl]propan-2-ol
BI 135585	HO N	(6R)-6-(2-hydroxy-2-methylpropyl)-3-
(CAS number 1114561-85-1)		[(1R)-1-[4-(1-methyl-2-oxopyridin-4-
(6)		yl)phenyl]ethyl]-6-phenyl-1,3-oxazinan-2-
		one
INCB-13739 (CAS number	o. N H	(3S)-1-[(3-Chloro-2-
872506-67-7)	5,00	methylphenyl)sulfonyl]-N-cyclohexyl-3-
	CI	piperidinecarboxamide
UE2343	O HOHN	[(1R,5S)-3-hydroxy-3-pyrimidin-2-yl-8-
(CAS number 1346013-80-6)		azabicyclo[3.2.1]octan-8-yl]-[5-(1 <i>H</i> -
	N S H	pyrazol-4-yl)thiophen-3-yl]methanone
UE2316		[4-(2-chlorophenyl)-4-fluoro-1-piperidyl]-
	N S T N F	[5-(1H-pyrazol-4-yl)-3-thienyl]methanone
CRx-401	CL	2-[4-[2-[(4-chlorobenzoyl)amino]
		ethyl]phenoxy]-2-methylpropanoic acid
	H ₃ C CH ₃	
carbenoxolone	√)—он	(2S,4aS,6aR,6aS,6bR,8aR,10S,12aS,14bR)-
(CAS number: 5697-56-3)	0	10-(3-carboxypropanoyloxy)-
(4)		2,4a,6a,6b,9,9,12a-heptamethyl-13-oxo-
Glycyrrhetinic acid derivatives	HO HO	3,4,5,6,6a,7,8,8a,10,11,12,14b-
(comparative compound- non	-	dodecahydro-1H-picene-2-carboxylic acid
selective HSD11B1 inhibitor)		

According to another particular embodiment, a HSD11B1 inhibitor according to the invention is selected from:

 $(10 J \ or \ (+/-)-2-(7-bromo-1'-((2-adamantyl)carbamoyl)-2,3-dihydrospiro[indene-1]-((2-adamantyl)carbamoyl)-2,3-dihydr$

1,4'-piperidine]-3-yl)acetic acid);

(PF-915275 or N-(6-aminopyridin-2-yl)-4'-cyanobiphenyl-4-sulfonamide); and

(BMS-823778 or 2-[3-[1-(4-chlorophenyl)cyclopropyl]-[1,2,4]triazolo[4,3-a]pyridin-8-

yl]propan-2-ol) or any pharmaceutically acceptable salts thereof.

According to another particular embodiment, a HSD11B1 inhibitor according to the invention is selected from:

(10J or (+/-)-2-(7-bromo-1'-((2-adamantyl)carbamoyl)-2,3-dihydrospiro[indene-

1,4'-piperidine]-3-yl)acetic acid);

 $(PF-915275\ or\ N-(6-aminopyridin-2-yl)-4'-cyanobiphenyl-4-sulfonamide);$

(BMS-823778 or 2-[3-[1-(4-chlorophenyl)cyclopropyl]-[1,2,4]triazolo[4,3-a]pyridin-8-

yl]propan-2-ol);

(MK-0736 or 3-{4-[3-(ethanesulfonyl)propyl]bicyclo[2.2.2]octan-1-yl}-4-

methyl-5-[2-(trifluoromethyl)phenyl]-4H-1,2,4-triazole);

Further inhibitors can be identified by *in silico* models, as described in *Liu et al., 2019, J. Chem. Inf. Model., 59, 3422–3436*. **Table 3** below shows the selectivity of HSD11B1 inhibitors for HSD11B1 over HSD11B2. The selectivity was calculated as follow: $(IC_{50} \text{ HSD11B2})/(IC_{50} \text{ HSD11B1})$ from published literature. Carbenoxolone is a dual inhibitor (non-selective HSD11B1 inhibitor).

Table 3

Compounds	Selectivity over HSD11B2	Source
MK-0916	>100	National Center for Biotechnology Information (2021). PubChem Bioassay Record for Bioactivity AID 332064 - SID 103563653, Bioactivity for AID 332064 - SID 103563653, Source: ChEMBL. Retrieved February 10, 2021 fromhttps://pubchem.ncbi.nlm.nih.gov/bioassay/332064#sid=103563653
MK-0736 (9)	>100	Maletic et al., 2011, Bioorg Med Chem Lett. 2011, 21(8):2568-72
AMG-221	>100	Véniant et al., 2010, J. Med. Chem. 2010, 53, 11, 4481-4487
ABT-384 (8)	>1000	https://doi.org/10.1002/bdd.1912

Compounds	Selectivity over HSD11B2	Source	
AZD4017 (5)	>1000	dx.doi.org/10.1021/jm300592r J.Med.Chem.2012, 55, 5951–5964	
10J (3)	>1000	Tice et al., 2010, Bioorg., Med. Chem. Lett., 20(3):881-6	
BMS-823778 (1)	>1000	Li et al., 2018, ACS Med Chem Lett., 9(12):1170-1174	
PF-915275 (2)	>1000	Siu et al., 2009, Bioorg Med Chem Lett., 19(13):3493-7	
HSD-016	>1000	https://doi.org/10.1021/jm8004948	
BI 135585 (6)	>1000	Zuang, bioorganic and medicinal, chemistry, 2017, 25(14) :3649-3657	
Carbenoxolone (4)	<10	Chapman et al, 2013, Physiol Rev 93: 1139 – 1206 <u>10.1152/physrev.00020.2012</u>	

The expression "immunotherapy" includes strategies used to activate effector immune cells to increase the efficacy of the patient's own immune response against neoplastic cells (melanoma, lung carcinoma, glioblastoma, renal carcinoma, gastrointestinal stromal carcinoma and leukemia). Immunotherapy includes the use of cancer vaccines, oncolytic viruses, cell therapy and/or immune system modulators.

The expression "immune system modulators" covers small molecules and large molecules (peptides, chimeric proteins, antibodies, bispecific antibodies) that induce an anti-cancer immune response or that aim to neutralize immune suppressive mechanisms driven by T regulators cells, tumor associated macrophages, myeloid derived suppressor cells or immune checkpoints.

Vaccines can be used in an immunotherapy according to the invention and work against cancer by boosting the immune system's response to cancer cells. Therapeutic vaccines are different from vaccines that help prevent disease. Examples of therapeutic vaccines include sipuleucel-T (*Topalian et al., 2011, J. Clin. Oncol., 29: 4828-36, Dendreon*).

Oncolytic viruses represent a novel drug class in which native or modified viruses mediate tumor regression through selective replication within and lysis of tumor cells as well as induction of systemic antitumor immunity capable of eradicating tumor at distant, uninjected sites. An example of oncolytic viruses includes the herpesvirus-based treatment T-VEC (talimogene laherparepvec, *Liu et al., Gene Therapy, 2003 10(4):292-303, Amgen*).

Cell therapy includes treatments based on *in vitro* expanded and/or genetically modified lymphocytes (T cells or NK cells). For instance, T-cell transfer therapy, also called adoptive cell therapy, adoptive immunotherapy, or immune cell therapy includes tumor-infiltrating lymphocytes as starting material and genetically engineered CAR T-cells, which specifically recognize and kill tumor cells, such as described for the treatment of relapsed or refractory B-cell malignancies, such as B-cell non-Hodgkin lymphoma (NHL), acute lymphoblastic leukemia (ALL) and chronic lymphocytic leukemia (CLL) in pediatric and adult patients (*Miliotou et al, 2018, Current pharmaceutical biotech., 19(1):5-18.*). Example of T cell transfer therapies includes tisagenlecleucel (Novartis, Forsberg et al., 2018, Ther Clin Risk Manag. 14:1573-1584 and Vairy, 2018, Drug Design, Development and Therapy, 12: 3885–3898), and axicabtagene ciloleucel (Gilead Sciences, Jain et al., 2018, Therapeutics and Clinical Risk Management, 14: 1007–1017).

Immune system modulators enhance the body's immune response against cancer. Some of these agents affect specific parts of the immune system, whereas others affect the immune system in a more general way. This class includes cytokines (interferons, interleukins, granulocyte-macrophage colony-stimulating factor and granulocyte colony-stimulating factor), Bacillus Calmette-Guérin, immunomodulatory drugs (thalidomide, lenalidomide, pomalidomide, imiquimod) and chemotherapeutic agents that induce immunogenic cell death (cyclophosphamide, bleomycin, shikonin, anthracyclines).

Are included as immune system modulators monoclonal antibodies and antibody-derived constructs used as immunotherapy according to the invention, which are proteins designed to bind to specific targets on cancer cells. Some monoclonal antibodies and antibody-derived constructs mark cancer cells so that they will be better seen and destroyed by the immune system. Monoclonal antibodies may also be called therapeutic antibodies. For example, those monoclonal antibodies can be rituximab (Biogen, Genentech, Hoffmann-La Roche, Chugai Pharmaceuticals, Zenyaku Kogyo and AryoGen, DOI: 10.1016/j.trac.2013.02.014). For example, antibody-derived constructs can include short-chain variable antibody fragments (scFv) and can be bispecific T-cell engagers (BiTE) such as blinatumomab (*Amgen, Wu et al., 2015, J. Hematol. Oncol., 8, 104*).

Are also included as immune system modulators the immune checkpoint blockers targeting PD-1 such as pembrolizumab (Merck, US 2010/0266617, DOI: 10.1158/1078-04), nivolumab (Bristol-Myers Squibb, WO 2006/121168), cemiplimab (Regeneron, DOI: 10.1158/1535-71), spartalizumab (PDR001, Novartis, US 9,683,048), camrelizumab (SHR1210, Jiangsu Hengrui Medicinem, https://doi.org/10.1007/s40265-019-01167-0), sintilimab (IBI308, Innovent Biologics and Eli Lilly, DOI: 10.1080/19420862.2019.1654303, tislelizumab (BGB-A317, BeiGene and Celgene Corp, US 8,735,553),

toripalimab (JS 001, Shanghai Junshi Bioscience, *Keam, 2019, Drugs 79, 573–578*), AMP-224 (GlaxoSmithKline, Amplimmune, *Infante et al. 2013, J Clin Oncol, 31, 3044*), AMP-514, AstraZeneca, *Naing et al. 2019, J. Immunotherapy Cancer 7, 225*). Are also included the CTLA-4 inhibitors such as ipilimumab (Bristol-Myers Squibb, WO 2001/014424, EP1503794). Are also included the PD-L1 inhibitors atezolizumab (Tecentriq[™], Roche, US 8,217,149, *Powles et al., 2014, Nature, 515, 558–562*), avelumab (Bavencio[™], Pfizer, Merk KGaA, WO 2013/079174 A1), BMS-936559 (Bristol-Myers Squibb) and durvalumab (Imfinzi[™], AstraZeneca, WO 2011/066389).

Are included as immune system modulators the immunoconjugates that are antibodies, peptides or proteins conjugated to a second molecule, which can include immune cell death inducer agents and toxins or immune system modulators (cytokines, Bacillus Calmette-Guérin and immunomodulatory drugs).

The term "pharmaceutically acceptable salts or complexes" refers to salts or complexes of the below-specified compounds of the invention. Examples of such salts include, but are not restricted, to base addition salts formed by reaction of compounds of the invention with organic or inorganic bases such as hydroxide, carbonate, bicarbonate or the like, of a metal cation such as those selected in the group consisting of alkali metals (sodium, potassium or lithium), alkaline earth metals (e.g. calcium or magnesium), or with an organic primary, secondary or tertiary alkyl amine. Other examples of such salts include, but are not restricted, to acid addition salts formed by reaction of compounds of the invention with organic or inorganic acids such as hydrochloric acid, hydrobromic acid, sulphuric acid, para-toluene sulfonic acid, 2-naphtalene sulfonic acid, camphosulfonic acid, benzene sulfonic acid, oxalic acid or the like.

Combined use and combined compositions

The invention provides pharmaceutical or therapeutic agents as compositions and methods useful for the treatment of cancer.

According to a particular embodiment, the HSD11B1 inhibitors of the invention are to be used in combination with an immunotherapy selected from anti-cancer vaccine, adoptive cell therapy such as T-cell transfer therapy (inhibitors and genetic approaches), a small or a large molecules such as chemotherapies inducing immune cell death, anti-cancer monoclonal antibody, immunoconjugates, bispecific proteins, and cytokines.

According to a further particular aspect, the invention provides a use of a combination comprising at least one selective HSD11B1 inhibitor and at least one immune checkpoint inhibitor.

According to a further particular aspect, an immune checkpoint inhibitor is selected from a PD-1 inhibitor, a CTLA-4 inhibitor and a PD-L1 inhibitor.

According to a further particular aspect, a PD-1 inhibitor is pembrolizumab or nivolumab.

According to another aspect, the invention provides a use of a combination comprising at least one selective HSD11B1 inhibitor and at least one CTLA-4 inhibitor for the treatment of cancer, in particular of cancers associated with melanoma, lung carcinoma, glioblastoma, renal carcinoma, gastrointestinal stromal carcinoma and leukemia.

According to a further particular aspect, a CTLA-4 inhibitor is ipilimumab.

According to another aspect, the invention provides a use of a combination comprising at least one selective HSD11B1 inhibitor and at least one PD-L1 inhibitor for the treatment of cancer, in particular of cancers associated with melanoma, lung carcinoma, glioblastoma, renal carcinoma, gastrointestinal stromal carcinoma and leukemia.

According to a further particular aspect, a PD-L1 inhibitor is atezolizumab.

According to another particular aspect, the invention provides a use of a combination comprising at least one selective HSD11B1 inhibitor and at least one at least one anti-cancer vaccine.

According to another particular aspect, the invention provides a use of a combination comprising at least one selective HSD11B1 inhibitor and at least one anti-cancer monoclonal antibody.

According to another further aspect, is provided a pharmaceutical composition comprising a combination according to the invention and at least one more pharmaceutically acceptable carrier.

Compositions of this invention may further comprise one or more pharmaceutically acceptable additional ingredient(s) such as alum, stabilizers, antimicrobial agents, buffers, colouring agents, flavouring agents, adjuvants, and the like.

The compositions according to the invention, together with a conventionally employed adjuvant, carrier, diluent or excipient may be placed into the form of pharmaceutical compositions and may be employed as solids, such as tablets or filled capsules, or liquids such as solutions, suspensions, ointments, emulsions, elixirs, or capsules filled with the same, films or gels, all for oral use. The compositions may also be formulated as a dry product for reconstitution with water or other suitable vehicle before use.

Compositions of this invention as liquid formulations including, but not limited to, aqueous or oily suspensions, solutions, emulsions, syrups, and elixirs.

Such liquid preparations may contain additives including, but not limited to, suspending agents, emulsifying agents, non-aqueous vehicles and preservatives. Suspending agents include, but are not limited to, sorbitol syrup, methyl cellulose, glucose/sugar syrup, gelatin, hydroxyethyl cellulose, carboxymethyl cellulose, aluminum stearate gel, and hydrogenated edible fats. Emulsifying agents include, but are not limited to, lecithin, sorbitan monooleate, and acacia. Preservatives include, but are not limited to, methyl or propyl p-hydroxybenzoate and sorbic acid. Dispersing or wetting agents include but are not limited to poly(ethylene glycol), glycerol, bovine serum albumin, Tween®, Span®.

Further materials as well as formulation processing techniques and the like are set out in *The Science* and *Practice of Pharmacy (Remington: The Science & Practice of Pharmacy), 22nd Edition, 2012, Lloyd, Ed. Allen, Pharmaceutical Press, which is incorporated herein by* reference.

Solid compositions of this invention may be in the form of tablets or lozenges formulated in a conventional manner. For example, tablets and capsules for oral administration may contain conventional excipients including, but not limited to, binding agents, fillers, lubricants, disintegrants and wetting agents. Binding agents include, but are not limited to, syrup, acacia, gelatin, sorbitol, tragacanth, mucilage of starch and polyvinylpyrrolidone. Fillers include, but are not limited to, lactose, sugar, microcrystalline cellulose, maize starch, calcium phosphate, and sorbitol. Lubricants include, but are not limited to, magnesium stearate, stearic acid, talc, polyethylene glycol, and silica. Disintegrants include, but are not limited to, potato starch and sodium starch glycolate. Wetting agents include, but are not limited to, sodium lauryl sulfate. Tablets may be coated according to methods well known in the art.

In a particular embodiment, the invention provides a pharmaceutical formulation according to the invention for use as a medicament.

• Mode of administration

According to the invention, the HSD11B1 inhibitor or a pharmaceutical formulation thereof, are administered to an individual prior to, or simultaneously with an anti-cancer immunotherapeutic agent, for example concomitantly through the same formulation or separately through different formulations, in particular through different formulation routes.

According to a particular aspect of the invention, a HSD11B1 inhibitor according to the invention and pharmaceutical formulations thereof is to be administered chronically (e.g. daily or weekly) for the duration of treatment and prior to the administration of an anti-cancer immunotherapeutic agent treatment.

According to another particular aspect of the invention, a HSD11B1 inhibitor according to the invention and pharmaceutical formulations thereof is to be administered concomitantly with an anti-cancer immunotherapeutic agent.

Compositions of this invention may be administered in any manner, including, but not limited to, orally, intravenously, intramuscularly, subcutaneously, parenterally, nasally, intralesionally or combinations thereof. Parenteral administration includes, but is not limited to subcutaneous and intramuscular. The compositions of this invention may also be administered in the form of an implant, which allows slow release of the compositions as well as a slow controlled i.v. infusion. In a particular embodiment, one or more HSD11B1 inhibitor is administered orally.

The compounds of a combination of this invention may be administered independently by any manner by oral route such as sublingually, via buccal administration, including to the mucosal surfaces of the oral cavity including the gingiva, the floor of the oral cavity, cheeks, lips, tongue, teeth.

According to a particular embodiment, compositions of this invention may be administered by intravenous or intra-muscular or sub-cutaneous injection.

The dosage administered, as single or multiple doses, to an individual will vary depending upon a variety of factors, including pharmacokinetic properties, patient conditions and characteristics (age, body weight, health, body size), extent of symptoms, frequency of treatment and the effect desired.

Patients

In an embodiment, patients according to the invention are patients suffering from a cancer.

In a particular embodiment, patients according to the invention are patients suffering from a cancer selected from melanoma, lung carcinoma, glioblastoma, renal carcinoma, gastrointestinal stromal carcinoma and leukemia.

In a particular embodiment, patients according to the invention are patients suffering from tumors of the skin, melanoma, lung, pancreas, breast, colon, rectum, brain, laryngeal, ovarian, prostate, colorectal, head, neck, testicular, lymphoid, marrow, bone, sarcoma, renal, gastrointestinal tract, sweat gland, and the like tissues.

In a particular embodiment, patients according to the invention are patients suffering from melanoma.

In another particular embodiment, patients according to the invention are patients suffering from lung carcinoma.

In a particular embodiment, patients according to the invention are patients suffering from glioblastoma.

In a particular embodiment, patients according to the invention are patients suffering from renal carcinoma.

In a particular embodiment, patients according to the invention are patients suffering from gastrointestinal stromal carcinoma.

In a particular embodiment, patients according to the invention are patients suffering from leukemia.

In another further embodiment, patients according to the invention are patients suffering from breast and renal cancer.

• Use and methods according to the invention

In a particular embodiment, the use of compounds of the invention or methods of treatment using those increases responsiveness to immunotherapy.

In another particular embodiment, the combined use of compounds of the invention and methods using this combination induce the level of IFN gamma.

Therefore, the use of inhibitory agents or methods that would silence or down-regulate or selectively inhibit HSD11B1 would be beneficial to subject's responsiveness to immunotherapeutic treatment of cancer.

According to another aspect of the invention, is provided a method for treating a subject who is suffering from a cancer, said method comprising administering a therapeutically effective amount of an agent inducing selective HSD11B1 inhibition or any suitable pharmaceutically acceptable formulation thereof, in a subject in need thereof in combination with immunotherapy.

According to another further embodiment, such agent inducing HSD11B1 inhibition can be agents that knock out or knock down HSD11B1 at the genetic level using methods such as CRISPR-Cas9 technology (Pickar-Olivier and Gerbach, 2019, Nature Reviews Molecular Cell Biology, 20, 490–50) and small interference RNA (Chakraborty et al., Mol Ther Nucleic Acids. 2017, 8: 132–143.) or gene therapy (Dunbar et al., 2018, Science 359, 6372).

In another embodiment, the invention provides a method of identifying agents useful in the potentiation of immunotherapy, said method comprising the following steps:

 exposing at least one immune cell such as dendritic cells, macrophages, neutrophils, T cells with cancer cells (alone or in co-culture) with HSD11B1 substrates (e.g. cortisone or 11-DHC);

- contacting said at least one cell with at least one candidate agents;
- identifying agents that are able to inhibit selectively HSD11B1 in said cells.

Examples illustrating the invention will be described hereinafter in a more detailed manner and by reference to the embodiments represented in the Figures.

EXAMPLES

The following abbreviations refer respectively to the definitions below:

BMDC (Bone marrow derived dendritic cells); **DMEM** (Modified Eagle's minimal essential medium); **DMSO** (Dimethyl Sulfoxyde); **FBS** (Fetal bovine serum); **GFP** (green fluorescent protein); **GMCSF** (Granulocyte-macrophage colony-stimulating factor); **RPMI** (Roswell Park Memorial Institute).

Example 1: Assessing the effect of inhibition of HSD11B1 in combination with immunotherapy for the use as treatment of cancer in an antigen recall assay

Response to immunotherapy rely on critical biological steps including antigen presentation and T cell activation. Therefore, the therapeutic potential of combining immunotherapy with HSD11B1 inhibition was investigated in an antigen recall assay as described below.

Antigen recall assay is the gold standard *in vitro* method to assess the bioactivity of immune checkpoint inhibitors because it measures at the same time the potential of antigen presenting cells to activate T cell and the actual T cell activation, taking into account thereby the two critical mechanisms required for an optimal response to immunotherapy. The level of IFN γ secreted in this human immune cell-based assay is considered as a good indicator of the T cells activation to immunomodulatory molecules. Cryopreserved human peripheral blood mononuclear cell (PBMC) isolated from cytomegalovirus (CMV) positive heathy donors were thawed in a 37°C water bath and seeded in round bottom 96 well plates at 2 X 10⁵ cells/well in 150 μ L final volume of RPMI media supplemented with 10% fetal bovin serum, 1% non-essential amino acids, 0.01M Hepes, 1% Penicilin/Streptomycin, 1% L-glutamine and 50 ng/ml cortisone). PBMC were stimulated with 1 μ g/ml CMV antigen (Astarte) and with 1 μ g/ml anti PD-1 (G4K) or isotype control (Biovision) and with 1 μ M of a HSD11B1 inhibitors (10J (3), carbenoxolone (4) and BMS-823778 (1) all from Sigma, AZD4017 (5), BI-135585 (6), AZD8329 (7), ABT-384 (8) and MK-0736 (9), all from custom synthesis and PF-915275 (2) from R&D Systems) or DMSO control (10). Plates were incubated at 37°C, 6% CO₂.

After 6 days, supernatants were assayed for IFNy by ELISA (Biolegend).

As illustrated in **Fig. 1**, the level of immune activation measured by IFNy secretion in PBMC supernatant was increased in the presence of the anti-PD-1 compared to isotype control in the absence of

cortisone. Addition of cortisone strongly reduced the therapeutic activity of the anti-PD-1. The treatment with HSD11B1 inhibitors increased the immune activation in isotype control and anti-PD-1 treated conditions.

As shown in **Table 4** below, the combination of HSD11B1 inhibitors plus the anti-PD-1 led to an unexpected synergistic effect that increased the immune activation to a superior level than the addition of anti-PD-1 plus HSD11B1 inhibitor taken separately.

Table 4

Compounds	Additive effect	Synergic effect	Synergic factor
4			
(comparative)	1,4	3,3	1,9
1	3,9	8,2	4,3
5	3,5	8,7	5,2
6	4	7,2	3,1
3	2,1	6,8	4,6
2	2,8	6,9	4,1
7	2,8	8,3	5,5
8	4,4	8,7	4,2
9	3	9,5	6,4

Importantly, the treatment with selective HSD11B1 inhibitors (1, 2, 3, 5, 6, 7, 8, 9) in combination with the anti-PD-1 not only completely abolished the immune suppressive effect of cortisone but led to a higher level of immune activation than the anti-PD-1 alone. Only the none selective HSD11B1 inhibitor carbenoxolone was not able to abolish the immune suppressive effect of cortisone.

This experiment therefore provides evidence that treatment with selective HSD11B1 inhibitors synergies with immunotherapy and represent an effective option to improve the efficacy of immunotherapy.

Example 2: Assessing the effect of inhibition of HSD11B1 in combination with immunotherapy for the use as treatment of cancer in a cell growth assay

Another critical biological mechanism required for an optimal response to immunotherapy of cancer is the capacity of T cells to kill the tumor target cells. The therapeutic potential of combining immunotherapy with HSD11B1 inhibition for the treatment of cancer was therefore assessed in a murine T cell-mediated tumor cell-killing assay.

Wild type C57BL/6J murine bone marrow progenitors cells were maintained with 20 ng/ml GMCSF (Peprotech) to induce differentiation into bone marrow derived dendritic cells (BMDCs) for 6 days. At day 6, 2×10^4 BMDCs/well together with 2×10^3 Renca tumor cells/well were seeded in flat bottom 96

well plate in RPMI 1640 supplemented with 10% FBS, 1% Penicillin/streptomycin, 1% L-glutamine, 50 mM betamercaptoethanol and 0.5% of sodium pyruvate, 32 ng/ml R848 (Invivogen) and 25 μg/ml ovalbumin (Invivogen). After 24 hours, cell supernatant was removed and 1x10⁵ OT-I CD8⁺ T cells/well were added in very low endotoxin RPMI 1640 medium supplemented with 10% fetal bovine serum, 1% L-glutamine, 1% penicillin-streptomycin, 1% sodium-pyruvate, 1% glutamine, 1%, non-essential amino acids and 50 mM beta-mercaptoethanol. After 24 hours, 5x10³ H2kb-recombined; SEQ ID NO: 1 SIINFEKL (Invivogen) loaded-GFP-expressing Renca cells/well were added. The growth of GFP Renca cells was measured and quantified in real time by cell imaging using the Incucyte technology. 200 ng/ml 11-DHC (US Biological), 10 μM HSD11B1 inhibitor (BMS-823778 (1) and carbenoxolone (4) from Sigma, ABT-384 (8) and MK-0736 (9) from custom synthesis) or vehicle DMSO and anti-PD-1 (Invivogen) or isotype control (Invivogen) were maintained from day 6 until the end of the experiment.

As illustrated in **Fig. 2**, the combination of an HSD11B1 inhibitor with an anti-PD-1 (mouse) inhibited the growth of tumor cells more efficiently than the single treatments. Further, the data supports that treatment with selective HSD11B1 inhibitors only was able to stimulate the antitumor immune response leading to the inhibition of tumor cell growth whereas no efficacy was observed with a none selective HSD11B1 inhibitor such as carbenoxolone.

These data provide therefore strong evidences that the selective inhibition of HSD11B1 is effective to improve the efficacy of immunotherapy for the treatment of cancer.

Example 3: Genetic deletion of HSD11B1

In order to assess the utility of genetic loss of function particularly for adoptive cell therapy (CAR T cell), genetic deletion of HSD11B1 can be performed using CRISPR-Cas9 *technology* (*Pickar-Olivier and Gerbach, 2019, Nature Reviews Molecular Cell Biology, 20, 490–50*) in mouse T cells. Isolated CD8⁺ T cell from OT-1 mouse are grown for 24 hours with 5 ng/ml IL-7 (R&D system) in RPMI 1640 medium supplemented with 10% fetal bovine serum, 1% L-glutamine, 1% sodium-pyruvate, 1% glutamine, 1%, non-essential amino acids and 50 mM beta-mercaptoethanol. After 24h, cells are electroporated with Cas9/crRNA complex targeting HSD11B1 (crRNA sequence 1: 5′-GCTGGGCACAAGTTCGAGTTAGG-3′ (SEQ ID NO: 2); crRNA sequence 2: 5′-ATGGTGGTCATCTTGGTCGTAGG-3′ (SEQ ID NO: 3)) with Neon electroporation (Thermofisher) as described by *Seki et al. 2018, JEM, 5;215(3):985-997*. T cells are then activated with ovalbumin loaded BMDCs as described in Example 2. Three days post activation, 5x10³ H2kb-recombined; SIINFEKL (SEQ ID NO: 1) loaded-GFP-expressing Renca cells/well are added. The growth of GFP Renca cells is then measured and quantified in real time by cell imaging using the Incucyte technology. 200 ng/ml 11-DHC (US Biological), 10 μM HSD11B1 inhibitor (BMS-823778 from

3) Results

Sigma) or vehicle DMSO and anti-PD-1 (Invivogen) or isotype control (Invivogen) are maintained from

day 2 post T cell activation until the end of the experiment.

SEQUENCE LISTING

SEQ ID NO: 1 - Ovalbumin peptide (chicken)

SIINFEKL

SEQ ID NO: 2 - crRNA sequence (gRNA targeting mouse hsd11b1)

5'-GCTGGGCACAAGTTCGAGTTAGG-3'

SEQ ID NO: 3 - crRNA sequence (gRNA targeting mouse hsd11b1)

5'-ATGGTGGTCATCTTGGTCGTAGG-3'

Claims:

1. A selective HSD11B1 inhibitor for use in the treatment of a cancer, wherein said selective

HSD11B1 inhibitor is to be administered in combination with immunotherapy.

A selective HSD11B1 inhibitor for use according to claim 1 in combination with at least one

immunotherapeutic agent selected from a cancer vaccine, oncolytic virus and an immune

system modulator.

3. A selective HSD11B1 inhibitor for use according to claim 1 in combination with cell therapy.

4. A selective HSD11B1 inhibitor for use according to claim 1 or 2 in combination with at least

one immune checkpoint inhibitor.

A selective HSD11B1 inhibitor for use according to claim 4, wherein said at least one immune

checkpoint inhibitor is selected from a PD-1inhibitor, an CTLA-4 inhibitor and an PD-L1

inhibitor.

6. A selective HSD11B1 inhibitor for use according to any one of claims 1 to 5 in combination with

at least one PD-1inhibitor.

7. A selective HSD11B1 inhibitor for use according to claim 6, wherein said at least one PD-1

inhibitor is pembrolizumab.

112

- 8. A selective HSD11B1 inhibitor for use according to any one of claims 1 to 5 in combination with at least one CTLA-4 inhibitor.
- 9. A selective HSD11B1 inhibitor for use according to claim 1 or 2 in combination with at least one anti-cancer vaccine.
- 10. A selective HSD11B1 inhibitor for use according to any one of claims 1 to 9, wherein said HSD11B1 inhibitor is a selective over HSD11B2 with a factor or 100 or more.
- 11. A selective HSD11B1 inhibitor for use according to any one of claims 1 to 10, wherein said selective HSD11B1 inhibitor is selected from a 3,4,5-trisubstituted-4-1,2,4-triazole, an adamantane, in particular an adamantyltriazole, an arylsulfonamide, in particular an arylsulfonamidothiazole, an anilinothiazolone and a spirocyclic urea.
- 12. A selective HSD11B1 inhibitor for use according to any one of claims 1 to 11, wherein said HSD11B1 inhibitor is a 3,4,5-trisubstituted-4-1,2,4-triazole.
- 13.A selective HSD11B1 inhibitor for use according to any one of claims 1 to 11, wherein said HSD11B1 inhibitor is an adamantane.
- 14. A selective HSD11B1 inhibitor for use according to any one of claims 1 to 11, wherein said selective HSD11B1 inhibitor is selected from:

(BI 135585 or (6R)-6-(2-hydroxy-2-methylpropyl)-3-[(1R)-1-[4-(1-methyl-2-oxopyridin-4-yl)phenyl]ethyl]-6-phenyl-1,3-oxazinan-2-one); any pharmaceutically acceptable salts thereof.

- 15. A selective HSD11B1 inhibitor for use according to any one of claims 1 to 11, wherein said selective HSD11B1 inhibitor is selected from ABT-384 and BMS-83778.
- 16. A selective HSD11B1 inhibitor for use according to any one of claims 1 to 15, wherein cancer is selected from melanoma, lung carcinoma, glioblastoma, renal carcinoma, gastrointestinal stromal carcinoma and leukemia.
- 17. A pharmaceutical composition comprising at least one selective HSD11B1 inhibitor and at least one agent useful in immunotherapy and at least one pharmaceutically acceptable carrier.
- A pharmaceutical composition according to claim 17, wherein said selective HSD11B1 inhibitor is selected from 10J, PF-915275, BMS-823778, MK-0736, AZD8329, ABT-384, AZD4017 and BI 135585.
- 19. A pharmaceutical composition according to claim 17 or 18, wherein said at least one immunotherapeutic agent selected from a cancer vaccine, oncolytic virus and an immune system modulator.
- 20. A pharmaceutical composition according to any one of claims 17 to 19 for use as a medicament.

3) Results

- 21. A pharmaceutical composition according to any one of claims 17 to 19 for use in the treatment of a cancer.
- 22. A pharmaceutical composition for use according to claim 21, wherein cancer is selected from melanoma, lung carcinoma, glioblastoma, renal carcinoma, gastrointestinal stromal carcinoma and leukemia.
- 23. A method of identifying agents useful in the potentiation of immunotherapy, said method comprising the following steps:
 - exposing at least one immune cell such as dendritic cell, macrophage, neutrophil, T
 cell with cancer cell with at least one selective HSD11B1 substrate;
 - contacting said at least one cell with at least one candidate agent;
 - identifying agents that are able to inhibit selective HSD11B1 in said cells.
- 24. A method for treating a subject who is suffering from a cancer, said method comprising administering a therapeutically effective amount of an agent inducing selective HSD11B1 inhibition or any suitable pharmaceutically acceptable formulation thereof, in a subject in need thereof in combination with immunotherapy.

Abstract of the invention

The present invention relates to HSD11B1 inhibitors useful for increasing antitumor immune response in combination with immunotherapy, in particular for the treatment of cancers and to related compositions and methods using those.

II.C. Supplementary results

To test the efficacy of HSD11B1 inhibitors in combination with immunotherapy, a human *ex vivo* assay was developed in which several inhibitors of HSD11B1 covering different chemotypes (presented in Table 1 of the patent) were used. This is described in Example 1 and Figure 1 of the patent. To complete the results published in the patent, the potency and therapeutic efficacy of the various inhibitors were measured and compared in this assay. Moreover, a dose response of the most promising inhibitor was performed.

II.C.1. Materials and methods

To use pharmacological inhibitors in a cell assay, their dilution in proper solvent was necessary. Chemical inhibitors of HSD11B1 were solubilized in the appropriate solvent in 10 μ M stock solution for BI-135585 (in chloroform), HSD-016 (in DMSO, 10 % EtOH), AZD8329 (in DMSO), ABT-384 (in DMSO), BMS-823778 (in DMSO), AZD4017 (in DMSO), BVT-3498 (in DMSO), or MK-0736 (in DMSO), or in 100 μ M stock solution for 10J (in DMSO, 1/10 EtOH), PF915275 (in DMSO, 10 % EtOH), BVT-2733 (in DMSO, 10 % EtOH), and CBX (in PBS). The inhibitors were then used at the concentrations previously described in Examples 1 and 2 of the patent.

II.C.2. Results

To test the therapeutic potential of HSD11B1 inhibitors in immune oncology, an antigen recall assay with PBMCs was set up as explained in Example 1 of the patent. This assay was selected because PBMCs contain APCs and T cells, which allowed us to investigate the antigen presentation mechanism. Moreover, anti-PD-1 treatment was effective in this assay, allowing us to study the effect of the combination of HSD11B1 inhibitors and immune checkpoint blockade.

IFN- γ concentration was used to follow the antigen-dependent T cell activation in the presence of human HSD11B1 substrate (cortisone). The maximum IFN- γ produced during T cell activation was reached in the absence of cortisone and the presence of anti-PD-1. Therefore, the concentration of IFN- γ obtained in this condition treated with anti-PD-1 without cortisone was set as the maximum level and called the maximum effect.

As indicated in Table 4, seven out of the twelve HSD11B1 inhibitors tested reached over 100 % of the maximum effect, thus allowing HSD11B1 inhibition to be overcome. Moreover, as the IFN- γ concentration produced was higher than that in the condition without cortisone, which explains why the maximum effect was > 100 %, these seven inhibitors were demonstrated to be able to improve anti-PD-1 response. Among these seven HSD11B1 inhibitors, only BMS-823778 and ABT-3842 had an EC50 below 1 nM, with ABT-384 being the more efficient with EC50 = 0.01671 nM. Therefore, an additional response curve was created with ABT-384. As represented in Figure 9, ABT-384 reached its maximum effect at 0.1 nM in combination with anti-PD-1 treatment. As the more potent inhibitor, ABT-384 was retained for subsequent *in vivo* testing in different renal cancer models to study whether the anti-PD-1 response could be improved *in vivo*.

Inhibitor	Maximum Effect (%)	EC50 (nM)	R2
AZD8329	167.8	298.2	0.8595
AZD4017	154.5	131.9	0.8025
BI-135585	150.5	8.115	0.773
ABT-384	144.4	0.01671	0.8478
BMS-823778	137.8	0.6708	0.9666
PF915275	135.2	261.4	0.8292
MK-0736	133.6	8.158	0.8779
10J	82.12	2.264	0.7475
BVT-3498	68.41	0.0647	0.9813
Carbenoxolone	47.99	0.7827	0.8495
HSD-016	47.48	0.54	0.7341
BVT-2733	32.99	0.4662	0.8922

Table 4: Effect of HSD11B1 inhibitors on restoration of immune response. Potency and efficacy of HSD11B1 pharmacological inhibitors in combination with anti-PD-1 treatment during antigen recall assay. Effect maximum expressed in percentage of IFN-y concentration in the condition without cortisone with anti-PD-1. Half maximal effective concentration expressed in nM. Goodness of fit to the regression model is represented as R2. R2 close to 1 means a low variance of the variable compare to the model.

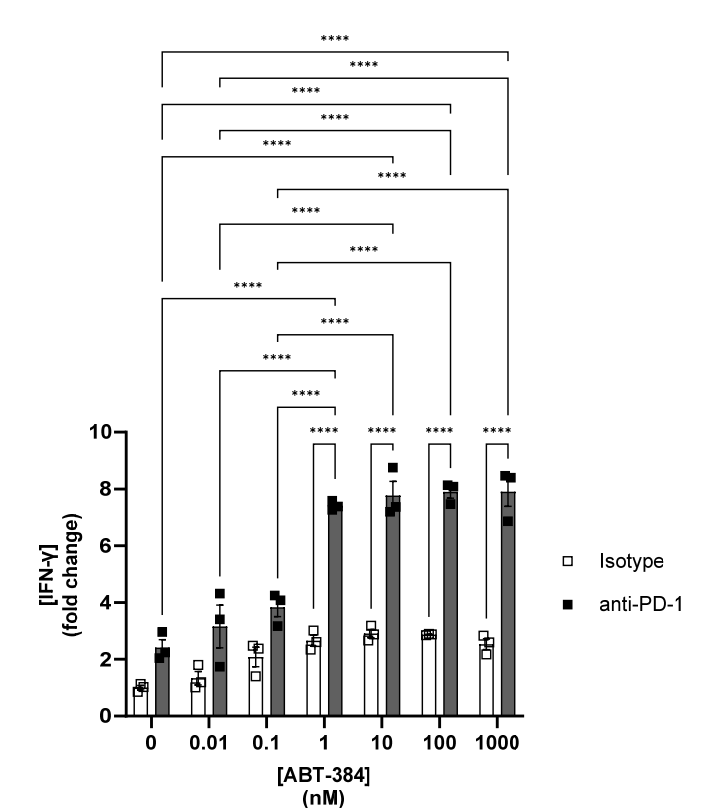


Figure 9: ABT-384 inhibits HSD11B1 in human ex vivo model. Conditions with 50 ng/mL of cortisone. IFN-y concentration was measured in supernatant after 1 week of antigen stimulation of PBMCs. Fold change compared to the condition with isotype and without ABT-384 is represented as mean +/- SEM of 3 technical replicates in one experiment. Data are representative of 2 independent experiments on the same donor. Statistical test: ordinary two-way ANOVA, alpha 0.05, Tukey's multiple comparison test, **** p value < 0.0001.

III. Effect of *Hsd11b1* genetic modulation on the antitumor immune response in a renal cancer model

Pharmacological inhibitors of HSD11B1 are administered systemically and can exhibit an activity against non-target proteins when concentrations are excessively high. Thus, to study the effect of HSD11B1 only in tumor cells as well as the impact of a specific inhibition of HSD11B1 in the host mouse, we performed an overexpression in the tumor cell line and the constitutive KO of *Hsd11b1* in mice.

The authors' contributions to this work are detailed as follows:

Aurélien Pommier, Carole Bourquin, and Hélène Poinot designed and planned the study. Hélène Poinot performed and analyzed all of the experiments with the help of Eulalia Olesti for steroid measurement. Hélène Poinot maintained the $Hsd11b1^{KO}$ mouse lines with the help of Aurélien Pommier and Fabrizio Thorel (Transgenic Core Facility of Geneva University) for their obtention, and of Montserrat Alvarez, Barbara Pinheiro Tonneau, and Isis Senoner for the genotyping during back-crossing. Aurélien Pommier supervised the study. This paragraph was written by Hélène Poinot.

III.A. Material and methods

Overexpression of *Hsd11b1*

Renal tumor cells (Renca) were genetically engineered to overexpress Hsd11b1 with a lentiviral plasmid. The plasmid #52961 (Addgene) and Hsd11b1 plasmid (ordered from Genscript, transcript sequence inserted between BamHI and XbaI restriction sites in a pUC57-Kan plasmid) were digested by BamHI and XbaI and ligated together. Hsd11b1 was located in front of the P2A sequence and the puromycin resistance gene, which necessarily allowed the expression of Hsd11b1 at the same time as the antibiotic resistance before peptide cleavage. The plasmid #52961 is a third-generation lentiviral plasmid; lentiviruses were produced and Renca cells infected before being placed in selection pressure (puromycin). To obtain a relevant negative control for subsequent in vivo tumor experiments, a random sequence of 29 amino acids (determined with http://www.faculty.ucr.edu/~mmaduro/random.htm) was inserted before the P2A sequence instead of $\mathit{Hsd11b1}$ transcript. The cells that overexpressed HSD11B1 were called Renca HSD11B1 $^{\text{HIGH}}$ and their negative controls were called Renca WT control.

Expression and activity of HSD11B1 measurement

Renca cell lines were cultured for few passages (kept below fifteen passages and always subconfluent) in RPMI, 10 % FBS, 1 % MEM Non-Essential Amino Acids, 2 mM L-glutamine, and 0.5 mM sodium pyruvate. To measure whether HSD11B1 was active in Renca that overexpressed the protein, 1.10⁵/well of Renca were cultured in 3 mL of medium in a six-well plate. Then, 11-DHC at a final concentration of 200 nM was added as it is the HSD11B1 substrate. After 48 h, the supernatant was collected and sent for mass spectrometry analysis of corticosterone and 11-DHC, as detailed in the material and methods of Section 3)I (with the method used for steroid measurement in kidney and plasma after D₄-cortisol injection).

Constitutive knockout of Hsd11b1 in mice

The KO of the *Hsd11b1* gene was performed in mice with the CRISPR/Cas9 method with the help of the Transgenic Core Facility of Geneva University. After *in vitro* fecundation, the embryos were injected with Cas9 protein and guide RNA (gRNA), allowing the *Hsd11b1* gene to be targeted. Two gRNAs were used to lead to two double strands cut and the elimination of a part of the gene, not only the creation of a frameshift (gRNA 1 and gRNA 2; Supplementary Table 1). The two gRNAs were located around exons 4 and 5 (HSD11B1 being composed of seven exons), leading to the removal of 552 base pairs (bp) out of the gene. To assess whether both cuts were happening, mice were genotyped with two PCR primers around exons 4 and 5 (Fw1 and Rv1 primers; Supplementary Table 1). The PCR product was

3) Results

1080 bp long in WT mice and 552 bp in full KO mice. After the obtention of $Hsd11b1^{KO}$ mice in the strain used for *in vitro* fecundation (B6D2F1 mice), back-crossing was carried into the two strains of interest, namely C57BL/6 and Balb/c. To increase the genetic background of each of the strains, $Hsd11b1^{+/KO}$ mice were crossed with WT mice and the heterozygotes of the next generation were kept for further crossing.

Subcutaneous tumor model

Subcutaneous (s.c.) Renca tumors were induced and anti-PD-1 treatment performed as described in the materials and methods of Section 3)I. The tumor volume was calculated with the following formula:²⁵⁸

$(\pi/6)$ *length*width*height

Steroid quantification in plasma was performed as described in the materials and methods of Section 3)I, with the method used for steroid measurement in plasma. The lower limits of quantification were 0.1 nmol/L for corticosterone and 2 nmol/L for 11-DHC.

Flow cytometry staining

All flow cytometry staining and analyses were performed as described in the materials and methods of Section 3)I.

Statistical analyses

All statistical tests were performed as described in the materials and methods of Section 3)I. The tests performed are indicated in the legends of figures.

III.B. Effect of intratumoral HSD11B1 over-expression on the antitumor immune response in a subcutaneous tumor model

During our investigation of HSD11B1 expression in a ccRCC tumor by immunohistochemistry (represented in Figure 2A of the manuscript in Section 3)I.B), we found that HSD11B1 was expressed in tumor cells in some patients (data not shown). Therefore, we hypothesized that HSD11B1 activity in tumor cells could affect tumor growth and the antitumor immune response.

To further investigate the impact of HSD11B1 tumor expression on the antitumor immune response, Renca cells overexpressing HSD11B1 were produced. To validate the phenotype of Renca HSD11B1^{HIGH} cells, the consumption of 11-DHC, HSD11B1 substrate, and production of corticosterone in the supernatant of the cells were measured. The amounts of corticosterone and 11-DHC were measured by LC-MS after 48 h of culture. As Figure 10 A and B indicate, the amount of 11-DHC in the culture medium was too low for us to detect basal activity of HSD11B1 without 11-DHC supplementation in these experimental conditions. Thus, known concentrations of 11-DHC were added to the medium. Corticosterone was only detected in the presence of cells. As Figure 10 A and B indicate, Renca HSD11B1^{HIGH} cells consumed more 11-DHC and produced more corticosterone than the WT control cells. Overall, the murine renal cancer cell line exhibited HSD11B1 activity, which increased with the overexpression of Hsd11b1.

We then engrafted Renca HSD11B1^{HIGH} and WT control cells in WT mice to study the impact of intratumoral HSD11B1 expression on the antitumor immune response. As Figure 10 C indicates, the overexpression of HSD11B1 in tumor cells did not affect tumor growth. Moreover, an examination of the immune population infiltrating the tumor revealed no differences between the groups (Figure 10 D–I).

We conclude that despite a higher *in vitro* production of corticosterone, HSD11B1 overexpression in tumor cells does not impact tumor growth nor the immune response to the tumor.

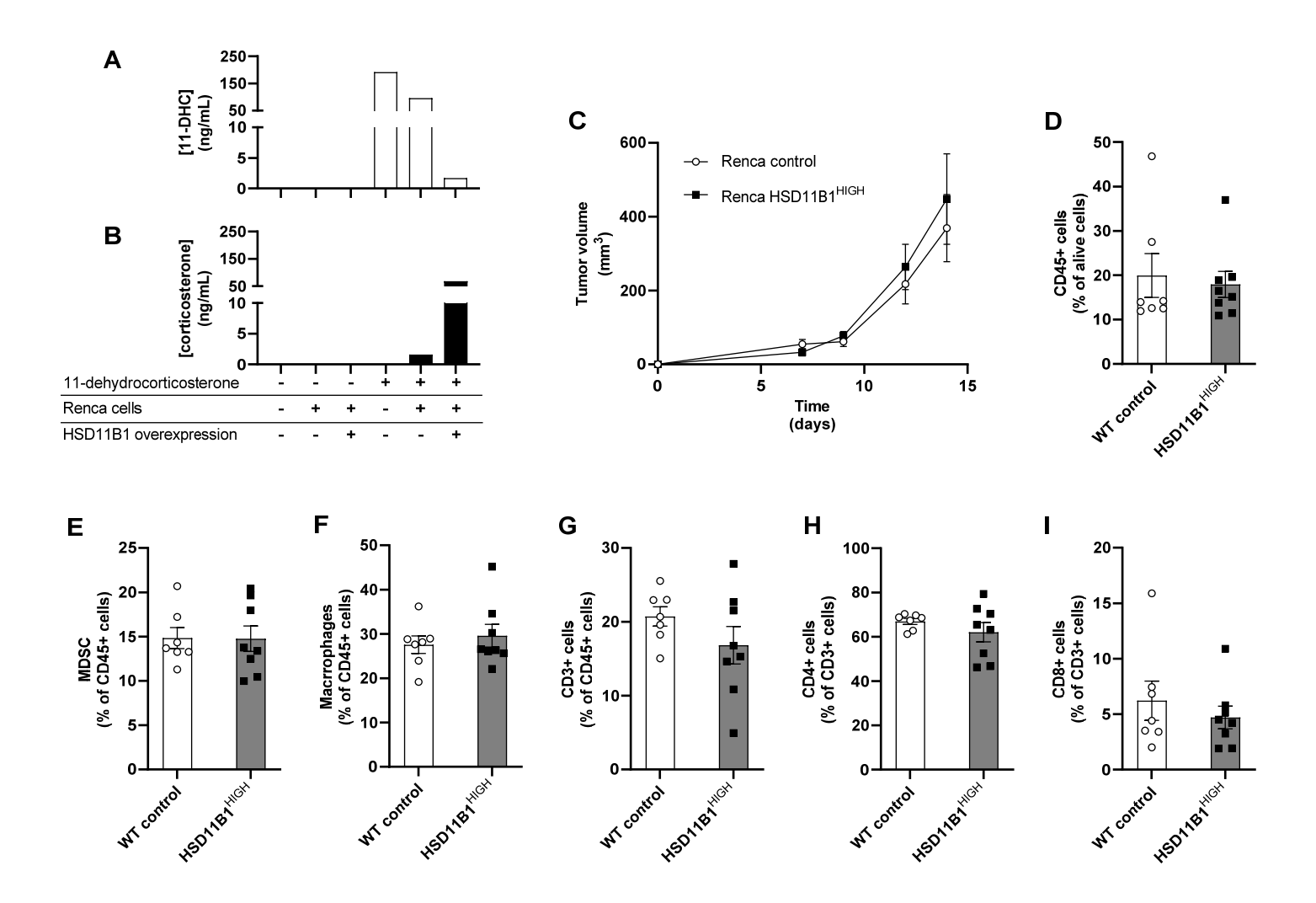


Figure 10: Intratumoral hsd11b1 over-expression does not have an effect on the antitumor immune response. **A-B.** 11-DHC (**A**) and corticosterone (**B**) concentrations in cell supernatant measured by mass spectrometry. **C.** Tumor growth of s.c. Renca B1^{high} tumor in WT mice. Data are shown as mean of tumor volume +/- SEM. 7 to 8 mice per group. **D-I.** Immunophenotyping results of the tumor by flow cytometry. Percentage of cells represented as % of alive cells (**D**), CD45⁺ cells (**E-G**) and CD3⁺ cells (**H-I**). Data are shown as mean +/- SEM. Each dot represents one mouse, 7 to 8 mice per group.

III.C. Impact of *Hsd11b1* knockout in mice on the antitumor immune response in a subcutaneous tumor model

To test the role of *Hsd11b1* expressed by the host mouse on the antitumor immune response, a mouse line with constitutive loss of *Hsd11b1* was produced.

First, we measured the effect of *Hsd11b1* loss on the immune system. Immunophenotyping of spleen and lymph nodes was performed on naïve *Hsd11b1*^{KO} mice and their littermate controls. No differences were found between genotypes in the total number of leukocytes (data not shown) nor in the proportion of DCs, T lymphocytes, or other immune subpopulations in the spleen, as indicated in Figure 11 A and B (and **Supplementary Figure 1** A–C), or in the lymph nodes (Figure 11 C–D and **Supplementary Figure 1** D–F).

Constitutive *Hsd11b1^{KO}* mice were then subcutaneously injected with Renca WT cells to study the effect of HSD11B1 activity in the host compartment on the antitumor immune response. Treatment with anti-PD-1 was administered to study the effect of the constitutive loss of *Hsd11b1* on the immune checkpoint response. Unexpectedly, anti-PD-1 treatment did not have an effect on the tumor growth in *Hsd11b1^{KO}* mice. By contrast, in WT mice, anti-PD-1 treatment reduced tumor growth, as indicated in Figure 11 E. The intratumoral infiltration of immune cells was similar in all groups, despite a slight increase in the mice treated with anti-PD-1 in both genotypes, although this was nonsignificant (Figure 11 F, **Supplementary Figure 1** G–J). The only significant difference regarding the tumor immune infiltration between *Hsd11b1^{KO}* and control mice was found for the MDSCs. Indeed, a higher MDSC infiltration was observed in the WT group compared with the *hsd11b1^{KO}* group with anti-PD-1 treatment (Figure 11 G). As Figure 11 H illustrates, the *Hsd11b1^{KO}* mice exhibited a lower ratio of plasmatic corticosterone to 11-DHC. Despite a significant difference in 11-DHC concentration between *Hsd11b1^{KO}* and WT mice (Figure 11 I), the corticosterone concentration and corticosterone-to-11-DHC ratio were not significantly different between the anti-PD-1 treated groups (**Supplementary Figure 1** K and Figure 11 H).

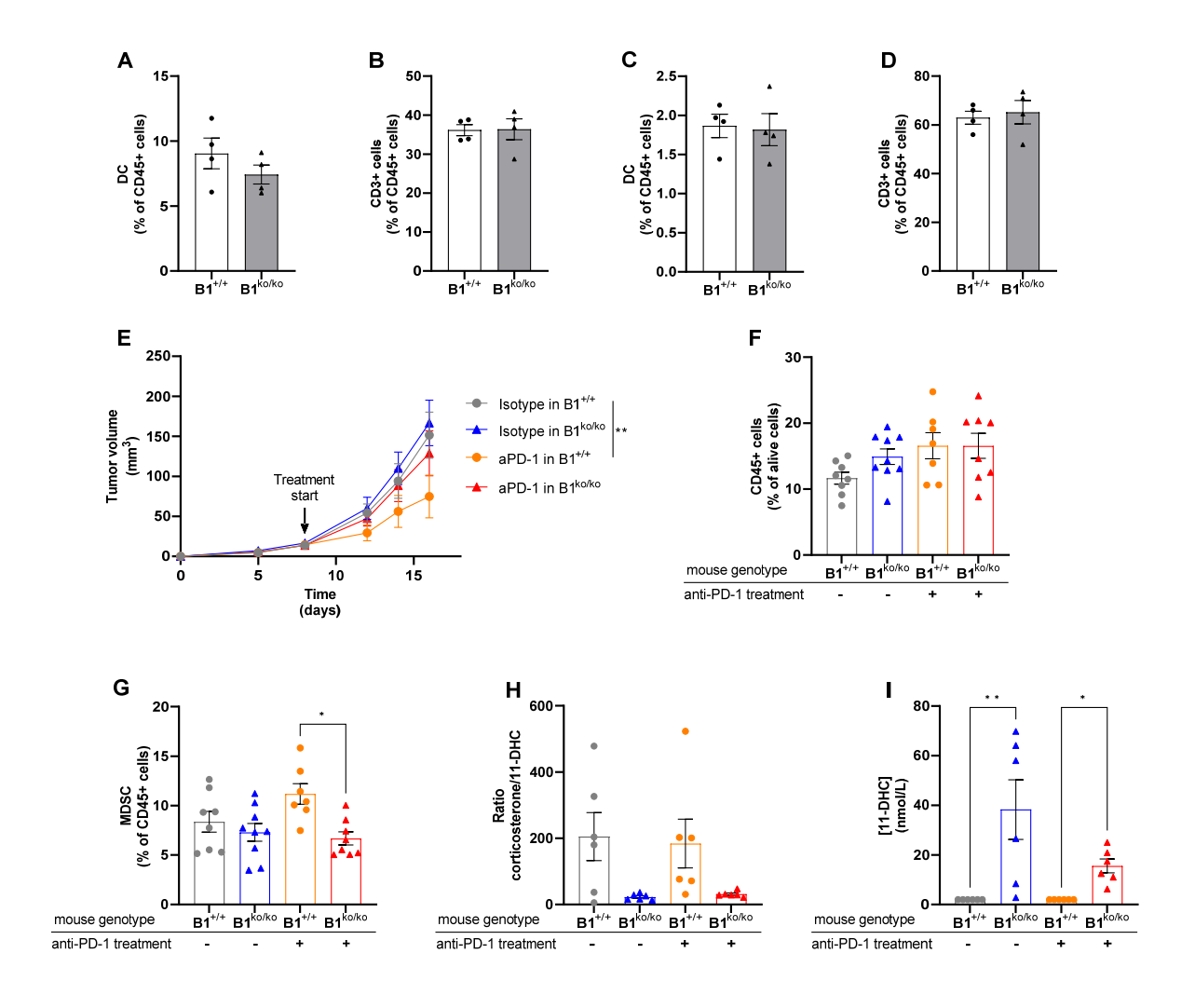


Figure 11: Constitutive knock out of Hsd11b1 prevents anti-PD-1 response in a subcutaneous tumor model. **A-D.** Immunophenotyping results of spleen (**A-B**) and lymph nodes (**C-D**) of naïve WT and Hsd11b1^{KO} mice by flow cytometry. Percentage of cells represented as % of CD45 $^+$ cells. Data are shown as mean +/- SEM. Each dot represents one mouse, 4 per group. **E.** Tumor growth of Renca s.c. tumor in Hsd11b1^{KO} mouse females and control littermate. Treatment started at day 7. Data are shown as mean of tumor volume +/- SEM. 10 mice per group. Statistical analysis: results showed for day 16, ordinary two-way ANOVA, alpha 0.05, Tukey's multiple comparisons tests, ** p value < 0.01, *** p value < 0.001. **F-G.** Immunophenotyping results of the tumor by flow cytometry. Percentage of cells represented as % of alive cells (**F**), or CD45 $^+$ cells (**G**). Data are shown as mean +/- SEM. Each dot represents one mouse, 8 to 10 mice per group. Statistical analysis: Kruskal–Wallis test, alpha 0.05, Dunn's multiple comparisons test, * p value < 0.05. **H-I.** Corticosterone and 11-DHC concentrations measured in plasma of s.c. tumor bearing mice by mass spectrometry represented as ratio (**H**) or nmol/L (**I**). Data are shown as mean +/- SEM. Each dot represents one mouse, 6 mice per group. Statistical analysis: Kruskal–Wallis test, alpha 0.05, Dunn's multiple comparisons test, * p value < 0.05, ** p value < 0.01.

III.D. Discussion

As corticosterone inhibits the immune response and we demonstrated that a higher expression of *Hsd11b1* is associated with more corticosterone (Figure 10 A and B), immunosuppression was expected in the Renca HSD11B1^{HIGH} tumors. However, s.c. Renca tumors overexpressing HSD11B1 displayed the same growth as Renca WT control tumors (Figure 10 C). Moreover, they were not less infiltrated by immune cells than the WT tumors (Figure 10 D), and we found no differences in the immune infiltrate (Figure 10 E–I).

One hypothesis regarding this absence of difference between Renca HSD11B1^{HIGH} and WT tumors was a lack of HSD11B1 substrate in the tumor microenvironment. Indeed, the absence of 11-DHC available for HSD11B1 in the tumor microenvironment would prevent increased corticosterone production even though *Hsd11b1* was overexpressed in tumor cells. As 11-DHC is produced by HSD11B2, which is mainly expressed in the kidney and not in the skin, a solution for overcoming this lack of HSD11B1 substrate could be an orthotopic tumor model. Indeed, in this case, Renca HSD11B1^{HIGH} tumor cells would be directly in the kidney, and thus, 11-DHC would be available directly in the tumor microenvironment. One could expect an increase of corticosterone production by HSD11B1 compared with Renca WT cells in this orthotopic condition.

Another hypothesis to explain why *Hsd11b1* overexpression in tumor cells did not lead to any change in tumor growth nor in the intratumoral immune infiltration, is that the activity of HSD11B1 was more decisive in the tumor microenvironment cells as immune cells. Thus, the constitutive loss of *Hsd11b1* was performed in mice.

However, $Hsd11b1^{KO}$ in the host appeared to be detrimental to the mice as there was a loss of anti-PD-1 response in $Hsd11b1^{KO}$ mice compared with WT mice. MDSC infiltration in WT anti-PD-1 treated tumors was increased compared with $Hsd11b1^{KO}$ tumors. MDSCs are known to be immunosuppressors, and immunosuppressive infiltration in tumors is associated with resistance to immune checkpoint blockade and higher tumor growth. Therefore, as the number of MDSCs is the lowest in the only group that responded regarding tumor growth, one could assume that their role in the resistance to treatment is not substantial, and other factors must be of importance. Functionality of T cells could be particularly impacted by Hsd11b1 loss as HSD11B1 plays a role in their thymic development.

This lack of anti-PD-1 response in $Hsd11b1^{KO}$ could suggest an adrenal compensation of the steroid level in these mice, which could lead to high concentrations of steroids, as already described for some mouse strains. However, we did not observe this, as indicated in Figure 11 H, which reveals a relative decrease in active glucocorticoids in KO mice compared with WT mice. Nevertheless, these results regarding steroid levels must be carefully considered, especially for the corticosterone concentration

(Supplementary Figure 1 K). Indeed, corticosterone is rapidly increased by stress, and a particular setup must be followed during euthanasia to avoid pre-mortem stress and obtain a reliable corticosterone level. During tumor experiments, the mice were placed in a quiet and calm environment at least 1 h before euthanasia to limit their stress. However, the method used for euthanasia (CO_2) did not cause a fast enough death to ensure a lack of pre-mortem stress. Therefore, corticosterone concentrations could be higher in $Hsd11b1^{KO}$ mice compared with WT mice, while the plasmatic level in WT mice could increase pre-mortem due to the stress of euthanasia leading to the average of all groups (Supplementary Figure 1 K).

Overall, increased HSD11B1 activity in tumor cells, which was expected to be pro-tumoral, did not exhibit an effect on tumor growth in our s.c. renal model. We also demonstrated an inhibitory effect of HSD11B1 activity on immune response in *in vitro* assays, and therefore, we hypothesized a potential benefit to its loss in a cancer model. This hypothesis was not confirmed by the results obtained with the tumor model in $Hsd11b1^{KO}$ mice. Even though loss of HSD11B1 reduces the level of active glucocorticoids, and thus, should decrease the immunosuppression in a tumor context, antitumor immune response was not improved in $Hsd11b1^{KO}$ mice. Moreover, despite no difference in immune cells between $Hsd11b1^{KO}$ and WT mice, we demonstrated a pro-tumoral effect of constitutive Hsd11b1 KO as we lost the anti-PD-1 response in $Hsd11b1^{KO}$ mice. Further investigations are needed to decipher the impact of constitutive loss of Hsd11b1 such as extensive characterization of T cells as HSD11B1 is known to play a role in their differentiation. 260

3) Results

IV. Effect of glucocorticoid receptor antagonism on tumor growth and antitumor immune response

To investigate not only the effect of glucocorticoid regeneration through HSD11B1 but also the total effect of endogenous glucocorticoids, we tested the impact of GR antagonism on the antitumor immune response.

Because RU486 (mifepristone) is a GR antagonist already delivered in clinic (as explained in Section 1)III.D.2.a), we used it in combination with anti-PD-1 in an s.c. renal tumor model to examine the GR inhibition effect.

The authors' contributions to this work are detailed as follows:

Aurélien Pommier and Hélène Poinot designed and planned the study. Hélène Poinot performed and analyzed all of the experiments with the help of Eloïse Dupuychaffray for the Bulk RNA barcoding and sequencing protocol as well as advice from Aurélien Pommier. Aurélien Pommier supervised the study. This paragraph was written by Hélène Poinot.

IV.A. Material and methods

Pharmacological inhibition of the glucocorticoid receptor in a renal cancer subcutaneous model

An s.c. renal tumor model was obtained with the induction of Renca tumors as explained in the material and methods of Section 3)I. The tumor volume was calculated using the following formula:²⁵⁸

$(\pi/6)$ *length*width*height

At day 7 after tumor induction, mice were assigned to treatment groups with the aim of obtaining groups of comparable average tumor areas. The mice were not moved from their initial cages to avoid stress and conflict. Treatments were started at day 7 after tumor induction. RU486 suspension (35 mg/kg) or vehicle (0.5 % (hydroxypropyl)methyl cellulose + 0.2 % tween 80) were administered in $100~\mu L$ per os twice a day. Then, anti-PD-1 ($200~\mu g/mouse$) or isotype were injected intraperitoneally three times a week in $200~\mu L$ of PBS.

Steroid quantification in plasma was performed as described in the material and methods of Section 3)I, with the method used for steroid measurement in plasma. The lower limits of quantification were 0.1 nmol/L for corticosterone and 2 nmol/L for 11-DHC.

RNA sequencing

Tumors were collected post-mortem, snap frozen, and stocked at -80°C before RNA extraction with TRIzol reagent. Then, 1 mL of cold TRIzol reagent was added to tumor samples and homogenized with tissue homogenizer (two times successively, 25 Hz, 2 min, 4°C). After 5 min of incubation at room temperature, the samples were centrifuged (10 min, 18,000 g, 4°C) and the supernatants were vigorously mixed with 200 μ L of biophenol:chloroform:isoamylalcohol (25:24:1). After 10 min of incubation at room temperature, samples were centrifuged (15 min, 13,000 g, 4°C) and the upper aqueous phase pipetted out into a new tube with 500 μ L of isopropanol. After 10 min of incubation at room temperature, the samples were centrifuged (10 min, 13,000 g, 4°C) and the supernatants were discarded. RNA pellets were washed with 1 mL of ethanol (centrifugation 5 min, 7,500 g, 4°C) and air dried for 5–10 min before being resuspended in water.

A library for bulk RNA barcoding and sequencing was prepared following the provider's protocol (Alithea Genomics, Barcoded Oligo-dT V4D2 module #10511 and Library Preparation module #10521). The library was sequenced using the Genomics platform of Geneva University.

Next, RNA sequencing data were filtered and normalized using the Voom method with the Automated Single-Cell Analysis Pipeline from the *Ecole Polytechnique Fédérale de Lausanne* (EPFL). Normalized log2(expression) data were downloaded for subsequent analysis.

Hierarchical clustering was generated with the TIBCO Spotfire software package. Gene clustering was calculated using Ward's method and distance was measured with the half square Euclidean distance, with the weight of expression ordered by the average value and normalization with Z-score calculation.

Gene set enrichment analysis was performed with gene expressions obtained with GSEA software. One-to-one comparisons were performed with the gene sets database m2.cp.v2022.1.Mm.symbols of GSEA, which contains mouse curated canonical pathway gene sets from BioCarta, Reactome, and WikiPathways.

IV.B. Results

The combination of RU486 and anti-PD-1 treatment was tested in an s.c. renal tumor model in mice. GR activation leads to the inhibition of the immune response (as explained in Section 1)III.C), and because RU486 is known to antagonize the GR, its effect on the immune system was expected to be beneficial for the antitumor immune response.

As illustrated in Figure 12 A, the combination of RU486 and anti-PD-1 treatment significantly decreased tumor growth compared with anti-PD-1 alone. However, this effect on tumor growth could not be detected in the immune populations by FACS analysis (Supplementary Figure 2 A–G). To investigate the effect of the combination of RU486 + anti-PD-1 on the steroid pathway further, we examined the steroid levels in the plasma of the tumor-bearing mice. The ratio of corticosterone to 11-DHC concentrations decreased in the combination group compared with mice receiving only anti-PD-1, as indicated in Figure 12 B. Despite no differences in tumor immune infiltration, the mice treated with the combination therapy exhibited a higher percentage of CD45⁺ cells in the spleen compared with untreated mice (Figure 12 C and Supplementary Figure 2 H–K).

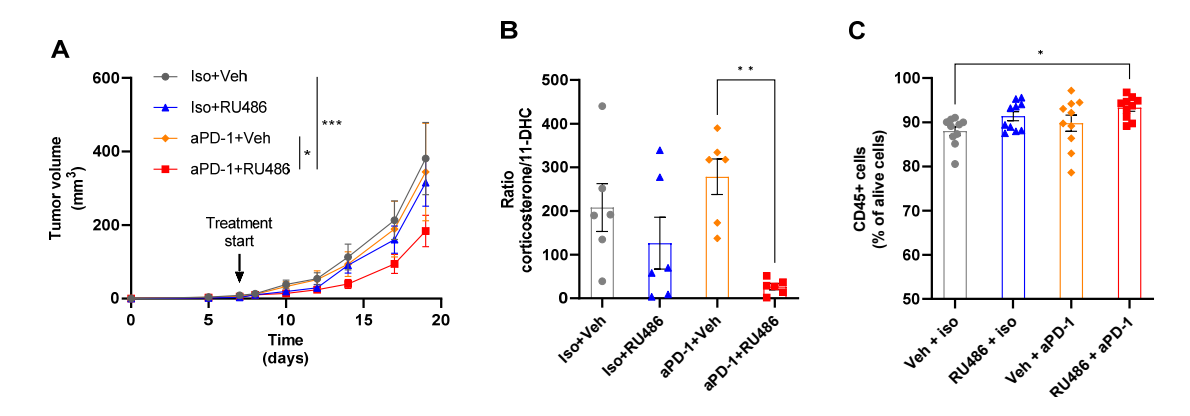


Figure 12: Inhibition of GR improved anti-PD-1 response in tumor-bearing mice. **A.** Growth of Renca s.c. tumors in female mice. Treatment started at day 7. Data are presented as the mean of tumor volume +/- SEM. 10 mice per group. Statistical analysis: results presented for day 19, ordinary two-way ANOVA, alpha 0.05, Tukey's multiple comparisons test, * p value < 0.05, *** p value < 0.001. **B.** Concentrations of corticosterone and 11-DHC measured in the plasma of s.c. tumor bearing mice by mass spectrometry and represented as the ratio. Data are presented as mean +/- SEM. Each dot represents one mouse, 6 mice per group. Statistical analysis: Kruskal–Wallis test, alpha 0.05, Dunn's multiple comparisons test, ** p value < 0.01. **C.** Immunophenotyping results of the spleen of tumor bearing mice by flow cytometry. Percentage of CD45⁺ cells represented as % of alive cells. Data are presented as mean +/- SEM. Each dot represents one mouse, 10 mice per group. Statistical analysis: Kruskal–Wallis test, alpha 0.05, Dunn's multiple comparisons test, * p value < 0.05.

To further identify biomarkers of the response to the combination therapy, RNA sequencing analyses were performed on the tumor samples and gene expression was investigated in the different treatment groups.

Several approaches were employed to explore gene expression data to detect changes between the treatment groups. First, a gene ontology-based approach was employed to identify the physiological pathways differentially expressed in the different treatment groups. This approach is a broad method compared with the second approach described next. Indeed, this first method of analysis is based on gene sets. One gene set corresponds to one pathway ontology, which considers the expression of several genes simultaneously. Therefore, one individual gene can be analyzed inside several gene sets, and even a low difference of gene expression can be considered within a gene set. However, this method allowed us to identify the main physiological pathways differentially expressed between the groups.

The second approach was based on the results of a t test performed to compare the gene expression between groups. Two-by-two comparisons were performed to compare tumor gene expression between the treatment groups. This method was more precise and reduced the result to individual differentially expressed genes. However, it made understanding the overall picture difficult as no physiological pathway was associated with each gene.

First, to obtain a comprehensive view of the biological functions impacted in the anti-PD-1+RU486 group versus the other groups, a gene ontology analysis was performed with GSEA software. As presented in Figure 13 A, gene ontology analysis revealed an enrichment in genes involved in immune pathways, such as the TYROBP signaling pathway, PD-1 signaling, and chemokines signaling pathways, or the phosphorylation of CD3 and TCR in the anti-PD-1+RU486 group compared with all other groups. As all of the genes from a gene set are not automatically enriched to obtain a significantly enriched gene set, the first 10 gene sets enriched in anti-PD-1+RU486 from the comparison in Figure 13 are detailed in Supplementary Table 2.

Subsequent to the GSEA analysis, the fifty more and fifty less enriched genes in the anti-PD-1+RU486 group, compared with all other groups, were extracted and represented in a heat map, which is presented in Figure 14.

This comparison of the anti-PD-1+RU486 group with the other groups led to the average of the genes expressed in the three other groups, as represented in the heat map in Figure 14. Therefore, all of the two-by-two comparisons were performed in the same way and are presented in Supplementary Figure 3 to Supplementary Figure 7. Noteworthily, the genes involved in collagen metabolism were enriched in the tumors of mice treated with the combination treatment compared with those treated with anti-

PD-1 alone (Supplementary Figure 7). This suggests an important role of the extracellular matrix metabolism in the anti-PD-1 response.

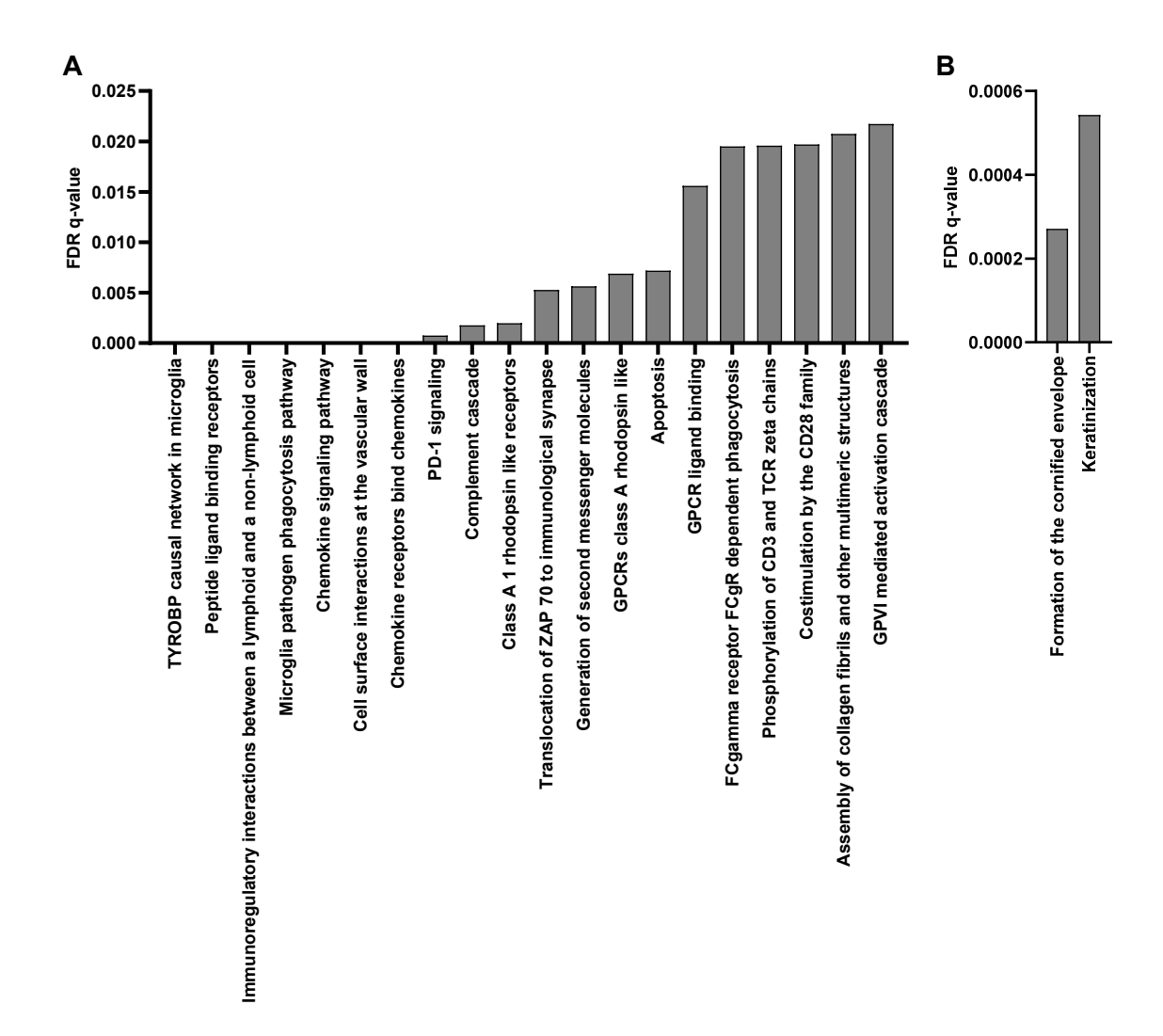


Figure 13: Physiological pathways differentially expressed in tumor of mice. Comparison of gene expression in tumors of females receiving anti-PD-1+RU486 to all the other groups of treatment (Iso+Veh, Iso+RU486 and anti-PD-1+Veh) with GSEA software. RNA from bulk s.c. Renca tumors from the experiment presented in Figure 12. Gene sets obtained from GSEA software, using the mouse canonical pathways data base. Gene set are ranked on the x axis from the smallest to the largest nominal p value. Only the first 20 statistically differentially expressed gene sets are showed (p value < 0.05 and FDR < 0.25). 9 to 10 mice per group. A. Physiological pathways enriched in tumor of mice treated with anti-PD-1+RU486. B. Physiological pathways reduced in tumor of mice treated with anti-PD-1+RU486.

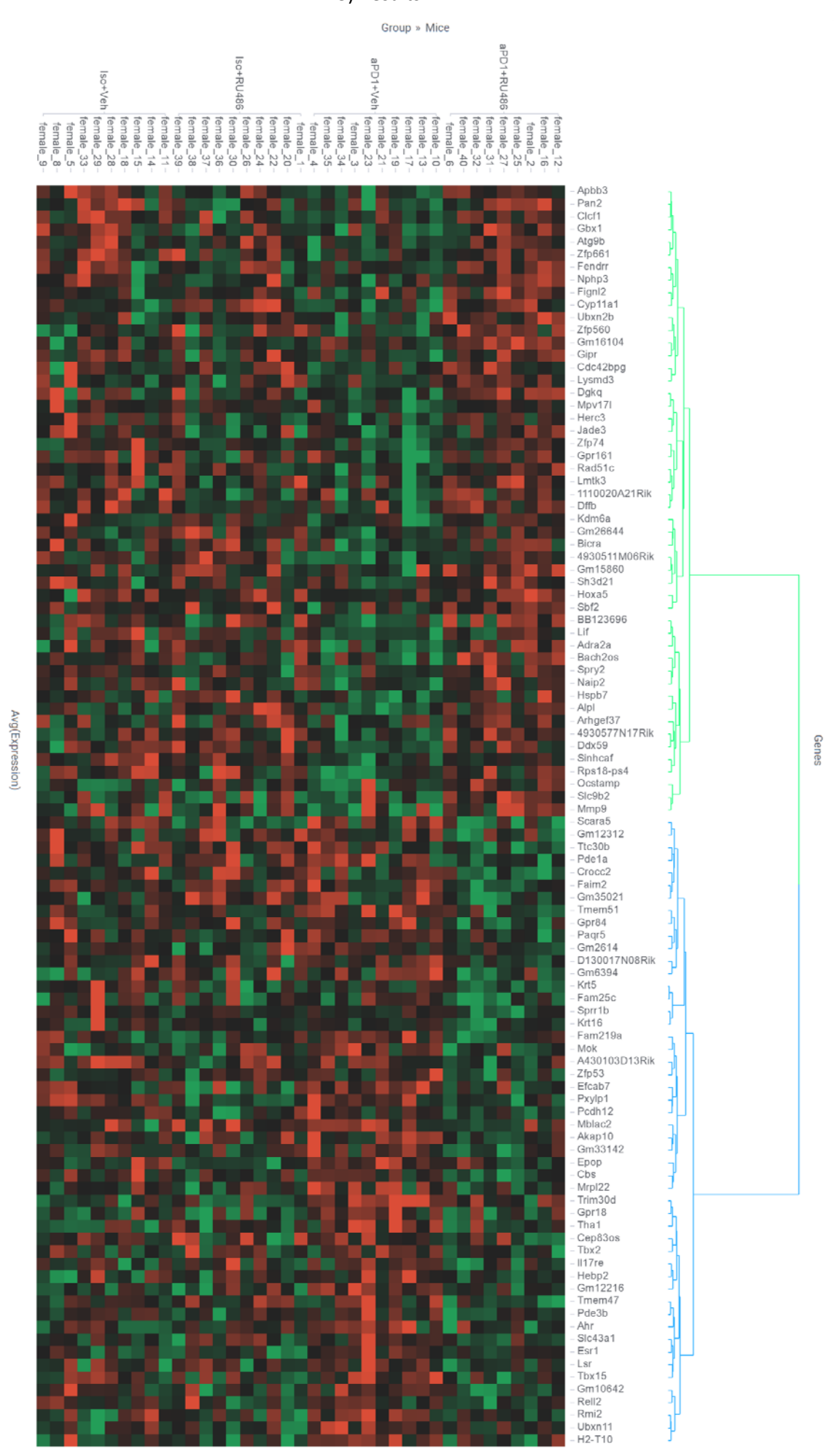


Figure 14: Combination of anti-PD-1+RU486 led to a modification of the intratumoral gene profile. This heat map represents the hierarchical clustering of the 50 most and 50 least expressed genes in the tumors of mice receiving anti-PD-1+RU486 compared with all other treatment groups. The gene selection is based on the GSEA analysis in Figure 13. Genes are along the horizontal axis and mice are along the vertical axis (clustered by treatment group).

The second approach increased the level of precision of the gene expression analysis. First, based on tumor growth, we identified three non-responder groups (Iso+Veh, Iso+RU486, and anti-PD-1+Veh) and one responder group (anti-PD-1+RU486). Comparisons of gene expression were performed between the responder group and each of the non-responder groups. With these comparisons, a Venn diagram was obtained to visualize the intersection of differentially expressed genes between the groups in Figure 15 A. Forty common genes were found to be differentially expressed in the anti-PD-1+RU486 in the three comparisons, which were used to create the heat map presented in Figure 15 B.

To further explore the effect of the anti-PD-1+RU486 combination on gene expression, bibliographic research was conducted. The aim was to determine whether these gene expressions were known to be immune-specific or to play a role in immune cells. The results are indicated in Table 5 and Table 6. Several upregulated genes were immune-specific, especially in the innate immune response, such as *Spag9*, or *Ppp6r3* and *Mark3*, which are expressed in eosinophils (Table 5). Some genes involved in the adaptive immune response were also enhanced, such as *Ptpn4* and *Casp6*, which are implicated in TCR signaling, or *Cd5I*, whose activation leads to the differentiation of T cells into Th₁₇ (Table 5).

Moreover, some of these genes were known to be modulated depending on the glucocorticoid context, such as *Zbtb43*, which is enriched in low glucocorticoid conditions, or *Tomm34*, which inhibits GR nuclear activation.

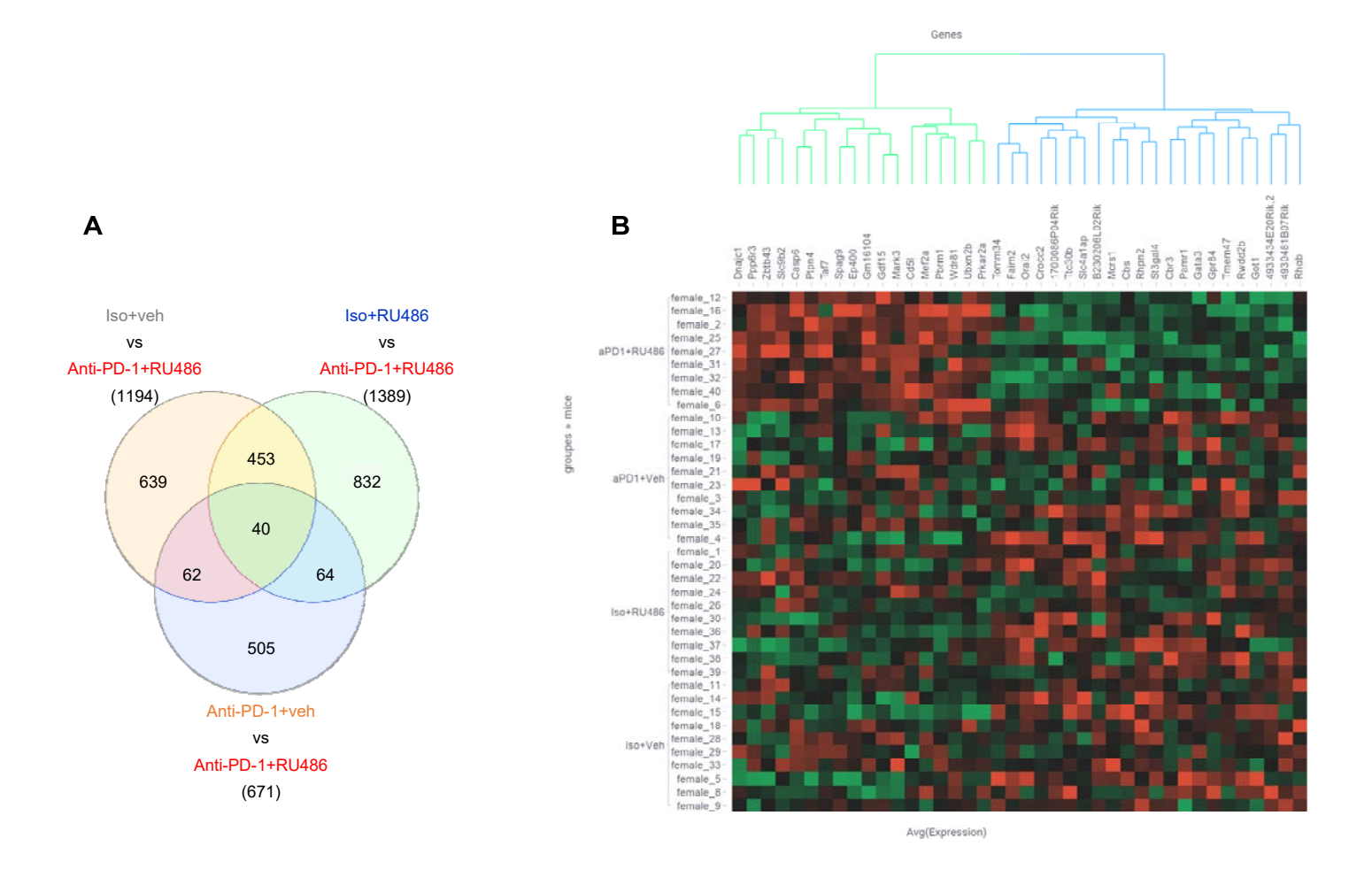


Figure 15: Combination of a GR inhibitor and anti-PD-1 impacts gene expression in the tumor. **A.** Venn diagram of differentially expressed genes in Renca s.c. tumors of female mice. The number of significantly differentially expressed genes between groups Iso+Veh and anti-PD-1+RU486, groups Iso+RU486 and anti-PD-1+RU486, group anti-PD-1+Veh and anti-PD-1+RU486, are represented in the brackets below the respective comparison (Statistical analysis: Student test, alpha 0.05, data of 9 to 10 mice). Numbers indicated in the diagram represent the number of genes which are differentially expressed in several comparison or exclusive of 1 comparison. **B.** Heat map representing the hierarchical clustering of the genes differentially expressed in all the comparisons of A (40 genes). Genes are in the horizontal axis and mice are in the vertical axis (clustered by treatment group).

Gene	Function involved	Immune cell expression
Dnajc1	Protein synthesis	Low in immune cells
Ppp6r3	Maintenance of immune self-tolerance	Low in immune cells Eosinophils
Zbtb43	Transcriptional regulation	Low in immune cells Basophils
Slc9b2	Intracellular pH, sodium homeostasis, and cell volume	Enhanced in immune cells NK cells
Casp6	Programmed cell death, innate immunity Cleaves NFkB and CREBBP	Low in immune cells T cell (T cell receptor)
Ptpn4	Negatively regulates: TLR4-induced IFN-β production and TCR-mediated signaling pathway	Adaptive immune response T cell
Taf7	Initiation of RNA polymerase II	Low in immune cells Granulocytes
Spag9	Scaffold protein Involved in tumor growth and development	Innate immune response Myeloid cells
Ep400	Transcriptional activation of select genes of NuA4 histone acetyltransferase complex	Low in immune cells Plasmacytoid DC
Gdf15	Stress-induced hormone Food intake, energy consumption in response to stresses	Enhanced in immune cells Neutrophil
Mark3		Innate immune response Eosinophil
Cd5l	Regulation of lipid synthesis Macrophages: promotes anti-inflammatory cytokine profile in response to TLR activation ²⁶¹ Key regulator of metabolic switch in Th ₁₇ cells	Macrophage Th ₁₇ cells
Mef2a	Activation of numerous growth factor and stress-induced genes	Low in immune cells Monocyte
Pbrm1	Negative regulator of cell proliferation Stability of the SWI/SNF chromatin remodeling complex	Low in immune cells Eosinophil
Wdr81	Negative regulator of PI3 kinase/PI3K activity Endosome fusion, recycling, sorting, transport	Low in immune cells Eosinophil
Ubxn2b	Adapter protein required for Golgi and endoplasmic reticulum biogenesis	Innate immune response Neutrophil
Prkar2a	cAMP signaling in cells CREB pathway signaling	Low in immune cells Monocyte

Table 5: Genes enhanced in the tumor of mice receiving anti-PD-1+RU486. Genes enhanced in tumors of anti-PD-1+RU486 group compare to all the other groups (from the 40 genes showed in Figure 15).

Gene	Function involved	Immune cell expression
Tomm34	Protein import into mitochondria Antigen presentation	Antigen presenting cell
Faim2	Protects cells uniquely from Fas-induced apoptosis	Enhanced in immune cells T _{reg}
Orai2	Ca ²⁺ release-activated Ca ²⁺ -like channel subunit	Innate immune response Eosinophil
Crocc2	Bone formation, plasticity, and evolution	Not detected in immune cells
Ttc30b	Required for polyglutamylation of axonemal tubulin	Low in immune cells Basophil
Slc4a1ap	May be involved in inflammatory response	Low in immune cells
Mcrs1	Cellular respiration	Low in immune cells Basophil
Cbs	Elimination of L-methionine and L-homocysteine Production of H2S	Innate immune response Neutrophil
Rhpn2	Involved in stress fiber formation and turnover of actin	Not detected in immune cells
St3gal4	Selectin-mediated rolling and adhesion of leukocytes during extravasation	Basophil, plasmacytoid DC, neutrophil
Cbr3	NADPH-dependent oxidoreductase	No immune specificity
Pamr1	In breast cancer: tumor suppressor Suppresses MYC target and mTORC1 signaling	Not detected in immune cells
Gata3	Promotes Th2 response Driver of T cell differentiation and <i>IL-5</i> and <i>IL-13</i> transcription.	
Gpr84	Receptor for medium-chain free fatty acid Regulation of the immune system.	Myeloid DCs Neutrophils
Tmem47	Regulates cell junction organization. Involved in podocyte differentiation.	Not detected in immune cells
Rwdd2b	Cellular respiration	Basophils
Got1	Biosynthesis of L-glutamate Regulates source of H2S	Low in immune cells Plasmacytoid DC
4933434E20Rik,2	General regulator of phagocytosis	Macrophages
Rhob	Apoptosis in transformed cells after DNA damage Intracellular protein trafficking	Innate immune response Eosinophil

Table 6: Genes downregulated in the tumor of mice receiving anti-PD-1+RU486. Genes downregulated in tumors of anti-PD-1+RU486 group compare to all the other groups (from the 40 genes showed in Figure 15).

IV.C. Discussion

In the s.c. renal cancer model used in this study, we demonstrated that the combination of anti-PD-1 and RU486 improved the antitumor response, as already demonstrated in stress conditions in several tumor models by *Yang et al.*²⁰⁰ Moreover, the combination of RU486 and anti-PD-1 treatment induced a decrease in active glucocorticoids. As glucocorticoids are known to have an immunosuppressive function (as explained in Section 1)III.C), we expected to produce a better immune response. However, no major change was detected in the immune populations infiltrating the tumor by flow cytometry despite a response in tumor growth.

Noteworthily, even though the tumor immune compartment was not modified by the treatment at the cell level, genes involved in immune pathways were particularly enriched in the tumor of the anti-PD-1+RU486 group, which highlights the importance of the treatment to the immune response. Indeed, our RNA sequencing analysis revealed that tumors treated with RU486 and anti-PD-1 expressed more genes involved in the PD-1 signaling pathway and in signaling through TCR. The enhancement of these two signaling pathways could indicate the presence of an antitumor immune response, which correlates with the decrease in tumor growth in this treatment group. Moreover, several genes differentially expressed in the anti-PD-1+RU486 group are known to be involved in immune functions, as exemplified in Table 5 and Table 6. One example is *Gata3* expression, which promoted T_H2 response in T cells and decreased in the combination treatment group.

Some of these findings support the hypothesis that even though no modulations were seen in the results of tumor immunophenotyping, the combination of anti-PD-1+RU486 led to an enhanced intratumoral immune response. However, an inconsistency seemed to exist in our results for validating this hypothesis. Indeed, some genes downregulated in the tumors of mice treated with RU486+anti-PD-1 (Table 6) are known to be involved in the immune response, such as *Tomm34*, which is implicated in antigen presentation. By contrast, some genes enhanced in tumors treated with the combination treatment are known to be anti-inflammatory, such as *Ptpn4* and *Cd5I*. Therefore, one should expect an increase of *Tomm34* expression and a decrease of *Ptpn4* and *Cd5I* expressions in the tumors of the responder group. Yet, there could also be genes with ambiguous immune functions, such as *Gpr84*, which is involved in the activation of neutrophils and ROS production.²⁶² However, neutrophils can have an antitumoral role, whereas the production of ROS can have a pro-tumoral role.²⁶³

Overall, we demonstrated an improvement of the anti-PD-1 response in combination with the GR antagonist in a renal cancer model. Further investigations must be performed to understand the effect of the GR antagonist on the antitumor immune response.

I. Impact of stress-induced glucocorticoids on the anti-PD-1 response in cancer

Our work on the impact of HSD11B1 on the antitumor immune response highlights the role of endogenous cortisol in cancer and its impact on the response to immunotherapy. Active glucocorticoids such as cortisol and corticosterone are increased during stress conditions, ²⁶⁴ and they are also known to play a role in cancer progression. ^{231,265–267} Stress increases the risk of cancer and, through its impact on immune cell activity, impairs the antitumor immune response, leading to enhanced tumor growth and tumor cell dissemination. ^{268,269} A study recently demonstrated that stress-induced cortisol impacts the function of DCs during the anti-cancer immune response, especially through GILZ expression. ²⁰⁰ Consistent with these data, we demonstrated that HSD11B1 produced cortisol and impacted the function of APCs in a renal cancer model. Moreover, we demonstrated an improvement of the response to immunotherapy, which was associated with a decrease of the active glucocorticoid level in two different renal cancer models (the intra-kidney model [Figure 5] of Poinot et al. and the s.c. model [data not shown] from the experiment in Figure 6 of Poinot et al.).

Noteworthily, we found that the response to anti-PD-1 monotherapy in our experiments was not consistent with data in the literature. The Renca model is usually described as a non-responder to anti-PD-1 monotherapy. 119,270–273 However, we found tumor sensitivity to anti-PD-1 in several of our experiments. These results could be due to the animal facility conditions, as some mice were produced in the animal facility (such as the *Hsd11b1* KO mice) and others were received from a supplier (even though they had an adaptation period before experiments). It could also be due to variable stress conditions, such as changes in animal caretakers or higher occupancy of the animal room. This discrepancy needs to be further elucidated and highlights the impact of stress on the response to immune checkpoint blockade.

Stress-induced glucocorticoids impair the antitumor immune response, which raises the question of the impact of corticosteroid use during immune checkpoint blockade. Indeed, corticosteroids are widely administered to cancer patients to manage immune-related side effects that occur during treatment with immune checkpoint inhibitors, and their effect on antitumor immune response is poorly understood.²⁷⁴ Some studies have demonstrated that such immunosuppressant treatments have no effect on the antitumor immune response or only impact the anti-PD-1 response and not the anti-CTLA-4 response.^{204–206} Moreover, the onset of corticosteroid treatment seems to be crucial, and the initiation of the immune checkpoint blockade response must precede glucocorticoid administration.²⁰⁷ However, these results are not consistent in the literature, as other studies have demonstrated a reduction of the overall survival of patients when corticosteroids were administered

during immune checkpoint blockade.^{275,276} Our data are in line with this impairment of the immunotherapy response in the presence of the administration of exogenous corticosteroids, even though the plasmatic concentration of endogenous glucocorticoids was much lower than that of exogenous glucocorticoids. Our data emphasize the negative effect of glucocorticoids on immune response during cancer immunotherapy as well as support the need for more research on the inhibition of the glucocorticoid pathway in combination with immune checkpoint blockade.

II. Role of HSD11B1 and the dual effect of its inhibitor ABT-384 on the antitumor immune response in a renal cancer model

In this study, we assessed the efficacy and potency of several HSD11B-specific pharmacological inhibitors from different chemotypes. Several molecules already developed by pharmaceutical companies were tested for their ability to restore the anti-PD-1 immune response. Bristol-Myers Squibb, AstraZeneca, Boehringer Ingelheim, AbbVie, and other companies or academic teams have developed HSD11B1 inhibitors such as BMS-823778, 277,278 AZD8329 and AZD4017, 279,280 BI-135585, 281 BVT-2733 and BVT-3498,²⁸² PF915275,²⁸³ MK-0736,²⁸⁴ HSD-016,^{285,286} and ABT-384.^{223,224,287,288} All of these molecules have been demonstrated to inhibit HSD11B1 and mainly been studied to improve symptoms of metabolic syndrome, particularly due to their effect on the regulation of glucose and insulin. However, in a recent study, Melo et al. demonstrated a benefit of the combination with 10J or carbenoxolone and immunotherapy in a melanoma model. 250,289,290 In this work, ABT-384, an adamantane, was found to be the molecule in all of the inhibitors tested in vitro that improved the anti-PD-1 response the most, which was inhibited in the presence of HSD11B1 substrate. Therefore, ABT-84 was selected for an in vivo study with the stated goal of repurposing this molecule in cancer treatment. We confirmed the activity of ABT-384 in not only naïve mice but also tumor-bearing mice. Indeed, we found that ABT-384 was active when administered per os and led to a decrease of cortisone-to-cortisol conversion and a decrease of the plasmatic ratio of corticosterone-to-11-DHC, which was consistent with the decrease of the urine ratio of cortisol-to-cortisone observed in humans.²⁸⁸

As discussed by Poinot et al., our findings highlight the importance of glucocorticoid regeneration through HSD11B1 on the impairment of the antitumor immune response in renal cancer. We demonstrated the involvement of the myeloid compartment, especially DCs, in the reestablishment of a proper immune response during combination with immunotherapy and HSD11B1 inhibitor. These results were confirmed by a recent study that also found an improvement of the anti-PD-1 response in a melanoma model due to the inhibition of HSD11B1 activity in myeloid cells, especially macrophages, as well as in CD8+ cells.²⁵⁰ To further investigate HSD11B1's impact on immune cells,

especially myeloid cells, it would be interesting to pursue the combination of HSD11B1 inhibitor and R848 in an intra-kidney model. Indeed, the tumor microenvironment of this model contains more HSD11B1 substrate – 11-DHC – since the 11-DHC-producer enzyme HSD11B2 is highly expressed in the kidney. Moreover, HSD11B1's combination with anti-PD-1 demonstrated an anti-PD-1 response improvement in the intra-kidney model compared with the s.c. model, which could indicate a greater impact of HSD11B1 activity in this orthotopic model.

Adaptation through metabolic change, such as an increase of adrenal-glucocorticoid production, or acquired resistance to the HSD11B1 pharmacological inhibitor could be a concern.^{279,291} However, the results that we obtained with the intra-kidney model suggest that if such an adaptation was happening, our treatment timing was too short to detect it. Indeed, we measured a decrease of plasmatic glucocorticoid in animals treated with ABT-384 at the end of the experiment (Figure 5D in Poinot et al.). Adaptation through metabolic change would involve adrenal compensation to restore a normal level of plasmatic glucocorticoids. The fact that glucocorticoids were still lower in the ABT-384 treated mice suggests an absence of adrenal compensation. Therefore, the results that we obtained with the orthotopic cancer model suggest that the lack of efficacy of anti-PD-1+ABT-384 in the s.c. model was not due to acquired adaptation, as the treatment time was even shorter than that for the intra-kidney model.

Moreover, monotherapy with HSD11B1 inhibitor in the intra-kidney model had a pro-tumoral effect. One hypothesis for explaining this tumorigenic effect could be increased angiogenesis favoring tumor progression. Indeed, numerous studies have investigated the role of HSD11B1, especially in cardiovascular events and ischemia. 181-184 In this context, glucocorticoids are known to impede angiogenesis. Thus, decrease of glucocorticoid production by HSD11B1 inhibition leads to an increase of angiogenesis. 181 However, the role of HSD11B1 in angiogenesis in cancer is unknown. RCC is a particularly vascularized tumor.²⁹² Yet, contrary to other solid tumors, a high density of vessels in the tumor does not correlate with poor prognosis in renal cancer.²⁹³ Despite this absence of a correlation between high vascularization and poor prognosis, treatments administered to patients target the angiogenesis such as anti-VEGF therapy. 122 In our work, the tumor progression was higher in the intrakidney model treated with ABT-384 compared with the vehicle, which also correlated with higher tumor metabolism. Through PET imaging analysis, the consumption of glucose was measured, and tumors treated with ABT-384 exhibited a higher consumption of glucose than tumors treated with the vehicle (data not shown). Beyond glucose consumption translating the metabolic activity of the tumor, PET signals also correlate with vascularization.²⁹⁴ Therefore, one can assume that the tumors treated with ABT-384 were more vascularized than those treated with the vehicle. Therefore, our hypothesis for explaining the antitumor effect obtained in the combination of anti-PD-1+ABT-384 is that it could

be due to improved tumor access of the treatment due to the presence of more vessels. Indeed, increased access of anti-PD-1 to the tumor improves the antitumor immune response, as one study demonstrated it with anti-PD-1 intratumor injection.²⁹⁵ Moreover, the metastasis count in the lung suggested a pro-metastatic effect of ABT-384 monotherapy, despite a lack of significant statistics (data not shown). These results could also be explained by increased angiogenesis in this group as well as increased access to the blood circulation. However, if it is confirmed, a pro-metastatic effect would exclude usage in the clinic. Therefore, further investigation should be pursued to determine a potential impact of HSD11B1 in the formation of metastasis, and in the angiogenesis pathway. First histology analysis could be easily performed, then RNA sequencing analysis of an intra-kidney tumor would bring more precise results.

III. Glucocorticoid receptor as a new target for improving immune checkpoint blockade response

In line with the inhibition the glucocorticoid pathway, we took a step back and focused on the GR to ensure a wider inhibitory effect. Indeed, with the inhibition of the receptor, we also prevented the effect of glucocorticoids produced by the adrenal gland and not only by HSD11B1. With this aim in mind, we reviewed the use of mifepristone, a glucocorticoid receptor antagonist, in cancer patients. Mifepristone or RU486 is used in the clinic as progesterone and a GR antagonist. It was studied in a preclinical cancer model as pre-treatment as well as for its direct role in cancer cells, especially because it downregulates the expression of integrin in cancer cells, which decreases metastasis development.²⁹⁶ Mifepristone was also studied for its impact on immune cells and, in this context, it improved immune checkpoint blockade when mice were subjected to stress conditions.²⁰⁰ Moreover, the compassionate use of mifepristone and clinical trials with this drug have been performed in cancers. Despite a lack of efficacy in meningioma patients or metastatic prostate cancer in combination with an androgen receptor antagonist, 297-299 encouraging results have been obtained in patients with pancreatic and lung cancer. 300,301 Moreover, in this thesis, we demonstrated an improvement of anti-PD-1 therapy in combination with RU486 in a renal cancer model, which was associated with an increased immune response. These pre-clinical results and case reports strengthen the use of GR antagonists in combination with immune checkpoint blockade in non-responder cancer patients.

Noteworthily, the inhibition of the GR in an anti-PD-1 context limits tumor growth. Moreover, RNA sequencing analysis revealed an upregulation of genes involved in collagen metabolism and extracellular matrix modulation as illustrated in the comparison of anti-PD.1+RU486 to anti-PD-1+Veh group in Supplementary Figure 7. Collagen metabolism is known to be important in angiogenesis, 302 therefore, the enhancement of such a pathway would support increased angiogenesis, which could be

verified using histological staining. Noteworthily, collagen degradation using metalloproteinases (MMP) and the crosslinking of collagen fibers using lysyl oxidase (LOX), which enhances the stiffness of the extracellular matrix, are both associated with an increase of tumor progression and invasion in the literature. 303 Therefore, our findings of low tumor growth being associated with the enhancement of collagen metabolism genes, such as MMP, contradict the literature and must be repeated.³⁰⁴ However, we can also hypothesize that the modification of the extracellular matrix detected through RNA sequencing analysis allows improved access to effective immune cells, even though no changes were detectable by flow cytometry. We can also hypothesize that the timing of tumor analysis was different between groups. Indeed, we saw a decrease of tumor growth in the combination group and an enhancement of collagen pathway genes, whereas in tumors of the anti-PD-1 monotherapy group, immune response pathways were enhanced but no effects on tumor growth could be detected. Therefore, we can assume that the kinetic of the immune response is different in both groups, and thus, the metabolic pathways and cells infiltrated were different.³⁰⁵ Tumor growth may have decreased in the combination group because the immune response occurred more rapidly, and collagen pathway genes were enhanced to create new tissues after the resolution of the immune response. On the other hand, in the anti-PD-1 monotherapy group, the response could have been slower and upon initiation; therefore, we found more immune genes enhanced in the tumors of this group.

IV. Repurposing drugs in cancer treatment to improve patients' quality of life

Although the results obtained with mifepristone encourage research on the inhibition of the GR in cancer treatment, we cannot rule out an antitumoral effect of the drug due to its antagonism of progesterone receptors. Indeed, PR antagonists are known to be beneficial in cancer, especially in cancers that affect women, such as breast and ovarian cancers, and one-third of renal tumors express PR. 114,306,307 Studies of specific GR antagonists in cancer treatment are therefore required. Some molecules are already under development for treating stress disorders, such as the stress-mediated development of Alzheimer's disease in NCT04601038 and posttraumatic stress disorder in veterans in NCT04452500. It will be interesting to test these molecules in combination with immune checkpoint blockade from a repurposing perspective while being particularly cautious in case of immune-related side effects.

A weak aspect of GR inhibition is the impossibility of using glucocorticoids if irAEs frequently occur during immune checkpoint blockade.³⁰⁸ Contrary to HSD11B1 inhibition, which allows the activation of the GR through the therapeutic administration of corticosteroids, GR antagonism could lead to the irreversible inhibition of the glucocorticoid pathway. Indeed, the receptor would not be available for

synthetic glucocorticoids. Therefore, we explored the possibility of targeting proteins that have an upstream role in the glucocorticoid pathway other than the GR.

V. Beyond glucocorticoids: The steroid pathway and its impact on renal cancer development

Based on the results obtained with HSD11B1 inhibition, which confirmed the importance of glucocorticoids in the tumor immune response, we hypothesized that other glucocorticoid producer enzymes could be important. We demonstrated that CYP21A2 expression in tumors was also correlated with poor prognosis in RCC patients of the TCGA cohort. CYP21A2 is involved in active glucocorticoid production upstream of HSD11B1 and is normally expressed in the adrenal gland. ^{309,310} As it is upstream of HSD11B1 in the steroid pathway, CYP21A2 inhibition in the tumor could have more of an effect on the active glucocorticoid amount available. However, this inhibition could also be associated with more side effects, such as the symptoms of congenital adrenal hyperplasia, ³¹¹ as it would affect adrenal steroidogenesis and more steroids than HSD11B1 (which directly regenerates cortisol). However, treatment with glucocorticoids could be possible in case of severe immune side effects, as the GR would still be available and functional. To accelerate this line of research, the repurposing of drugs could also be considered for targeting CYP21A2, as efavirenz inhibits this enzyme and is already approved for HIV treatment. ³¹²

Finally, we also identified two targets that could potentially be used as prognostic markers, namely AKR1C4 and HSD11B2, which are correlated with a good prognosis in patients. These two enzymes are involved in the elimination of active glucocorticoids. Further investigations should be conducted to understand their precise role, especially in immune cells, to determine whether their expression and activity are associated with an enhanced antitumor immune response.

5) Conclusion and Perspectives

Overall, this thesis has investigated the therapeutic potential of inhibiting the glucocorticoid pathway to improve the response to immunotherapy in renal cancer. We demonstrated the inhibitory impact of an HSD11B1 activity on DC activation and antigen-mediated T cell activation. The immune activation of DC and T cell was restored *in vitro* with HSD11B1 inhibition. Moreover, combination of an HSD11B1 inhibitor with immunotherapy revealed an improvement in the efficacy of immunostimulatory treatment such as anti-PD-1 and R848. We also investigated the role of GR in the antitumor immune response in an s.c. renal tumor model. We found that inhibition of GR with mifepristone in combination with ICI also displayed an enhancement of the antitumor immune response. Our findings indicate that HSD11B1 or GR inhibition in combination with ICIs improved the outcome in the renal cancer model.

Our results indicate that ABT-384 and mifepristone seem to represent good candidates for drug repurposing in cancer treatment and should be further investigated. Indeed, both of them are safe in humans, ^{223,296} and their use in renal cancer treatment should be considered, especially for patients who exhibited resistance to first- and second-line treatments.

However, our results also displayed unfavorable points which need to be elucidated. For example, further studies must be carried out to understand the discrepancy of the antitumor immune response obtained with the pharmacological inhibition of HSD11B1 and with the genetic ablation in $Hsd11b1^{KO}$ mice that did not respond to anti-PD-1 as expected. Moreover, the underlying mechanism of the antitumor immune response occurring with the combination of mifepristone and anti-PD-1 needs to be further investigated to understand the potential role of novel mechanism involved, beyond antigen presentation. Finally, the trend towards an increase of lung metastasis with ABT-384 monotherapy should be carefully investigated as it would prevent a use in patients.

Moreover, as sex hormones are also part of the steroid pathway, the effects noticed in this thesis might be different depending on the sex, especially as there is a sex dimorphism in renal cancer as explained in the paragraph 1)II.B.4.a. ^{161,163,164} Therefore, studies taking in account the sex of the mice should be carried out to determine if, as expected, a sex difference occurs concerning the antitumor immune response in renal cancer.

Finally, targeting the glucocorticoid pathway could also increase the risk of immune-related adverse events, which are commonly occurring during ICI treatment. This point raises one of the benefits of treatment with an HSD11B1 inhibitor compared to mifepristone. Indeed, HSD11B1 inhibition would not prevent GR activation through exogenous glucocorticoids as GR would not be occupied by an antagonist, whereas it is the case with mifepristone treatment. Therefore, HSD11B1 inhibition would allow the management of irAEs with exogenous glucocorticoids during ICI treatment.

5) Conclusion and Perspectives

To conclude, this thesis demonstrated the central role of endogenous steroids in the antitumor immune response in renal cancer. This work also emphasized that careful attention must be given to the effect of glucocorticoid pathway inhibition as it could lead to side effect such as adrenal hyperplasia for the inhibition of CYP21A2. We demonstrated the important role of endogenous glucocorticoids on the inhibition of the immune response in renal cancer treatment with immunotherapy. Moreover, this thesis emphasized the need for more studies on the combination of immune checkpoint blockade with existing drugs, especially those that reduce glucocorticoid production. Indeed, drug repurposing presents the advantage to ease the access to new treatment solution for renal cancer patients who developed resistance to ICI.

6) **Bibliography**

- 1. Ahmad, F.B., and Anderson, R.N. (2021). The Leading Causes of Death in the US for 2020. JAMA 325, 1829–1830. 10.1001/jama.2021.5469.
- 2. European Commission, Eurostat (online data code: hlth_cd_aro) (2023). Major causes of death in the EU in 2020. https://ec.europa.eu/eurostat/statistics-explained/index.php?title=Causes_of_death_statistics.
- 3. Hanahan, D., and Weinberg, R.A. (2011). Hallmarks of Cancer: The Next Generation. Cell *144*, 646–674. 10.1016/j.cell.2011.02.013.
- 4. Chen, D.S., and Mellman, I. (2013). Oncology Meets Immunology: The Cancer-Immunity Cycle. Immunity *39*, 1–10. 10.1016/j.immuni.2013.07.012.
- 5. Schreiber, R.D., Old, L.J., and Smyth, M.J. (2011). Cancer Immunoediting: Integrating Immunity's Roles in Cancer Suppression and Promotion. Science *331*, 1565–1570. 10.1126/science.1203486.
- 6. Dunn, G.P., Bruce, A.T., Ikeda, H., Old, L.J., and Schreiber, R.D. (2002). Cancer immunoediting: from immunosurveillance to tumor escape. Nature Immunology *3*, 991–998. 10.1038/ni1102-991.
- 7. Hastings, K.T. (2008). Innate and Adaptive Immune Responses to Cancer. In Fundamentals of Cancer Prevention, D. S. Alberts and L. M. Hess, eds. (Springer), pp. 79–108. 10.1007/978-3-540-68986-7_4.
- 8. Wang, S., and Zhang, Y. (2020). HMGB1 in inflammation and cancer. Journal of Hematology & Oncology *13*, 116. 10.1186/s13045-020-00950-x.
- 9. Gardner, A., and Ruffell, B. (2016). Dendritic Cells and Cancer Immunity. Trends in Immunology *37*, 855–865. 10.1016/j.it.2016.09.006.
- 10. Sánchez-Paulete, A.R., Teijeira, A., Cueto, F.J., Garasa, S., Pérez-Gracia, J.L., Sánchez-Arráez, A., Sancho, D., and Melero, I. (2017). Antigen cross-presentation and T-cell cross-priming in cancer immunology and immunotherapy. Ann Oncol *28*, xii44–xii55. 10.1093/annonc/mdx237.
- 11. Jhunjhunwala, S., Hammer, C., and Delamarre, L. (2021). Antigen presentation in cancer: insights into tumour immunogenicity and immune evasion. Nat Rev Cancer *21*, 298–312. 10.1038/s41568-021-00339-z.
- 12. Hiam-Galvez, K.J., Allen, B.M., and Spitzer, M.H. (2021). Systemic immunity in cancer. Nat Rev Cancer *21*, 345–359. 10.1038/s41568-021-00347-z.
- 13. Schmidt, S.V., Nino-Castro, A.C., and Schultze, J.L. (2012). Regulatory dendritic cells: there is more than just immune activation. Front Immunol *3.* 10.3389/fimmu.2012.00274.
- 14. Kerkar, S.P., and Restifo, N.P. (2012). Cellular Constituents of Immune Escape within the Tumor Microenvironment. Cancer Research *72*, 3125–3130. 10.1158/0008-5472.CAN-11-4094.
- 15. Liu, J., Geng, X., Hou, J., and Wu, G. (2021). New insights into M1/M2 macrophages: key modulators in cancer progression. Cancer Cell International *21*, 389. 10.1186/s12935-021-02089-2.

- 16. Boutilier, A.J., and Elsawa, S.F. (2021). Macrophage Polarization States in the Tumor Microenvironment. Int J Mol Sci *22*, 6995. 10.3390/ijms22136995.
- 17. Masucci, M.T., Minopoli, M., and Carriero, M.V. (2019). Tumor Associated Neutrophils. Their Role in Tumorigenesis, Metastasis, Prognosis and Therapy. Front Oncol *9*, 1146. 10.3389/fonc.2019.01146.
- Cassetta, L., Fragkogianni, S., Sims, A.H., Swierczak, A., Forrester, L.M., Zhang, H., Soong, D.Y.H., Cotechini, T., Anur, P., Lin, E.Y., et al. (2019). Human Tumor-Associated Macrophage and Monocyte Transcriptional Landscapes Reveal Cancer-Specific Reprogramming, Biomarkers, and Therapeutic Targets. Cancer Cell, S1535610819301047. 10.1016/j.ccell.2019.02.009.
- 19. Veglia, F., Sanseviero, E., and Gabrilovich, D.I. (2021). Myeloid-derived suppressor cells in the era of increasing myeloid cell diversity. Nat Rev Immunol *21*, 485–498. 10.1038/s41577-020-00490-y.
- 20. Song, W., Shao, Y., He, X., Gong, P., Yang, Y., Huang, S., Zeng, Y., Wei, L., and Zhang, J. (2020). IGFLR1 as a Novel Prognostic Biomarker in Clear Cell Renal Cell Cancer Correlating With Immune Infiltrates. Frontiers in Molecular Biosciences 7.
- 21. Raskov, H., Orhan, A., Christensen, J.P., and Gögenur, I. (2021). Cytotoxic CD8+ T cells in cancer and cancer immunotherapy. Br J Cancer *124*, 359–367. 10.1038/s41416-020-01048-4.
- Li, F., Li, C., Cai, X., Xie, Z., Zhou, L., Cheng, B., Zhong, R., Xiong, S., Li, J., Chen, Z., et al. (2021). The association between CD8+ tumor-infiltrating lymphocytes and the clinical outcome of cancer immunotherapy: A systematic review and meta-analysis. EClinicalMedicine 41, 101134. 10.1016/j.eclinm.2021.101134.
- 23. Brummel, K., Eerkens, A.L., de Bruyn, M., and Nijman, H.W. (2023). Tumour-infiltrating lymphocytes: from prognosis to treatment selection. Br J Cancer *128*, 451–458. 10.1038/s41416-022-02119-4.
- 24. Liu, S., Lachapelle, J., Leung, S., Gao, D., Foulkes, W.D., and Nielsen, T.O. (2012). CD8+ lymphocyte infiltration is an independent favorable prognostic indicator in basal-like breast cancer. Breast Cancer Research *14*, R48. 10.1186/bcr3148.
- 25. Schulze, A.B., Evers, G., Görlich, D., Mohr, M., Marra, A., Hillejan, L., Rehkämper, J., Schmidt, L.H., and Heitkötter, B. (2020). Tumor infiltrating T cells influence prognosis in stage I–III non-small cell lung cancer. Journal of Thoracic Disease 12. 10.21037/jtd-19-3414a.
- 26. Zhu, J., and Paul, W.E. (2010). Heterogeneity and plasticity of T helper cells. Cell Res *20*, 4–12. 10.1038/cr.2009.138.
- 27. Walker, J.A., and McKenzie, A.N.J. (2018). TH2 cell development and function. Nat Rev Immunol *18*, 121–133. 10.1038/nri.2017.118.
- 28. Togashi, Y., Shitara, K., and Nishikawa, H. (2019). Regulatory T cells in cancer immunosuppression implications for anticancer therapy. Nat Rev Clin Oncol *16*, 356–371. 10.1038/s41571-019-0175-7.
- 29. Crespo, J., Sun, H., Welling, T.H., Tian, Z., and Zou, W. (2013). T cell anergy, exhaustion, senescence, and stemness in the tumor microenvironment. Current Opinion in Immunology *25*, 214–221. 10.1016/j.coi.2012.12.003.

- 30. Buchbinder, E.I., and Desai, A. (2016). CTLA-4 and PD-1 Pathways: Similarities, Differences, and Implications of Their Inhibition. Am J Clin Oncol *39*, 98–106. 10.1097/COC.000000000000239.
- 31. Sharma, P., and Allison, J.P. (2015). Immune Checkpoint Targeting in Cancer Therapy: Towards Combination Strategies with Curative Potential. Cell *161*, 205–214. 10.1016/j.cell.2015.03.030.
- 32. Esfahani, K., Roudaia, L., Buhlaiga, N., Del Rincon, S.V., Papneja, N., and Miller, W.H. (2020). A review of cancer immunotherapy: from the past, to the present, to the future. Curr Oncol *27*, S87–S97. 10.3747/co.27.5223.
- 33. Waldman, A.D., Fritz, J.M., and Lenardo, M.J. (2020). A guide to cancer immunotherapy: from T cell basic science to clinical practice. Nat Rev Immunol *20*, 651–668. 10.1038/s41577-020-0306-5.
- 34. Qu, T., Li, B., and Wang, Y. (2022). Targeting CD47/SIRP α as a therapeutic strategy, where we are and where we are headed. Biomarker Research 10, 20. 10.1186/s40364-022-00373-5.
- 35. Vaddepally, R.K., Kharel, P., Pandey, R., Garje, R., and Chandra, A.B. (2020). Review of Indications of FDA-Approved Immune Checkpoint Inhibitors per NCCN Guidelines with the Level of Evidence. Cancers (Basel) *12*, 738. 10.3390/cancers12030738.
- 36. Robert, C. (2020). A decade of immune-checkpoint inhibitors in cancer therapy. Nat Commun *11*, 3801. 10.1038/s41467-020-17670-y.
- Boukouris, A.E., Theochari, M., Stefanou, D., Papalambros, A., Felekouras, E., Gogas, H., and Ziogas, D.C. (2022). Latest evidence on immune checkpoint inhibitors in metastatic colorectal cancer: A 2022 update. Critical Reviews in Oncology/Hematology 173, 103663. 10.1016/j.critrevonc.2022.103663.
- 38. Naimi, A., Mohammed, R.N., Raji, A., Chupradit, S., Yumashev, A.V., Suksatan, W., Shalaby, M.N., Thangavelu, L., Kamrava, S., Shomali, N., et al. (2022). Tumor immunotherapies by immune checkpoint inhibitors (ICIs); the pros and cons. Cell Communication and Signaling *20*, 44. 10.1186/s12964-022-00854-y.
- 39. Robert, C., Schachter, J., Long, G.V., Arance, A., Grob, J.J., Mortier, L., Daud, A., Carlino, M.S., McNeil, C., Lotem, M., et al. (2015). Pembrolizumab versus Ipilimumab in Advanced Melanoma. N Engl J Med *372*, 2521–2532. 10.1056/NEJMoa1503093.
- Motzer, R.J., Tannir, N.M., McDermott, D.F., Arén Frontera, O., Melichar, B., Choueiri, T.K., Plimack, E.R., Barthélémy, P., Porta, C., George, S., et al. (2018). Nivolumab plus Ipilimumab versus Sunitinib in Advanced Renal-Cell Carcinoma. New England Journal of Medicine 378, 1277– 1290. 10.1056/NEJMoa1712126.
- 41. Reck, M., Rodríguez-Abreu, D., Robinson, A.G., Hui, R., Csőszi, T., Fülöp, A., Gottfried, M., Peled, N., Tafreshi, A., Cuffe, S., et al. (2016). Pembrolizumab versus Chemotherapy for PD-L1—Positive Non—Small-Cell Lung Cancer. N Engl J Med *375*, 1823—1833. 10.1056/NEJMoa1606774.
- 42. Martins, F., Sofiya, L., Sykiotis, G.P., Lamine, F., Maillard, M., Fraga, M., Shabafrouz, K., Ribi, C., Cairoli, A., Guex-Crosier, Y., et al. (2019). Adverse effects of immune-checkpoint inhibitors: epidemiology, management and surveillance. Nat Rev Clin Oncol *16*, 563–580. 10.1038/s41571-019-0218-0.

- 43. Zhong, L., Wu, Q., Chen, F., Liu, J., and Xie, X. (2021). Immune-related adverse events: promising predictors for efficacy of immune checkpoint inhibitors. Cancer Immunol Immunother *70*, 2559–2576. 10.1007/s00262-020-02803-5.
- 44. Das, S., and Johnson, D.B. (2019). Immune-related adverse events and anti-tumor efficacy of immune checkpoint inhibitors. J Immunother Cancer *7*, 306. 10.1186/s40425-019-0805-8.
- 45. Schachter, J., Ribas, A., Long, G.V., Arance, A., Grob, J.-J., Mortier, L., Daud, A., Carlino, M.S., McNeil, C., Lotem, M., et al. (2017). Pembrolizumab versus ipilimumab for advanced melanoma: final overall survival results of a multicentre, randomised, open-label phase 3 study (KEYNOTE-006). The Lancet *390*, 1853–1862. 10.1016/S0140-6736(17)31601-X.
- 46. Syn, N.L., Teng, M.W.L., Mok, T.S.K., and Soo, R.A. (2017). De-novo and acquired resistance to immune checkpoint targeting. The Lancet Oncology *18*, e731–e741. 10.1016/S1470-2045(17)30607-1.
- 47. Dammeijer, F., Lau, S.P., van Eijck, C.H.J., van der Burg, S.H., and Aerts, J.G.J.V. (2017). Rationally combining immunotherapies to improve efficacy of immune checkpoint blockade in solid tumors. Cytokine & Growth Factor Reviews *36*, 5–15. 10.1016/j.cytogfr.2017.06.011.
- 48. Ventola, C.L. (2017). Cancer Immunotherapy, Part 3: Challenges and Future Trends. P T 42, 514–521.
- 49. Zheng, L., Qin, S., Si, W., Wang, A., Xing, B., Gao, R., Ren, X., Wang, L., Wu, X., Zhang, J., et al. (2021). Pan-cancer single-cell landscape of tumor-infiltrating T cells. Science *374*, abe6474. 10.1126/science.abe6474.
- 50. Niknafs, N., Balan, A., Cherry, C., Hummelink, K., Monkhorst, K., Shao, X.M., Belcaid, Z., Marrone, K.A., Murray, J., Smith, K.N., et al. (2023). Persistent mutation burden drives sustained anti-tumor immune responses. Nat Med *29*, 440–449. 10.1038/s41591-022-02163-w.
- 51. Zheng, M. (2022). Tumor mutation burden for predicting immune checkpoint blockade response: the more, the better. J Immunother Cancer *10*, e003087. 10.1136/jitc-2021-003087.
- 52. Maleki Vareki, S. (2018). High and low mutational burden tumors versus immunologically hot and cold tumors and response to immune checkpoint inhibitors. Journal for ImmunoTherapy of Cancer *6*, 157. 10.1186/s40425-018-0479-7.
- 53. Sharma, P., Hu-Lieskovan, S., Wargo, J.A., and Ribas, A. (2017). Primary, Adaptive, and Acquired Resistance to Cancer Immunotherapy. Cell *168*, 707–723. 10.1016/j.cell.2017.01.017.
- 54. Lecoester, B., Wespiser, M., Marguier, A., Mirjolet, C., Boustani, J., and Adotévi, O. (2023). Chapter Six Chemotherapy to potentiate the radiation-induced immune response. In International Review of Cell and Molecular Biology Ionizing Radiation and the Immune Response Part A., C. Mirjolet and L. Galluzzi, eds. (Academic Press), pp. 143–173. 10.1016/bs.ircmb.2023.01.004.
- 55. Tsuchikawa, T., Takeuchi, S., Nakamura, T., Shichinohe, T., and Hirano, S. (2016). Clinical impact of chemotherapy to improve tumor microenvironment of pancreatic cancer. World Journal of Gastrointestinal Oncology *8*, 786–792. 10.4251/wjgo.v8.i11.786.

- 56. Sharabi, A.B., Lim, M., DeWeese, T.L., and Drake, C.G. (2015). Radiation and checkpoint blockade immunotherapy: radiosensitisation and potential mechanisms of synergy. The Lancet Oncology *16*, e498–e509. 10.1016/S1470-2045(15)00007-8.
- 57. Fumet, J.-D., Limagne, E., Thibaudin, M., and Ghiringhelli, F. (2020). Immunogenic Cell Death and Elimination of Immunosuppressive Cells: A Double-Edged Sword of Chemotherapy. Cancers (Basel) *12*, 2637. 10.3390/cancers12092637.
- 58. Lucarini, V., Melaiu, O., Tempora, P., D'Amico, S., Locatelli, F., and Fruci, D. (2021). Dendritic Cells: Behind the Scenes of T-Cell Infiltration into the Tumor Microenvironment. Cancers (Basel) *13*, 433. 10.3390/cancers13030433.
- 59. Schoenfeld, A.J., and Hellmann, M.D. (2020). Acquired Resistance to Immune Checkpoint Inhibitors. Cancer Cell *37*, 443–455. 10.1016/j.ccell.2020.03.017.
- 60. Jenkins, R.W., Barbie, D.A., and Flaherty, K.T. (2018). Mechanisms of resistance to immune checkpoint inhibitors. Br J Cancer *118*, 9–16. 10.1038/bjc.2017.434.
- 61. Liu, D., Jenkins, R.W., and Sullivan, R.J. (2019). Mechanisms of Resistance to Immune Checkpoint Blockade. Am J Clin Dermatol *20*, 41–54. 10.1007/s40257-018-0389-y.
- 62. Biga, L.M., Dawson, S., Harwell, A., Hopkins, R., Kaufmann, J., LeMaster, M., Matern, P., Morrison-Graham, K., Quick, D., and Runyeon, J. (2019). 25.2 Microscopic Anatomy of the Kidney: Anatomy of the Nephron.
- 63. Jourde-Chiche, N., Fakhouri, F., Dou, L., Bellien, J., Burtey, S., Frimat, M., Jarrot, P.-A., Kaplanski, G., Le Quintrec, M., Pernin, V., et al. (2019). Endothelium structure and function in kidney health and disease. Nat Rev Nephrol *15*, 87–108. 10.1038/s41581-018-0098-z.
- 64. Lennon, R., Randles, M.J., and Humphries, M.J. (2014). The Importance of Podocyte Adhesion for a Healthy Glomerulus. Frontiers in Endocrinology 5.
- 65. Scott, R.P., and Quaggin, S.E. (2015). The cell biology of renal filtration. Journal of Cell Biology 209, 199–210. 10.1083/jcb.201410017.
- 66. Biga, L.M., Dawson, S., Harwell, A., Hopkins, R., Kaufmann, J., LeMaster, M., Matern, P., Morrison-Graham, K., Quick, D., and Runyeon, J. (2019). 25.1 Internal and External Anatomy of the Kidney.
- 67. Dalal, R., Bruss, Z.S., and Sehdev, J.S. (2022). Physiology, Renal Blood Flow and Filtration. In StatPearls (StatPearls Publishing).
- 68. Hoenig, M.P., and Zeidel, M.L. (2014). Homeostasis, the Milieu Intérieur, and the Wisdom of the Nephron. Clin J Am Soc Nephrol *9*, 1272–1281. 10.2215/CJN.08860813.
- 69. Biga, L.M., Dawson, S., Harwell, A., Hopkins, R., Kaufmann, J., LeMaster, M., Matern, P., Morrison-Graham, K., Quick, D., and Runyeon, J. (2019). 25.3 Physiology of Urine Formation: Overview.
- 70. Wallace, M.A. (1998). Anatomy and Physiology of the Kidney. AORN Journal *68*, 799–820. 10.1016/S0001-2092(06)62377-6.
- 71. Blaine, J., Chonchol, M., and Levi, M. (2015). Renal Control of Calcium, Phosphate, and Magnesium Homeostasis. CJASN *10*, 1257–1272. 10.2215/CJN.09750913.

- 72. Palsson, R., and Waikar, S.S. (2018). Renal Functional Reserve Revisited. Advances in Chronic Kidney Disease *25*, e1–e8. 10.1053/j.ackd.2018.03.001.
- 73. Schreiber, A., Shulhevich, Y., Geraci, S., Hesser, J., Stsepankou, D., Neudecker, S., Koenig, S., Heinrich, R., Hoecklin, F., Pill, J., et al. (2012). Transcutaneous measurement of renal function in conscious mice. American Journal of Physiology-Renal Physiology *303*, F783–F788. 10.1152/ajprenal.00279.2012.
- 74. Firsov, D., and Bonny, O. (2018). Circadian rhythms and the kidney. Nat Rev Nephrol *14*, 626–635. 10.1038/s41581-018-0048-9.
- 75. Ames, M.K., Atkins, C.E., and Pitt, B. (2019). The renin-angiotensin-aldosterone system and its suppression. Journal of Veterinary Internal Medicine *33*, 363–382. 10.1111/jvim.15454.
- 76. Pan, S.-Y., Tsai, P.-Z., Chou, Y.-H., Chang, Y.-T., Chang, F.-C., Chiu, Y.-L., Chiang, W.-C., Hsu, T., Chen, Y.-M., Chu, T.-S., et al. (2021). Kidney pericyte hypoxia-inducible factor regulates erythropoiesis but not kidney fibrosis. Kidney International *99*, 1354–1368. 10.1016/j.kint.2021.01.017.
- 77. Donnelly, S. (2001). Why is erythropoietin made in the kidney? The kidney functions as a critmeter. American Journal of Kidney Diseases *38*, 415–425. 10.1053/ajkd.2001.26111.
- 78. Peti-Peterdi, J., and Harris, R.C. (2010). Macula Densa Sensing and Signaling Mechanisms of Renin Release. J Am Soc Nephrol *21*, 1093–1096. 10.1681/ASN.2009070759.
- 79. J. Gordon Betts, Kelly A. Young, James A. Wise, Eddie Johnson, Brandon Poe, Dean H. Kruse, Oksana Korol, Jody E. Johnson, Mark Womble, and Peter DeSaix (2013). Anatomy and Physiology (OpenStax).
- 80. Biga, L.M., Dawson, S., Harwell, A., Hopkins, R., Kaufmann, J., LeMaster, M., Matern, P., Morrison-Graham, K., Quick, D., and Runyeon, J. (2019). 25.4 Physiology of Urine Formation: Glomerular Filtration.
- 81. Lindgren, D., Sjölund, J., and Axelson, H. (2018). Tracing Renal Cell Carcinomas back to the Nephron. Trends in Cancer 4, 472–484. 10.1016/j.trecan.2018.05.003.
- 82. Warren, A.Y., and Harrison, D. (2018). WHO/ISUP classification, grading and pathological staging of renal cell carcinoma: standards and controversies. World J Urol *36*, 1913–1926. 10.1007/s00345-018-2447-8.
- 83. Padala, S.A., Barsouk, A., Thandra, K.C., Saginala, K., Mohammed, A., Vakiti, A., Rawla, P., and Barsouk, A. (2020). Epidemiology of Renal Cell Carcinoma. World J Oncol *11*, 79–87. 10.14740/wjon1279.
- 84. Frew, I.J., and Moch, H. (2015). A Clearer View of the Molecular Complexity of Clear Cell Renal Cell Carcinoma. Annu. Rev. Pathol. Mech. Dis. *10*, 263–289. 10.1146/annurev-pathol-012414-040306.
- 85. Comprehensive Molecular Characterization of Papillary Renal-Cell Carcinoma (2016). New England Journal of Medicine *374*, 135–145. 10.1056/NEJMoa1505917.

- 86. Chen, S.-H., Xu, L.-Y., Wu, Y.-P., Ke, Z.-B., Huang, P., Lin, F., Li, X.-D., Xue, X.-Y., Wei, Y., Zheng, Q.-S., et al. (2021). Tumor volume: a new prognostic factor of oncological outcome of localized clear cell renal cell carcinoma. BMC Cancer *21*, 79. 10.1186/s12885-021-07795-8.
- 87. Sun, M., Lughezzani, G., Jeldres, C., Isbarn, H., Shariat, S.F., Arjane, P., Widmer, H., Pharand, D., Latour, M., Perrotte, P., et al. (2009). A Proposal for Reclassification of the Fuhrman Grading System in Patients with Clear Cell Renal Cell Carcinoma. European Urology *56*, 775–781. 10.1016/j.eururo.2009.06.008.
- 88. Hsieh, J.J., and Cheng, E.H. (2016). The panoramic view of clear cell renal cell carcinoma metabolism: values of integrated global cancer metabolomics. Transl Androl Urol *5*, 984–986. 10.21037/tau.2016.11.03.
- 89. Lee, C., Park, J.-W., Suh, J.H., Nam, K.H., and Moon, K.C. (2013). Histologic Variations and Immunohistochemical Features of Metastatic Clear Cell Renal Cell Carcinoma. Korean J Pathol 47, 426–432. 10.4132/KoreanJPathol.2013.47.5.426.
- 90. Luo, Z., Tian, M., Yang, G., Tan, Q., Chen, Y., Li, G., Zhang, Q., Li, Y., Wan, P., and Wu, J. (2022). Hypoxia signaling in human health and diseases: implications and prospects for therapeutics. Sig Transduct Target Ther 7, 1–30. 10.1038/s41392-022-01080-1.
- 91. Kieran, M.W., Kalluri, R., and Cho, Y.-J. (2012). The VEGF Pathway in Cancer and Disease: Responses, Resistance, and the Path Forward. Cold Spring Harb Perspect Med *2*, a006593. 10.1101/cshperspect.a006593.
- 92. Shibuya, M. (2011). Vascular Endothelial Growth Factor (VEGF) and Its Receptor (VEGFR) Signaling in Angiogenesis. Genes Cancer *2*, 1097–1105. 10.1177/1947601911423031.
- 93. Perl, A. (2016). Activation of mTOR (mechanistic target of rapamycin) in rheumatic diseases. Nat Rev Rheumatol *12*, 169–182. 10.1038/nrrheum.2015.172.
- 94. Faes, S., Demartines, N., and Dormond, O. (2021). Mechanistic Target of Rapamycin Inhibitors in Renal Cell Carcinoma: Potential, Limitations, and Perspectives. Frontiers in Cell and Developmental Biology 9.
- 95. Ganner, A., Gehrke, C., Klein, M., Thegtmeier, L., Matulenski, T., Wingendorf, L., Wang, L., Pilz, F., Greidl, L., Meid, L., et al. (2021). VHL suppresses RAPTOR and inhibits mTORC1 signaling in clear cell renal cell carcinoma. Sci Rep *11*, 14827. 10.1038/s41598-021-94132-5.
- 96. Zhang, Y., Narayanan, S.P., Mannan, R., Raskind, G., Wang, X., Vats, P., Su, F., Hosseini, N., Cao, X., Kumar-Sinha, C., et al. (2021). Single-cell analyses of renal cell cancers reveal insights into tumor microenvironment, cell of origin, and therapy response. PNAS *118*. 10.1073/pnas.2103240118.
- 97. Şenbabaoğlu, Y., Gejman, R.S., Winer, A.G., Liu, M., Van Allen, E.M., de Velasco, G., Miao, D., Ostrovnaya, I., Drill, E., Luna, A., et al. (2016). Tumor immune microenvironment characterization in clear cell renal cell carcinoma identifies prognostic and immunotherapeutically relevant messenger RNA signatures. Genome Biology *17*, 231. 10.1186/s13059-016-1092-z.
- 98. Nistala, R., Meuth, A., Smith, C., and Annayya, A. (2016). Reliable and High Efficiency Extraction of Kidney Immune Cells. J Vis Exp, 54368. 10.3791/54368.

- 99. Su, S., Akbarinejad, S., and Shahriyari, L. (2021). Immune classification of clear cell renal cell carcinoma. Sci Rep *11*, 4338. 10.1038/s41598-021-83767-z.
- 100. Borcherding, N., Vishwakarma, A., Voigt, A.P., Bellizzi, A., Kaplan, J., Nepple, K., Salem, A.K., Jenkins, R.W., Zakharia, Y., and Zhang, W. (2021). Mapping the immune environment in clear cell renal carcinoma by single-cell genomics. Commun Biol 4, 1–11. 10.1038/s42003-020-01625-6.
- 101. Wang, Q., Tang, H., Luo, X., Chen, J., Zhang, X., Li, X., Li, Y., Chen, Y., Xu, Y., and Han, S. (2022). Immune-Associated Gene Signatures Serve as a Promising Biomarker of Immunotherapeutic Prognosis for Renal Clear Cell Carcinoma. Frontiers in Immunology 13.
- 102. Hirsch, L., Flippot, R., Escudier, B., and Albiges, L. (2020). Immunomodulatory Roles of VEGF Pathway Inhibitors in Renal Cell Carcinoma. Drugs *80*, 1169–1181. 10.1007/s40265-020-01327-7.
- 103. Wheeler, K.C., Jena, M.K., Pradhan, B.S., Nayak, N., Das, S., Hsu, C.-D., Wheeler, D.S., Chen, K., and Nayak, N.R. (2018). VEGF may contribute to macrophage recruitment and M2 polarization in the decidua. PLoS One *13*, e0191040. 10.1371/journal.pone.0191040.
- 104. Geindreau, M., Ghiringhelli, F., and Bruchard, M. (2021). Vascular Endothelial Growth Factor, a Key Modulator of the Anti-Tumor Immune Response. Int J Mol Sci 22, 4871. 10.3390/ijms22094871.
- 105. Huang, H., Langenkamp, E., Georganaki, M., Loskog, A., Fuchs, P.F., Dieterich, L.C., Kreuger, J., and Dimberg, A. (2015). VEGF suppresses T-lymphocyte infiltration in the tumor microenvironment through inhibition of NF-κB-induced endothelial activation. The FASEB Journal *29*, 227–238. 10.1096/fj.14-250985.
- 106. Zhang, Y., Huang, H., Coleman, M., Ziemys, A., Gopal, P., Kazmi, S.M., and Brekken, R.A. VEGFR2 activity on myeloid cells mediates immune suppression in the tumor microenvironment. JCI Insight *6*, e150735. 10.1172/jci.insight.150735.
- 107. Sung, H., Ferlay, J., Siegel, R.L., Laversanne, M., Soerjomataram, I., Jemal, A., and Bray, F. (2021). Global Cancer Statistics 2020: GLOBOCAN Estimates of Incidence and Mortality Worldwide for 36 Cancers in 185 Countries. CA: A Cancer Journal for Clinicians 71, 209–249. 10.3322/caac.21660.
- 108. Mancini, M., Righetto, M., and Baggio, G. (2020). Gender-Related Approach to Kidney Cancer Management: Moving Forward. Int J Mol Sci *21*, 3378. 10.3390/ijms21093378.
- 109. Woldrich Jeffrey M., Mallin Katherine, Ritchey Jamie, Carroll Peter R., and Kane Christopher J. (2008). Sex Differences in Renal Cell Cancer Presentation and Survival: An Analysis of the National Cancer Database, 1993–2004. Journal of Urology 179, 1709–1713. 10.1016/j.juro.2008.01.024.
- 110. Grigg, C., Trufan, S., Clark, P.E., Riggs, S.B., Zhu, J., Matulay, J.T., Raghavan, D., and Burgess, E.F. (2021). Survival trends of men and women with metastatic clear cell renal cell carcinoma. JCO 39, 4566–4566. 10.1200/JCO.2021.39.15_suppl.4566.
- 111. Peired, A.J., Campi, R., Angelotti, M.L., Antonelli, G., Conte, C., Lazzeri, E., Becherucci, F., Calistri, L., Serni, S., and Romagnani, P. (2021). Sex and Gender Differences in Kidney Cancer: Clinical and Experimental Evidence. Cancers (Basel) *13*, 4588. 10.3390/cancers13184588.

- 112. Conforti, F., Pala, L., Bagnardi, V., De Pas, T., Martinetti, M., Viale, G., Gelber, R.D., and Goldhirsch, A. (2018). Cancer immunotherapy efficacy and patients' sex: a systematic review and meta-analysis. The Lancet Oncology *19*, 737–746. 10.1016/S1470-2045(18)30261-4.
- 113. Lucca, I., Klatte, T., Fajkovic, H., de Martino, M., and Shariat, S.F. (2015). Gender differences in incidence and outcomes of urothelial and kidney cancer. Nat Rev Urol *12*, 585–592. 10.1038/nrurol.2015.232.
- 114. Czarnecka, A.M., Niedzwiedzka, M., Porta, C., and Szczylik, C. (2016). Hormone signaling pathways as treatment targets in renal cell cancer (Review). International Journal of Oncology 48, 2221–2235. 10.3892/ijo.2016.3460.
- 115. Yu, C.-P., Ho, J.-Y., Huang, Y.-T., Cha, T.-L., Sun, G.-H., Yu, D.-S., Chang, F.-W., Chen, S.-P., and Hsu, R.-J. (2013). Estrogen Inhibits Renal Cell Carcinoma Cell Progression through Estrogen Receptor-β Activation. PLOS ONE *8*, e56667. 10.1371/journal.pone.0056667.
- 116. Noh, S.J., Jae Kang, M., Min Kim, K., Sang Bae, J., Sung Park, H., Sung Moon, W., Chung, M.J., Lee, H., Lee, D.G., and Yun Jang, K. (2013). Acetylation status of P53 and the expression of DBC1, SIRT1, and androgen receptor are associated with survival in clear cell renal cell carcinoma patients. Pathology *45*, 574–580. 10.1097/PAT.0b013e3283652c7a.
- 117. Pak, S., Kim, W., Kim, Y., Song, C., and Ahn, H. (2019). Dihydrotestosterone promotes kidney cancer cell proliferation by activating the STAT5 pathway via androgen and glucocorticoid receptors. J Cancer Res Clin Oncol *145*, 2293–2301. 10.1007/s00432-019-02993-1.
- 118. Zhang, Q., Chen, P., Tian, R., He, J., Han, Q., and Fan, L. (2022). Metabolic Syndrome is an Independent Risk Factor for Fuhrman Grade and TNM Stage of Renal Clear Cell Carcinoma. Int J Gen Med *15*, 143–150. 10.2147/IJGM.S346972.
- 119. Boi, S.K., Orlandella, R.M., Gibson, J.T., Turbitt, W.J., Wald, G., Thomas, L., Buchta Rosean, C., Norris, K.E., Bing, M., Bertrand, L., et al. (2020). Obesity diminishes response to PD-1-based immunotherapies in renal cancer. J Immunother Cancer 8, e000725. 10.1136/jitc-2020-000725.
- 120. Heng, D.Y.C., Xie, W., Regan, M.M., Harshman, L.C., Bjarnason, G.A., Vaishampayan, U.N., Mackenzie, M., Wood, L., Donskov, F., Tan, M.-H., et al. (2013). External validation and comparison with other models of the International Metastatic Renal-Cell Carcinoma Database Consortium prognostic model: a population-based study. Lancet Oncol *14*, 141–148. 10.1016/S1470-2045(12)70559-4.
- 121. Dy, H., W, X., Mm, R., Ma, W., Ar, G., C, S., Bj, E., Jd, R., T, C., S, N., et al. (2009). Prognostic factors for overall survival in patients with metastatic renal cell carcinoma treated with vascular endothelial growth factor-targeted agents: results from a large, multicenter study. Journal of clinical oncology: official journal of the American Society of Clinical Oncology 27. 10.1200/JCO.2008.21.4809.
- 122. Choueiri, T.K., and Motzer, R.J. (2017). Systemic Therapy for Metastatic Renal-Cell Carcinoma. N Engl J Med *376*, 354–366. 10.1056/NEJMra1601333.
- 123. Renal Cell Cancer Treatment (PDQ®)—Health Professional Version National Cancer Institute (2022). https://www.cancer.gov/types/kidney/hp/kidney-treatment-pdq.
- 124. Sharma, R., Kadife, E., Myers, M., Kannourakis, G., Prithviraj, P., and Ahmed, N. (2021). Determinants of resistance to VEGF-TKI and immune checkpoint inhibitors in metastatic renal

- cell carcinoma. Journal of Experimental & Clinical Cancer Research *40*, 186. 10.1186/s13046-021-01961-3.
- 125. Moreira, M., Pobel, C., Epaillard, N., Simonaggio, A., Oudard, S., and Vano, Y.-A. (2020). Resistance to cancer immunotherapy in metastatic renal cell carcinoma. Cancer Drug Resistance 3, 454–471. 10.20517/cdr.2020.16.
- 126. Atkins, M.B., and Tannir, N.M. (2018). Current and emerging therapies for first-line treatment of metastatic clear cell renal cell carcinoma. Cancer Treatment Reviews 70, 127–137. 10.1016/j.ctrv.2018.07.009.
- 127. Powles, T., Albiges, L., Bex, A., Grünwald, V., Porta, C., Procopio, G., Schmidinger, M., Suárez, C., and de Velasco, G. (2021). ESMO Clinical Practice Guideline update on the use of immunotherapy in early stage and advanced renal cell carcinoma. Annals of Oncology *32*, 1511–1519. 10.1016/j.annonc.2021.09.014.
- 128. Escudier, B., Porta, C., Schmidinger, M., Rioux-Leclercq, N., Bex, A., Khoo, V., Grünwald, V., Gillessen, S., and Horwich, A. (2019). Renal cell carcinoma: ESMO Clinical Practice Guidelines for diagnosis, treatment and follow-up††Approved by the ESMO Guidelines Committee: September 2008, last update January 2019. This publication supersedes the previously published version—Ann Oncol 2016; 27 (Suppl 5): v58–v68. Annals of Oncology 30, 706–720. 10.1093/annonc/mdz056.
- 129. Hou, W., and Ji, Z. (2018). Generation of autochthonous mouse models of clear cell renal cell carcinoma: mouse models of renal cell carcinoma. Exp Mol Med *50*, 30. 10.1038/s12276-018-0059-4.
- 130. Liu, J., Xu, J., Zhang, T., Xu, K., Bao, P., Zhang, Z., Xue, K., He, R., Ma, L., and Wang, Y. (2022). Decoding the Immune Microenvironment of Clear Cell Renal Cell Carcinoma by Single-Cell Profiling to Aid Immunotherapy. Frontiers in Immunology *13*.
- 131. Gong, M., Li, Y., Song, E., Li, M., Qiu, S., Dong, W., and Yuan, R. (2022). OIP5 Is a Novel Prognostic Biomarker in Clear Cell Renal Cell Cancer Correlating With Immune Infiltrates. Frontiers in Immunology 13.
- 132. Brodaczewska, K.K., Szczylik, C., Fiedorowicz, M., Porta, C., and Czarnecka, A.M. (2016). Choosing the right cell line for renal cell cancer research. Molecular Cancer *15*, 83. 10.1186/s12943-016-0565-8.
- 133. Wolf, M.M., Kimryn Rathmell, W., and Beckermann, K.E. (2020). Modeling clear cell renal cell carcinoma and therapeutic implications. Oncogene *39*, 3413–3426. 10.1038/s41388-020-1234-3.
- 134. Sobczuk, P., Brodziak, A., Khan, M.I., Chhabra, S., Fiedorowicz, M., Wełniak-Kamińska, M., Synoradzki, K., Bartnik, E., Cudnoch-Jędrzejewska, A., and Czarnecka, A.M. (2020). Choosing The Right Animal Model for Renal Cancer Research. Translational Oncology *13*, 100745. 10.1016/j.tranon.2020.100745.
- 135. Noonan, H.R., Metelo, A.M., Kamei, C.N., Peterson, R.T., Drummond, I.A., and Iliopoulos, O. (2016). Loss of vhl in the zebrafish pronephros recapitulates early stages of human clear cell renal cell carcinoma. Dis Model Mech *9*, 873–884. 10.1242/dmm.024380.

- 136. Nargund, A.M., Pham, C.G., Dong, Y., Wang, P.I., Osmangeyoglu, H.U., Xie, Y., Aras, O., Han, S., Oyama, T., Takeda, S., et al. (2017). The SWI/SNF Protein PBRM1 Restrains VHL Loss-Driven Clear Cell Renal Cell Carcinoma. Cell Rep *18*, 2893–2906. 10.1016/j.celrep.2017.02.074.
- 137. Slominski, R.M., Tuckey, R.C., Manna, P.R., Jetten, A.M., Postlethwaite, A., Raman, C., and Slominski, A.T. (2020). Extra-adrenal glucocorticoid biosynthesis: implications for autoimmune and inflammatory disorders. Genes Immun *21*, 150–168. 10.1038/s41435-020-0096-6.
- 138. Miller, W.L., and Auchus, R.J. (2011). The Molecular Biology, Biochemistry, and Physiology of Human Steroidogenesis and Its Disorders. Endocrine Reviews *32*, 81–151. 10.1210/er.2010-0013.
- 139. Mahata, B., Pramanik, J., van der Weyden, L., Polanski, K., Kar, G., Riedel, A., Chen, X., Fonseca, N.A., Kundu, K., Campos, L.S., et al. (2020). Tumors induce de novo steroid biosynthesis in T cells to evade immunity. Nat Commun *11*, 3588. 10.1038/s41467-020-17339-6.
- 140. Taves, M.D., and Ashwell, J.D. (2021). Glucocorticoids in T cell development, differentiation and function. Nat Rev Immunol *21*, 233–243. 10.1038/s41577-020-00464-0.
- 141. Megha, R., Wehrle, C.J., Kashyap, S., and Leslie, S.W. (2022). Anatomy, Abdomen and Pelvis, Adrenal Glands (Suprarenal Glands). In StatPearls (StatPearls Publishing).
- 142. Haas, A., Borsook, D., Adler, G., and Freeman, R. (2022). Stress, hypoglycemia, and the autonomic nervous system. Autonomic Neuroscience *240*, 102983. 10.1016/j.autneu.2022.102983.
- 143. Chapman, K.E., Coutinho, A.E., Zhang, Z., Kipari, T., Savill, J.S., and Seckl, J.R. (2013). Changing glucocorticoid action: 11β-Hydroxysteroid dehydrogenase type 1 in acute and chronic inflammation. J Steroid Biochem Mol Biol *137*, 82–92. 10.1016/j.jsbmb.2013.02.002.
- 144. Harris, H.J., Kotelevtsev, Y., Mullins, J.J., Seckl, J.R., and Holmes, M.C. (2001). Intracellular Regeneration of Glucocorticoids by11β-Hydroxysteroid Dehydrogenase (11β-HSD)-1 Plays a KeyRole in Regulation of the Hypothalamic-Pituitary-Adrenal Axis: Analysisof 11β-HSD-1-Deficient Mice**The Wellcome Trust supported this work through a program grant (to J.J.M. and J.R.S.) and a Career Development Fellowship (to M.C.H.). Endocrinology *142*, 114–120. 10.1210/endo.142.1.7887.
- 145. Evans, A.N., Liu, Y., MacGregor, R., Huang, V., and Aguilera, G. (2013). Regulation of Hypothalamic Corticotropin-Releasing Hormone Transcription by Elevated Glucocorticoids. Mol Endocrinol *27*, 1796–1807. 10.1210/me.2013-1095.
- 146. Kriegsfeld, L.J., LeSauter, J., Hamada, T., Pitts, S.M., and Silver, R. (2002). 18 Circadian Rhythms in the Endocrine System. In Hormones, Brain and Behavior, D. W. Pfaff, A. P. Arnold, S. E. Fahrbach, A. M. Etgen, and R. T. Rubin, eds. (Academic Press), pp. 33–91. 10.1016/B978-012532104-4/50020-2.
- 147. Whitfield, G.K., Jurutka, P.W., Haussler, C.A., and Haussler, M.R. (1999). Steroid hormone receptors: Evolution, ligands, and molecular basis of biologic function. Journal of Cellular Biochemistry 75, 110–122. 10.1002/(SICI)1097-4644(1999)75:32+<110::AID-JCB14>3.0.CO;2-T.
- 148. Kino, T., Su, Y.A., and Chrousos, G.P. (2009). Human Glucocorticoid Receptor (GR) Isoform β : Recent Understanding of its Potential Implications in Physiology and Pathophysiology. Cell Mol Life Sci 66, 3435–3448. 10.1007/s00018-009-0098-z.

- 149. Weikum, E.R., Knuesel, M.T., Ortlund, E.A., and Yamamoto, K.R. (2017). Glucocorticoid receptor control of transcription: precision and plasticity via allostery. Nat Rev Mol Cell Biol *18*, 159–174. 10.1038/nrm.2016.152.
- 150. Gomez-Sanchez, E., and Gomez-Sanchez, C.E. (2014). The Multifaceted Mineralocorticoid Receptor. Compr Physiol *4*, 965–994. 10.1002/cphy.c130044.
- 151. Louw, A. (2019). GR Dimerization and the Impact of GR Dimerization on GR Protein Stability and Half-Life. Front Immunol *10*, 1693. 10.3389/fimmu.2019.01693.
- 152. Gerber, A.N., Newton, R., and Sasse, S.K. (2021). Repression of transcription by the glucocorticoid receptor: A parsimonious model for the genomics era. Journal of Biological Chemistry *296*. 10.1016/j.jbc.2021.100687.
- 153. Deng, Y., Xia, X., Zhao, Y., Zhao, Z., Martinez, C., Yin, W., Yao, J., Hang, Q., Wu, W., Zhang, J., et al. (2021). Glucocorticoid receptor regulates PD-L1 and MHC-I in pancreatic cancer cells to promote immune evasion and immunotherapy resistance. Nat Commun 12, 7041. 10.1038/s41467-021-27349-7.
- 154. Hunter, R.W., Ivy, J.R., and Bailey, M.A. (2014). Glucocorticoids and renal Na ⁺ transport: implications for hypertension and salt sensitivity: Glucocorticoids and renal Na ⁺ transport. J Physiol *592*, 1731–1744. 10.1113/jphysiol.2013.267609.
- 155. Nishi, M., Tanaka, M., Matsuda, K., Sunaguchi, M., and Kawata, M. (2004). Visualization of Glucocorticoid Receptor and Mineralocorticoid Receptor Interactions in Living Cells with GFP-Based Fluorescence Resonance Energy Transfer. J Neurosci *24*, 4918–4927. 10.1523/JNEUROSCI.5495-03.2004.
- 156. Viengchareun, S., Menuet, D.L., Martinerie, L., Munier, M., Tallec, L.P.-L., and Lombès, M. (2007). The mineralocorticoid receptor: insights into its molecular and (patho)physiological biology. Nuclear Receptor Signaling 5. 10.1621/nrs.05012.
- 157. Bienvenu, L.A., Morgan, J., Rickard, A.J., Tesch, G.H., Cranston, G.A., Fletcher, E.K., Delbridge, L.M.D., and Young, M.J. (2012). Macrophage Mineralocorticoid Receptor Signaling Plays a Key Role in Aldosterone-Independent Cardiac Fibrosis. Endocrinology *153*, 3416–3425. 10.1210/en.2011-2098.
- 158. Pooley, J.R., Rivers, C.A., Kilcooley, M.T., Paul, S.N., Cavga, A.D., Kershaw, Y.M., Muratcioglu, S., Gursoy, A., Keskin, O., and Lightman, S.L. (2020). Beyond the heterodimer model for mineralocorticoid and glucocorticoid receptor interactions in nuclei and at DNA. PLoS One *15*, e0227520. 10.1371/journal.pone.0227520.
- 159. Mifsud, K.R., and Reul, J.M.H.M. (2016). Acute stress enhances heterodimerization and binding of corticosteroid receptors at glucocorticoid target genes in the hippocampus. Proceedings of the National Academy of Sciences *113*, 11336–11341. 10.1073/pnas.1605246113.
- 160. Sofer, Y., Osher, E., Limor, R., Shefer, G., Marcus, Y., Shapira, I., Tordjman, K., Greenman, Y., Berliner, S., and Stern, N. (2016). Gender Determines Serum Free Cortisol: Higher Levels in Men. Endocrine Practice *22*, 1415–1421. 10.4158/EP161370.OR.
- 161. Reschke-Hernández, A.E., Okerstrom, K.L., Edwards, A.B., and Tranel, D. (2017). Sex and stress: Men and women show different cortisol responses to psychological stress induced by the Trier

- Social Stress Test and the Iowa Singing Social Stress Test. J Neurosci Res *95*, 106–114. 10.1002/jnr.23851.
- 162. Van Cauter, E., Leproult, R., and Kupfer, D.J. (1996). Effects of gender and age on the levels and circadian rhythmicity of plasma cortisol. The Journal of Clinical Endocrinology & Metabolism *81*, 2468–2473. 10.1210/jcem.81.7.8675562.
- 163. Bourke, C.H., Harrell, C.S., and Neigh, G.N. (2012). Stress-Induced Sex Differences: Adaptations Mediated by the Glucocorticoid Receptor. Horm Behav *62*, 210–218. 10.1016/j.yhbeh.2012.02.024.
- 164. Rohleder, N., Schommer, N.C., Hellhammer, D.H., Engel, R., and Kirschbaum, C. (2001). Sex Differences in Glucocorticoid Sensitivity of Proinflammatory Cytokine Production After Psychosocial Stress. Psychosomatic Medicine *63*, 966–972.
- 165. Dakin, R.S., Walker, B.R., Seckl, J.R., Hadoke, P.W.F., and Drake, A.J. (2015). Estrogens protect male mice from obesity complications and influence glucocorticoid metabolism. Int J Obes *39*, 1539–1547. 10.1038/ijo.2015.102.
- 166. Yan, C., Yang, Q., and Gong, Z. (2017). Tumor-Associated Neutrophils and Macrophages Promote Gender Disparity in Hepatocellular Carcinoma in Zebrafish. Cancer Res 77, 1395–1407. 10.1158/0008-5472.CAN-16-2200.
- 167. McTernan, P.G., Anderson, L.A., Anwar, A.J., Eggo, M.C., Crocker, J., Barnett, A.H., Stewart, P.M., and Kumar, S. (2002). Glucocorticoid Regulation of P450 Aromatase Activity in Human Adipose Tissue: Gender and Site Differences. The Journal of Clinical Endocrinology & Metabolism 87, 1327–1336. 10.1210/jcem.87.3.8288.
- 168. Karmakar, S., Jin, Y., and Nagaich, A.K. (2013). Interaction of Glucocorticoid Receptor (GR) with Estrogen Receptor (ER) α and Activator Protein 1 (AP1) in Dexamethasone-mediated Interference of ERα Activity. J Biol Chem *288*, 24020–24034. 10.1074/jbc.M113.473819.
- 169. Bereshchenko, O., Bruscoli, S., and Riccardi, C. (2018). Glucocorticoids, Sex Hormones, and Immunity. Front. Immunol. *9*. 10.3389/fimmu.2018.01332.
- 170. Zhang, Y., Leung, D.Y.M., Nordeen, S.K., and Goleva, E. (2009). Estrogen Inhibits Glucocorticoid Action via Protein Phosphatase 5 (PP5)-mediated Glucocorticoid Receptor Dephosphorylation. J Biol Chem 284, 24542–24552. 10.1074/jbc.M109.021469.
- 171. Chen, S., Wang, J., Yu, G., Liu, W., and Pearce, D. (1997). Androgen and Glucocorticoid Receptor Heterodimer Formation: A POSSIBLE MECHANISM FOR MUTUAL INHIBITION OF TRANSCRIPTIONAL ACTIVITY*. Journal of Biological Chemistry *272*, 14087–14092. 10.1074/jbc.272.22.14087.
- 172. Delettré, J., Mornon, J.P., Lepicard, G., Ojasoo, T., and Raynaud, J.P. (1980). Steroid flexibility and receptor specificity. Journal of Steroid Biochemistry *13*, 45–59. 10.1016/0022-4731(80)90112-0.
- 173. Raynaud, J.P., Bouton, M.M., Moguilewsky, M., Ojasoo, T., Philibert, D., Beck, G., Labrie, F., and Mornon, J.P. (1980). Steroid hormone receptors and pharmacology. Journal of Steroid Biochemistry *12*, 143–157. 10.1016/0022-4731(80)90264-2.

- 174. Sheppard, K.E., and Funder, J.W. (1987). Equivalent affinity of aldosterone and corticosterone for type I receptors in kidney and hippocampus: Direct binding studies. Journal of Steroid Biochemistry *28*, 737–742. 10.1016/0022-4731(87)90406-7.
- 175. Rupprecht, R., Arriza, J.L., Spengler, D., Reul, J.M., Evans, R.M., Holsboer, F., and Damm, K. (1993). Transactivation and synergistic properties of the mineralocorticoid receptor: relationship to the glucocorticoid receptor. Molecular Endocrinology *7*, 597–603. 10.1210/mend.7.4.8388999.
- 176. Yeh, S., Miyamoto, H., Shima, H., and Chang, C. (1998). From estrogen to androgen receptor: A new pathway for sex hormones in prostate. Proc Natl Acad Sci U S A *95*, 5527–5532.
- 177. Ray, D.W., Suen, C.-S., Brass, A., Soden, J., and White, A. (1999). Structure/Function of the Human Glucocorticoid Receptor: Tyrosine 735 Is Important for Transactivation. Molecular Endocrinology 13, 1855–1863. 10.1210/mend.13.11.0376.
- 178. Lei, K., Chen, L., Georgiou, E.X., Sooranna, S.R., Khanjani, S., Brosens, J.J., Bennett, P.R., and Johnson, M.R. (2012). Progesterone Acts via the Nuclear Glucocorticoid Receptor to Suppress IL-1β-Induced COX-2 Expression in Human Term Myometrial Cells. PLOS ONE *7*, e50167. 10.1371/journal.pone.0050167.
- 179. Miller, L., and Hunt, J.S. (1998). Regulation of TNF-α Production in Activated Mouse Macrophages by Progesterone. The Journal of Immunology *160*, 5098–5104.
- 180. Chapman, K., Holmes, M., and Seckl, J. (2013). 11β-Hydroxysteroid Dehydrogenases: Intracellular Gate-Keepers of Tissue Glucocorticoid Action. Physiol Rev *93*, 1139–1206. 10.1152/physrev.00020.2012.
- 181. Small, G.R., Hadoke, P.W.F., Sharif, I., Dover, A.R., Armour, D., Kenyon, C.J., Gray, G.A., and Walker, B.R. (2005). Preventing local regeneration of glucocorticoids by 11β-hydroxysteroid dehydrogenase type 1 enhances angiogenesis. Proc Natl Acad Sci U S A *102*, 12165–12170. 10.1073/pnas.0500641102.
- 182. Gong, R., Morris, D.J., and Brem, A.S. (2008). Variable expression of 11β Hydroxysteroid dehydrogenase (11β-HSD) isoforms in vascular endothelial cells. Steroids *73*, 1187–1196. 10.1016/j.steroids.2008.05.009.
- 183. Zhang, Z., Coutinho, A.E., Man, T.Y., Kipari, T.M.J., Hadoke, P.W.F., Salter, D.M., Seckl, J.R., and Chapman, K.E. (2017). Macrophage 11β-HSD-1 deficiency promotes inflammatory angiogenesis. Journal of Endocrinology *234*, 291–299. 10.1530/JOE-17-0223.
- 184. McSweeney, S.J., Hadoke, P.W.F., Kozak, A.M., Small, G.R., Khaled, H., Walker, B.R., and Gray, G.A. (2010). Improved heart function follows enhanced inflammatory cell recruitment and angiogenesis in 11βHSD1-deficient mice post-MI. Cardiovasc Res *88*, 159–167. 10.1093/cvr/cvq149.
- 185. Carter, R.N., Paterson, J.M., Tworowska, U., Stenvers, D.J., Mullins, J.J., Seckl, J.R., and Holmes, M.C. (2009). Hypothalamic-Pituitary-Adrenal Axis Abnormalities in Response to Deletion of 11β-HSD1 is Strain-Dependent. J Neuroendocrinol *21*, 879–887. 10.1111/j.1365-2826.2009.01899.x.
- 186. do Nascimento, F.V., Piccoli, V., Beer, M.A., von Frankenberg, A.D., Crispim, D., and Gerchman, F. (2015). Association of HSD11B1 polymorphic variants and adipose tissue gene expression with metabolic syndrome, obesity and type 2 diabetes mellitus: a systematic review. Diabetology & Metabolic Syndrome 7, 38. 10.1186/s13098-015-0036-1.

- 187. Bujalska, I.J., Kumar, S., Hewison, M., and Stewart, P.M. (1999). Differentiation of Adipose Stromal Cells: The Roles of Glucocorticoids and 11β-Hydroxysteroid Dehydrogenase*. Endocrinology *140*, 3188–3196. 10.1210/endo.140.7.6868.
- 188. Balachandran, A., Guan, H., Sellan, M., van Uum, S., and Yang, K. (2008). Insulin and Dexamethasone Dynamically Regulate Adipocyte 11β-Hydroxysteroid Dehydrogenase Type 1. Endocrinology *149*, 4069–4079. 10.1210/en.2008-0088.
- 189. Odermatt, A., Arnold, P., Stauffer, A., Frey, B.M., and Frey, F.J. The N-terminal Anchor Sequences of 11^{tt}-Hydroxysteroid Dehydrogenases Determine Their Orientation in the Endoplasmic Reticulum Membrane. 10.
- 190. Zhang, Z.-H., Kang, Y.-M., Yu, Y., Wei, S.-G., Schmidt, T.J., Johnson, A.K., and Felder, R.B. (2006). 11β-Hydroxysteroid Dehydrogenase Type 2 Activity in Hypothalamic Paraventricular Nucleus Modulates Sympathetic Excitation. Hypertension 48, 127–133. 10.1161/01.HYP.0000224296.96235.dd.
- 191. Wyrwoll, C.S., Holmes, M.C., and Seckl, J.R. (2011). 11β-Hydroxysteroid dehydrogenases and the brain: From zero to hero, a decade of progress. Frontiers in Neuroendocrinology *32*, 265–286. 10.1016/j.yfrne.2010.12.001.
- 192. Atanasov, A.G., Ignatova, I.D., Nashev, L.G., Dick, B., Ferrari, P., Frey, F.J., and Odermatt, A. (2007). Impaired Protein Stability of 11β-Hydroxysteroid Dehydrogenase Type 2: A Novel Mechanism of Apparent Mineralocorticoid Excess. JASN 18, 1262–1270. 10.1681/ASN.2006111235.
- 193. Seckl, J.R., Cleasby, M., and Nyirenda, M.J. (2000). Glucocorticoids, 11β-hydroxysteroid dehydrogenase, and fetal programming. Kidney International *57*, 1412–1417. 10.1046/j.1523-1755.2000.00984.x.
- 194. Bolt, R.J., van Weissenbruch, M. m., Lafeber, H. n., and Delemarre-van de Waal, H. a. (2001). Glucocorticoids and lung development in the fetus and preterm infant. Pediatric Pulmonology 32, 76–91. 10.1002/ppul.1092.
- 195. Sun, K., Yang, K., and Challis, J.R.G. (1998). Regulation of 11β-Hydroxysteroid Dehydrogenase Type 2 by Progesterone, Estrogen, and the Cyclic Adenosine 5′-Monophosphate Pathway in Cultured Human Placental and Chorionic Trophoblasts1. Biology of Reproduction *58*, 1379–1384. 10.1095/biolreprod58.6.1379.
- 196. Huang, W. I., Harper, C. g., Evans, S. f., Newnham, J. p., and Dunlop, S. a. (2001). Repeated prenatal corticosteroid administration delays astrocyte and capillary tight junction maturation in fetal sheep. International Journal of Developmental Neuroscience *19*, 487–493. 10.1016/S0736-5748(01)00035-1.
- 197. Coutinho, A.E., Kipari, T.M.J., Zhang, Z., Esteves, C.L., Lucas, C.D., Gilmour, J.S., Webster, S.P., Walker, B.R., Hughes, J., Savill, J.S., et al. (2016). 11β-Hydroxysteroid Dehydrogenase Type 1 Is Expressed in Neutrophils and Restrains an Inflammatory Response in Male Mice. Endocrinology 157, 2928–2936. 10.1210/en.2016-1118.
- 198. Freeman, L., Hewison, M., Hughes, S.V., Evans, K.N., Hardie, D., Means, T.K., and Chakraverty, R. (2005). Expression of 11β-hydroxysteroid dehydrogenase type 1 permits regulation of

- glucocorticoid bioavailability by human dendritic cells. Blood *106*, 2042–2049. 10.1182/blood-2005-01-0186.
- 199. Nucera, S., Biziato, D., and De Palma, M. (2011). The interplay between macrophages and angiogenesis in development, tissue injury and regeneration. Int. J. Dev. Biol. *55*, 495–503. 10.1387/ijdb.103227sn.
- 200. Yang, H., Xia, L., Chen, J., Zhang, S., Martin, V., Li, Q., Lin, S., Chen, J., Calmette, J., Lu, M., et al. (2019). Stress–glucocorticoid–TSC22D3 axis compromises therapy-induced antitumor immunity. Nat Med 25, 1428–1441. 10.1038/s41591-019-0566-4.
- 201. Wang, C., Lutes, L.K., Barnoud, C., and Scheiermann, C. (2022). The circadian immune system. Science Immunology 7, eabm2465. 10.1126/sciimmunol.abm2465.
- 202. Scheiermann, C., Gibbs, J., Ince, L., and Loudon, A. (2018). Clocking in to immunity. Nat Rev Immunol *18*, 423–437. 10.1038/s41577-018-0008-4.
- 203. Brahmer, J.R., Lacchetti, C., Schneider, B.J., Atkins, M.B., Brassil, K.J., Caterino, J.M., Chau, I., Ernstoff, M.S., Gardner, J.M., Ginex, P., et al. (2018). Management of Immune-Related Adverse Events in Patients Treated With Immune Checkpoint Inhibitor Therapy: American Society of Clinical Oncology Clinical Practice Guideline. JCO 36, 1714–1768. 10.1200/JCO.2017.77.6385.
- 204. Wakuda, K., Miyawaki, T., Miyawaki, E., Mamesaya, N., Kawamura, T., Kobayashi, H., Omori, S., Nakashima, K., Ono, A., Kenmotsu, H., et al. (2019). The impact of steroid use on efficacy of immunotherapy among patients with lung cancer who have developed immune-related adverse events. JCO *37*, e20583–e20583. 10.1200/JCO.2019.37.15_suppl.e20583.
- 205. Horvat, T.Z., Adel, N.G., Dang, T.-O., Momtaz, P., Postow, M.A., Callahan, M.K., Carvajal, R.D., Dickson, M.A., D'Angelo, S.P., Woo, K.M., et al. (2015). Immune-Related Adverse Events, Need for Systemic Immunosuppression, and Effects on Survival and Time to Treatment Failure in Patients With Melanoma Treated With Ipilimumab at Memorial Sloan Kettering Cancer Center. J Clin Oncol *33*, 3193–3198. 10.1200/JCO.2015.60.8448.
- 206. Giles, A.J., Hutchinson, M.-K.N.D., Sonnemann, H.M., Jung, J., Fecci, P.E., Ratnam, N.M., Zhang, W., Song, H., Bailey, R., Davis, D., et al. (2018). Dexamethasone-induced immunosuppression: mechanisms and implications for immunotherapy. Journal for ImmunoTherapy of Cancer *6*, 51. 10.1186/s40425-018-0371-5.
- 207. Kalfeist, L., Galland, L., Ledys, F., Ghiringhelli, F., Limagne, E., and Ladoire, S. (2022). Impact of Glucocorticoid Use in Oncology in the Immunotherapy Era. Cells *11*, 770. 10.3390/cells11050770.
- 208. Cirillo, N., Morgan, D.J., Pedicillo, M.C., Celentano, A., Lo Muzio, L., McCullough, M.J., and Prime, S.S. (2017). Characterisation of the cancer-associated glucocorticoid system: key role of 11β-hydroxysteroid dehydrogenase type 2. British Journal of Cancer 117, 984–993. 10.1038/bjc.2017.243.
- 209. Veneris, J.T., Darcy, K.M., Mhawech-Fauceglia, P., Tian, C., Lengyel, E., Lastra, R.R., Pejovic, T., Conzen, S.D., and Fleming, G.F. (2017). High glucocorticoid receptor expression predicts short progression-free survival in ovarian cancer. Gynecologic Oncology *146*, 153–160. 10.1016/j.ygyno.2017.04.012.

- 210. Pan, D., Kocherginsky, M., and Conzen, S.D. (2011). Activation of the Glucocorticoid Receptor Is Associated with Poor Prognosis in Estrogen Receptor-Negative Breast Cancer. Cancer Res *71*, 6360–6370. 10.1158/0008-5472.CAN-11-0362.
- 211. Diamantopoulou, Z., Castro-Giner, F., Schwab, F.D., Foerster, C., Saini, M., Budinjas, S., Strittmatter, K., Krol, I., Seifert, B., Heinzelmann-Schwarz, V., et al. (2022). The metastatic spread of breast cancer accelerates during sleep. Nature *607*, 156–162. 10.1038/s41586-022-04875-y.
- 212. Hadadi, E., Taylor, W., Li, X.-M., Aslan, Y., Villote, M., Rivière, J., Duvallet, G., Auriau, C., Dulong, S., Raymond-Letron, I., et al. (2020). Chronic circadian disruption modulates breast cancer stemness and immune microenvironment to drive metastasis in mice. Nat Commun *11*, 3193. 10.1038/s41467-020-16890-6.
- 213. Nakayama, J., Lu, J.-W., Makinoshima, H., and Gong, Z. (2020). A Novel Zebrafish Model of Metastasis Identifies the HSD11β1 Inhibitor Adrenosterone as a Suppressor of Epithelial–Mesenchymal Transition and Metastatic Dissemination. Molecular Cancer Research 18, 477–487. 10.1158/1541-7786.MCR-19-0759.
- 214. Dalm, S., Karssen, A.M., Meijer, O.C., Belanoff, J.K., and de Kloet, E.R. (2019). Resetting the Stress System with a Mifepristone Challenge. Cell Mol Neurobiol *39*, 503–522. 10.1007/s10571-018-0614-5.
- 215. Kroon, J., Koorneef, L.L., van den Heuvel, J.K., Verzijl, C.R.C., van de Velde, N.M., Mol, I.M., Sips, H.C.M., Hunt, H., Rensen, P.C.N., and Meijer, O.C. (2018). Selective Glucocorticoid Receptor Antagonist CORT125281 Activates Brown Adipose Tissue and Alters Lipid Distribution in Male Mice. Endocrinology *159*, 535–546. 10.1210/en.2017-00512.
- 216. Havel, P.J., Busch, B.L., Curry, D.L., Johnson, P.R., Dallman, M.F., and Stern, J.S. (1996). Predominately glucocorticoid agonist actions of RU-486 in young specific-pathogen-free Zucker rats. The American journal of physiology *271*, R710–R717. 10.1152/ajpregu.1996.271.3.r710.
- 217. Albertson, D., and Hill, R.B. Effect of the antiglucocorticoid RU486 on adrenal steroidogenic enzyme activity and steroidogenesis. 6.
- 218. Southwest Oncology Group (2019). Double Blind Randomized Trial of the Anti-Progestational Agent Mifepristone In The Treatment of Unresectable Meningioma (clinicaltrials.gov).
- 219. Corcept Therapeutics (2018). Phase 1 Study of Mifepristone in Combination With Eribulin in Patients With Locally Advanced/Metastatic Breast or Other Specified Solid Tumors, With a Dose Expansion Cohort in Patients With Triple Negative Breast Cancer. (clinicaltrials.gov).
- 220. University of Chicago (2023). A Randomized, Placebo-Controlled, Double-Blind, Phase II Trial of Nanoparticle Albumin-Bound Paclitaxel (Nab-Paclitaxel, Abraxane®) With or Without Mifepristone for Advanced, Glucocorticoid Receptor-Positive, Triple-Negative Breast Cancer (clinicaltrials.gov).
- 221. Taplin, M.-E., Manola, J., Oh, W.K., Kantoff, P.W., Bubley, G.J., Smith, M., Barb, D., Mantzoros, C., Gelmann, E.P., and Balk, S.P. (2008). A phase II study of mifepristone (RU-486) in castration-resistant prostate cancer, with a correlative assessment of androgen-related hormones. BJU International *101*, 1084–1089. 10.1111/j.1464-410X.2008.07509.x.
- 222. Hardy, R.S., Botfield, H., Markey, K., Mitchell, J.L., Alimajstorovic, Z., Westgate, C.S.J., Sagmeister, M., Fairclough, R.J., Ottridge, R.S., Yiangou, A., et al. (2020). 11βHSD1 Inhibition with AZD4017

- Improves Lipid Profiles and Lean Muscle Mass in Idiopathic Intracranial Hypertension. J Clin Endocrinol Metab *106*, 174–187. 10.1210/clinem/dgaa766.
- 223. Marek, G.J., Katz, D.A., Meier, A., Greco IV, N., Zhang, W., Liu, W., and Lenz, R.A. (2014). Efficacy and safety evaluation of HSD-1 inhibitor ABT-384 in Alzheimer's disease. Alzheimer's & Dementia 10, S364–S373. 10.1016/j.jalz.2013.09.010.
- 224. An, G., Liu, W., Katz, D.A., Marek, G., Awni, W., and Dutta, S. (2013). Effect of Ketoconazole on the Pharmacokinetics of the 11 *β* -Hydroxysteroid Dehydrogenase Type 1 Inhibitor ABT-384 and Its Two Active Metabolites in Healthy Volunteers: Population Analysis of Data from a Drug-Drug Interaction Study. Drug Metab Dispos *41*, 1035–1045. 10.1124/dmd.112.049742.
- 225. Tung, I., and Sahu, A. (2021). Immune Checkpoint Inhibitor in First-Line Treatment of Metastatic Renal Cell Carcinoma: A Review of Current Evidence and Future Directions. Front Oncol *11*, 707214. 10.3389/fonc.2021.707214.
- 226. Lasorsa, F., di Meo, N.A., Rutigliano, M., Milella, M., Ferro, M., Pandolfo, S.D., Crocetto, F., Tataru, O.S., Autorino, R., Battaglia, M., et al. (2023). Immune Checkpoint Inhibitors in Renal Cell Carcinoma: Molecular Basis and Rationale for Their Use in Clinical Practice. Biomedicines *11*, 1071. 10.3390/biomedicines11041071.
- 227. Braun, D.A., Bakouny, Z., Hirsch, L., Flippot, R., Van Allen, E., Wu, C.J., and Choueiri, T.K. (2021). Beyond Conventional Immune Checkpoint Inhibition: Renal Cell Carcinoma at the Forefront of Solid Tumor Immunology. Nat Rev Clin Oncol *18*, 199–214. 10.1038/s41571-020-00455-z.
- 228. Chowdhury, N., and Drake, C.G. (2020). Kidney Cancer: An Overview of Current Therapeutic Approaches. Urologic Clinics of North America *47*, 419–431. 10.1016/j.ucl.2020.07.009.
- 229. Zhang, S., Zhang, E., Long, J., Hu, Z., Peng, J., Liu, L., Tang, F., Li, L., Ouyang, Y., and Zeng, Z. (2019). Immune infiltration in renal cell carcinoma. Cancer Science *110*, 1564–1572. 10.1111/cas.13996.
- 230. Liu, R., Yang, F., Yin, J.-Y., Liu, Y.-Z., Zhang, W., and Zhou, H.-H. (2021). Influence of Tumor Immune Infiltration on Immune Checkpoint Inhibitor Therapeutic Efficacy: A Computational Retrospective Study. Frontiers in Immunology *12*.
- 231. Larsson, S.C., Lee, W.-H., Kar, S., Burgess, S., and Allara, E. (2021). Assessing the role of cortisol in cancer: a wide-ranged Mendelian randomisation study. Br J Cancer *125*, 1025–1029. 10.1038/s41416-021-01505-8.
- 232. Zhang, L., Pan, J., Chen, W., Jiang, J., and Huang, J. (2020). Chronic stress-induced immune dysregulation in cancer: implications for initiation, progression, metastasis, and treatment. Am J Cancer Res *10*, 1294–1307.
- 233. Albiges, L., Tannir, N.M., Burotto, M., McDermott, D., Plimack, E.R., Barthélémy, P., Porta, C., Powles, T., Donskov, F., George, S., et al. (2020). Nivolumab plus ipilimumab versus sunitinib for first-line treatment of advanced renal cell carcinoma: extended 4-year follow-up of the phase III CheckMate 214 trial. ESMO Open 5, e001079. 10.1136/esmoopen-2020-001079.
- 234. Strehl, C., Ehlers, L., Gaber, T., and Buttgereit, F. (2019). Glucocorticoids—All-Rounders Tackling the Versatile Players of the Immune System. Front Immunol *10*, 1744. 10.3389/fimmu.2019.01744.

- 235. Mahata, B., Zhang, X., Kolodziejczyk, A.A., Proserpio, V., Haim-Vilmovsky, L., Taylor, A.E., Hebenstreit, D., Dingler, F.A., Moignard, V., Göttgens, B., et al. (2014). Single-Cell RNA Sequencing Reveals T Helper Cells Synthesizing Steroids De Novo to Contribute to Immune Homeostasis. Cell Reports 7, 1130–1142. 10.1016/j.celrep.2014.04.011.
- 236. Suzuki, T., Moriya, T., Ishida, T., Ohuchi, N., and Sasano, H. (2003). Intracrine mechanism of estrogen synthesis in breast cancer. Biomedicine & Pharmacotherapy *57*, 460–462. 10.1016/j.biopha.2003.09.007.
- 237. Stuchbery, R., McCoy, P.J., Hovens, C.M., and Corcoran, N.M. (2017). Androgen synthesis in prostate cancer: do all roads lead to Rome? Nat Rev Urol *14*, 49–58. 10.1038/nrurol.2016.221.
- 238. Frycz, B.A., Murawa, D., Borejsza-Wysocki, M., Wichtowski, M., Spychała, A., Marciniak, R., Murawa, P., Drews, M., and Jagodziński, P.P. (2017). mRNA expression of steroidogenic enzymes, steroid hormone receptors and their coregulators in gastric cancer. Oncology Letters *13*, 3369–3378. 10.3892/ol.2017.5881.
- 239. Li, C.-F., Liu, T.-T., Wang, J.-C., Yu, S.-C., Chen, Y.-Y., Fang, F.-M., Li, W.-S., and Huang, H.-Y. (2018). Hydroxysteroid 11-Beta Dehydrogenase 1 Overexpression with Copy-Number Gain and Missense Mutations in Primary Gastrointestinal Stromal Tumors. Journal of Clinical Medicine *7*, 408. 10.3390/jcm7110408.
- 240. Hasan, M.N., Capuk, O., Patel, S.M., and Sun, D. (2022). The Role of Metabolic Plasticity of Tumor-Associated Macrophages in Shaping the Tumor Microenvironment Immunity. Cancers (Basel) *14*, 3331. 10.3390/cancers14143331.
- 241. Edwards, C.R.W., Burt, D., Mcintyre, M.A., Kloet, E.R.D., Stewart, P.M., Brett, L., Sutanto, W.S., and Monder, C. PROTECTOR OF THE MINERALOCORTICOID RECEPTOR.
- 242. Spinetti, T., Spagnuolo, L., Mottas, I., Secondini, C., Treinies, M., Rüegg, C., Hotz, C., and Bourquin, C. (2016). TLR7-based cancer immunotherapy decreases intratumoral myeloid-derived suppressor cells and blocks their immunosuppressive function. Oncolmmunology *5*, e1230578. 10.1080/2162402X.2016.1230578.
- 243. Bourquin, C., Hotz, C., Noerenberg, D., Voelkl, A., Heidegger, S., Roetzer, L.C., Storch, B., Sandholzer, N., Wurzenberger, C., Anz, D., et al. (2011). Systemic Cancer Therapy with a Small Molecule Agonist of Toll-like Receptor 7 Can Be Improved by Circumventing TLR Tolerance. Cancer Research 71, 5123–5133. 10.1158/0008-5472.CAN-10-3903.
- 244. Bourquin, C., Pommier, A., and Hotz, C. (2020). Harnessing the immune system to fight cancer with Toll-like receptor and RIG-I-like receptor agonists. Pharmacological Research *154*, 104192. 10.1016/j.phrs.2019.03.001.
- 245. Fridman, W.H., Zitvogel, L., Sautès–Fridman, C., and Kroemer, G. (2017). The immune contexture in cancer prognosis and treatment. Nature Reviews Clinical Oncology *14*, 717–734. 10.1038/nrclinonc.2017.101.
- 246. Braun, D.A., Hou, Y., Bakouny, Z., Ficial, M., Sant' Angelo, M., Forman, J., Ross-Macdonald, P., Berger, A.C., Jegede, O.A., Elagina, L., et al. (2020). Interplay of somatic alterations and immune infiltration modulates response to PD-1 blockade in advanced clear cell renal cell carcinoma. Nat Med *26*, 909–918. 10.1038/s41591-020-0839-y.

- 247. Lawrence, M.S., Stojanov, P., Polak, P., Kryukov, G.V., Cibulskis, K., Sivachenko, A., Carter, S.L., Stewart, C., Mermel, C.H., Roberts, S.A., et al. (2013). Mutational heterogeneity in cancer and the search for new cancer-associated genes. Nature *499*, 214–218. 10.1038/nature12213.
- 248. Albiston, A.L., Obeyesekere, V.R., Smith, R.E., and Krozowski, Z.S. Cloning and tissue distribution of the human 1l/%hydroxysteroid dehydrogenase type 2 enzyme.
- 249. Han, D., Yu, Z., Zhang, H., Liu, H., Wang, B., and Qian, D. (2021). Microenvironment-associated gene HSD11B1 may serve as a prognostic biomarker in clear cell renal cell carcinoma: a study based on TCGA, RT-qPCR, Western blotting, and immunohistochemistry. Bioengineered *12*, 10891–10904. 10.1080/21655979.2021.1994908.
- 250. Melo, L.M.N., Herrera-Rios, D., Hinze, D., Löffek, S., Oezel, I., Turiello, R., Klein, J., Leonardelli, S., Westedt, I.-V., Al-Matary, Y., et al. (2023). Glucocorticoid activation by HSD11B1 limits T cell-driven interferon signaling and response to PD-1 blockade in melanoma. J Immunother Cancer 11, e004150. 10.1136/jitc-2021-004150.
- 251. Soulier, A., Blois, S.M., Sivakumaran, S., Fallah-Arani, F., Henderson, S., Flutter, B., Rabbitt, E.H., Stewart, P.M., Lavery, G.G., Bennett, C., et al. (2013). Cell-intrinsic regulation of murine dendritic cell function and survival by prereceptor amplification of glucocorticoid. Blood *122*, 3288–3297. 10.1182/blood-2013-03-489138.
- 252. Acharya, N., Madi, A., Zhang, H., Klapholz, M., Escobar, G., Dulberg, S., Christian, E., Ferreira, M., Dixon, K.O., Fell, G., et al. (2020). Endogenous Glucocorticoid Signaling Regulates CD8+ T Cell Differentiation and Development of Dysfunction in the Tumor Microenvironment. Immunity *53*, 658-671.e6. 10.1016/j.immuni.2020.08.005.
- 253. Chuanxin, Z., Shengzheng, W., Lei, D., Duoli, X., Jin, L., Fuzeng, R., Aiping, L., and Ge, Z. (2020). Progress in 11β-HSD1 inhibitors for the treatment of metabolic diseases: A comprehensive guide to their chemical structure diversity in drug development. European Journal of Medicinal Chemistry 191, 112134. 10.1016/j.ejmech.2020.112134.
- 254. Kelton, W., Waindok, A.C., Pesch, T., Pogson, M., Ford, K., Parola, C., and Reddy, S.T. (2017). Reprogramming MHC specificity by CRISPR-Cas9-assisted cassette exchange. Sci Rep *7*, 45775. 10.1038/srep45775.
- 255. Andrieu, T., du Toit, T., Vogt, B., Mueller, M.D., and Groessl, M. (2022). Parallel targeted and non-targeted quantitative analysis of steroids in human serum and peritoneal fluid by liquid chromatography high-resolution mass spectrometry. Anal Bioanal Chem *414*, 7461–7472. 10.1007/s00216-022-03881-3.
- 256. Bindea, G., Mlecnik, B., Tosolini, M., Kirilovsky, A., Waldner, M., Obenauf, A.C., Angell, H., Fredriksen, T., Lafontaine, L., Berger, A., et al. (2013). Spatiotemporal Dynamics of Intratumoral Immune Cells Reveal the Immune Landscape in Human Cancer. Immunity *39*, 782–795. 10.1016/j.immuni.2013.10.003.
- 257. Pommier, A., and Bourquin, C. (2021). Hsd11b1 Inhibitors for Use in Immunotherapy and Uses Thereof.
- 258. Tomayko, M.M., and Reynolds, C.P. (1989). Determination of subcutaneous tumor size in athymic (nude) mice. Cancer Chemother. Pharmacol. *24*, 148–154. 10.1007/BF00300234.

- 259. Tie, Y., Tang, F., Wei, Y., and Wei, X. (2022). Immunosuppressive cells in cancer: mechanisms and potential therapeutic targets. Journal of Hematology & Oncology *15*, 61. 10.1186/s13045-022-01282-8.
- 260. Rocamora-Reverte, L., Reichardt, H.M., Villunger, A., and Wiegers, Gj. (2017). T-cell autonomous death induced by regeneration of inert glucocorticoid metabolites. Cell Death & Disease 8, e2948. 10.1038/cddis.2017.344.
- 261. Sanjurjo, L., Aran, G., Téllez, É., Amézaga, N., Armengol, C., López, D., Prats, C., and Sarrias, M.-R. (2018). CD5L Promotes M2 Macrophage Polarization through Autophagy-Mediated Upregulation of ID3. Frontiers in Immunology *9*.
- 262. Mårtensson, J., Sundqvist, M., Manandhar, A., Ieremias, L., Zhang, L., Ulven, T., Xie, X., Björkman, L., and Forsman, H. (2021). The Two Formyl Peptide Receptors Differently Regulate GPR84-Mediated Neutrophil NADPH Oxidase Activity. JIN *13*, 242–256. 10.1159/000514887.
- 263. Konaté, M.M., Antony, S., and Doroshow, J.H. (2020). Inhibiting the Activity of NADPH Oxidase in Cancer. Antioxidants & Redox Signaling *33*, 435–454. 10.1089/ars.2020.8046.
- 264. Gong, S., Miao, Y.-L., Jiao, G.-Z., Sun, M.-J., Li, H., Lin, J., Luo, M.-J., and Tan, J.-H. (2015). Dynamics and Correlation of Serum Cortisol and Corticosterone under Different Physiological or Stressful Conditions in Mice. PLoS ONE *10*, e0117503. 10.1371/journal.pone.0117503.
- 265. Volden, P.A., and Conzen, S.D. (2013). The influence of glucocorticoid signaling on tumor progression. Brain, Behavior, and Immunity *30*, S26–S31. 10.1016/j.bbi.2012.10.022.
- 266. Bernabé, D.G., Tamae, A.C., Miyahara, G.I., Sundefeld, M.L.M., Oliveira, S.P., and Biasoli, É.R. (2012). Increased plasma and salivary cortisol levels in patients with oral cancer and their association with clinical stage. Journal of Clinical Pathology 65, 934–939. 10.1136/jclinpath-2012-200695.
- 267. Ayroldi, E., Cannarile, L., Adorisio, S., Delfino, D.V., and Riccardi, C. (2018). Role of Endogenous Glucocorticoids in Cancer in the Elderly. International Journal of Molecular Sciences *19*, 3774. 10.3390/ijms19123774.
- 268. Di Rosso, M.E., Sterle, H.A., Cremaschi, G.A., and Genaro, A.M. (2018). Beneficial Effect of Fluoxetine and Sertraline on Chronic Stress-Induced Tumor Growth and Cell Dissemination in a Mouse Model of Lymphoma: Crucial Role of Antitumor Immunity. Front. Immunol. 9. 10.3389/fimmu.2018.01341.
- 269. Obradović, M.M.S., Hamelin, B., Manevski, N., Couto, J.P., Sethi, A., Coissieux, M.-M., Münst, S., Okamoto, R., Kohler, H., Schmidt, A., et al. (2019). Glucocorticoids promote breast cancer metastasis. Nature, 1. 10.1038/s41586-019-1019-4.
- 270. Chon, H.J., Lee, W.S., Yang, H., Kong, S.J., Lee, N.K., Moon, E.S., Choi, J., Han, E.C., Kim, J.H., Ahn, J.B., et al. (2018). Tumor microenvironment remodeling by intratumoral oncolytic vaccinia virus enhances the efficacy of immune checkpoint blockade. Clin Cancer Res, clincanres.1932.2018. 10.1158/1078-0432.CCR-18-1932.
- 271. O'Shaughnessy, M.J., Murray, K.S., Rosa, S.P.L., Budhu, S., Merghoub, T., Somma, A., Monette, S., Kim, K., Corradi, R.B., Scherz, A., et al. Systemic Antitumor Immunity by PD-1/PD-L1 Inhibition Is Potentiated by Vascular-Targeted Photodynamic Therapy of Primary Tumors. Clinical Cancer Research, 9.

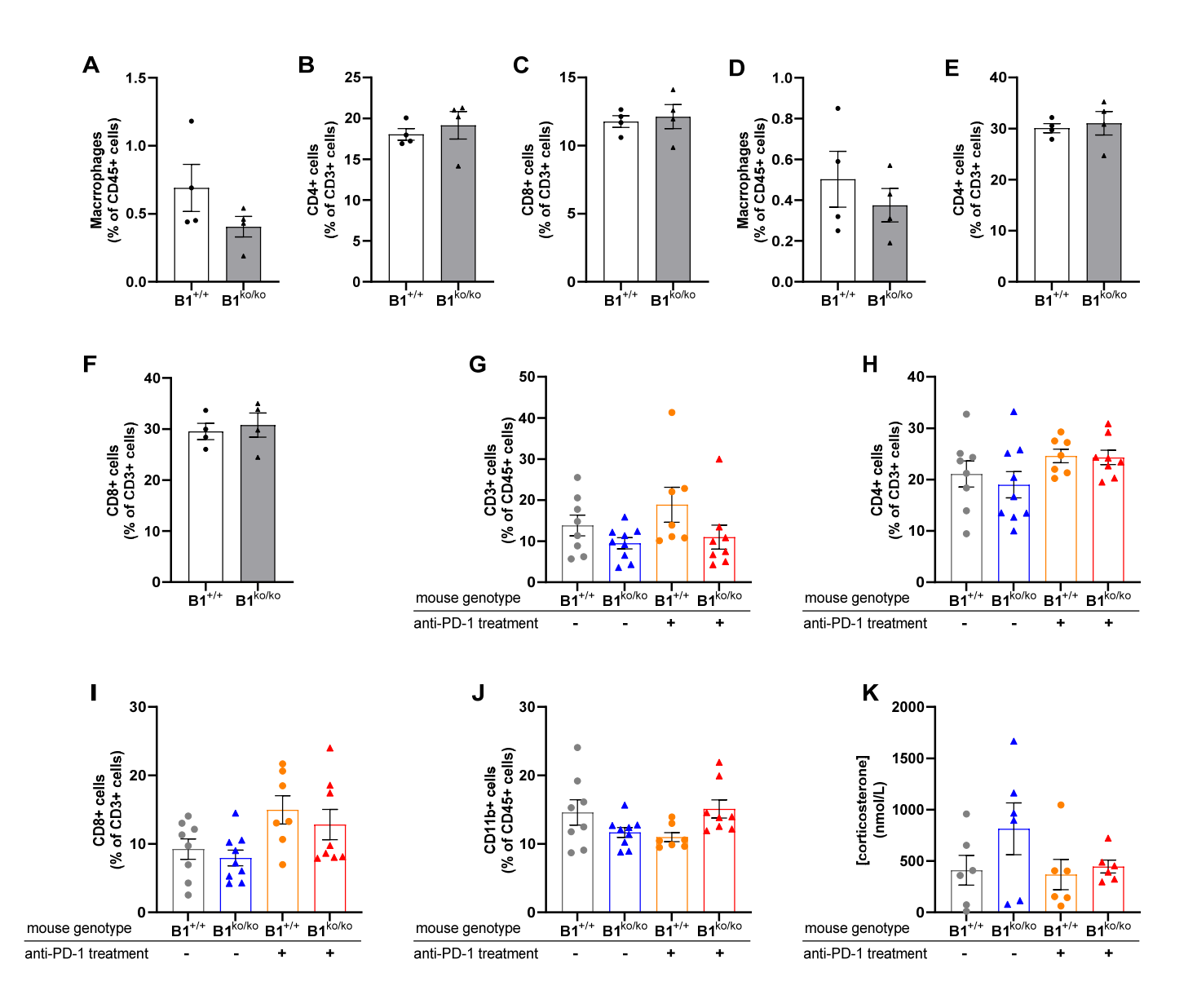
- 272. Zhang, X., Shi, X., Li, J., Hu, Z., Gao, J., Wu, S., and Long, Z. (2019). Combination immunotherapy with interleukin-2 surface-modified tumor cell vaccine and programmed death receptor-1 blockade against renal cell carcinoma. Cancer Sci *110*, 31–39. 10.1111/cas.13842.
- 273. Mosely, S.I.S., Prime, J.E., Sainson, R.C.A., Koopmann, J.-O., Wang, D.Y.Q., Greenawalt, D.M., Ahdesmaki, M.J., Leyland, R., Mullins, S., Pacelli, L., et al. (2017). Rational Selection of Syngeneic Preclinical Tumor Models for Immunotherapeutic Drug Discovery. Cancer Immunol Res *5*, 29–41. 10.1158/2326-6066.CIR-16-0114.
- 274. Bruera, S., and Suarez-Almazor, M.E. (2022). The effects of glucocorticoids and immunosuppressants on cancer outcomes in checkpoint inhibitor therapy. Frontiers in Oncology 12.
- 275. Li, J., Yang, K., Zhao, L., Bai, C., and Sun, Z. (2020). Impact of corticosteroids use on efficacy of immune checkpoint inhibitors in cancer patients: A meta-analysis. JCO *38*, e15234–e15234. 10.1200/JCO.2020.38.15_suppl.e15234.
- 276. Maslov, D.V., Tawagi, K., Kc, M., Simenson, V., Yuan, H., Parent, C., Bamnolker, A., Goel, R., Blake, Z., Matrana, M.R., et al. (2021). Timing of steroid initiation and response rates to immune checkpoint inhibitors in metastatic cancer. J Immunother Cancer *9*, e002261. 10.1136/jitc-2020-002261.
- 277. Li, J., Robl, J.A., Li, J.J., Kennedy, L.J., Wang, H., Li, J.J., Qian, X., Deshpande, R.P., Kolla, L.R., Cann, R.O., et al. (2012). Triazolopyridine 11-β hydroxysteroid dehydrogenase type I inhibitors. US8119658B2.
- 278. Li, J., Robl, J.A., Li, J.J., Kennedy, L.J., Wang, H., Li, J.J., Wei, C., and Galella, M. (2013). Triazolopyridine 11-beta hydroxysteroid dehydrogenase type I inhibitors. US8541444B2.
- 279. Gutierrez, P.M., Gyte, A., deSchoolmeester, J., Ceuppens, P., Swales, J., Stacey, C., Eriksson, J.W., Sjöstrand, M., Nilsson, C., and Leighton, B. (2015). Continuous inhibition of 11β-hydroxysteroid dehydrogenase type I in adipose tissue leads to tachyphylaxis in humans and rats but not in mice. British Journal of Pharmacology *172*, 4806–4816. 10.1111/bph.13251.
- 280. Scott, J.S., Bowker, S.S., deSchoolmeester, J., Gerhardt, S., Hargreaves, D., Kilgour, E., Lloyd, A., Mayers, R.M., McCoull, W., Newcombe, N.J., et al. (2012). Discovery of a Potent, Selective, and Orally Bioavailable Acidic 11β-Hydroxysteroid Dehydrogenase Type 1 (11β-HSD1) Inhibitor: Discovery of 2-[(3 *S*)-1-[5-(Cyclohexylcarbamoyl)-6-propylsulfanylpyridin-2-yl]-3-piperidyl]acetic Acid (AZD4017). J. Med. Chem. *55*, 5951–5964. 10.1021/jm300592r.
- 281. Zhuang, L., Tice, C.M., Xu, Z., Zhao, W., Cacatian, S., Ye, Y.-J., Singh, S.B., Lindblom, P., McKeever, B.M., Krosky, P.M., et al. (2017). Discovery of BI 135585, an in vivo efficacious oxazinanone-based 11β hydroxysteroid dehydrogenase type 1 inhibitor. Bioorganic & Medicinal Chemistry 25, 3649–3657. 10.1016/j.bmc.2017.04.033.
- 282. Wang, L., Liu, J., Zhang, A., Cheng, P., Zhang, X., Lv, S., Wu, L., Yu, J., Di, W., Zha, J., et al. (2012). BVT.2733, a Selective 11β-Hydroxysteroid Dehydrogenase Type 1 Inhibitor, Attenuates Obesity and Inflammation in Diet-Induced Obese Mice. PLOS ONE *7*, e40056. 10.1371/journal.pone.0040056.
- 283. Courtney, R., Stewart, P.M., Toh, M., Ndongo, M.-N., Calle, R.A., and Hirshberg, B. (2008). Modulation of 11β-Hydroxysteroid Dehydrogenase (11βHSD) Activity Biomarkers and

- Pharmacokinetics of PF-00915275, a Selective 11βHSD1 Inhibitor. The Journal of Clinical Endocrinology & Metabolism *93*, 550–556. 10.1210/jc.2007-1912.
- 284. Shah, S., Hermanowski-Vosatka, A., Gibson, K., Ruck, R.A., Jia, G., Zhang, J., Hwang, P.M.T., Ryan, N.W., Langdon, R.B., and Feig, P.U. (2011). Efficacy and safety of the selective 11β-HSD-1 inhibitors MK-0736 and MK-0916 in overweight and obese patients with hypertension. Journal of the American Society of Hypertension *5*, 166–176. 10.1016/j.jash.2011.01.009.
- 285. Wan, Z.-K., Chenail, E., Li, H.-Q., Kendall, C., Wang, Y., Gingras, S., Xiang, J., Massefski, W.W., Mansour, T., S., and Saiah, E. (2011). Synthesis of Potent and Orally Efficacious 11β-Hydroxysteroid Dehydrogenase Type 1 Inhibitor HSD-016. J. Org. Chem. *76*, 7048–7055. 10.1021/jo200958a.
- 286. Xiang, J.S., Saiah, E., Tam, S.Y., McKew, J.C., Chen, L., Ipek, M., Lee, K., Li, H.-Q., Li, J., Li, W., et al. (2010). 11-Beta HSD1 Inhibitors. US20100029648A1.
- 287. Liu, W., Katz, D.A., Locke, C., Daszkowski, D., Wang, Y., Rieser, M.J., Awni, W., Marek, G.J., and Dutta, S. (2013). Clinical Safety, Pharmacokinetics, and Pharmacodynamics of the 11β-Hydroxysteroid Dehydrogenase Type 1 Inhibitor ABT-384 in Healthy Volunteers and Elderly Adults: Clinical Pharmacology in Drug Development. Clinical Pharmacology in Drug Development 2, 133–151. 10.1002/cpdd.5.
- 288. Katz, D.A., Liu, W., Locke, C., Jacobson, P., Barnes, D.M., Basu, R., An, G., Rieser, M.J., Daszkowski, D., Groves, F., et al. (2013). Peripheral and central nervous system inhibition of 11β-hydroxysteroid dehydrogenase type 1 in man by the novel inhibitor ABT-384. Transl Psychiatry 3, e295. 10.1038/tp.2013.67.
- 289. Tice, C.M., Zhao, W., Xu, Z., Cacatian, S.T., Simpson, R.D., Ye, Y.-J., Singh, S.B., McKeever, B.M., Lindblom, P., Guo, J., et al. (2010). Spirocyclic ureas: Orally bioavailable 11β-HSD1 inhibitors identified by computer-aided drug design. Bioorganic & Medicinal Chemistry Letters *20*, 881–886. 10.1016/j.bmcl.2009.12.082.
- 290. Taylor, A., Irwin, N., McKillop, A.M., Flatt, P.R., and Gault, V.A. (2008). Sub-chronic administration of the 11β-HSD1 inhibitor, carbenoxolone, improves glucose tolerance and insulin sensitivity in mice with diet-induced obesity. *389*, 441–445. 10.1515/BC.2008.049.
- 291. Cooper, M.S., and Stewart, P.M. (2009). 11β-Hydroxysteroid Dehydrogenase Type 1 and Its Role in the Hypothalamus-Pituitary-Adrenal Axis, Metabolic Syndrome, and Inflammation. The Journal of Clinical Endocrinology & Metabolism *94*, 4645–4654. 10.1210/jc.2009-1412.
- 292. Aziz, S.A., Sznol, J., Adeniran, A., Colberg, J.W., Camp, R.L., and Kluger, H.M. (2013). Vascularity of primary and metastatic renal cell carcinoma specimens. J Transl Med *11*, 15. 10.1186/1479-5876-11-15.
- 293. Mertz, K.D., Demichelis, F., Kim, R., Schraml, P., Storz, M., Diener, P.-A., Moch, H., and Rubin, M.A. (2007). Automated immunofluorescence analysis defines microvessel area as a prognostic parameter in clear cell renal cell cancer. Human Pathology *38*, 1454–1462. 10.1016/j.humpath.2007.05.017.
- 294. Mirus, M., Tokalov, S.V., Abramyuk, A., Heinold, J., Prochnow, V., Zöphel, K., Kotzerke, J., and Abolmaali, N. (2019). Noninvasive assessment and quantification of tumor vascularization using [18F]FDG-PET/CT and CE-CT in a tumor model with modifiable angiogenesis—an animal experimental prospective cohort study. EJNMMI Res *9*, 55. 10.1186/s13550-019-0502-0.

- 295. Melero, I., Castanon, E., Alvarez, M., Champiat, S., and Marabelle, A. (2021). Intratumoural administration and tumour tissue targeting of cancer immunotherapies. Nat Rev Clin Oncol *18*, 558–576. 10.1038/s41571-021-00507-y.
- 296. Wang, J., Chen, J., Zhu, Y., Zheng, N., Liu, J., Xiao, Y., Lu, Y., Dong, H., Xie, J., Yu, S., et al. (2016). In vitro and in vivo efficacy and safety evaluation of metapristone and mifepristone as cancer metastatic chemopreventive agents. Biomedicine & Pharmacotherapy *78*, 291–300. 10.1016/j.biopha.2016.01.017.
- 297. Ji, Y., Rankin, C., Grunberg, S., Sherrod, A.E., Ahmadi, J., Townsend, J.J., Feun, L.G., Fredericks, R.K., Russell, C.A., Kabbinavar, F.F., et al. (2015). Double-Blind Phase III Randomized Trial of the Antiprogestin Agent Mifepristone in the Treatment of Unresectable Meningioma: SWOG S9005. JCO *33*, 4093–4098. 10.1200/JCO.2015.61.6490.
- 298. Cossu, G., Levivier, M., Daniel, R.T., and Messerer, M. (2015). The Role of Mifepristone in Meningiomas Management: A Systematic Review of the Literature. BioMed Research International *2015*, e267831. 10.1155/2015/267831.
- 299. Serritella, A.V., Shevrin, D., Heath, E.I., Wade, J.L., Martinez, E., Anderson, A., Schonhoft, J., Chu, Y.-L., Karrison, T., Stadler, W.M., et al. (2022). Phase I/II Trial of Enzalutamide and Mifepristone, a Glucocorticoid Receptor Antagonist, for Metastatic Castration-Resistant Prostate Cancer. Clinical Cancer Research *28*, 1549–1559. 10.1158/1078-0432.CCR-21-4049.
- 300. Check, J.H., Check, D., Srivastava, M.D., Poretta, T., and Aikins, J.K. (2020). Treatment With Mifepristone Allows a Patient With End-stage Pancreatic Cancer in Hospice on a Morphine Drip to Restore a Decent Quality of Life. Anticancer Research 40, 6997–7001. 10.21873/anticanres.14724.
- 301. Check, J.H., Check, D., and Poretta, T. (2019). Mifepristone Extends Both Length and Quality of Life in a Patient With Advanced Non-small Cell Lung Cancer that Has Progressed Despite Chemotherapy and a Check-point Inhibitor. Anticancer Research 39, 1923–1926. 10.21873/anticanres.13301.
- 302. Nicosia, R.F., Belser, P., Bonanno, E., and Diven, J. (1991). Regulation of angiogenesis in vitro by collagen metabolism. In Vitro Cell Dev Biol *27A*, 961–966. 10.1007/BF02631124.
- 303. Fang, M., Yuan, J., Peng, C., and Li, Y. (2014). Collagen as a double-edged sword in tumor progression. Tumor Biol. *35*, 2871–2882. 10.1007/s13277-013-1511-7.
- 304. Rømer, A.M.A., Thorseth, M.-L., and Madsen, D.H. (2021). Immune Modulatory Properties of Collagen in Cancer. Frontiers in Immunology *12*.
- 305. Capasso, A., Lang, J., Pitts, T.M., Jordan, K.R., Lieu, C.H., Davis, S.L., Diamond, J.R., Kopetz, S., Barbee, J., Peterson, J., et al. (2019). Characterization of immune responses to anti-PD-1 mono and combination immunotherapy in hematopoietic humanized mice implanted with tumor xenografts. J Immunother Cancer 7, 37. 10.1186/s40425-019-0518-z.
- 306. Elía, A., Saldain, L., Vanzulli, S.I., Helguero, L.A., Lamb, C.A., Fabris, V., Pataccini, G., Martínez-Vazquez, P., Burruchaga, J., Caillet-Bois, I., et al. (2023). Beneficial Effects of Mifepristone Treatment in Patients with Breast Cancer Selected by the Progesterone Receptor Isoform Ratio: Results from the MIPRA Trial. Clinical Cancer Research *29*, 866–877. 10.1158/1078-0432.CCR-22-2060.

- 307. Goyeneche, A.A., Carón, R.W., and Telleria, C.M. (2007). Mifepristone Inhibits Ovarian Cancer Cancer Cell Growth In Vitro and In Vivo. Clin Cancer Res *13*, 3370–3379. 10.1158/1078-0432.CCR-07-0164.
- 308. Wang, H., Zhou, J., Guo, X., Li, Y., Duan, L., SI, X., and Zhang, L. (2020). Use of glucocorticoids in the management of immunotherapy-related adverse effects. Thorac Cancer *11*, 3047–3052. 10.1111/1759-7714.13589.
- 309. Kanumakala, S., and Warne, G.L. (2004). 21-Hydroxylase Deficiency, Classical. In Encyclopedia of Endocrine Diseases, L. Martini, ed. (Elsevier), pp. 476–484. 10.1016/B0-12-475570-4/00632-6.
- 310. Stewart, P.M., and Newell-Price, J.D.C. (2016). The Adrenal Cortex. In Williams Textbook of Endocrinology (Elsevier), pp. 489–555. 10.1016/B978-0-323-29738-7.00015-0.
- 311. Prado, M.J., Singh, S., Ligabue-Braun, R., Meneghetti, B.V., Rispoli, T., Kopacek, C., Monteiro, K., Zaha, A., Rossetti, M.L.R., and Pandey, A.V. (2021). Characterization of Mutations Causing CYP21A2 Deficiency in Brazilian and Portuguese Populations. Int J Mol Sci *23*, 296. 10.3390/ijms23010296.
- 312. Malikova, J., Zingg, T., Fingerhut, R., Sluka, S., Grössl, M., Brixius-Anderko, S., Bernhardt, R., McDougall, J., Pandey, A.V., and Flück, C.E. (2019). HIV Drug Efavirenz Inhibits CYP21A2 Activity with Possible Clinical Implications. Hormone Research in Paediatrics *91*, 262–270. 10.1159/000500522.
- 313. Rižner, T.L., and Penning, T.M. (2014). Role of aldo–keto reductase family 1 (AKR1) enzymes in human steroid metabolism. Steroids *79*, 49–63. 10.1016/j.steroids.2013.10.012.
- 314. Ferrari, P. (2010). The role of 11β-hydroxysteroid dehydrogenase type 2 in human hypertension. Biochimica et Biophysica Acta (BBA) Molecular Basis of Disease *1802*, 1178–1187. 10.1016/j.bbadis.2009.10.017.

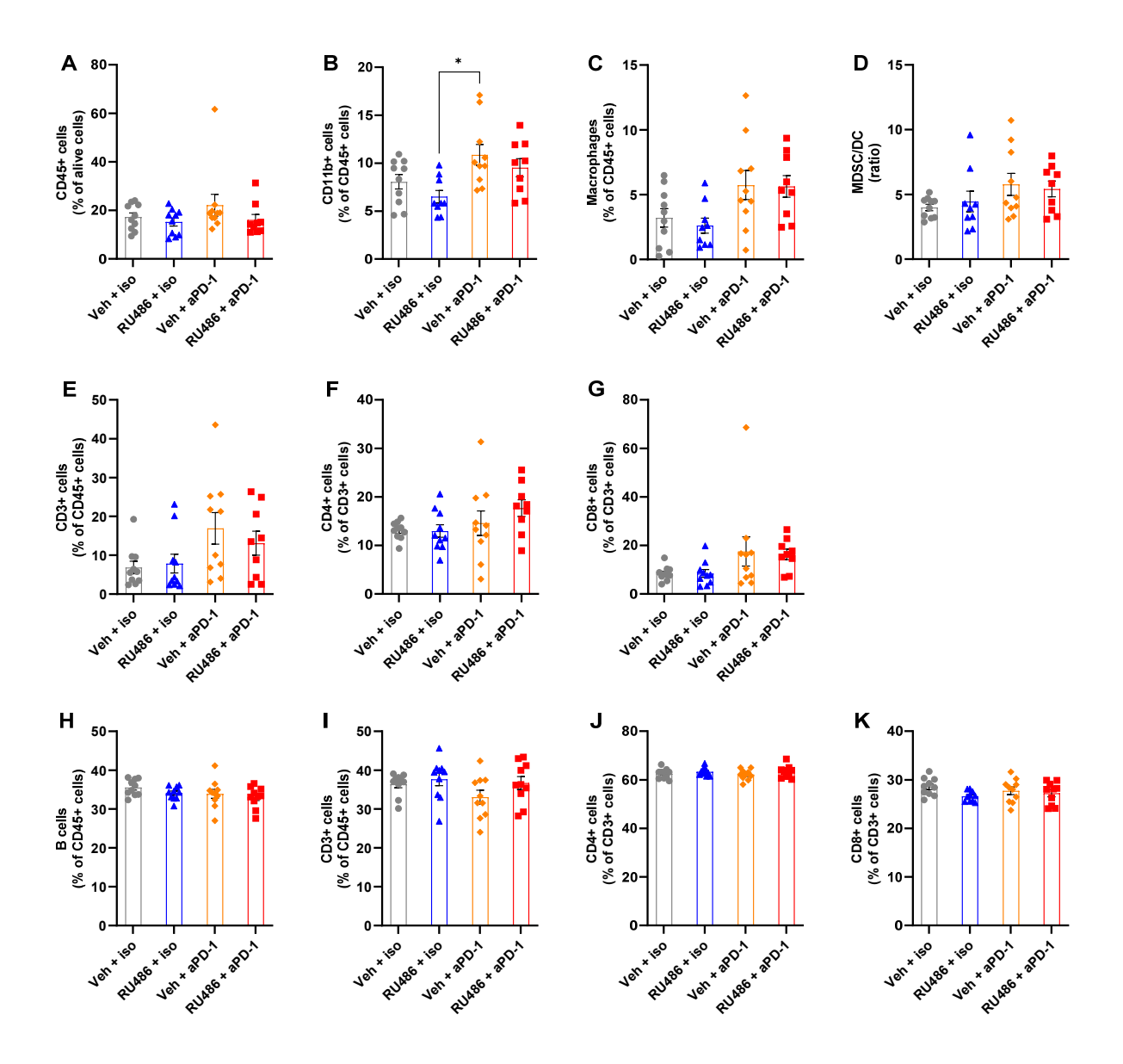
I. Supplementary data



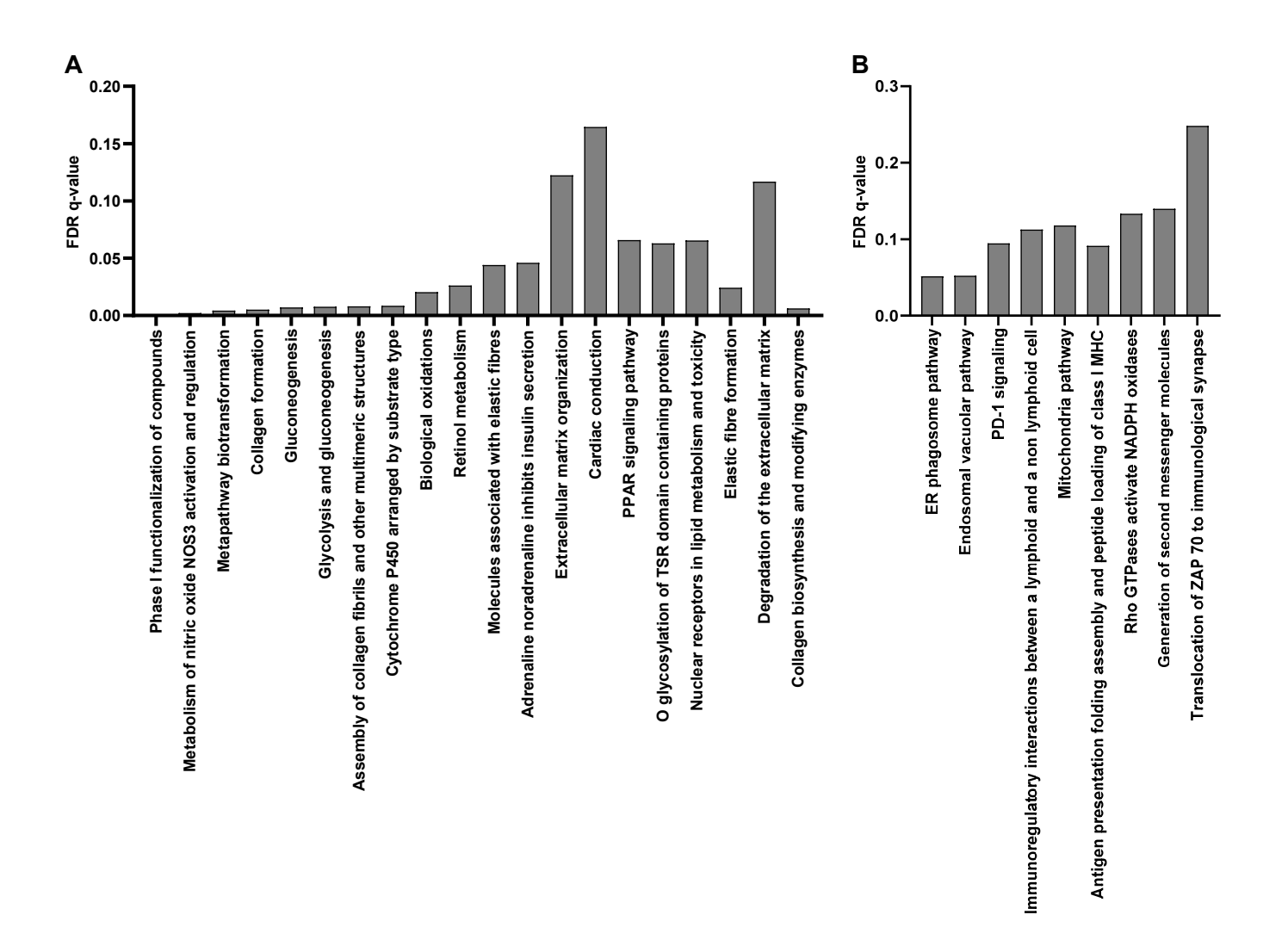
Supplementary Figure 1: Constitutive loss of hsd11b1 prevents anti-PD-1 response in subcutaneous tumor model. **A-F.** Immunophenotyping results of spleen (**A-C**) and lymph nodes (**D-F**) of naïve mice by flow cytometry. Percentage of cells represented as % of CD45⁺ cells (**A, D**) or as % of CD3⁺ cells (**B-C, E-F**). Data are shown as mean +/- SEM. 4 mice per group. **G-J.** Immunophenotyping results of the tumor by flow cytometry. Percentage of cells represented as % of CD45⁺ cells (**G, J**) or as % of CD3⁺ cells (**H-I**). Data are shown as mean +/- SEM. 8 to 10 mice per group. **K.** Corticosterone concentration measured in plasma of s.c. tumor bearing mice by mass spectrometry. Data are shown as mean +/- SEM. 6 mice per group.

Usage	Sequence
gRNA 1 for hsd11b1 KO in mouse with Cas9	GCTGGGCACAAGTTCGAGTT
gRNA 2 for hsd11b1 KO in mouse with Cas9	ATGGTGGTCATCTTGGTCGT
Fw1 primer for genotyping PCR of mouse hsd11b1	CATGTCCCTTCCTCACCGAG
Rv1 primer for genotyping PCR of mouse hsd11b1	TGTTGGCATGCCCCATAGTC

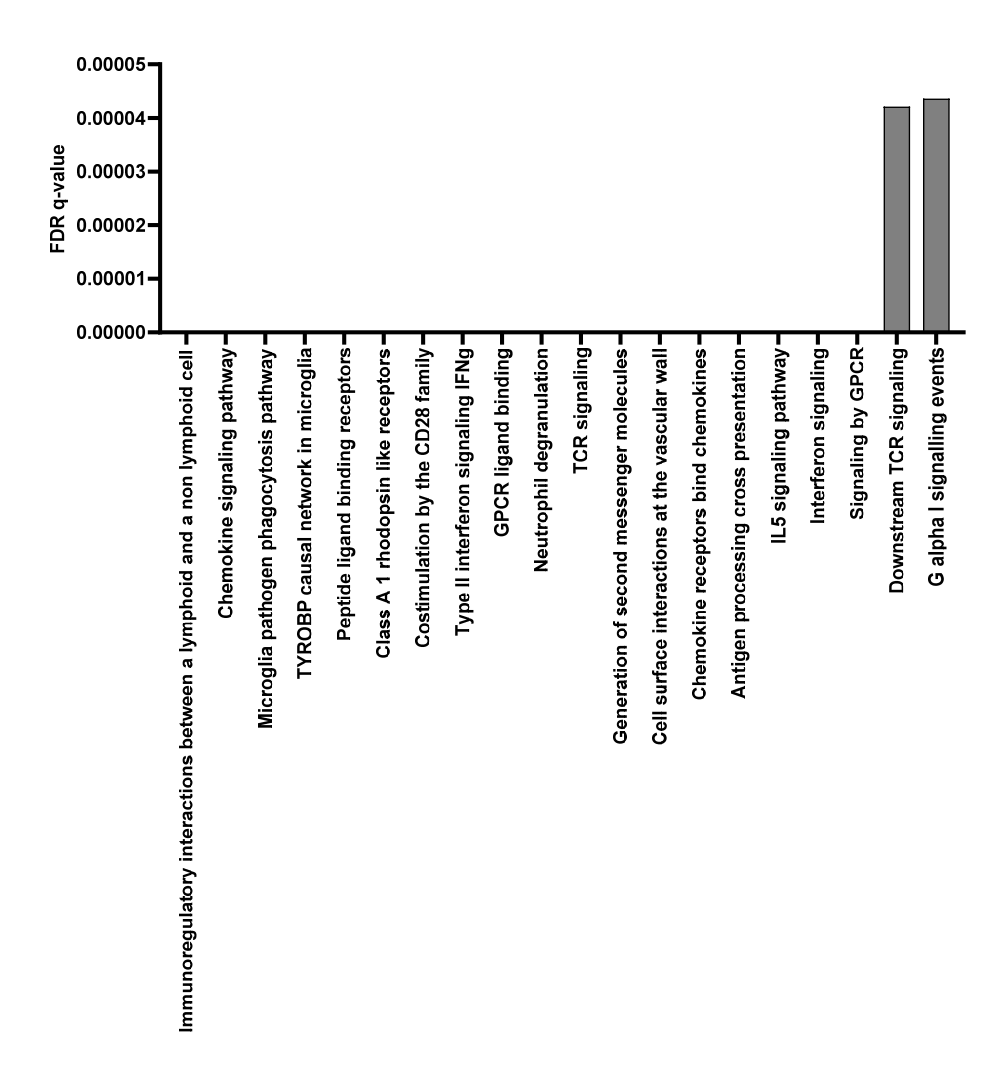
Supplementary Table 1: DNA sequences used to perform knock out of hsd11b1 and primers used to genotype hsd11b1 in mouse DNA.



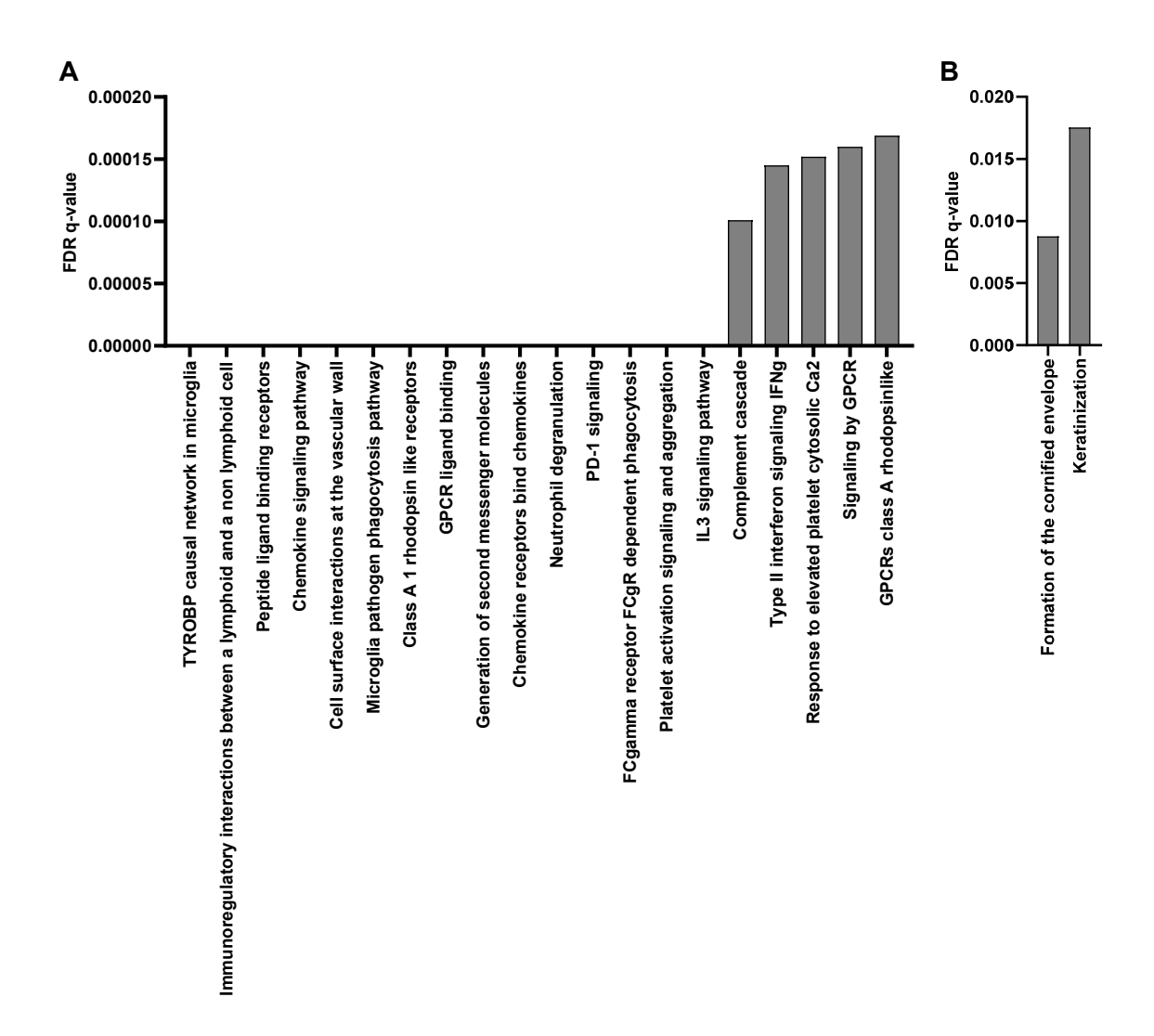
Supplementary Figure 2: Immune population in tumor and spleen of Renca tumor bearing mice. **A-G**. Immunophenotyping results of tumor by flow cytometry. Percentage of cells represented as % of alive cells (**A**), % of CD45⁺ cells (**B-C**, **E**), % of CD3⁺ cells (**F-G**) or as cells ratio based on the % of MDCS/CD45⁺ cells and % of DC/CD45⁺ cells (**D**). Data are shown as mean +/- SEM. 10 mice per group. Statistical analysis: Kruskal–Wallis test, alpha 0.05, Dunn's multiple comparisons test, * p value < 0.05. **H-K**. Immunophenotyping results of the spleen of tumor bearing mice by flow cytometry. Percentage of cells represented as % of CD45⁺ cells (**H-I**), % of CD3⁺ cells (**J-K**). Data are shown as mean +/- SEM. 10 mice per group.



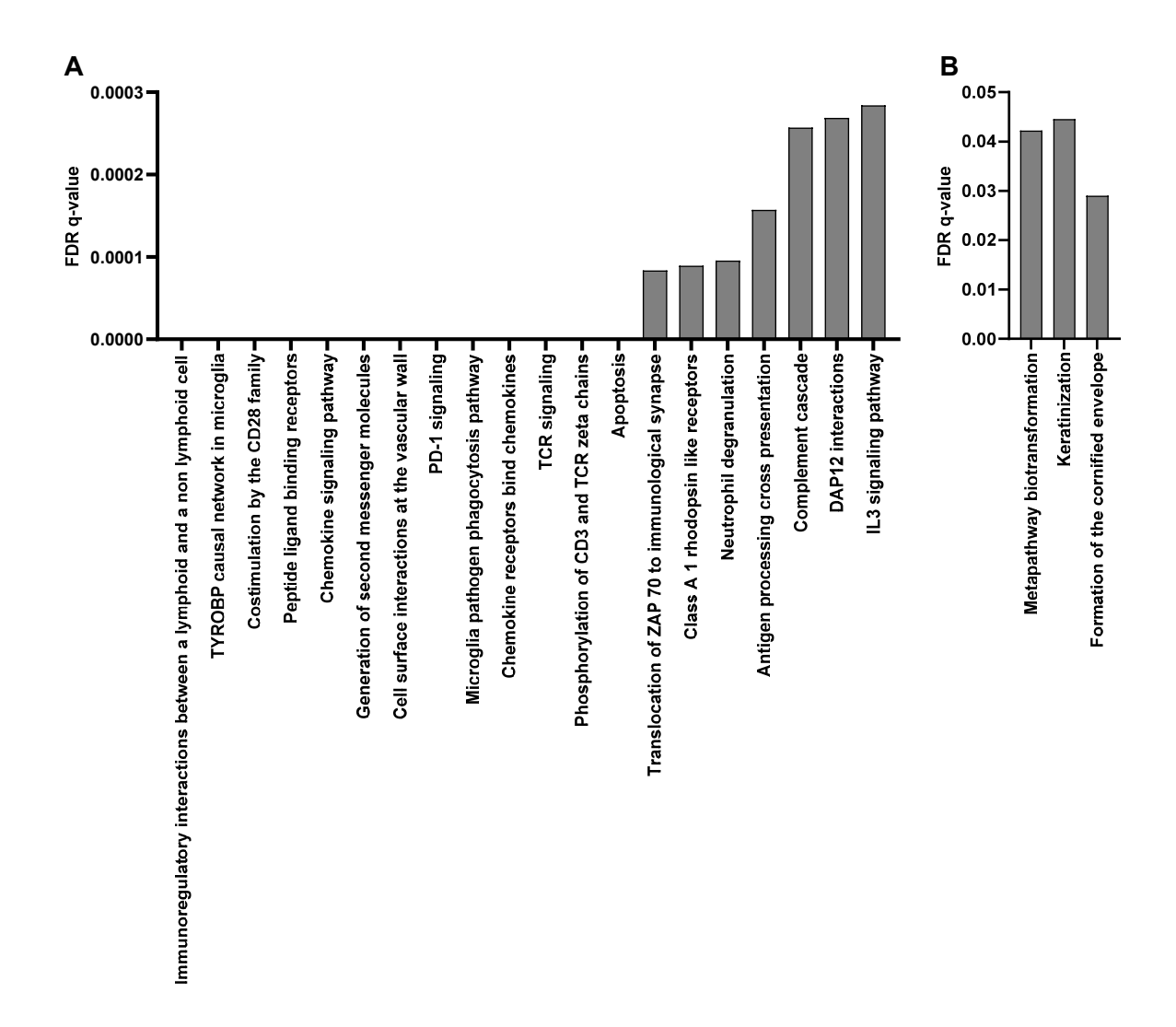
Supplementary Figure 3: Physiological pathways differentially expressed in tumor of mice. Comparison of tumors of females receiving Iso+RU486 to Iso+Veh group with GSEA software. Gene sets obtained from GSEA software, using the mouse canonical pathways data base. Gene set are ranked on the x axis from the smallest to the largest nominal p value. Only the first 20 statistically differentially expressed gene sets are showed (p value < 0.05 and FDR < 0.25). 10 mice per group. **A.** Physiological pathways enriched in tumor of mice treated with Iso+RU486. **B.** Physiological pathways reduced in tumor of mice treated with Iso+RU486.



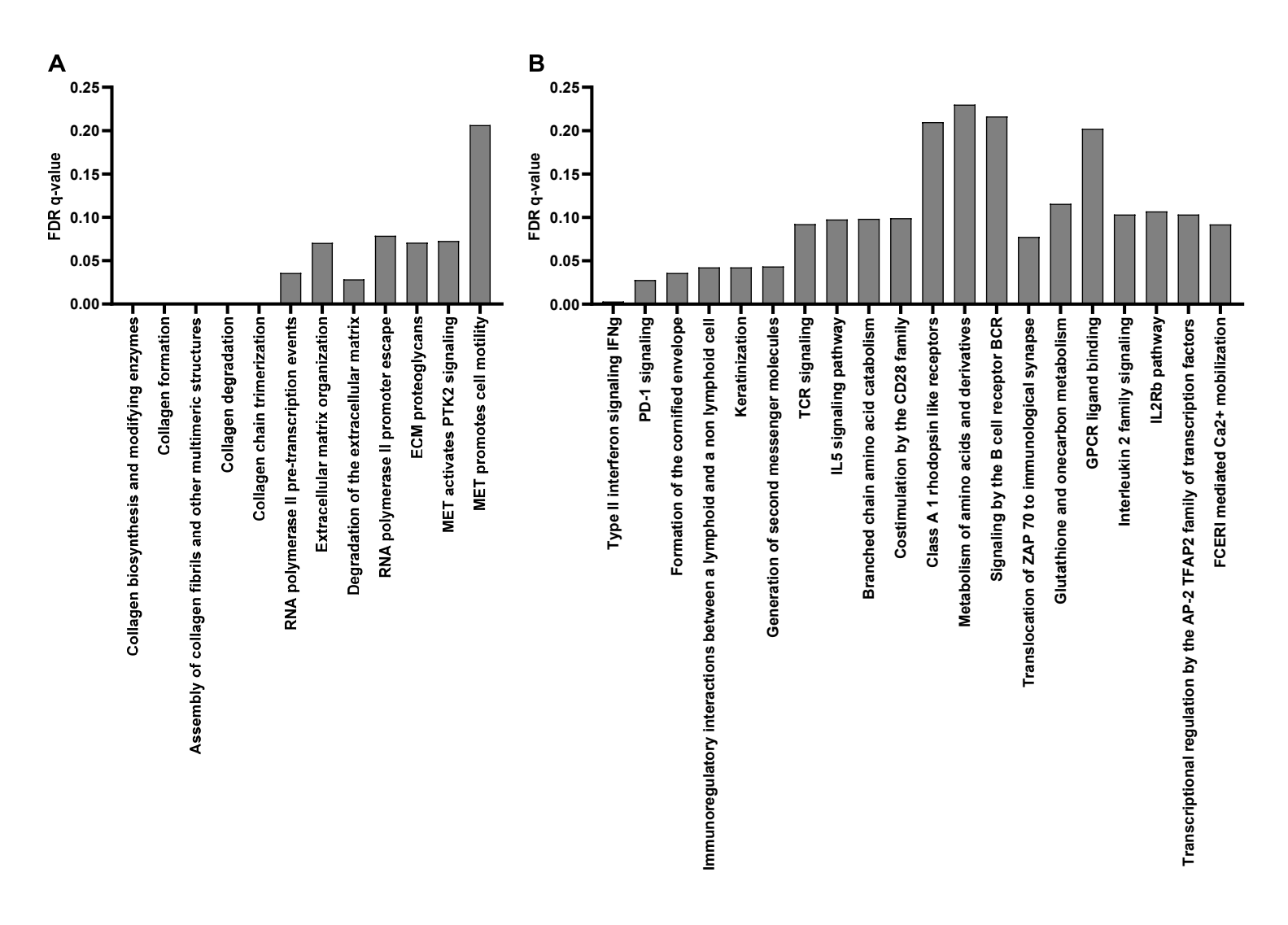
Supplementary Figure 4: Physiological pathways differentially expressed in tumor of mice. Comparison of tumors of females receiving anti-PD-1+Veh to Iso+Veh group with GSEA software. Gene sets obtained from GSEA software, using the mouse canonical pathways data base. Gene set are ranked on the x axis from the smallest to the largest nominal p value. Only the first 20 statistically differentially expressed gene sets are showed (p value < 0.05 and FDR < 0.25). 10 mice per group. Physiological pathways enriched in tumor of mice treated with anti-PD-1+Veh. No physiological pathway was found statistically reduced in tumor of mice treated with anti-PD-1+Veh in this comparison.



Supplementary Figure 5: Physiological pathways differentially expressed in tumor of mice. Comparison of tumors of females receiving anti-PD-1+RU486 to Iso+Veh group with GSEA software. Gene sets obtained from GSEA software, using the mouse canonical pathways data base. Gene set are ranked on the x axis from the smallest to the largest nominal p value. Only the first 20 statistically differentially expressed gene sets are showed (p value < 0.05 and FDR < 0.25). 9 to 10 mice per group. A. Physiological pathways enriched in tumor of mice treated with anti-PD-1+RU486. B. Physiological pathways reduced in tumor of mice treated with anti-PD-1+RU486.



Supplementary Figure 6: Physiological pathways differentially expressed in tumor of mice. Comparison of tumors of females receiving anti-PD-1+RU486 to Iso+RU486 group with GSEA software. Gene sets obtained from GSEA software, using the mouse canonical pathways data base. Gene set are ranked on the x axis from the smallest to the largest nominal p value. Only the first 20 statistically differentially expressed gene sets are showed (p value < 0.05 and FDR < 0.25). 9 to 10 mice per group. **A.** Physiological pathways enriched in tumor of mice treated with anti-PD-1+RU486. **B.** Physiological pathways reduced in tumor of mice treated with anti-PD-1+RU486.



Supplementary Figure 7: Physiological pathways differentially expressed in tumor of mice. Comparison of tumors of females receiving anti-PD-1+RU486 to anti-PD-1+Veh group with GSEA software. Gene sets obtained from GSEA software, using the mouse canonical pathways data base. Gene set are ranked on the x axis from the smallest to the largest nominal p value. Only the first 20 statistically differentially expressed gene sets are showed (p value < 0.05 and FDR < 0.25). 9 to 10 mice per group. **A.** Physiological pathways enriched in tumor of mice treated with anti-PD-1+RU486. **B.** Physiological pathways reduced in tumor of mice treated with anti-PD-1+RU486.

TYROBP causal network in	Cd84, Itgam, II10ra, Itgax, Hlx, Itgb2, Ncf2, Nrros, Samsn1, Rgs1, Tmem106a,	
microglia	Nckap1l, Plek, Kcne3, Zfp36l2, Cxcl16, Hcls1, Apbb1ip, Tgfbr1, Tyrobp, Lyl1, Igsf6,	
- merogna	Tnfrsf1b, C1qc, C3	
Peptide ligand binding	Cxcl13, Ccl6, Pf4, Ccl9, Ccr5, Ednrb, Ccl25, Cxcr6, C3ar1, Penk, Cxcl1, Ccl4, Fpr1,	
	Ccr9, Cxcl9, C5ar1, Xcr1, Cxcl12, Ccl5, Ccl3, Ccl7, Aplnr, Cxcl2, Kiss1r, Cxcl16, Fpr2,	
receptors	Xcl1, Cxcr4, Cxcr3, C3, Cxcl10, Ccl12, Ccl11, Cxcl11, Ccrl2, Mc1r, Cxcl5	
Immunoregulatory	Cd300a, Ifitm6, Siglec1, Itga4, Itgb2, Cd3d, H2-Q7, Jaml, Cd300c2, Fcgr2b, Cd1d1,	
interactions between a	Siglech, H2-M3, Cd8a, Trbc1, Trac, Cd22, Slamf6, Lair1, Pilra, Siglece, H2-Q6, H2-	
lymphoid and a non-	Q10, H2-Q4, Trem2, Fcgr4, Cd3e, Icam1, Col3a1, Hcst, Klrk1, H2-Q1, C3, Icam4,	
lymphoid cell	Slamf7, Cd8b1, H2-T23, Sell, Siglecg, Ifitm1	
Microglia pathogen	Itgam, Rac3, Itgb2, Ncf2, Ncf1, Cybb, Rac2, Lat, Nckap1l, Vav1, Pik3r6, Vav3,	
phagocytosis pathway	Fcgr1, Siglece, Tyrobp, C1qa, Syk, Trem2, Fcer1g, C1qb, C1qc, Ptpn6	
	Pik3r5, Fgr, Cxcl13, Ccl6, Pf4, Ccl9, Cxcl14, Ccr5, Ccl8, Prkcb, Ccl25, Cxcr6, Braf,	
Chemokine signaling	Shc4, Cxcl1, Ccl4, Plcb4, Dock2, Ncf1, Ccr1, Adcy9, Ccr9, Gnb4, Rac2, Cxcl9, Xcr1,	
pathway	Cxcl12, Ccl5, Ccl3, Ccl7, Adcy7, Cxcl2, Vav1, Ccr2, Adcy4, Cxcl16, Xcl1, Vav3, Cxcr4,	
patriway	Akt3, Plcb2, Rock1, Cxcr3, Gng2, Plcb1, Ccl2, Jak2, Cxcl10, Rock2, Gng11, Sos2,	
	Ccl12, Ccl11, Tiam1, Cxcl5, Ccl24, Pik3r1, Prkx, Chuk, Pak1, Stat1, Prkcd, Pik3ca	
Cell surface interactions at	Igha, Selp, Dok2, Cd84, Itgam, Ceacam1, Pf4, Gm5150, Mertk, Itga4, Itgax, Sdc3,	
the vascular wall	Fyn, Itgb2, Jaml, Inpp5d, Cd48, Fn1, Fcer1g, Ptpn6, Yes1, Cd74, Pros1, Sell, Selplg,	
the vascular wall	Pik3r1, Tnfrsf10b, Pik3ca, Jchain, Col1a2, Pecam1, Pik3cb	
Chemokine receptors bind	Cxcl13, Pf4, Ccr5, Ccl25, Cxcr6, Cxcl1, Ccl4, Ccr9, Cxcl9, Xcr1, Cxcl12, Ccl5, Ccl3, Ccl7,	
chemokines	Cxcl2, Cxcl16, Xcl1, Cxcr4, Cxcr3, Cxcl10, Ccl12, Ccl11, Cxcl11, Ccrl2, Cxcl5	
PD-1 signaling	Pdcd1, Cd3d, Trbc1, H2-Ea, Trac, H2-Eb1, Cd3e, Cd274, H2-Ab1, Ptpn6, Pdcd1lg2,	
PD-1 Signating	H2-Aa, Cd4	
Complement cascade	Fcna, Cfb, C6, C3ar1, C4b, C5ar1, Cfp, C1qa, Serping1, C1qb, Cd55, C1qc, Ighg1, C3	
	Ptafr, Cxcl13, Ccl6, Pf4, Ccl9, Lpar1, P2ry14, Ccr5, Adra2a, Ednrb, Ptger4, Ccl25,	
Class A 1 rhodopsin like	Cxcr6, C3ar1, Penk, Cxcl1, Ccl4, Fpr1, Ccr9, Cxcl9, C5ar1, Xcr1, Cxcl12, Ccl5, Ccl3,	
receptors	Ccl7, Hcar2, Aplnr, Cxcl2, Cmklr1, Kiss1r, Cxcl16, Fpr2, Xcl1, Cxcr4, S1pr4, Cxcr3,	
	Gpr183, C3, P2ry6, Cxcl10, Ccl12, Ccl11, Cxcl11, Ccrl2, Mc1r, Gpr132, Cxcl5, Gpr35	
	l	

Supplementary Table 2: Genes upregulated in the comparison Figure 13 A and the associated gene set.

Genes are represented with their gene symbols. Only the first 10 gene set are showed.

II. Abbreviations

CYP:

ER:

cytochrome P

estrogen receptor

ACTH: adrenocorticotropic hormone GILZ: GC-induced leucine-zipper protein

APC: antigen presenting cell GR: glucocorticoid receptor

AR: androgen receptor GRE: glucocorticoid response element

BAP1: BRCA1-associated protein 1 gene gRNA: guide RNA

BMDC: bone marrow-derived dendritic cell GSEA: gene set enrichment analysis

bp: base pair HIF-1: hypoxia-inducible factor 1

ccRCC: clear cell renal cell carcinoma HLA: human leukocyte antigen

cDNA: complementary DNA HMGB1: high mobility group box 1 protein

chRCC: chromophobe RCC HPA: hypothalamic-pituitary-adrenal axis

CMV: cytomegalovirus HR: hazard ratio

CO₂: carbon dioxide HRP: horseradish peroxidase

CRH: corticotropin-releasing hormone HSD: hydroxysteroid dehydrogenase

CT: computed tomography HSD11B1: hydroxysteroid 11-beta

dehydrogenase type 1

CTLA-4: cytotoxic T-lymphocyte-associated protein 4 HSD11B2: hydroxysteroid 11-beta

dehydrogenase type 2

DC: dendritic cells HSP: heat shock protein

DHT: dihydrotestosterone H6PDH: hexose-6-phosphate dehydrogenase

DMSO: dimethyl sulfoxide

DNA: deoxyribonucleotide acid

EC50: half maximal effective concentration IFN-γ: interferon γ

irAEs: immune-related adverse events EPFL: Ecole Polytechnique fédérale de

Lausanne IUPAC: international union of pure and

EPO: erythropoietin applied chemistry

IVF: in vitro fecundation

KEGG: Kyoto encyclopedia of genes and

EtOH: ethanol genomes

FACS: fluorescence activated cell sorting KO: knockout

FBS: fetal bovine serum LDL: low-density lipoprotein

FDR: false discovery rate LOX: lysyl oxidase

FFPE: formalin-fixed paraffin-embedded MBq: megabecquerel

fw: forward primer MDSC: myeloid-derived suppressor cells

GC: glucocorticoid MFI: mean fluorescence intensity

MHC: major histocompatibility complex ROS: reactive oxygen species

MMP: matrix metalloprotease RR: relative risk

MR: mineralocorticoid receptor RU486: mifepristone

MRI: magnetic resonance imaging rv: reverse primer

mRNA: messenger RNA R848: resiguimod

mTOR: mammalian target of rapamycin s.c.: subcutaneous

N2: standard error of the mean nitrogen SEM:

Na⁺: sodium SETD2: SET domain-containing 2 gene

SSIGN: stage, size, grade, and necrosis score NAD: oxidized form of nicotinamide adenine

dinucleotide StAR: steroidogenic acute regulatory protein NADH: reduced form of nicotinamide adenine

TCGA: the cancer genome atlas program dinucleotide

TCR: T cell receptor NADP: oxidized form of nicotinamide adenine

dinucleotide phosphate TGF- β : transforming growth factor β

NADPH: reduced form of nicotinamide T_H1: type 1 T helper cell adenine dinucleotide phosphate

TIL: tumor-infiltrating lymphocyte OS: overall survival

TKI: tyrosine kinase inhibitors PBMC: peripheral blood mononuclear cell

TLR: toll-like receptor PBS: phosphate buffer saline

TNF- α : tumor necrosis factor α PBRM1: polybromo 1 gene

TNM: tumor-node-metastasis system PCR: polymerase chain reaction

TP53: tumor protein 53 gene PD-1: programmed cell death protein 1

T_{reg}: regulatory T cells PD-L1: programmed death-ligand 1

USA: United States of America PET: positron emission tomography

VEGF: vascular endothelial growth factor PI3K: phosphoinositide 3-kinase

VEGFR: vascular endothelial growth factor PR:

progesterone receptor receptor

pRCC: papillary RCC VHL: von Hippel-Lindau

RAAS: renin-angiotensin-aldosterone system WT: wild type

RCC: renal cell carcinoma 11-DHC: 11-dehydrocorticosterone

RNA: ribonucleotide acid 95%CI: 95 % confidence interval

ROI: region of interest [18F]FDG: Fluorodeoxyglucose F18

III. List of Figures and Tables

Figure number	Title	Page number
Figure 1	The cancer-immunity cycle: A schematic representation of immune activity during cancer development	1
Figure 2	Anatomy of the kidney and the associated histology	8
Figure 3	Renin-angiotensin system for the regulation of blood pressure	10
Figure 4	Section of normal kidney and primary ccRCC stained with hematoxylin and eosin	12
Figure 5	Pathways and current drugs in metastatic renal-cell carcinoma	17
Figure 6	Algorithm for treatment choice in ccRCC	18
Figure 7	Steroidogenesis pathway that occurs in the adrenal gland and its spatial localization	23
Figure 8	Glucocorticoid pathway in peripheral organ cells	29
Figure 9	ABT-384 inhibits HSD11B1 in human ex vivo model	118
Figure 10	Intratumoral hsd11b1 over-expression does not have an effect on the antitumor immune response	123
Figure 11	Constitutive knock out of Hsd11b1 prevents anti-PD-1 response in a subcutaneous tumor model	125
Figure 12	Inhibition of GR improved anti-PD-1 response in tumor-bearing mice	131
Figure 13	Physiological pathways differentially expressed in tumor of mice	133
Figure 14	Combination of anti-PD-1+RU486 led to a modification of the intratumoral gene profile	135
Figure 15	Combination of a GR inhibitor and anti-PD-1 impacts gene expression in the tumor	136
Supplementary	Constitutive loss of hsd11b1 prevents anti-PD-1 response in	173
Figure 1	subcutaneous tumor model	1/5
Supplementary Figure 2	Immune population in tumor and spleen of Renca tumor bearing mice	175
Supplementary	Physiological pathways differentially expressed in tumor of mice.	176
Figure 3	Comparison of Iso+RU486 to Iso+Veh group	170
Supplementary	Physiological pathways differentially expressed in tumor of mice.	177
Figure 4	Comparison of anti-PD-1+Veh to Iso+Veh group	1//

Supplementary	Physiological pathways differentially expressed in tumor of mice.	178	
Figure 5	Comparison of anti-PD-1+RU486 to Iso+Veh group		
Supplementary	Physiological pathways differentially expressed in tumor of mice.	179	
Figure 6	Comparison of anti-PD-1+RU486 to Iso+RU486 group		
Supplementary	Physiological pathways differentially expressed in tumor of mice.	190	
Figure 7	Comparison of anti-PD-1+RU486 to anti-PD-1+Veh group	180	

Table number	Title	Page number
Table 1	Immune checkpoint inhibitors and their current indications	5
Table 2	ccRCC stages from the tumor-node-metastasis (TNM) classification	12
Table 3	Ranking of steroid affinity for steroid receptors	28
Table 4	Effect of HSD11B1 inhibitors on restoration of immune response	118
Table 5	Genes enhanced in the tumor of mice receiving anti-PD-1+RU486	137
Table 6	Genes downregulated in the tumor of mice receiving anti-PD-1+RU486	138
Supplementary	DNA sequences used to perform knock out of hsd11b1 and primers	174
Table 1	used to genotype hsd11b1 in mouse DNA	
Supplementary	Genes upregulated in the comparison Figure 13 A and the associated	181
Table 2	gene set	_ 5-

IV. Curriculum vitae

Date of birth 04/07/1993
French nationality
In honoinot@gmail.com
A allée de la Coopérative,
74100 Annemasse – France
+33(0)6 07 64 42 67

https://www.linkedin.com/in/helene-poinot/

0009-0006-8347-8430

French B permit

French (mother tongue)

English (proficient, working language)

Hélène POINOT M. Sc.

Immunologist, researcher, post-doctoral researcher



Skills:

Diploma:

Animal research experimentation (Swiss authorization, module 1)

Lab technics:

- Cell culture, in vitro and ex vivo experiments with primary cells and cell lines (human and murine)
- Immunophenotyping of tumor by flow cytometry (up to 13 colors panels)
- In vivo experiment with mice: injection of tumor (subcutaneous, intra-kidney), MRI of tumor bearing mice, per os, intraperitoneal and subcutaneous injections of compounds
- ELISA, Western blot, bacteria culture
- Molecular biology: PCR, qPCR, cloning, CRISPR/Cas9 knock out

Lab responsibilities:

- Management of 2 genetically modified mouse lines for 3 years: genotyping and back-crossing, management of the breeding for maintenance of the line and production of homozygote KO animals for experiments
- Main responsible of the FACS machine for 2.5 years (Novocyte 3000): maintenance of the machine and troubleshooting adviser, design of antibody panels, formation of new users, adviser for experiments with multicolor flow cytometry

Teaching responsibilities:

- Supervision of 3 master projects (4 to 5 months each): training and management of the master student
- Teaching to bachelor students

Work experience:

2017

2014

2023

2015

2023 Research assistant and PhD candidate, laboratory of Immunopharmacology of Cancer (Geneva University, Geneva, 2018 Switzerland)

Graduate researcher for 4 months in Innovation department of Oncology (Centre d'Immunologie Pierre Fabre, France).

Undergraduate researcher for 6 months in Innovation department of Oncology (Centre d'Immunologie Pierre Fabre, France). Supervisor: Dr. Aurélien Pommier, master thesis obtained with honors:

"Immunophenotypic characterization and in vitro modeling of syngeneic tumor"

Internship for 2 months. Supervisor: Pr. Pierre-Antoine Defossez
(Unité épigénétique et destin cellulaire, CNRS, France), thesis:
Epigenetic control of Cancer/Testis antigen in lung tumor

Internship for 2 months. Supervisor: Pr. Oliver Nüsse (SCICF, INSERM, France), thesis: Detection of reactive oxygen species during phagocytosis of *Candida glabrata* and *Saccharomyces cerevisiae* by human PLB cells

Internship for 2 months. Supervisor: Dr. Kathrin Marheineke (I2BC, CNRS, France), thesis: Quantification of Chk1 in the nucleus during replication in *Xenopus laevis*

Education:

PhD in Pharmaceutical Sciences, Geneva University, Geneva, Switzerland (defense in August 2023)

Thesis title: "Targeting the Glucocorticoid Pathway Improves the Outcome of Immunotherapyin a Renal Cancer Model" Thesis co-directors: Pr. Carole Bourquin, Dr. Aurélien Pommier Grant: IMMUTRAIN – EU's Horizon 2020 research and innovation program, Innosuisse – Swiss Innovation Agency

2017 Master of Oncology, Institut Gustave Roussy, University of Paris-Saclay, France

Magister of Biology, Magistère de Biologie d'Orsay, University of Paris-Sud, France, highly selective training which focus on the business world

Bachelor of Biology, University of Paris-Sud, France, diploma obtained with honors.

Scientific communications:

Short oral presentations:

MT180, Final 2023 of Geneva University, Geneva (Switzerland) 32th PhD retreat 2018, Zermatt (Switzerland)

Oral presentations:

Immune Responses in Cancer Infection, IRCI 2022, Lyon (France) PhD day 2022 of the pharmaceutical science doctoral school, Geneva (Switzerland)

World Immune Regulation Meeting-XIV 2020 (WIRM), online 8th ProDoc Cell Migration Retreat 2020, Eggiwil (Switzerland)

Poster presentations:

11th faculty & staff annual retreat of the Swiss Cancer Center Leman 2022, Geneva (Switzerland) 18th Annual Meeting of the Association for Cancer Immunotherapy 2021 (CIMT), online 7th ProDoc Cell Migration Retreat 2019, Bern (Switzerland)

7th ProDoc Cell Migration Retreat 2019, Bern (Switzerland) Spring Meeting of the Swiss Society of Pharmacology and Toxicology 2019, Bern (Switzerland)

6th ProDoc Cell Migration Retreat 2018, Bern (Switzerland)